

AD-772 831

PARTICLE DISPERSION STUDIES

Robert Kaiser

Avco Corporation

Prepared for:

Air Force Technical Applications Center
Advanced Research Projects Agency

9 August 1973

DISTRIBUTED BY:

NTIS

National Technical Information Service
U. S. DEPARTMENT OF COMMERCE
5285 Port Royal Road, Springfield Va. 22151

AD772831

PARTICLE DISPERSION STUDIES

Short Title: VT/1415

AFTAC Project Authorization
No. VT/1415/-/ASD (U)
ARPA Order No. 1702
Contract No. F33657-72-C-0388
Program Code No. 2F10

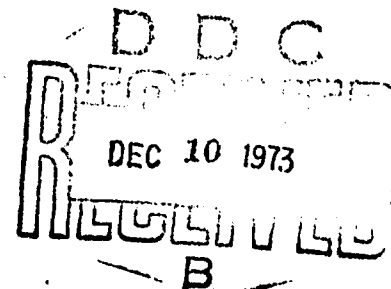
Date of Contract: 10 December 1971
Contract Expiration Date: 9 August 1973

Sponsored by

Advanced Research Projects Agency
ARPA Order No. 1702

Prepared by

Robert Kaiser (617-452-8961, X492)
Avco Corporation
Systems Division
Lowell, Massachusetts 01851



Approved for public release; distribution unlimited.

Unclassified

Security Classification

DOCUMENT CONTROL DATA - R&D		
(Security classification of title, body of abstract and indexing annotation must be entered when the overall report is classified)		
1. ORIGINATING ACTIVITY (Corporate author) AVCO Corporation, Systems Division Systems Division Lowell, Massachusetts 01851		2a. REPORT SECURITY CLASSIFICATION Unclassified
		2b. GROUP
3. REPORT TITLE Particle Dispersion Studies Short Title: VT/1415		
4. DESCRIPTIVE NOTES (Type of report and inclusive dates) Final Report December 1971 to December 1972		
5. AUTHOR(S) (Last name, first name, initial) Kaiser, Robert (NMI)		
6. REPORT DATE 9 August 1973	7a. TOTAL NO. OF PAGES 245 250	7b. NO. OF REFS 40
8a. CONTRACT OR GRANT NO. F33657-72-C-0388		9a. ORIGINATOR'S REPORT NUMBER(S)
b. PROJECT NO. AFTAC No. VT/1415/-/ASD		
c. ARPA Order No. 1702		
d. Program Code No. 2F10		9b. OTHER REPORT NO(S) (Any other numbers that may be assigned this report)
10. AVAILABILITY/LIMITATION NOTICES Approved for public release; distribution unlimited.		
11. SUPPLEMENTARY NOTES		12. SPONSORING MILITARY ACTIVITY ARPA and AFTAC/-TRE Patrick AFB, Florida
13. ABSTRACT The objective of this program was to develop to a routine procedure the capability for using a perfluorinated surfactant as an agent in bringing about the dispersion of agglomerated or conglomerated particles smaller than 5 micrometers in size. The dispersion would be of such a nature as to allow subsequent analytical measurements to be made on the separated particles. In order to deposit individual particles from an agglomerate or conglomerate, it is necessary to first completely disperse the powder in a solution of a fluorinated surfactant, Krytox 157, in a fluorinated liquid, Freon E-3. The dispersed solid particles in suspension are then partitioned from the liquid phase by filtering through in Amicon XM-100A ultrafiltration membrane, which has a pore size of about 0.007 μm . The concentration of particles in the dispersion is adjusted to yield a powder loading of less than 1.0 $\mu\text{g}/\text{cm}^2$ of filter area. At this surface concentration level, re-agglomeration of the particles during washing is minimized. The deposited particles are then washed sequentially with two other fluorinated liquids, FC-43 and Freon C-51-12, to remove the dispersing medium, and dried. The particles adhere to the filter as a result of the same forces responsible for agglomerate formation. The deposited particles can now be examined and analyzed by a variety of methods including the analysis of individual particles.		

DD FORM 1473

1 JAN 64

Unclassified

Security Classification

Unclassified
Security Classification

14. KEY WORDS	LINK A		LINK B		LINK C	
	ROLE	WT	ROLE	WT	ROLE	WT
Fine Particles Agglomeration Dispersion Ultrafiltration Fluorinated Liquids Surfactants Powders						

INSTRUCTIONS

1. **ORIGINATING ACTIVITY:** Enter the name and address of the contractor, subcontractor, grantee, Department of Defense activity or other organization (corporate author) issuing the report.

2a. **REPORT SECURITY CLASSIFICATION:** Enter the overall security classification of the report. Indicate whether "Restricted Data" is included. Marking is to be in accordance with appropriate security regulations.

2b. **GROUP:** Automatic downgrading is specified in DoD Directive 5200.10 and Armed Forces Industrial Manual. Enter the group number. Also, when applicable, show that optional markings have been used for Group 3 and Group 4 as authorized.

3. **REPORT TITLE:** Enter the complete report title in all capital letters. Titles in all cases should be unclassified. If a meaningful title cannot be selected without classification, show title classification in all capitals in parenthesis immediately following the title.

4. **DESCRIPTIVE NOTES:** If appropriate, enter the type of report, e.g., interim, progress, summary, annual, or final. Give the inclusive dates when a specific reporting period is covered.

5. **AUTHOR(S):** Enter the name(s) of author(s) as shown on or in the report. Enter last name, first name, middle initial. If military, show rank and branch of service. The name of the principal author is an absolute minimum requirement.

6. **REPORT DATE:** Enter the date of the report as day, month, year; or month, year. If more than one date appears on the report, use date of publication.

7a. **TOTAL NUMBER OF PAGES:** The total page count should follow normal pagination procedures, i.e., enter the number of pages containing information.

7b. **NUMBER OF REFERENCES:** Enter the total number of references cited in the report.

8a. **CONTRACT OR GRANT NUMBER:** If appropriate, enter the applicable number of the contract or grant under which the report was written.

8b, 8c, & 8d. **PROJECT NUMBER:** Enter the appropriate military department identification, such as project number, subproject number, system numbers, task number, etc.

9a. **ORIGINATOR'S REPORT NUMBER(S):** Enter the official report number by which the document will be identified and controlled by the originating activity. This number must be unique to this report.

9b. **OTHER REPORT NUMBER(S):** If the report has been assigned any other report numbers (either by the originator or by the sponsor), also enter this number(s).

10. **AVAILABILITY/LIMITATION NOTICES:** Enter any limitations on further dissemination of the report, other than those imposed by security classification, using standard statements such as:

- (1) "Qualified requesters may obtain copies of this report from DDC."
- (2) "Foreign announcement and dissemination of this report by DDC is not authorized."
- (3) "U. S. Government agencies may obtain copies of this report directly from DDC. Other qualified DDC users shall request through _____."
- (4) "U. S. military agencies may obtain copies of this report directly from DDC. Other qualified users shall request through _____."
- (5) "All distribution of this report is controlled. Qualified DDC users shall request through _____."

If the report has been furnished to the Office of Technical Services, Department of Commerce, for sale to the public, indicate this fact and enter the price, if known.

11. **SUPPLEMENTARY NOTES:** Use for additional explanatory notes.

12. **SPONSORING MILITARY ACTIVITY:** Enter the name of the departmental project office or laboratory sponsoring (paying for) the research and development. Include address.

13. **ABSTRACT:** Enter an abstract giving a brief and factual summary of the document indicative of the report, even though it may also appear elsewhere in the body of the technical report. If additional space is required, a continuation sheet shall be attached.

It is highly desirable that the abstract of classified reports be unclassified. Each paragraph of the abstract shall end with an indication of the military security classification of the information in the paragraph, represented as (TS), (S), (C), or (U).

There is no limitation on the length of the abstract. However, the suggested length is from 150 to 225 words.

14. **KEY WORDS:** Key words are technically meaningful terms or short phrases that characterize a report and may be used as index entries for cataloging the report. Key words must be selected so that no security classification is required. Identifiers, such as equipment model designation, trade name, military project code name, geographic location, may be used as key words but will be followed by an indication of technical context. The assignment of links, rules, and weights is optional.

Unclassified
Security Classification

PARTICLE DISPERSION STUDIES

Short Title: VT/1415

AFTAC Project Authorization
No. VT/1415/-/ASD (U)
ARPA Order No. 1702
Contract No. F33657-72-C-0388
Program Code No. 2F10

Date of Contract: 10 December 1971
Contract Expiration Date: 9 August 1973

Sponsored by

Advanced Research Projects Agency
ARPA Order No. 1702

Prepared by

Robert Kaiser (617-452-8961, X492)
Avco Corporation
Systems Division
Lowell, Massachusetts 01851

Approved for public release; distribution unlimited.

NOTICE

Neither the Advanced Research Projects Agency nor the U.S. Air Force will be responsible for information contained herein which has been supplied by other organizations or contractors, and this document is subject to later revision as may be necessary. The views and conclusions presented are those of the author and should not be interpreted as necessarily representing the official policies, either expressed or implied, of the Advanced Research Projects Agency, the Air Force Technical Applications Center, or the U.S. Government.

ACKNOWLEDGEMENTS

This research was supported by the Advanced Research Projects Agency of the Department of Defense and was monitored by HQ USAF (AFTAC/NYRC), Patrick Air Force Base, Florida, under Contract No. F33657-72-C-0388.

The active cooperation and guidance of Major Richard N. Park, USAF, and Captain David F. O'Brien, USAF, is acknowledged and contributed significantly to the achievement of the program.

ABSTRACT

The objective of this program was to develop to a routine procedure the capability for using a perfluorinated surfactant as an agent in bringing about the dispersion of agglomerated or conglomerated particles smaller than 5 micrometers in size. The dispersion would be of such a nature as to allow subsequent analytical measurements to be made on the separated particles.

In order to deposit individual particles from an agglomerate or conglomerate, it is necessary to first completely disperse the powder in a solution of a fluorinated surfactant, Krytox 157, in a fluorinated liquid, Freon E-3. The dispersed solid particles in suspension are then partitioned from the liquid phase by filtering through an Amicon XM 100A ultrafiltration membrane, which has a pore size of about $0.007\mu\text{m}$. The concentration of particles in the dispersion is adjusted to yield a powder loading of less than $1.0\mu\text{g}/\text{cm}^2$ of filter area. At this surface concentration level, re-agglomeration of the particles during washing is minimized. The deposited particles are then washed sequentially with two other fluorinated liquids, FC 43 and Freon C51-12, to remove the dispersing medium, and dried. The particles adhere to the filter as a result of the same forces responsible for agglomerate formation.

The deposited particles can now be examined and analyzed by a variety of methods, including the analysis of individual particles.

SUMMARY

Technical Problem

Often the analysis of particles released to the environment from industrial facilities is hindered because these particles are combined with others in the form of agglomerates or conglomerates. If the particle(s) of interest are small in comparison to the others as is usually the case, useful and necessary information will be lost due to a present lack of capability for selectively analyzing single particles within an agglomerate/conglomerate.

The objective of this program was to develop to a routine procedure the capability for using a perfluorinated surfactant as an agent in bringing about the dispersion in fluorinated liquids of particles in an agglomerate/conglomerate. The dispersion would be of such a nature as to allow subsequent analytical measurements to be made on the separated particles. As a result of the advent of new instrumentation which potentially permits chemical analysis of particles much smaller than 1 micrometer in diameter, and because such particles are usually present as agglomerates, emphasis was directed toward developing a capability for dispersion of agglomerates/conglomerates comprised of particles in the size range of 0.005 to 5 micrometers released to the environment from industrial facilities.

The goals of the program were to develop a dispersion technique that had the following desirable characteristics:

1. No physical or chemical change in original particles due to the dispersion process (mandatory).
2. No sample loss.
3. Complete dispersion (100% efficiency).
4. No re-agglomeration of dispersed particles.
5. Final state of each individual dispersed particle compatible with analysis by various techniques (electron microprobe, scanning and transmission electron microscopes, ion microprobe, mass spectrometer, etc.).

The great ease with which fine powders can be dispersed in a liquid phase as compared to the gas phase formed the basis of the approach to the problem.

The requirement that the suspension method developed must disperse the agglomerated materials into separate particles without physical or chemical changes, placed stringent limitations on the choice of liquids that can be used to disperse the particles. The components of the candidate dispersing liquid mixtures must, therefore, not react nor combine irreversibly with any particle in the matrix. For these reasons fluorinated liquids, which are stable, chemically inert, and furthermore, not found in nature, were the dispersion media of choice.

Technical Results

The following preparative procedure was developed. The agglomerated powder sample, typically 50 mg or less, is first dispersed ultrasonically in a 1% solution of Krytox 157, a fluorinated surfactant, in Freon E-3, a fluorinated liquid. It is recommended that a high intensity ultrasonic probe, be used to carry out the dispersion and that the dispersion process be monitored with a nephelometer. In order to insure complete dispersion, the sample should be sonolated until no further change in turbidity is observed. An aliquot sample of the above dispersion is removed and diluted with additional dispersing solution. The size of the aliquot is adjusted to obtain a particle loading on the deposition filter of $0.1 \mu\text{g}/\text{cm}^2$ or less, depending on the particle size.

This dilute dispersion is then filtered through an Amicon XM-100A ultrafiltration membrane at an applied pressure of about 1 psig. The dispersing liquid passes through membranes which retains particles larger than $0.007 \mu\text{m}$ in size. The deposited particles are then washed with a second fluorinated liquid, FC 43, to remove the dispersing medium and adsorbed surfactant. Finally a very volatile fluorinated liquid, Freon C-51-12, is then added to remove the non-volatile FC 43. The Freon C-51-12 wet filter is easily air dried. The product is an assembly of individual particles, deposited on a flat laboratory filter, that could be readily examined on this filter by a variety of microanalytical tools.

DOD Implications

The major goals of the program have been met in that a preparative procedure has been developed which will permit normally agglomerated or conglomerated particles less than $1 \mu\text{m}$ in size, down to at least $0.02 \mu\text{m}$ in size, (which is the limit of resolution of a scanning electron microscope) to be analyzed individually. The procedure was tested with four powders representative of many classes of sub-micron particles found in the atmosphere.

The method required that the agglomerates be initially well dispersed and deposited at a low surface concentration. Just as the analysis of individual particles becomes increasingly more difficult to perform with decreasing particle size, the method of preparation becomes more difficult as the size of the particles decreases. As the size of particles decreases, the acoustic energy required for dispersion increases and the permissible surface concentration of deposited particles decreases. With very small ($\sim 0.007 \mu\text{m}$), the retention of particles becomes a problem.

Recommended Further Research

The preparative procedure was tested with known samples only. The technique should now be applied to samples of natural origin. Within the scope of the present program, it was not possible to carry out any detailed, indepth analysis of the deposited samples. This should be performed to obtain a sound statistical basis of deposited sample uniformity.

TABLE OF CONTENTS

<u>Section</u>	<u>Title</u>	<u>Page No.</u>
	NOTICE	ii
	ACKNOWLEDGEMENTS	iii
	ABSTRACT	iv
	SUMMARY	v
	TABLE OF CONTENTS	vii
	LIST OF ILLUSTRATIONS	xii
	LIST OF TABLES	xix
1.0	INTRODUCTION AND BACKGROUND	1-1
	1.1 Technical Objectives	1-1
	1.2 Definition of Terms	1-1
	1.3 Theoretical Background	1-2
	1.3.1 Mechanisms of Powder Agglomeration/ Conglomeration in Air	1-2
	1.3.2 Particle Dispersion Mechanisms in a Liquid Phase	1-3
	1.4 Proposed Method of Sample Preparation	1-4
	1.5 Specific Problems Studied in this Investigation	1-5
	1.5.1 Powder Dispersion	1-6
	1.5.2 Solid/Liquid Interaction	1-6
	1.5.3 Ultrafiltration System	1-6
	1.5.4 Deposition and Characterization of Dispersed Particles	1-6
	1.6 Assignment of Project Responsibility	1-6
2.0	PROPERTIES OF MATERIALS USED IN STUDY	2-1
	2.1 Candidate Powders used in Experimental Studies	2-1
	2.2 Initial Characterization of Candidate Powders	2-3
	2.2.1 Introduction	2-3
	2.2.2 Powder Structure	2-3

TABLE OF CONTENTS (Continued)

<u>Section</u>	<u>Title</u>	<u>Page No.</u>
2.2.3	Conglomerate Formation	2-7
2.3	Fluorinated Liquids	2-13
2.3.1	Description of Candidate Fluorocarbons	2-13
2.3.2	Solubility of Candidate Powders in Fluorinated Liquids	2-13
2.4	Fluorinated Dispersing Agent	2-18
2.4.1	Choice of Dispersing Agent	2-18
2.4.2	Properties of Krytox 157 Solutions	2-19
2.5	Filtration Membranes	2-23
2.5.1	Requirements	2-23
2.5.2	Hydraulic Permeability	2-26
2.5.3	Surfactant Retention	2-30
2.5.4	Surface Characteristics and Stability for Microscopic Evaluation	2-30
2.5.5	Final Selection of Filters for Deposition Work	2-32
3.0	SURFACTANT PARTITION STUDIES	3-1
3.1	Introduction	3-1
3.2	Experimental Procedure	3-1
3.2.1	Absorption of Krytox 157 from Solution	3-1
3.2.2	Absorption Studies in 90 mm Cell	3-5
3.2.3	Particle Retention	3-7
3.2.4	Desorption of Krytox 157	3-8
3.3	Experimental Results	3-8
3.3.1	Absorption Measurements	3-8
3.3.2	Particle Retention	3-10

TABLE OF CONTENTS (Continued)

<u>Section</u>	<u>Title</u>	<u>Page No.</u>
	2.2.3 Conglomerate Formation	2-7
2.3	Fluorinated Liquids	2-13
	2.3.1 Description of Candidate Fluorocarbons	2-13
	2.3.2 Solubility of Candidate Powders in Fluorinated Liquids	2-13
2.4	Fluorinated Dispersing Agent	2-18
	2.4.1 Choice of Dispersing Agent	2-18
	2.4.2 Properties of Krytox 157 Solutions	2-19
2.5	Filtration Membranes	2-23
	2.5.1 Requirements	2-23
	2.5.2 Hydraulic Permeability	2-26
	2.5.3 Surfactant Retention	2-30
	2.5.4 Surface Characteristics and Stability for Microscopic Evaluation	2-30
	2.5.5 Final Selection of Filters for Deposition Work	2-32
3.0	SURFACTANT PARTITION STUDIES	3-1
	3.1 Introduction	3-1
	3.2 Experimental Procedure	3-1
	3.2.1 Adsorption of Krytox 157 from Solution	3-1
	3.2.2 Adsorption Studies in 90 mm Cell	3-5
	3.2.3 Particle Retention	3-9
	3.2.4 Desorption of Krytox 157	3-9
	3.3 Experimental Results	3-8
	3.3.1 Adsorption Measurements	3-8
	3.3.2 Particle Retention	3-10

TABLE OF CONTENTS (Continued)

<u>Section</u>	<u>Title</u>	<u>Page No.</u>
	3.3.3 Washing Tests	3-10
3.4	Discussion of Results	3-10
	3.4.1 Effects of Partition Filters	3-10
	3.4.2 Adsorption Measurements	3-19
	3.4.3 Washing Tests	3-20
4.0	POWDER DISPERSION IN FLUORINATED LIQUIDS	4-1
	4.1 Introduction	4-1
	4.2 Ultrasonic Dispersion	4-1
	4.3 Experimental Method	4-2
	4.3.1 Introduction	4-2
	4.3.2 Turbidity Measurements	4-3
	4.3.3 Centrifugal Sedimentation	4-4
	4.3.4 Ultrasonic Dispersion Equipment	4-7
	4.4 Experimental Results	4-9
	4.4.1 Dispersion Tests in the Ultrasonic Bath	4-9
	4.4.2 Dispersion Tests with the Ultrasonic Probe	4-13
	4.4.3 Characterization of Dispersions by Sedimentation	4-13
	4.5 Discussion of Results	4-29
	4.5.1 Correlation of Turbidity with Size of Suspended Material	4-29
	4.5.2 Effect of Process Parameters on Particle Dispersion	4-33
	4.5.3 Postulated Dispersion Mechanism	4-35
	4.5.4 Conditions for Powder Dispersions	4-39

TABLE OF CONTENTS (Continued)

<u>Section</u>	<u>Title</u>	<u>Page No.</u>
5.0	PARTICLE DEPOSITION STUDIES	5-1
5.1	Basic Method of Sample Preparation	5-1
5.1.1	Preparation of Primary Particle Dispersions	5-1
5.1.2	Secondary Particle Dispersions	5-2
5.1.3	Particle Deposition	5-2
5.1.4	Washing of Deposited Particles	5-3
5.1.5	Drying of the Membrane	5-4
5.2	Other Methods of Sample Preparation	5-4
5.3	Precautions Taken to Prevent Sample Contamination	5-5
5.4	Examination of Deposited Particles	5-7
5.4.1	S.E.M. Examination	5-7
5.4.2	Analysis of Individual Particles	5-9
5.4.3	Electron Microprobe Analysis	5-9
5.5	Experimental Results	5-9
5.5.1	Introduction	5-9
5.5.2	SEM Examination of Deposited Samples	5-10
5.5.3	Analysis of Individual Particles	5-10
5.5.4	Electron Microprobe Analysis	5-44
5.6	Discussion of Results	5-44
5.6.1	Introduction	5-44
5.6.2	Suitability of the XM-100A Ultrafilter as a Deposition Substrate	5-49
5.6.3	Effect of Scale of Measurement on Apparent Size of Deposited Particles	5-52
5.6.4	Degree of Dispersion of Deposited Powders	5-53
5.6.5	Comparison of Agglomerated and Conglomerated Mixtures	5-62

TABLE OF CONTENTS (Continued)

<u>Section</u>	<u>Title</u>	<u>Page No.</u>
	5.6.6 Elemental Composition of Deposited Samples	5-63
	5.6.7 Further Evaluation of Uniformity of a Deposited Sample	5-64
6.0	SUMMARY, CONCLUSIONS AND RECOMMENDATIONS	6-1
6.1	Summary	6-1
6.1.1	Technical Problem	6-1
6.1.2	General Methodology	6-2
6.1.3	Technical Results	6-2
6.1.4	Preparative Method Developed	6-8
6.2	Conclusions	6-9
6.3	Recommended Further Research	6-10
7.0	LIST OF REFERENCES	7-1
	APPENDICES	
	APPENDIX A - Standard Avco Method of Preparation of Powder Support Films	A-1
	APPENDIX B - Adsorption of Krytox 157 from Fluorinated Solutions on Candidate Powders	B-1
	APPENDIX C - Surface Re-Agglomeration of Deposited Particles	C-1
	APPENDIX D - Turner Model 110 Fluorometer	D-1

LIST OF ILLUSTRATIONS

<u>Figure</u>	<u>Title</u>	<u>Page No.</u>
1-1	Material Flow Diagram for Ayco Dispersion Technique	1-5
2-1	Low Magnification Transmission Electron Micrograph of Peerless No. 2 Kaolin, R.T. Vanderbilt Co., Inc. (72150)	2-5
2-2	High Magnification Transmission Electron Micrograph of Peerless No. 2 Kaolin, R.T. Vanderbilt Co., Inc. (72154)	2-5
2-3	High Magnification Transmission Electron Micrograph of Thermal Black, Sterling FT, Cabot Corp. (72146)	2-5
2-4	High Magnification of Transmission Electron Micrograph of Thermal Black, Sterling MT, Cabot Corp. (72142)	2-5
2-5	High Magnification Transmission Electron Micrograph of Natural (Normal) Sinterable Uranium Dioxide, Specification ENL-1, Eldorado Nuclear Ltd. (72181)	2-6
2-6	Very High Magnification Transmission Electron Micrograph of Natural (Normal) Sinterable Uranium Dioxide, Specification ENL-1, Eldorado Nuclear Ltd. (72184)	2-6
2-7	High Magnification Transmission Electron Micrograph of Calcium Fluoride, Reagent Grade, J.T. Baker Chemical Co. (72162)	2-6
2-8	SEM Representation of ENL-1 Uranium Dioxide Powder as Received	2-8
2-9	SEM Representation of ENL-1 Uranium Dioxide Powder as Received	2-8
2-10	SEM Representation of Precipitated Calcium Fluoride Powder as Received	2-8
2-11	SEM Representation of Precipitated Calcium Fluoride Powder as Received	2-8
2-12	SEM Representation of Sterling MT Carbon Black Powder as Received	2-9
2-13	SEM Representation of Sterling MT Carbon Black Powder as Received	2-9
2-14	SEM Representation of Precipitated Peerless No. 2 Kaolin as Received	2-9
2-15	SEM Representation of Precipitated Peerless No. 2 Kaolin as Received	2-9

LIST OF ILLUSTRATIONS (Continued)

<u>Figure</u>	<u>Title</u>	<u>Page No.</u>
2-16	SEM Representation of Agglomerated Quarternary Mixture BQF-1 . . .	2-11
2-17	SEM Representation of Agglomerated Quarternary Mixture BQF-1 . . .	2-11
2-18	SEM Representation of Agglomerated Quarternary Mixture BQF-1 . . .	2-11
2-19	SEM Representation of Agglomerated ENL-1 UO ₂ /Sterling MT Binary Mixture	2-12
2-20	SEM Representation of Agglomerated ENL-1 UO ₂ /Sterling MT Binary Mixture	2-12
2-21	SEM Representation of Kaolin/Sterling MT Agglomerated Binary Mixture	2-12
2-22	SEM Representation of ENL-1 UO ₂ /CaF ₂ Agglomerated Binary Mixture .	2-12
2-23	Soxhlet Extraction Apparatus	2-15
2-24	Measurement of Krytox 157 Concentration with Wilks Miran I Infrared Spectrophotometer	2-23
2-25	Infrared Spectrum of Krytox 157 (Courtesy E.I. Dupont de Nemours and Co., Inc.)	2-24
2-26	Infrared Absorbance at 3.18 μ m of Freon E-3/Krytox 157 Solutions	2-25
2-27	SEM Representation of S&S Selectron B-14 Filter, 4500X 1:1 (Central Zone previously exposed for 4 min at 18000X)	2-33
2-28	SEM Representation of Millipore VS Filter, 9000X 1:1	2-33
2-29	SEM Representation of Pellicon PSED Ultrafilter, 4500X 1:1 (Central Zone previously exposed for 4 min at 18000X)	2-33
2-30	SEM Representation of Amicon XM-100A Membrane (4500X 1:1) (Center Zone previously exposed at 18000X for 4 min)	2-34
2-31	SEM Representation of Scratched Amicon XM-100A Membrane from New Package (Membranes Removed by Sliding)	2-34
3-1	25 mm Millipore Ultrafiltration Cell being Rinsed in Preparation for use in Adsorption Measurements	3-2
3-2	Adsorption Measurements - Sealed 25 mm Millipore Filtration Cell being Introduced in Ultrasonic Bath (Filter is at top of Cell	3-3

LIST OF ILLUSTRATIONS (Continued)

<u>Figure</u>	<u>Title</u>	<u>Page No.</u>
3-3	Adsorption Measurements - 25 mm Millipore Ultrafiltration Cells Immersed in Constant Temperature Bath for Filtration of Fluorinated Liquid. Cell Outlet Tubes lead to Receiving Vessels	3-4
3-4	Assembly of Millipore 90 mm Ultrafiltration Cell	3-6
3-5	Millipore 90 mm Ultrafiltration Cell after Assembly for a Freon E-3 Washing Run	3-7
3-6	Adsorption on Kaolin of Krytox 157 from Fluorinated Liquid Solutions	3-9
3-7	Effect of Membrane on Apparent Adsorption of Krytox 157 on ENL-1 Uranium Dioxide from Freon E-3 Solution at 25°C	3-12
3-8	Filtration and Wash of Kaolin Dispersion in a 1% Krytox 157/FC-43 Solution through FC-43 Wet Amicon XM 100 Filter (90 mm Diameter)	3-16
3-9	Electron Micrograph of a Suspension 70 (UO ₂ - FC-43 - Krytox 157) Filtered through Millipore VSWP Filter (26000X)	3-18
4-1	Joyce Loeb1 - Mk III Disc Centrifuge	4-5
4-2	Branson E Ultrasonic Bath and Power Supply	4-8
4-3	Sonifier Probe and Power Supply Placed in 50 ml Centrifuge Tube	4-10
4-4	Sterling MT Carbon Black being Dispersed in Fluorinated Liquid by Sonifier Probe (Sample taken out of Cooling Jacket for Photograph)	4-11
4-5	Samples of Candidate Powders in Fluorinated Liquids Before and After Dispersion	4-12
4-6	Ultrasonic Dispersion of ENL-1 Uranium Dioxide in Fluorinated Liquid	4-20
4-7	Ultrasonic Dispersion of CaF ₂ in Fluorinated Liquid	4-21
4-8	Ultrasonic Dispersion of Sterling MT Carbon Black in Fluorinated Liquid	4-22
4-9	Ultrasonic Dispersion of Kaolin in Fluorinated Liquid	4-23

LIST OF ILLUSTRATIONS (Continued)

<u>Figure</u>	<u>Title</u>	<u>Page No.</u>
4-10	Calibration Curve for Sedimentation of Powders in Joyce Loeb1 Mk III Centrifuge	4-25
4-11	Photosedimentation Curves for UO_2 Dispersion in Fluorinated Liquid obtained with Joyce Loeb1 Centrifuge	4-26
4-12	Effect of Sonolation Time on Size Distribution of UO_2 Dispersed in Fluorinated Liquid	4-27
4-13	Reproducibility of Size Distribution Curve for UO_2 Dispersion	4-28
4-14	Effect of Sonolation Time on Size Distribution of CaF_2 Dispersed in Fluorinated Liquid	4-30
4-15	Particle Size Distribution of Calcium Fluoride Dispersed in a 1% Krytox 157 - Freon E-3 Solution	4-32
5-1	Laminar Flow Bench used in Studies	5-6
5-2	Filter Sample in Scanning Electron Micrograph	5-8
5-3	Effect of Sonolation Time on Appearance of Dispersed ENL-1 Uranium Dioxide Powder Deposited on XM-100 Ultrafilter (Powder Loading = $10 \mu g/cm^2$).	5-25
5-4	Effect of Powder Loading on Appearance of Dispersed ENL-1 Uranium Dioxide Powder Deposited on XM-100 Ultrafilter (Sonolation Time 678 min)	5-26
5-5	SEM Photomicrograph of Deposited UO_2 Sample DA1-1	5-27
5-6	SEM Photomicrograph of Deposited UO_2 Sample DA1-3	5-27
5-7	SEM Photomicrograph of Deposited UO_2 Sample DA1-8	5-27
5-8	SEM Photomicrograph of Deposited UO_2 Sample DA1-14	5-27
5-9	SEM Photomicrograph of Deposited UO_2 Sample DA1-15	5-28
5-10	SEM Photomicrograph of Deposited UO_2 Sample DA1-17	5-28
5-11	SEM Photomicrograph of Deposited UO_2 Sample DA1-16 (450X, 1:1).	5-29
5-12	SEM Photomicrograph of Deposited UO_2 Sample DA1-16 (4500X, 1:1).	5-29
5-13	SEM Photomicrograph of Deposited UO_2 Sample DA1-16 (18000X, 1:1)	5-29

LIST OF ILLUSTRATIONS (Continued)

<u>Figure</u>	<u>Title</u>	<u>Page No.</u>
5-14	SEM Photomicrograph of Deposited Carbon Black Sample F1-3 (450X, 1:1)	5-30
5-15	SEM Photomicrograph of Deposited Carbon Black Sample F1-3 (4500X, 1:1)	5-30
5-16	SEM Photomicrograph of Deposited Carbon Black Sample F1-3 (18000X, 1:1)	5-30
5-17	SEM Photomicrograph of Deposited Carbon Black Sample F1-1 . . .	5-31
5-18	SEM Photomicrograph of Deposited Carbon Black Sample F1-2 . . .	5-31
5-19	SEM Photomicrograph of Deposited Carbon Black Sample F1-4 . . .	5-31
5-20	SEM Photomicrograph of Deposited Carbon Black Sample B1-1 . . .	5-31
5-21	SEM Photomicrograph of Deposited CaF ₂ Sample F3-1	5-32
5-22	SEM Photomicrograph of Deposited CaF ₂ Sample F3-2	5-32
5-23	SEM Photomicrograph of Deposited CaF ₂ Sample F3-3	5-32
5-24	SEM Photomicrograph of Deposited CaF ₂ Sample F3-4	5-32
5-25	SEM Photomicrograph of Deposited Kaolin Sample F2-1	5-33
5-26	SEM Photomicrograph of Deposited Kaolin Sample F2-2	5-33
5-27	SEM Photomicrograph of Deposited Kaolin Sample F2-3	5-33
5-28	SEM Photomicrograph of Deposited Kaolin Sample F2-4	5-33
5-29	SEM Photomicrograph of Binary (Kaolin-Carbon Black) Sample FB3-4 (450X, 1:1)	5-34
5-30	SEM Photomicrograph of Binary (Kaolin-Carbon Black) Sample FB3-4 (4500X, 1:1)	5-34
5-31	SEM Photomicrograph of Binary (Kaolin-Carbon Black) Sample FB3-4 (18000X, 1:1)	5-34
5-32	SEM Photomicrograph of Binary (Kaolin-Carbon Black) Sample FB3-2	5-35
5-33	SEM Photomicrograph of Binary (Kaolin-Carbon Black) Sample FB3-5	5-35
5-34	SEM Photomicrograph of Binary (Kaolin-Carbon Black) Sample FB3-6	5-35
5-35	SEM Photomicrograph of Binary (UO ₂ -Carbon Black) Sample FB1-10 (450X, 1:1)	5-36

LIST OF ILLUSTRATIONS (Continued)

<u>Figure</u>	<u>Title</u>	<u>Page No.</u>
5-36	SEM Photomicrograph of Binary (UO_2 -Carbon Black) Sample FBI-10 (4500X, 1:1)	5-36
5-37	SEM Photomicrograph of Binary (UO_2 -Carbon Black) Sample FBI-10 (18000X, 1:1)	5-36
5-38	SEM Photomicrograph of Binary (UO_2 -Carbon Black) Sample FBI-4	5-37
5-39	SEM Photomicrograph of Binary (UO_2 -Carbon Black) Sample FBI-11	5-37
5-40	SEM Photomicrograph of Binary (UO_2 -Carbon Black) Sample FBI-8 .	5-37
5-41	SEM Photomicrograph of Binary (UO_2 -Carbon Black) Sample FBI-9 .	5-37
5-42	SEM Photomicrograph of Binary (CaF_2 -Carbon) Sample FB2-4	5-38
5-43	SEM Photomicrograph of Binary (CaF_2 - UO_2) Sample FB4-4	5-38
5-44	SEM Photomicrograph of Binary (Kaolin- UO_2) Sample FB5-5	5-38
5-45	SEM Photomicrograph of Ternary (UO_2 -Carbon Black- CaF_2) Sample FT1-5	5-39
5-46	SEM Photomicrograph of Ternary (UO_2 -Carbon Black-Kaolin) Sample FT2-5	5-39
5-47	SEM Photomicrograph of Quarternary Sample FQ1-3 (450X, 1:1). . .	5-40
5-48	SEM Photomicrograph of Quarternary Sample FQ1-3 (4500X, 1:1) . .	5-40
5-49	SEM Photomicrograph of Quarternary Sample FQ1-3 (18000X, 1:1). .	5-40
5-50	SEM Photomicrograph of Quarternary Sample FQ1-8 (450X, 1:1). . .	5-41
5-51	SEM Photomicrograph of Quarternary Sample FQ1-8 (4500X, 1:1) . .	5-41
5-52	SEM Photomicrograph of Quarternary Sample FQ1-8 (18000X, 1:1). .	5-41
5-53	SEM Photomicrograph of Quarternary Sample FQ1-4, Showing a Large Kaolin Particle	5-42
5-54	SEM Photomicrograph of Quarternary Sample FQ1-9	5-42
5-55	SEM Photomicrograph of Quarternary Powder Sample FQ1-10	5-42

LIST OF ILLUSTRATIONS (Continued)

<u>Figure</u>	<u>Title</u>	<u>Page No.</u>
5-56	SEM Photomicrograph of Quarternary Sample FQ1-10	5-42
5-57	SEM Photomicrograph of Quarternary Deposited Sample FQ1-10 . . .	5-43
5-58	Background Spectrum of Gold Coated Filter, Spot B, Figure 5-57 showing Characteristic Au and Cl Peaks and Spectrum of Particle A (Kaolin) showing Characteristic Au, Al and Si Peaks .	5-43
5-59	Background Spectrum of Gold Coated Filter at Spot B, Figure 5-57 and Spectrum of Particle C (CaF ₂) showing Characteristic Au and Ca Peaks	5-43
5-60	Photomicrograph of Gold Coated Kaolin Particle from Quarternary Sample FQ1-8	5-45
5-61	Spectrum for this Gold Coated Kaolin Particle, showing Characteristic Al, Si and Au Peak, and Cl Peak due to Filter . .	5-45
5-62	SEM Photomicrograph of Kaolin Particle and ENL-1 UO ₂ Agglomerate from Sample FB5-4	5-46
5-63	Spectrum of Gold Coated Kaolin Particle D showing Characteristic Al, Si and Au Peaks	5-46
5-64	Spectrum of Gold Coated UO ₂ Agglomerate showing Characteristic Au and U Peaks	5-46
5-65	SEM Photomicrograph of Kaolin Particles Deposited on Millipore VS Filter. Note Breakdown of Filter due to SEM Electron Beam (Preliminary Sample No. 3)	5-50
5-66	SEM Photomicrograph of ENL-1 UO ₂ Particles Deposited on Pellicon PSJM Ultrafilter (Preliminary Sample D-28)	5-50
5-67	SEM Photomicrograph of ENL-1 UO ₂ Particles Deposited on Amicon XM-100A Ultrafilter (Sample DA1-17)	5-50
5-68	Effect of Powder Loading on Apparent Size of Deposited Particles	5-54
5-69	Schematic Diagram of Deposited Particles during Washing	5-59
5-70	Addition of Wash Liquid to Deposited Particles	5-67
5-71	SEM Photomicrograph of Deposited UO ₂ Sample DA1-11 (Near Center of Filter)	5-68
5-72	SEM Photomicrograph of Deposited UO ₂ Sample DA1-11 (Near Edge of Filter)	5-68
6-1	Material Flow Diagram for Avco Dispersion Technique	6-3

LIST OF TABLES

<u>Table</u>	<u>Title</u>	<u>Page No.</u>
2-1	Physical Properties of Candidate Powders	2-2
2-2	Composition of Conglomerated Powder Mixtures	2-10
2-3	Manufacturers' Published Data on Properties of Fluorinated Liquids Used in Study	2-14
2-4	Index of Powder Solubility in Fluorinated Liquids	2-17
2-5	Density of Solutions of Krytox 157 in Various Fluorinated Liquids at 25°C	2-20
2-6	Viscosity of Fluorinated Solutions	2-21
2-7	Filter Membranes Investigated in this Study	2-27
2-8	Initial Permeability of Surfactant Free Fluorinated Liquids through Candidate Filters	2-29
2-9	Rejection of Krytox 157 by Candidate Filters	2-31
3-1	Apparent Adsorption of Krytox 157 from Fluorinated Liquids on Candidate Powders	3-11
3-2	Retention of SAL-1 Uranium Dioxide Dispersions on Ultrafilter Ultrafilters	3-13
3-3	Filter Retention of Dispersed Calcium Fluoride	3-14
3-4	Results of FC-43 Washing Experiments at Ambient with AMICON XM-100 Filter	3-15
3-5	Results of Freon E-3 Washing Experiments at Ambient	3-15
4-1	Ultrasonic Bath Dispersion of Uranium Dioxide Powder (EMIL-1) in Fluorinated Liquids as Indexed by Turbidity Measurements	4-14
4-2	Ultrasonic Bath Dispersion of Precipitated Calcium Fluoride in Fluorinated Liquids as Indexed by Turbidity Measurements	4-15
4-3	Ultrasonic Dispersion of Sterling MT Carbon Black in Fluorinated Liquids as Indexed by Turbidity Measurements	4-16
4-4	Ultrasonic Bath Dispersion of No. 2 Kaolin in Fluorinated Liquids as Indexed by Turbidity Measurements	4-17
4-5	Ultrasonic Bath Dispersion of Binary Powder Mixtures in Fluorinated Liquids as Indexed by Turbidity Measurements	4-18
4-6	Ultrasonic Bath Dispersion of Multi-Powder Mixtures in Fluorinated Liquids as Indexed by Turbidity Measurements	4-19

LIST OF TABLES (Continued)

<u>Table</u>	<u>Title</u>	<u>Page No.</u>
4-7	Particle Size Distribution of CaF_2 Dispersion in 1% Krytox - Freon E-3 Solution by Sedimentation Analysis	4-31
4-8	Summary Results of Dispersion Studies Based on Turbidity Measurements	4-34
5-1	Summary of Deposited Samples Examined by SEM	5-11
5-2	Deposition and SEM Examination of ENL-1 Uranium Dioxide on AMICON XM-100 Ultrafilter	5-12
5-3	Deposition and SEM Examination of Sterling MF Carbon Black on AMICON XM-100A Ultrafilter	5-14
5-4	Deposition and SEM Examination of Precipitated Calcium Fluoride on AMICON XM-100A Ultrafilter	5-15
5-5	Deposition and SEM Examination of Peerless No. 2 Kaolin on AMICON XM-100A Ultrafilter	5-16
5-6	Deposition and SEM Examination of Kaolin/Carbon Black Binary Mixture	5-17
5-7	Deposition and SEM Examination of UO_2 /Carbon Black Binary Mixture	5-18
5-8	Deposition and SEM Examination of CaF_2 /Carbon Black Binary Mixture	5-19
5-9	Deposition and SEM Examination of UO_2 / CaF_2 Binary Mixture	5-20
5-10	Deposition and SEM Examination of UO_2 /Kaolin Binary Mixture	5-21
5-11	Deposition and SEM Examination of (UO_2 / CaF_2 /Carbon Black) Ternary Mixture	5-22
5-12	Deposition and SEM Examination of (UO_2 /Carbon Black/Kaolin) Ternary Mixture	5-23
5-13	Deposition and SEM Examination of (UO_2 / CaF_2 /Carbon Black/Kaolin) Quaternary Mixture	5-24
5-14	Results of Electron Microprobe Analysis	5-47
5-15	Effect of Electron Probe Intensity on AMICON XM-100A Ultrafilter	5-48

LIST OF TABLES (Continued)

<u>Table</u>	<u>Title</u>	<u>Page No.</u>
5-16	Effect of Particle Shape on Interpretation of \bar{d}_{vs}	5-55
5-17	Critical Surface Loading of Candidate Powders	5-61
5-18	Factors for Electron Microprobe Measurements	5-63
6-1	Powders Used in Study	6-4
6-2	Principal Fluorinated Liquids Used in Study	6-5

1.0 INTRODUCTION AND BACKGROUND

1.1 Technical Objectives

Often the analysis of particles released to the environment from industrial facilities is hindered because these particles are combined with others in the form of agglomerates or conglomerates. If the particle(s) of interest are small in comparison to the others, as is usually the case, useful and necessary information will be lost because of a present lack of capability for selectively analyzing single particles within an agglomerate/conglomerate. The objective of this program was to develop to a routine procedure the capability for using a perfluorinated surfactant as an agent in bringing about the dispersion of particles in an agglomerate/conglomerate. The dispersion would be of such a nature as to allow subsequent analytical measurements to be made on the separated particles. As a result of the advent of new instrumentation which potentially permits chemical analysis of particles much smaller than 1 micrometer in diameter, and because such particles are usually present as agglomerates, emphasis was directed toward developing a capability for dispersion of agglomerates/conglomerates comprised of particles in the size range of 0.005 to 5 micrometers, (μm) such as those released to the environment from industrial facilities.

The goals of the program were to develop a dispersion technique that had the following desirable characteristics:

- a. No physical or chemical change in original particles due to the dispersion process (mandatory).
- b. No sample loss.
- c. Complete dispersion (100% efficiency).
- d. No re-agglomeration of dispersed particles.
- e. Final state of each individual dispersed particle compatible with analysis by various techniques (electron microprobe, scanning and transmission electron microscopes, ion microprobe, mass spectrometer, etc.).

1.2 Definition of Terms

- a. Particle of Interest - An individual particle in the same physical and chemical state in which it was first released to the environment. This may include aggregates.
- b. Aggregate - A collection of particles bound together by strong chemical bonds.
- c. Agglomerate - A collection of particles or aggregates of the same element or compound bound together by physical forces as opposed to chemical bonds.

- d. Conglomerate - Similar to an agglomerate but including different elements and/or compounds.
- e. Dispersion - Separation of an agglomerate or conglomerate into its individual component particles or aggregates.

1.3 Theoretical Background

1.3.1 Mechanisms of Powder Agglomeration/Conglomeration in Air

Ultrafine powders in air, with a particle size less than 10 μm , exhibit cohesive characteristics, even in the dry state, which are not exhibited by macroscopic objects. Microscopic examination of these powders reveals that they consist of particles of characteristic geometry that adhere to form firm assemblies. Two types of assemblies are observed: aggregates and agglomerates. Groups of particles can be fused together to form aggregates bonded by primary valence (chemical) bonds. There is no distinguishable surface between the particles forming the primary aggregates. These aggregates are usually formed during the deposition of the ultimate particles.

These aggregates in turn are found to adhere by physical forces (Van der Waals forces) to form agglomerates. (The term conglomerate is used in the case where all the particles in the agglomerate do not have the same composition and origin.) This agglomerate formation becomes increasingly more apparent as the size of the ultimate particles or aggregates decreases. Agglomeration of fine powders becomes especially significant when the particles are smaller than 1 micrometer in diameter.

Agglomerates differ from aggregates in that there is a discontinuous surface zone between the constituting particles or aggregates. Actual contact of two adjacent particles is prevented by the presence of layers of adsorbed molecules on the particle surfaces. Such layers will always be present under atmospheric conditions, and they arise from either physical or chemical adsorption. These adsorbed films can greatly alter the magnitude of the interaction between fine particles since any interaction between two solids decays rapidly with increasing distance of separation of their surfaces.

Different mechanisms which can lead to an agglomerated/aggregated matrix have been recently reviewed by Davies et al⁽¹⁻¹⁾. Mechanisms of particle agglomeration have also been discussed by Meissner et al⁽¹⁻²⁾ and Rumpf^(1-3, 1-4). Fine particle agglomeration is considered to result primarily from secondary valence interaction between the particles. The concept of an attraction between two neutral atoms or molecules was introduced in 1873 by Van der Waals⁽¹⁻⁵⁾ in order to explain deviations of real gases from the perfect gas law. In 1932, in order to take into account the coagulation of colloidal dispersions, Kallmann and Willstatter⁽¹⁻⁶⁾ suggested that secondary valence forces or Van der Waals forces could also be an effective and universal force of attraction between macroscopic solids. This idea has since been expanded, developed and tested by various workers. At the present time, it is generally considered that these forces are responsible for the so-called "spontaneous" adhesions of finely divided solids.

General explanations for the nature of Van der Waals forces were first proposed by London⁽¹⁻⁷⁾ in 1930 and more recently by Lifschitz⁽¹⁻⁸⁾. These explanations were both based on quantum theory which considers that all atoms, even in their ground state, possess rapidly fluctuating dipole moments which lead to an attraction between these atoms. The force between two solid objects, which are viewed as assemblies of many atoms, is obtained from the summation of the individual interactions of all the atoms in the two bodies with the force between any two atoms being considered independent of the presence of other atoms. According to Lifschitz, the secondary valence force, F , between two spheres of diameter, d , whose surfaces are separated by a distance, a , can be expressed as follows:

$$F = \frac{-Bd}{36a^3} \quad (1-1)$$

In the above equation, B is a characteristic material constant whose value will depend on composition of the particles and the surrounding phase. According to Dejongh⁽¹⁻⁹⁾, the value of B is approximately 10^{-9} ergs/cm for particles of polar materials in a vacuum. It is to be noted that interaction decreases as the cube of the separation distance.

In air, agglomerate formation occurs in fine particle systems because the thickness of the adsorbed layers is small, of the order of 10 \AA . Under these conditions, the Van der Waals interaction between two particles separated by this distance is significantly higher than the potential energy of disruptive mechanisms, namely thermal energy, kT , where k is Boltzmann's constant and T is the absolute temperature, or inertial effects which are proportional to the volume of the particles. Thus, although the attractive force between two solids increases with diameter, the effect of Van der Waals forces becomes insignificant with macroscopic objects (e.g. particles greater than $10 \mu\text{m}$ - $20 \mu\text{m}$) in air since inertial effects increase with mass and are thus proportional to the third power of particle diameter.

Other factors may also lead to particle-particle interactions. Electrostatic charges can be induced in many powders and can result in significant transient forces. However, because of either bulk or surface conductivity due to moisture, the electrostatic potential will leak away and hence will have no lasting effect. An exception is the case of the electret, such as aminoazobenzene, where there is a charge retention. In a similar manner, magnetic dipole-dipole interaction is important only in materials that have a significant magnetic coercitivity, such as magnetic iron oxide. Mechanical interlocking occurs in systems which contain very irregularly shaped particles. Liquid particle bridging due to surface tension forces may also occur as a result of capillary condensation of a liquid (water). Solid particle bridging is a reflection of the origin of the particles and is representative of aggregation rather than agglomeration.

1.3.2 Particle Dispersion Mechanisms in a Liquid Phase

As in the gas phase, solid particles in a liquid are also subject to secondary valence forces which lead to agglomeration. While there are no obvious techniques of dispersing sub-micron particles in the gas phase, it is standard technology to disperse particles in the liquid phase. It is possible to disperse sub-micron particles in liquid system first, by

breaking the agglomerates through application of disruptive forces, and, second, by subsequently generating repulsion forces which prevent close approach of two particles and therefore prevent or minimize re-agglomeration.

Two repulsive mechanisms exist which result in stabilization of aliquid phase colloid:

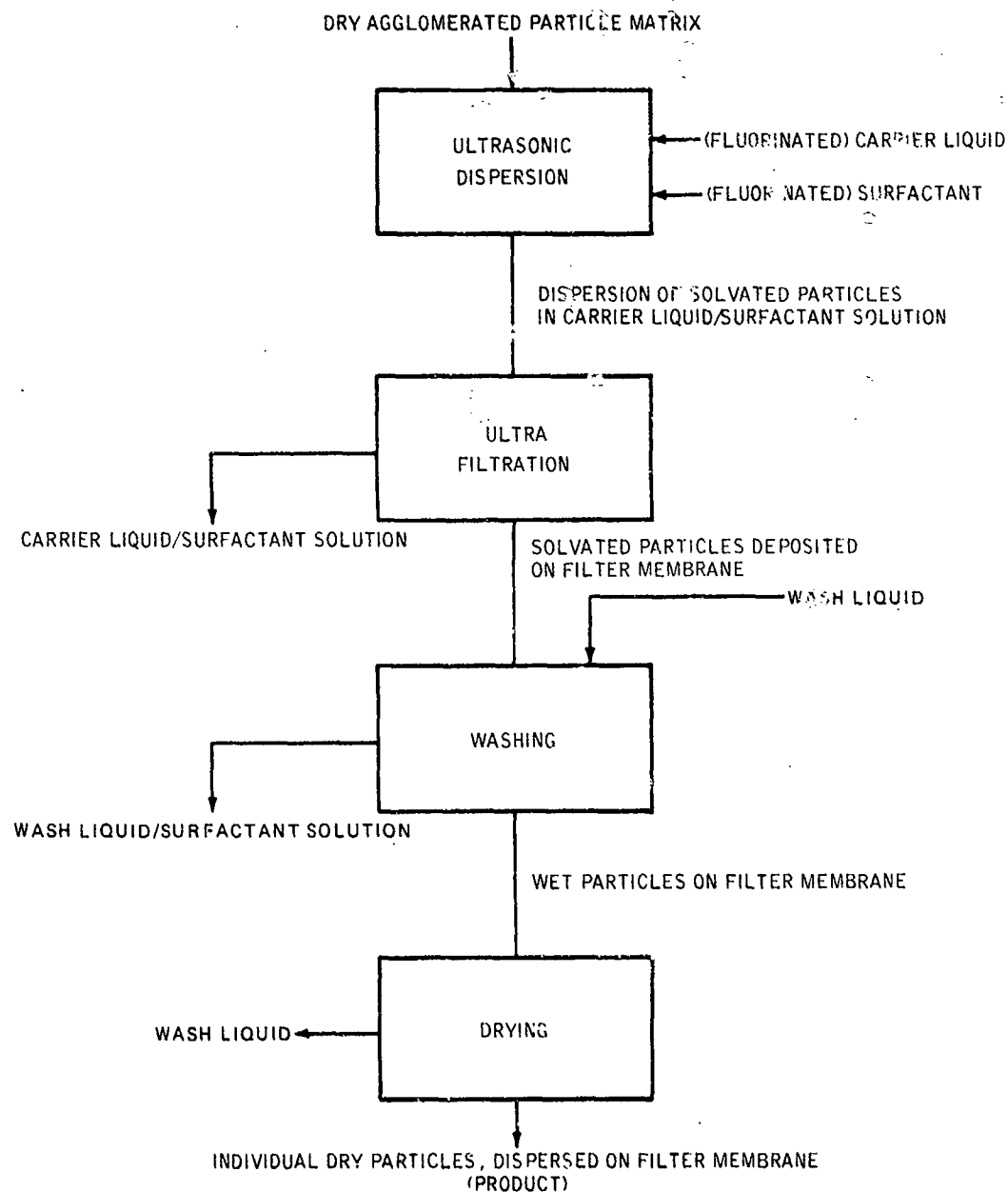
- a. Double layer electrostatic repulsion, and
- b. entropic repulsion of interacting molecules adsorbed on the particle surfaces⁽¹⁻¹⁰⁾.

The first mechanism results from the adsorption of charged species on and around the particle surfaces to form the well-known electrostatic double-layer. Stabilization occurs because of the electrostatic repulsion of two charged particles. The stability of hydrosols (aqueous colloidal dispersions) is usually due to electrostatic stabilization.

The second mechanism of entropic repulsion results from the adsorption on the particle surface of large molecules that solvate with the liquid⁽¹⁻¹¹⁾. This results in the formation of thick film of essentially bound liquid. When two particles collide, the particle-particle interaction becomes negligible in comparison to the thermal energy of these particles at the distance of separation equal to about twice the solvated film thickness. The mechanism of entropic repulsion predominates in colloid suspensions in non-polar media which are poor electrical conductors. In these liquids, it is possible to stably suspend solid particles by adding polar molecules wherein one end can adsorb at the particle surfaces and the other end of the molecule can be solvated by the carrier liquid. Carbon black is a typical example of a finely divided solid material with a characteristic particle size of less than 1 μm . The particles will not disperse in the gas phase, but they can be made to form stable suspensions in an immiscible liquid phase. Similar statements can be made for many other materials of widely diverse chemical structure and origin (titanium dioxide, zinc oxide, bentonite, organic dyes, etc.).

1.4 Proposed Method of Sample Preparation

The great ease with which fine powders can be dispersed in a liquid phase, as compared to the gas phase formed the basis of Avco's approach to the problem; this is outlined in Figure 1-1. The agglomerated matrix is first dispersed in a fluorinated organic liquid which is unlikely to dissolve or react irreversibly with any of the solid particles that form the matrix. The dispersed solid particles in suspension are then partitioned from the liquid phase by filtration, using a filtering membrane such as an ultrafilter, that has pores smaller than the smallest particles in suspension. By making the concentration of particles small enough and the area of the filter large enough for a given volume of suspension, not only will the particles be separated from the liquid phase, but the individual particles will also be separated from each other on a statistical basis when deposited on the filter. After removing the residual dispersing liquid adhering to the particles on the filter, by evaporation for example, a system of dry, isolated solid particles is obtained on the filter membrane. These particles can then be examined individually.



70-0974

Figure 1-1 MATERIAL FLOW DIAGRAM FOR AVCO DISPERSION TECHNIQUE

1.5 Specific Problems Studied in this Investigation

The purpose of the investigation was to develop and demonstrate the sample preparation technique described in Section 1.4 and outlined in Figure 1-1. The goal was to develop to a routine procedure a method of preparing agglomerated powders for analysis that made use only of commercially available materials and laboratory equipment. The principal factors that required study were:

1.5.1 Powder Dispersion

Define and determine the parameters which affect the de-agglomeration and dispersion of various agglomerated powder samples in a fluorinated liquid in order to specify processing conditions which will result in a well dispersed sample, irrespective of the initial degree of agglomeration of the powder sample to be treated.

1.5.2 Solid/Liquid Interaction

Determine the extent and reversibility of the interaction of fluorinated chemical compounds that could be used in the process with various powder samples of interest. While solid/liquid interaction is required in order to disperse the powder, this interaction has to be reversible in order to prevent contamination of the prepared particles by these fluorinated agents which might interfere with their subsequent analysis.

1.5.3 Ultrafiltration System

Determine which commercially available ultrafiltration membranes and filtration systems can be used in this technique. As outlined in more detail in Section 2.5, desirable filter characteristics include retention of the smallest particles of interest, inertness in fluorinated liquid media used to prepare the powder samples, high permeability and stability, and lack of interference with different methods of analysis.

1.5.4 Deposition and Characterization of Dispersed Particles

Utilizing the information obtained as described above, determine the conditions required to provide well-dispersed particles on a stable substrate. Demonstrate the effectiveness of the method by suitable comparative analyses of a variety of prepared samples and of the initial powders.

1.6 Assignment of Project Responsibility

The particle dispersion program was conducted in the Chemical Processes Department of Avco Systems Division, Lowell, Mass. 01851. Dr. Robert Kaiser, Leader of the Ferrofluid Group at Avco, was the principal investigator and Avco project manager. He reported to Dr. Val Krukoni, Manager, Chemical Processes Department. In addition the following Avco personnel contributed significantly to the technical effort:

Without the enthusiastic and diligent support of Mr. Richard Brown, Engineering Aide, it would not have been possible to obtain experimental

data of sufficient quality to develop meaningful conclusions. His special contribution should not go unnoticed.

Dr. Clark K. Colton, Assistant Professor of Chemical Engineering at M.I. T. and Avco Consultant, provided guidance and expertise in the areas of ultrafiltration and ultrasonic dispersion. Both Dr. Colton and Dr. Leon Mir, Senior Consulting Scientist, who acted as in-house consultant, willingly contributed their time to review and comment on the technical reports prepared during the course of the program.

Analytical measurements were performed by the Chemical Properties Group headed by Mr. W. S. Port. Transmission electron micrographs were taken by Mr. Charles Houck of the Ceramics R&D Section.

Examination of the deposited samples was sub-contracted to Advanced Metals Research, Inc. (AMR) of Burlington, Mass. 01803. The work at AMR was performed by Mr. George Bruno.

Through the courtesy of Mr. John K. Swift, of Joyce Loebl and Company, Burlington, Mass. 01803, access to a Joyce Loebl Disc Centrifuge MK III was obtained. Without Mr. Swift's cooperation, it would not have been possible to carry out meaningful sedimentation measurements on some of the dispersions of interest.

2.0 PROPERTIES OF MATERIALS USED IN STUDY

2.1 Candidate Powders used in Experimental Studies

The experimental work was performed with well characterized powders considered to be representative of those normally found in an airborne dust sample. The powders examined are listed in Table 2-1. These powders varied widely in source of origin, chemical composition, and particle shape. All had a characteristic size smaller than 1 μm , they were normally agglomerated in the dry state, and were insoluble in water. These powders were chosen to simulate a variety of solid effluents, as well as dust of natural origin which would also be present in a sample collected from the atmosphere.

A most common industrial effluent is soot which results from the intensive use of coal, petroleum and natural gas by our energy intensive technological society. Since soot is generated by myriads of industrial sources, it is quite likely that any airborne sample collected for analysis will contain some fine carbon particles. It was deemed imperative therefore that one of the powders studied be a well characterized grade of carbon black, or commercially produced soot. In order to minimize the effects of aggregation on the interpretation and evaluation of the data obtained, it was decided to study a thermal black. Medallia and co-workers (2-1, 2-2) have extensively studied the morphology of carbon black. The particles of commercial blacks consist of chains of fused spheres of different chain lengths and degree of branching. Thermal blacks have been found to be less aggregated than other types of commercial black. Thermal blacks are prepared under conditions which favor the formation of relatively discrete spherical particles, ranging from 0.1 to 1 μm in diameter. Through the courtesy of Dr. Medallia, experimental samples of two thermal blacks, Sterling MT and Sterling FT were obtained from the Cabot Corporation for further examination. Sterling MT was used as the carbon black of choice for the program on the basis of the results of the extraction studies discussed further below.

Metal oxides, as a class, are another common component of airborne effluents from industrial complexes. Metal oxides smokes are vented into the atmosphere, to varying degrees, not only by the metallurgical industry in the course of winning a metal from its ore, but by other manufacturers that make or use metal oxide powders for a variety of other commercial purposes: pigments for paints, memory elements for magnetic tapes, the fabrication of ceramic ware, etc. Because of the commercial importance of metal oxides, there were many well characterized candidate materials that could have been included in this study. A sinterable grade of natural uranium dioxide, UO_2 (Powder ENL-1 manufactured by Eldorado Nuclear Ltd. of Port Arthur, Canada) was used as a candidate powder on the basis of the following factors: size range, density, color, and the unlikely probability that uranium would be present in any of the system components (e.g. tanks, filters, glassware, etc.). ENL-1 uranium dioxide was also one of the few commercially available metal oxide powders that contained a significant number of particles smaller than 0.1 μm . A combination of the small particle size, the rarity of uranium compounds in commercial laboratory ware or ultrafiltration membranes, and the deep coloration of even very dilute uranium dioxide suspensions, made this powder an

Table 2-1
Physical Properties of Candidate Powders

Powder	Uranium Dioxide	Calcium Fluoride	Knolin	Carbon Black (1)	Carbon Black
Source	Elkhart Nuclear Ltd.	J.T. Baker Chemicals Co.	R.T. Vanderbilt Co.	Cabot Corporation	Cabot Corporation
Mfg's Designation	Natural (Normal) Sinterable UO ₂ Spec ENL-1, Issue 3	Precipitated CaF ₂ (Reagent Grade)	Peerless No. 2	Sterling FT	Sterling MT
Density, gr/cm ³ , ρ_p					
Apparent Bulk Density, ρ_B	1.53	0.95	0.49	0.45	0.44
Void Fraction in Powder Bed, ϵ_v (2)	0.85	0.70	0.81	0.75	0.75
Surface Area \pm /gram, A_s	6.0	10.1	12.5	9.6	8.5
Equivalent Spherical Diameter, \bar{d}_{vs} μ_m (3)	0.092	0.19	0.13	0.35	0.39
Particle Shape	Irregular	Irregular Prisms	Thin Platelets	Spherical	Spherical

(1) Powder tested but dropped from program

$$(2) \epsilon_v = 1 - \frac{\rho_B}{\rho_p}$$

$$(3) \bar{d}_{vs} = \frac{6}{A_s \rho_p}$$

excellent test material with which to determine the retentivity of various ultra-filtration membranes. As further discussed in the report, dispersions of ENL-1 uranium dioxide proved to be excellent tracer materials. The high density of uranium dioxide (10.9 gr/cm^3) was another attractive property of this material, because dispersions of this powder would be amenable to study by sedimentation techniques in spite of the small particle size and the relatively high density of the fluorinated liquids used in the program ($\rho = 1.7 - 1.9 \text{ gr/cm}^3$).

Any airborne effluent sample would also be contaminated with dust of natural origin, such as silicates or aluminosilicates. A well characterized grade of refined Kaolinite (Peerless No. 2 Clay marketed by R. T. Vanderbilt Company, Inc., New York, N. Y.), was included in the study program as characteristic of this type of dust. This grade of Kaolinite has been subjected to extensive prior study because of its common industrial use. A large sample of Peerless No. 2 Clay was obtained through the courtesy of R. T. Vanderbilt and Company.

There is the possibility that the presence of fluorine in the dispersed particles might not be detected if there is any significant residue on the fluorinated carrier liquid or fluorinated dispersing agent on these particles or on the filter substrate. Any residue of the dispersing medium would result in a background signal for fluorine analysis. It was therefore decided to include powdered calcium fluoride among the materials to be examined as a representative fluorine - containing material. The particular powder used was precipitated reagent grade calcium fluoride sold by J. T. Baker Company, Inc.

2.2 Initial Characterization of Candidate Powders

2.2.1 Introduction

The principal property of candidate powders of interest are listed in Table 2-1. The great advantage of using powders of industrial interest is that such materials are usually well characterized by their manufacturers. The manufacturers' published values were used for chemical composition and intrinsic physical properties of the candidate powders. Additional information was obtained at Avco related to the structure of the dry powder as received. This characterization included measurement of surface area by nitrogen adsorption, and of bulk density, as well as examination of the powder by transmission and scanning electron microscopy. Agglomerated mixtures of powders were also prepared. The solubility of the individual powders in the various liquids of interest was also examined.

2.2.2 Powder Structure

Specific surface area of the different candidate powders was measured by nitrogen adsorption in a Perkin Elmer Sorptometer (Model 212C). Duplicate single point surface area measurements were made on powder samples previously dried to 105°C and stored in a dessicator. The results are presented in Table 2-1. These measurements are accurate to within $\pm 5\%$.

The measurement of specific surface area by adsorption is independent of the degree of powder agglomeration. It is one of the few ways by which one can obtain an estimate of the ultimate particle size of an agglomerated powder without having to disperse it. The equivalent spherical average particle diameter, \bar{d}_{vs} , is related to specific surface area, A_s , and the density of the particles, ρ_p , by the following equation:

$$\bar{d}_{vs} = \frac{6}{A_s \rho_p} \quad (2-1)$$

Values of \bar{d}_{vs} are also presented in Table 2-1. This estimate is valid for all powders where the particles are not porous. It is to be noted that \bar{d}_{vs} is less than 1 μm for all the candidate powders.

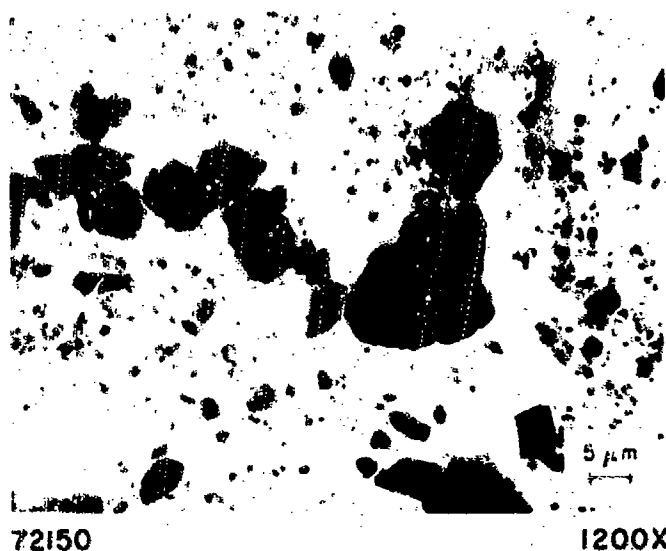
The void volume, which is one minus the ratio of bulk powder density to particle density, is usually much higher for agglomerated powders than for powder beds in which there are no interparticle forces. In the absence of interparticle forces, the volume fraction void in a powder is usually less than 0.50. With agglomerated powder, void volumes in excess of 0.90 are not uncommon. The bulk density of each candidate powder was measured by filling a 25 ml graduate with a known weight of powder, and gently tapping the graduate on a desk top until there was no further significant change in the bulk volume (usually about 20 taps) of the powder. This value was then used to calculate the bulk density. The void fraction in the powder bed ϵ_v , is derived from the bulk density, ρ_B , and the particle density, ρ_p , by the following equation:

$$\epsilon_v = 1 - \frac{\rho_B}{\rho_p} \quad (2-2)$$

As shown in Table 2-1, the measured bed void fraction is 0.70 or higher for all the candidate powders. This is a good indication that these powders have a tendency to agglomerate.

The powder samples were also examined by transmission and scanning electron microscopy. Transmission electron micrographs were obtained with Avco's 100 KV Seimens Elmiskop I. This microscope has a useful magnification range of 200 - 200,000X with a resolution of 10Å. Avco's standard preparation method was used to obtain micrographs such as the ones shown in Figure 2-1 to 2-7. This method is described in more detail in Appendix A. No specific instructions beyond the procedure described in the Appendix were given as to the presence of agglomerates in the original powder or the degree of dispersion desired.

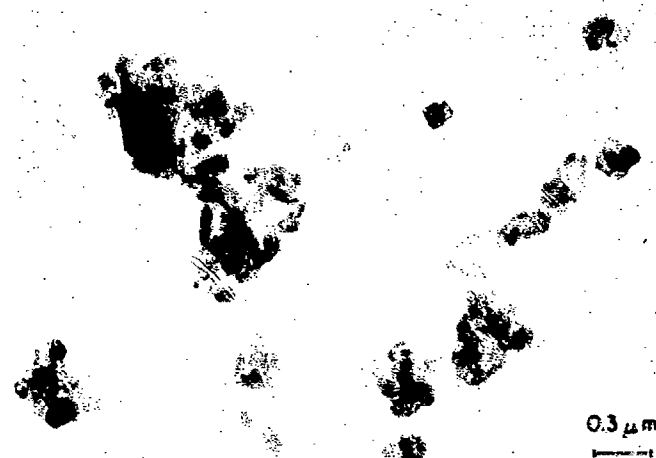
Scanning electron microscopy (SEM) work was done under sub-contract at Advanced Metals Research, Inc. (AMR) in Burlington, Mass. Scanning electron micrographs were obtained with an AMR Model 900 high resolution scanning electron microscope. This instrument has a resolution of the order of 100Å to 150Å with a useful magnification range of from about 10X up to about 50,000X. Powder sample preparation consisted in sprinkling



72150

1200X

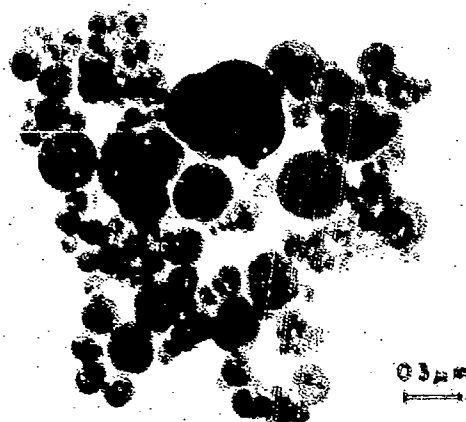
Figure 2-1 LOW MAGNIFICATION TRANSMISSION ELECTRON
MICROGRAPH OF PEERLESS NO. 2 KAOLIN,
R. T. VANDERBILT CO., INC.



72154

24,000X

Figure 2-2 HIGH MAGNIFICATION TRANSMISSION ELECTRON
MICROGRAPH OF PEERLESS NO. 2 KAOLIN,
R. T. VANDERBILT CO., INC.



72146

24,000X

Figure 2-3 HIGH MAGNIFICATION TRANSMISSION ELECTRON
MICROGRAPH OF THERMAL BLACK,
STERLING FT. CABOT CORP.



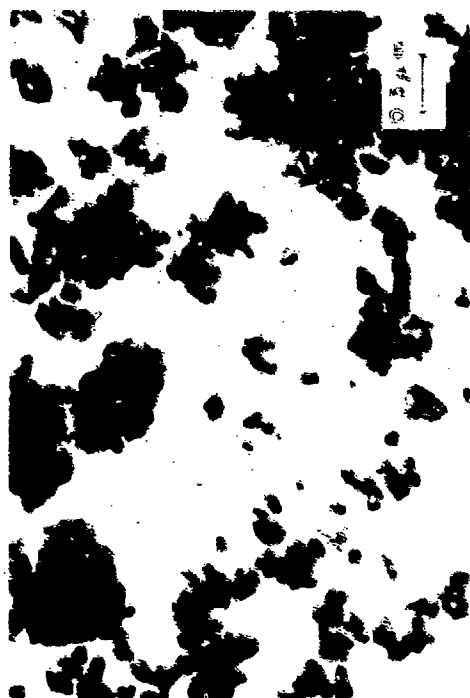
72142

24,000X

Figure 2-4 HIGH MAGNIFICATION TRANSMISSION ELECTRON
MICROGRAPH OF THERMAL BLACK,
STERLING FT. CABOT CORP.

63-1274

Reproduced from
best available copy.



72181

24,000X

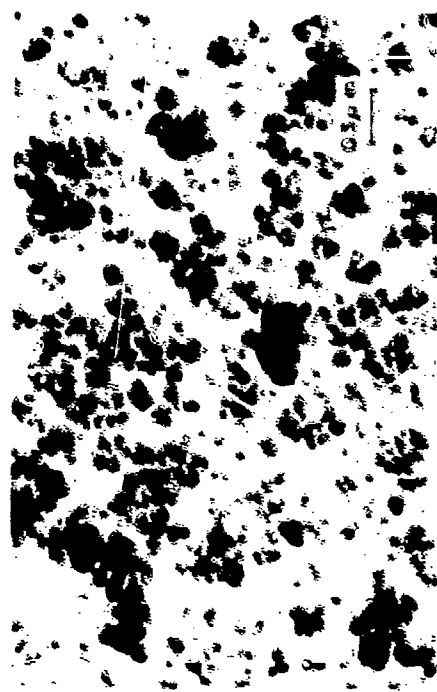
Figure 2-6 HIGH MAGNIFICATION TRANSMISSION ELECTRON
MICROGRAPH OF NATURAL (NORMAL) SINTERABLE
URANIUM DIOXIDE. SPECIFICATION ENL-1.
ELDORADO NUCLEAR LTD.



72184

96,000X

Figure 2-6 VERY HIGH MAGNIFICATION TRANSMISSION
ELECTRON MICROGRAPH OF NATURAL (NORMAL)
SINTERABLE URANIUM DIOXIDE. SPECIFICATION
ENL-1. ELDORADO NUCLEAR LTD.



72162

24,000X

Figure 2-7 HIGH MAGNIFICATION TRANSMISSION ELECTRON
MICROGRAPH OF CALCIUM FLUORIDE, REAGENT GRADE,
J. T. BAKER CHEMICAL CO.

some dry powder on a piece of transparent, double backed adhesive tape, which was already placed on a SEM target knob, and then blowing away excess powder. A thin gold-palladium coating estimated to be about 0.01 μm thick was then deposited on the samples to make them conductive. Striking photographs of well agglomerated powders were obtained as shown in Figures 2-8 to 2-15.*

As can be seen from these pictures, the powders are not well dispersed. In the SEM photographs, where there was no preliminary preparation, there are very large agglomerates. The various powders all look remarkably alike at 450X due to similarities in appearance of agglomerates. It becomes possible to identify particles to a greater or lesser degree, depending on the powder, at 4500X. Sterling MT appears to consist of bunches of grapes haphazardly thrown together. Calcium fluoride and uranium dioxide are fuzzy mosses. It is possible to identify individual particles of CaF_2 and UO_2 only at the edges of the agglomerates. It is possible to identify individual platelets of Kaolin within the agglomerated jumble represented by Figure 2-15.

The powders in the transmission electromicrographs are not as badly agglomerated because of their pretreatment. There is some degree of particle separation, and at higher magnifications it is possible to obtain some information on the geometry of primary particles, but these photographs are not very useful for quantitative analytical measurements because of the degree of agglomeration present. However, these photographs will serve as a basis of comparison, characteristic of the existing state of the art, against which electron micrographs of samples prepared by the proposed dispersion technique can be compared.

2.2.3 Conglomerate Formation

Binary and quaternary mixtures of the various powders required for deposition studies were prepared in a manner designed to promote good mixing and the formation of conglomerates. The technique involved small quantities of material and was very simple. As listed in Table 2-2, equal weights of various powders (60 mg total) were each added to a 50 ml screwcap polycarbonate centrifuge tube. The tubes and their contents were then agitated for 6 hours with a standard laboratory wrist shaker at about 1 oscillation/second. The various powders became mixed and also started to pelletize, much in the manner of a bed of zinc oxide or carbon black when tumbled in a cylindrical vessel for a long period of time (2-3). Small samples of powder mixtures after agitation were examined by SEM. Some representative electron micrographs are shown in Figures 2-16 to 2-22. These samples were prepared for microscopy in the same manner as the powder samples discussed in the previous section. As can be seen, spherical masses are formed which are significantly larger than the individual particles. Examination of the micrographs taken at higher magnification indicate that various particles appear to be well mixed within these masses or conglomerates. The particles adhere to other type particles as well as to their own kind. This result is a further indication that the particles adhere to each other by a non-specific mechanism as discussed in the introduction.

*SEM Photomicrographs presented in this report are 80% reductions of original photomicrographs. Quoted magnifications refer to original values.

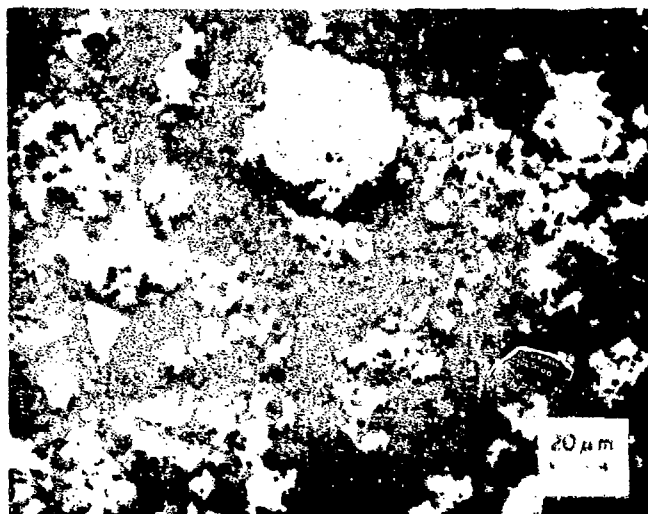


Figure 2-8 SEM REPRESENTATION OF ENL-1 URANIUM DIOXIDE POWDER AS RECEIVED

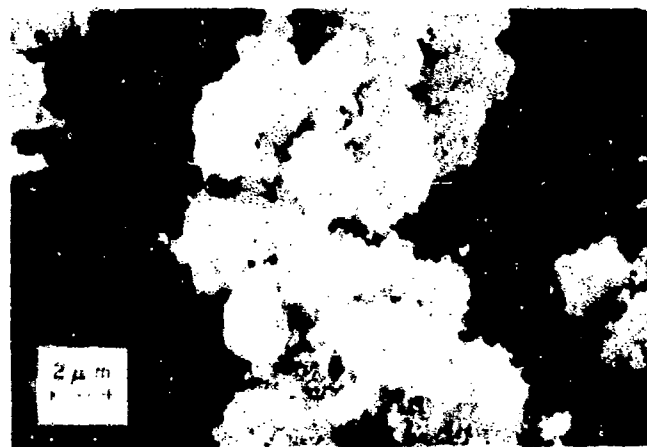


Figure 2-9 SEM REPRESENTATION OF ENL-1 URANIUM DIOXIDE POWDER AS RECEIVED

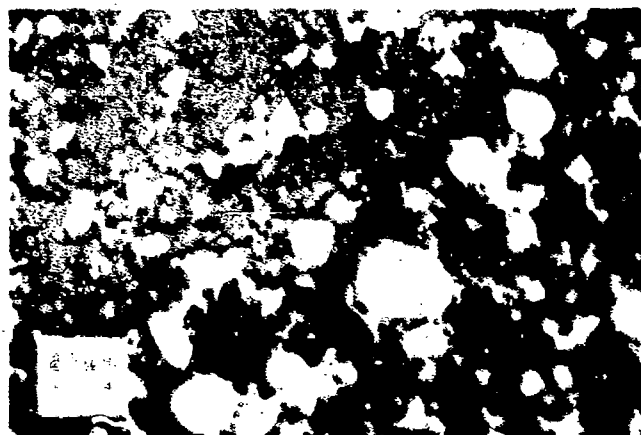


Figure 2-10 SEM REPRESENTATION OF PRECIPITATED CALCIUM FLUORIDE POWDER AS RECEIVED

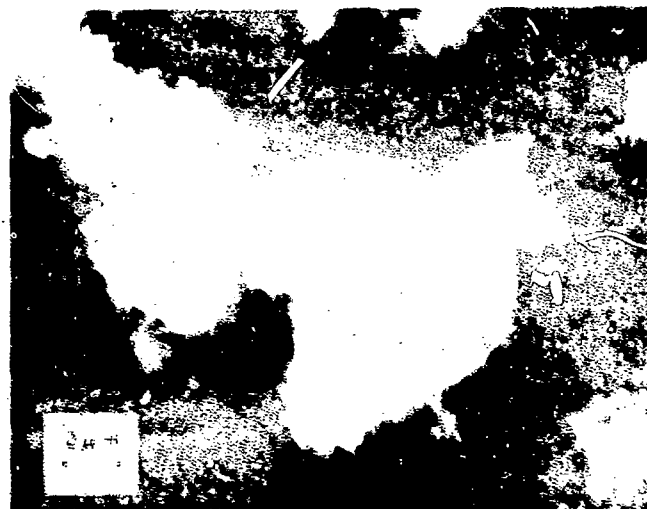


Figure 2-11 SEM REPRESENTATION OF PRECIPITATED CALCIUM FLUORIDE POWDER AS RECEIVED

53-1276

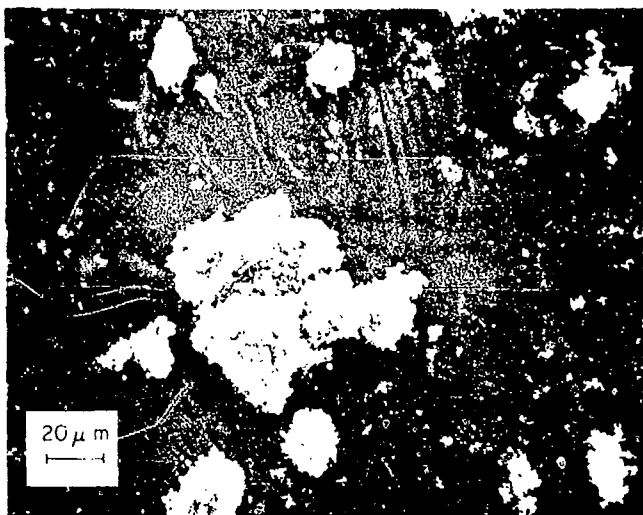


Figure 2-12 SEM REPRESENTATION OF STERLING MT CARBON BLACK POWDER AS RECEIVED

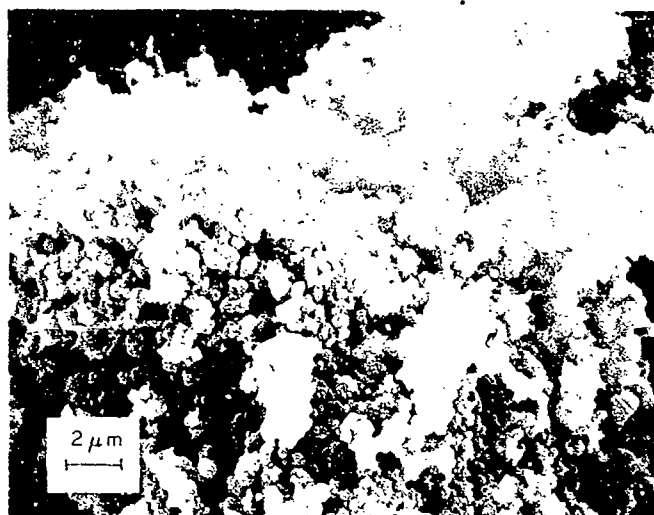


Figure 2-13 SEM REPRESENTATION OF STERLING MT CARBON BLACK POWDER AS RECEIVED



Figure 2-14 SEM REPRESENTATION OF PRECIPITATED PEERLESS NO. 2 KAOLIN AS RECEIVED

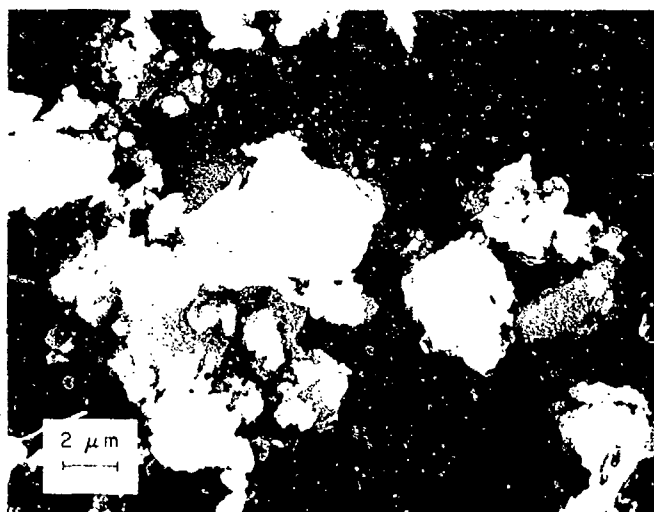


Figure 2-15 SEM REPRESENTATION OF PRECIPITATED PEERLESS NO. 2 KAOLIN AS RECEIVED

3-1277

TABLE 2-2

COMPOSITION OF CONGLOMERATED POWDER MIXTURES

<u>Mixture No.</u>	<u>Weight of Powders in Mixture, mg</u>				<u>Total</u>
	<u>UO₂</u>	<u>CaF₂</u>	<u>Kaolin</u>	<u>Sterling MT</u>	
BFB-1	30			30	60
BFB-2		30		30	60
BFB-3			30	30	60
BFB-4	30	30			60
BFB-5	30		30		60
BFB-6	15	15	15	15	60

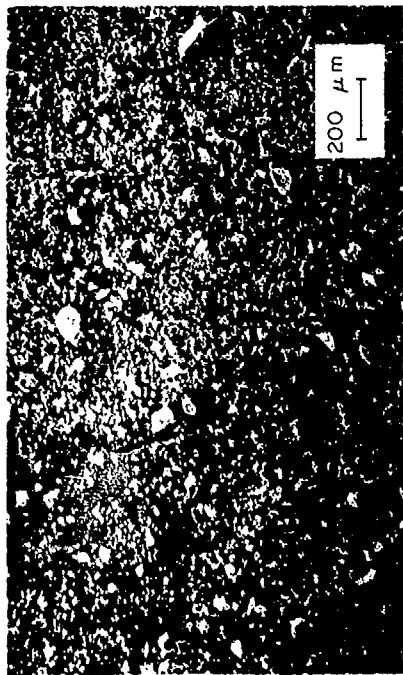


Figure 2-16 SEM REPRESENTATION OF AGGLOMERATED
QUARTERNARY MIXTURE BQF-1



Figure 2-17 SEM REPRESENTATION OF AGGLOMERATED
QUARTERNARY MIXTURE BQF-1



Figure 2-18 SEM REPRESENTATION OF AGGLOMERATED
QUARTERNARY MIXTURE BQF-1

Reproduced from
best available copy.



Figure 2-19 SEM REPRESENTATION OF AGGLOMERATED ENL-1
UO₂/STERLING MT BINARY MIXTURE



Figure 2-20 SEM REPRESENTATION OF AGGLOMERATED ENL-1
UO₂/STERLING MT BINARY MIXTURE



Figure 2-21 SEM REPRESENTATION OF KAOLIN/STERLING MT
AGGLOMERATED BINARY MIXTURE

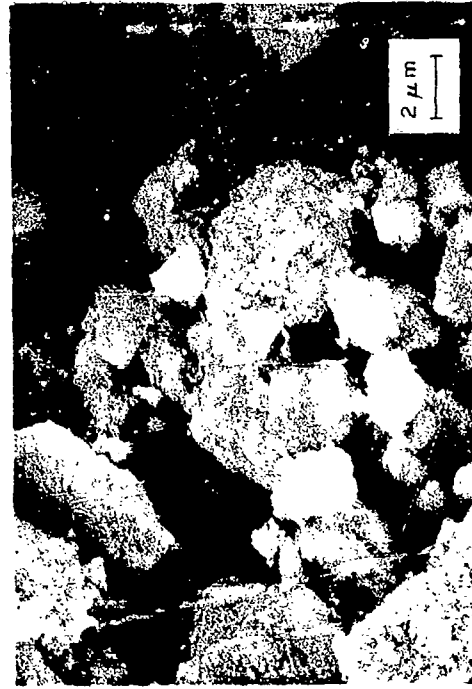


Figure 2-22 SEM REPRESENTATION OF ENL-1 UO₂/CaF₂
AGGLOMERATED BINARY MIXTURE

2.3 Fluorinated Liquids

2.3.1 Description of Candidate Fluorocarbons

The requirement that the suspension method developed must disperse the agglomerated materials into separate particles without physical or chemical changes places stringent limitations on the choice of liquids that can be used to disperse the particles. The components of the candidate dispersing liquid mixtures must, therefore, not react nor combine irreversibly with any particle in the matrix. Ideal candidate materials are the perfluorinated hydrocarbon liquids. They are fluorocarbons which are an unusually stable family of compounds (viz., teflon). They show as a class a remarkable degree of inertness and resistance to chemical attack. Furthermore, they are not found in nature so that the presence of any residual material is readily detectable.

A variety of perfluorinated or highly fluorinated organic liquids are available from different chemical manufacturers (e.g. E.I. Dupont de Nemours and Company, Inc. (Dupont), 3M Company, Inc., Allied Chemical Corporation, and Peninsular Chem Research, Inc.). These liquids have found industrial applications as heat transfer media, lubricants, electrical insulators, optical media, etc. They are presently being investigated for many other purposes. For example, a promising application is their use as a component of a synthetic blood (2-4).

The candidate fluorinated liquids used during the program are listed in Table 2-3. These liquids are all commercially available. The bulk of the experimental work involved dispersion in Freon E-3 (E-3), Freon C-51-12 (C-51-12) and FC-43. While these liquids are all generally highly fluorinated compounds, they differ in their molecular structure, and they do vary in their physical and chemical properties to a certain extent. E-3 is a highly fluorinated ether, C-51-12 is a perfluorinated cycloalkane, and FC-43 is a perfluorinated tertiary amine. The nitrogen atom in FC-43 does not behave in the same manner as the nitrogen atom in an ordinary tertiary amine. FC-43 is quite inert and behaves as an alkane. E-3 is essentially a linear molecule, C-51-12 has a ring structure, and FC-43 is highly branched. These liquids are mutually soluble.

In addition to the above liquids, the fourth fluorinated liquid listed in Table 2-3, FC-77, was used in the program as a preliminary rinse liquid because of its lower cost. It was not used in the bulk of the studies because it was found to have an effect on various candidate filters and to interact more with certain candidate powders than the other three liquids as discussed in the next section.

2.3.2 Solubility of Candidate Powders in Fluorinated Liquids

A key requirement of the study is that there be no interaction between the various fluorinated liquids and the powders under consideration. In order to determine the extent of interaction, each powder was systematically extracted by different fluorinated liquids in a standard Soxhlet extractor, as shown in Figure 2-23. In each test, about 10 gr of powder, dried overnight

TABLE 2-3

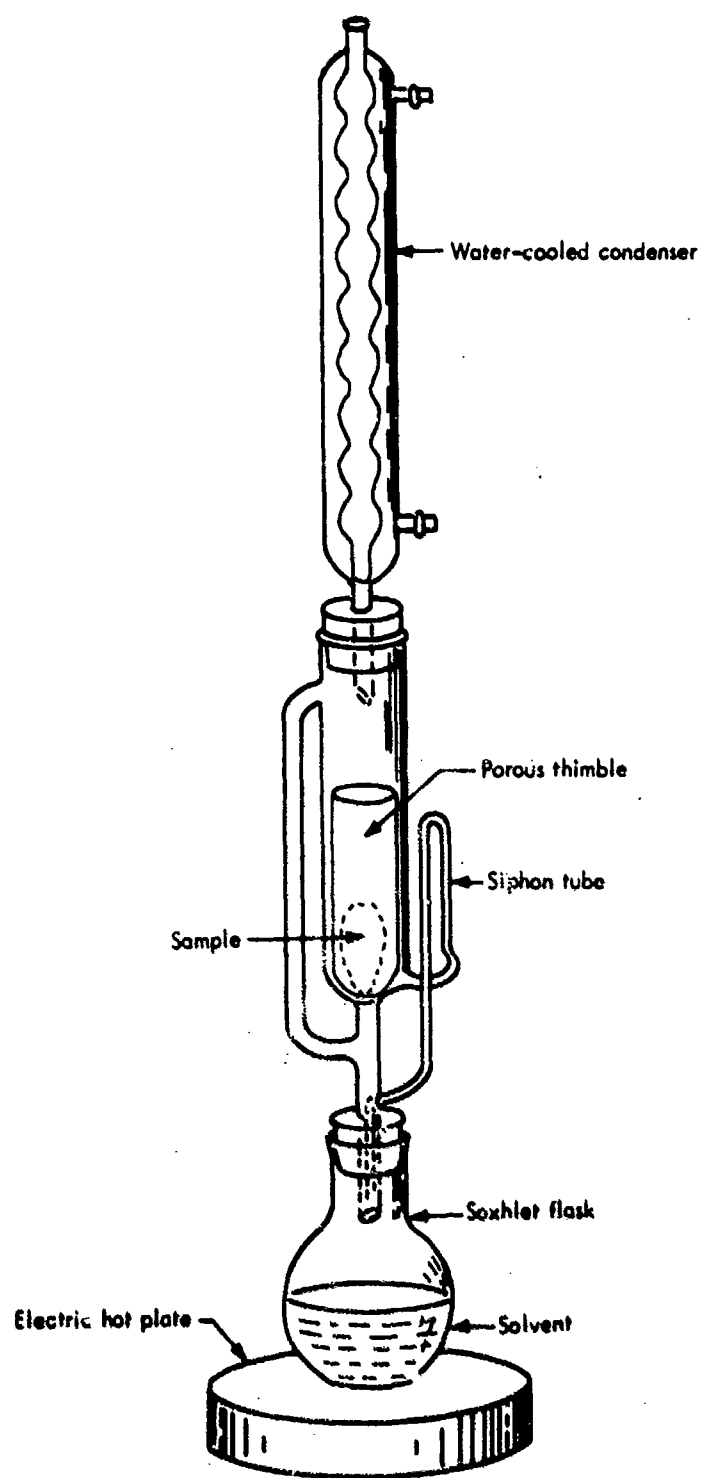
MANUFACTURERS' PUBLISHED DATA ON PROPERTIES OF FLUORINATED LIQUIDS USED IN STUDY

Trade Name	Freon E-3	Freon C-5L-12	FC-43	FC-77
Manufacturer	E.I. duPont de Nemours & Company, Inc.	E.I. duPont de Nemours & Company, Inc.	3M Company, Inc.	3M Company, Inc.
Generic Designation	Mono-hydrogen Hexafluoropropylene Oxide Trimer	Mixed Perfluorodimethyl Cyclobutane Isomers	Perfluorotributyl Amine	Mixture of perfluoro-cyclic ethers and perfluoronitrogen compounds***
Chemical Formula	$\begin{array}{c} \text{F} (\text{CFCF}_2\text{O})_3 \text{CHCF}_3 \\ \\ \text{CF}_3 \end{array}$	C_6F_6	$(\text{C}_4\text{F}_9)_3\text{N}$	Not known
Boiling Point °C	152	45	174	97
Density, gm/cm ³ (25°C)	1.723	1.6718	1.88	1.78
Viscosity, cp (25°C)	2.37	0.98	5.33	1.43
Surface Tension dynes/cm (25°C)	14.2	11.6		
Velocity of Sound in Liquid, m/sec (25°C)	720*		655**	595**
Reference:	(2-5)	(2-6)	(2-7, 2-8)	(2-7, 2-8, 2-9)

*Based on manufacturer's compressibility and density data, Reference 2-5.

** Reference 2-8

*** Reference 2-9



87-2809

Figure 2-23 SOXHLET EXTRACTION APPARATUS

in a 110°C oven, was placed in a tared, porous paper extraction thimble. The initial powder weight was measured to 0.1 mg on an analytical balance. After adding 50 ml of a given fluorinated liquid, the thimble was placed in the extraction tube and extracted for 6 hours. During the extraction process, the fluorinated liquid in the flask is heated to boiling. The resulting vapors flow through the by-pass in the extraction tube to a condenser where they are condensed. The resulting liquid drops into the thimble where it comes into contact with the powder sample. Liquid level builds up in the extractor until it exceeds the height of the syphon tube, at which time it syphons back into the reboiler flask. The process then repeats itself automatically. In this manner, the powder is continuously contacted with fresh liquid and any non-volatile dissolved material would be concentrated in the liquid in the extraction flask. At the end of each test, the thimble was dried to constant weight at 110°C, and the change in powder weight recorded (see Table 2-4). The appearance of the extractant was also noted. In addition, for the inorganic compounds, samples of the extraction liquids were sent to the Avco analytical laboratory to determine the concentration of a characteristic substance in each liquid by atomic adsorption (uranium for uranium dioxide, calcium for calcium fluoride, aluminum for kaolin).

The percent weight loss was less than 1% for the five powders studied, with the exception of the Sterling FT carbon black. In particular, for uranium dioxide the weight loss was less than 0.2%. For the inorganic compounds, the extraction liquid was clear after each test with one exception (CaF₂/Freon E-3). The weight losses observed are believed to result mainly from loss of adsorbed water (especially with FC-43 and Freon E-3 which boil at 345°F and 306°F, respectively), and to passage of some of the particles through the filter (Kaolin/C-51-12 and CaF₂/Freon E-3).

The extraction liquids from the Kaolin, uranium dioxide and calcium fluoride tests were analyzed for aluminum, calcium and uranium, respectively. None of these metals were detected in these liquids by atomic adsorption. This technique can detect trace quantities of calcium and aluminum (less than 1 ppm). Due to the low sensitivity of this method to uranium (2000 ppm detection limit), the presence of uranium in the UO₂ extracts was also analyzed by x-ray fluorescence which can detect 10 ppm uranium in the fluorinated liquids. These tests indicated that there was no uranium present in these fluorinated liquids.

There is some interaction between the fluorinated liquids and the carbon black samples, especially Sterling FT, where weight losses of about 1% and discoloration of the extraction liquid were noted. With Sterling MT weight losses were less than 1%. In this case, while some material was removed from the carbon black matrix, this material was apparently immiscible in the fluorinated liquids. These results are not unexpected in that Sterling MT and Sterling FT are both thermal blacks that exhibit a relatively high concentration of toluene extractable material. These materials are mainly hydrocarbons which would exhibit a limited solubility in the fluorinated liquids. However, even with these powders, the observed weight change was small. Since the weight losses were less for Sterling MT than for Sterling FT, and since the materials extracted from Sterling MT were not soluble in the fluorinated liquids used, this grade of carbon black was used in all further adsorption and dispersion studies.

TABLE 2-4

INDEX OF POWDER SOLUBILITY IN FLUORINATED LIQUIDS

(Weight Loss after 6 hours of Soxhlet Extraction)

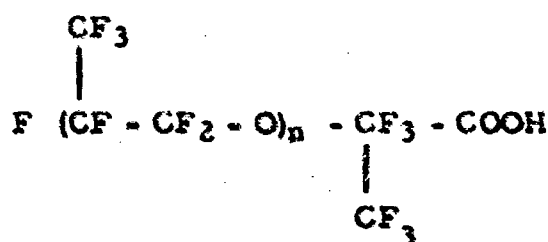
<u>Powder</u>	<u>Liquid</u>	<u>Initial Powder Weight, gr</u>	<u>ΔW Powder Grams</u>	<u>Percent Weight Loss</u>	<u>Comments on Liquid After Extraction</u>
UO ₂	Freon C-51-12	9.0918	-0.0032	0.03	Clear
	Freon E-3	7.4287	-0.0125	0.17	Clear
	FC-43	8.8872	-0.0121	0.14	Clear
	FC-77	16.8369	-0.0178	0.11	Clear
CaF ₂	Freon C-51-12	9.9846	-0.0542	0.54	Clear
	Freon E-3	9.9820	-0.0647	0.65	Slight Haze
	FC-43	9.7789	-0.0555	0.56	Clear
Kaolin	Freon C-51-12	10.5932	-0.0604	0.57	Clear
	Freon E-3	9.9829	-0.0315	0.32	Clear
	FC-43	8.9057	-0.0320	0.36	Clear
Sterling MT	Freon C-51-12	10.0529	-0.0568	0.56	Some yellow drops in liquid
	Freon E-3	10.0144	-0.0736	0.70	Clear
	FC-43	10.0138	-0.0705	0.70	Yellow line on glass at liquid surface
Sterling FT	Freon C-51-12	10.0648	-0.1170	1.16	Clear
	Freon E-3	9.9793	-0.1356	1.36	Yellowish
	FC-77	10.0309	-0.1553	1.55	Yellowish

2.4 Fluorinated Dispersing Agent

2.4.1 Choice of Dispersing Agent

Different surfactants will be needed for different fluids. A surfactant that stabilizes a dispersion in one fluid system will not usually stabilize it in any other fluid system. It is necessary to tailor the surfactant in each specific case in order to have proper transition from particle surface to bulk liquid properties. Numerous additives have been developed to stabilize suspensions in aqueous and hydrocarbon media. A typical example is oleic acid which is used to peptize suspensions in aliphatic and aromatic hydrocarbons. In this case the carboxylic acid "head" adsorbs at the particle surface and the organic "tail" interacts with the carrier liquid molecules to form a solvated sheath. While there exist many surface active agents which may be used to prepare stable colloidal sols in a hydrocarbon liquid or in water, this is not the case for perfluorinated liquid media where only a limited number of chemicals have been synthesized which are capable of stabilizing a suspension. Most commercially available fluorinated surfactants, such as perfluorooctanoic acid, do not have a molecular weight high enough to form the desired solvated film.

For a number of years, it had been desired to prepare colloidal dispersions in perfluorinated media (fluorosols) in order to take advantage of their inertness. In 1968, Kaiser recognized that chemical intermediates in the manufacture of hexafluoropropylene oxide (HFPO) polymers had the desired characteristics (2-10). These compounds have the following general chemical formula:



where n can vary between from 1 to more than 20.

Stable fluorocarbon dispersions of such diverse solids as silica, magnetite, carbon black, and sulfur have been prepared with HFPO acids that have a sufficient degree of polymerization ($n > 6$). In particular, dispersions of superparamagnetic magnetite particles stabilized by poly (HFPO) acid in a variety of fluorinated liquids have been extensively investigated at Avco S/D. These dispersions are a class of MagnecoTM ferrofluids and behave as magnetizable liquids (2-5). It has also been found that it is easier to disperse a given powder, and that the stability of the resulting dispersion is higher, when a high molecular weight poly (HFPO) acid is used as a stabilizer. These fluorosols have exhibited a shelf life in excess of one year. The particle size in these suspensions range from less than 50 Å to 10⁴ Å (1 µm).

Based on this prior experience, a high molecular weight mixture ($15 < n < 20$) of HFPO polymer acids, Krytox 157, was considered the surfactant of choice for the proposed program. It was expected that Krytox 157 would be a non-specific dispersant suitable for powders varying widely in size and composition. All the experimental work was performed with material drawn from one batch of Krytox 157 (Lots No. 2 and 3) obtained from the Petroleum Division of Dupont.

2.4.2 Properties of Krytox 157 Solutions

The following physical properties of solutions of Krytox 157 in the various fluorinated liquids were measured in order to carry out various subsequent experiments during the course of the program. These were density, viscosity, and adsorption in the near infrared. These solutions were prepared by adding a known amount of fluorinated liquid to a known amount of Krytox 157 in a tared container and then mixing these liquids in this container. The weights were determined to within 0.1 mg on a Mettler HT6 analytical balance.

The densities of various solutions of Krytox 157 and Krytox 157 alone were measured at 25°C in a jacketed cell by weight displacement, using toluene ($\rho = 0.86230 \text{ gm/cm}^3$ at 25°C (2-11)) as the liquid of reference. These results are presented in Table 2-5. The measured densities of the base liquids agree closely with available manufacturers published data.

Viscosity measurements are presented in Table 2-6. These values were required for the sedimentation studies. The viscosities of the solutions were measured on a Wells-Brookfield cone and plate viscosimeter at a shear rate of 230 sec^{-1} . The viscosity of pure Krytox 157 was measured at a lower shear rate of 1.1 sec^{-1} . These measurements are accurate to 1%.

Infrared analysis is the simplest method of analyzing the concentration of Krytox 157 HFPO acid in various fluorinated liquids of interest. Measurements were made with a Miran I infrared analyzer shown in Figure 2-24, which is a single beam infrared spectrometer that can be used with a variety of sampling systems. This instrument is particularly suited for quantitative analysis through the accurate measurement of sample absorbance at a particular wave length:

$$\ln \frac{I}{I_0} = -a \lambda c; \quad \log_{10} \left(\frac{I_0}{I} \right) = \frac{a \lambda c}{2.303} \quad (2-3)$$

where

- I = signal with sample
- I_0 = signal with no sample
- $\log_{10} \left(\frac{I_0}{I} \right)$ = sample absorbance
- λ = cell pathlength
- c = Sample concentration expressed in any convenient units
- a = Absorbance coefficient, a constant characteristic of the sample and the units chosen for concentration and pathlength.

TABLE 2-5

DENSITY OF SOLUTIONS OF KRYTOX 157
IN VARIOUS FLUORINATED LIQUIDS AT 25°C

<u>Liquid</u>	<u>Freon E-3</u>	<u>C-51-12</u>	<u>FC-43</u>	<u>FC-77</u>
Krytox 157 Concentration Weight-Percent	<u>Density, gr/cm³</u>			
0	1.727		1.886	1.768
0.01	1.727	1.674		
0.10	1.727	1.673		
1.00	1.729	1.675	1.893	1.769
5.00	1.735	<u>1.688</u>		1.774
Krytox 157 (100%)		1.892		

TABLE 2-6

VISCOSITY OF FLUORINATED SOLUTIONS

<u>Liquid</u>	<u>Viscosity, cp^a</u>	
	<u>T = 25°C</u>	<u>T = 30°C</u>
FC-43	5.53	4.78
FC-43 - 1% Kr. tox 157 ^b	5.72	5.57
E-3	2.37	2.17
E-3 - 1% Krytox 157 ^b	3.05	2.57
Krytox 157	1700	1300

a - Measured at a shear rate of 230 sec^{-1} , except for Krytox 157 which was measured at a shear rate of 1.1 sec^{-1} .

b - By weight.

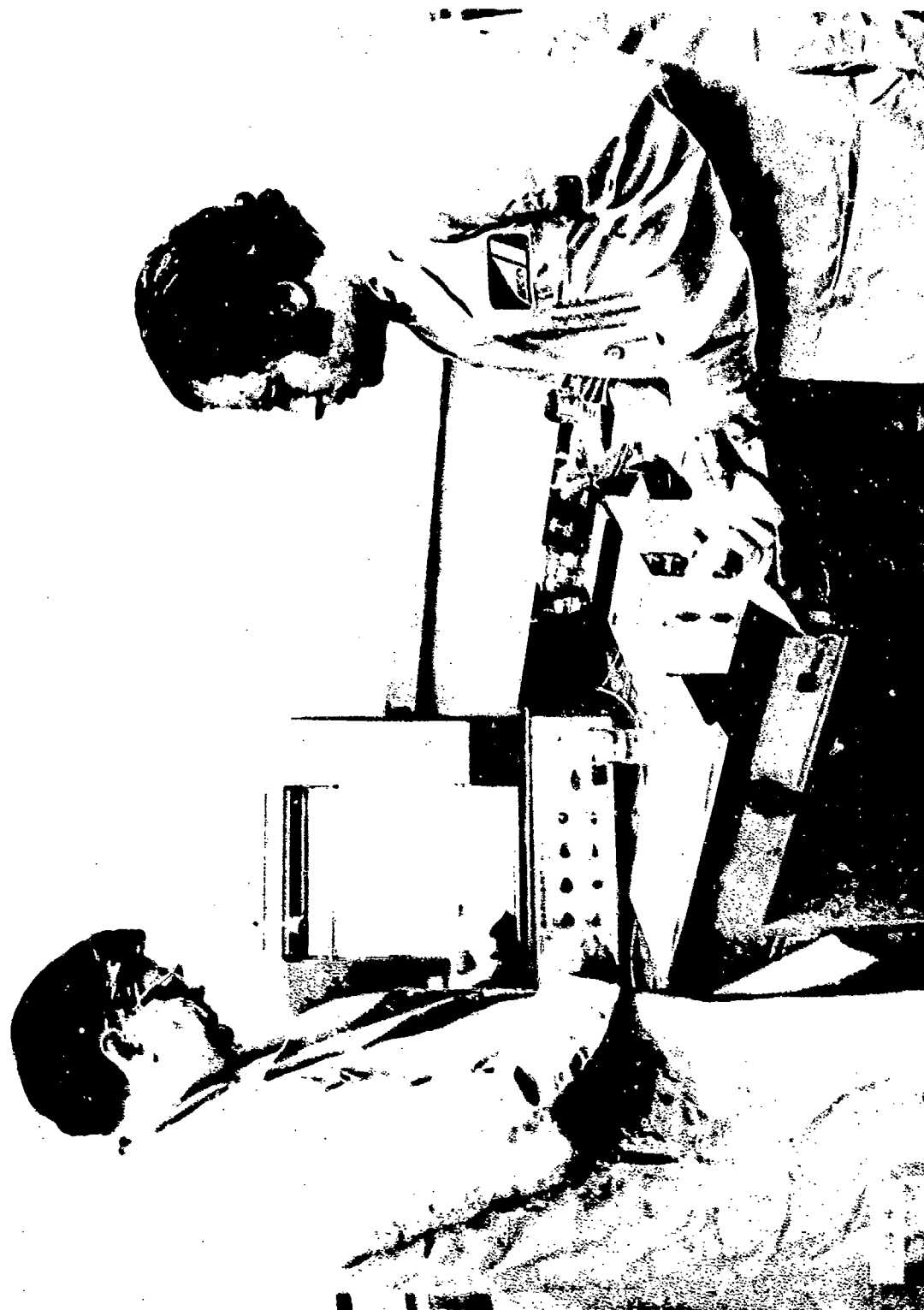


Figure 7 24 MEASUREMENT OF KRYTOX 157 CONCENTRATION
WITH WILKS MIRAN I INFRARED SPECTROPHOTOMETER

By proper choice of cell pathlength, signal intensity and wave length, it is possible to obtain conditions which are sensitive to the concentration of the unknown species one wishes to measure.

After preliminary examination of the adsorption spectrum in the near infrared of various fluorinated liquids and solutions of Krytox 157 in these liquids, all measurements were made in the near infrared at a wave length of $3.18\text{ }\mu\text{m}$ where Krytox 157 shows a significant absorbance peak (See Figure 2-25). The peak at $3.18\text{ }\mu\text{m}$ was used in preference to the very strong peak at $5.58\text{ }\mu\text{m}$ because the measurements were easier to perform. Measurements at $5.58\text{ }\mu\text{m}$ would have required the use of NaCl cells and a path length of 0.1 cm or less, whereas a standard 1 cm quartz cell could be used at $3.18\text{ }\mu\text{m}$. The quartz cell could be cleaned easily and not have to be stored in a dessicator. The Miran I could be adjusted to measure the concentration of Krytox 157 over any desired range of concentrations. A series of reference samples that contained known concentrations of Krytox 157 in a given fluorinated liquid were used to establish calibration curves from which the concentration of an unknown sample was obtained. A typical calibration curve for a broad concentration range of Krytox 157 in Freon E-3 is shown in Figure 2-26. The minimum detectable concentration of Krytox 157 was 0.01% in Freon E-3, which was the least sensitive measurement. The error in each measurement was less than 1% of the full scale reading.

2.5 Filtration Membranes

2.5.1 Requirements

In terms of the primary goals the present program, where it was planned to filter a dispersed powder from a solution of relatively high molecular weight surfactant in a carrier liquid, the allowable pore size of the membrane had to be large enough to allow passage of the high molecular component but not of the smallest particles one wished to retain. It was felt that a suitable membrane should have the following general properties:

- a. The minimum pore size should be large enough to allow the surfactant in solution to permeate.
- b. The maximum pore size should be smaller than the diameter of the smallest particle one wishes to examine.
- c. There should be minimum interaction between the membrane and any of the components of the solutions of perfluorinated liquids used to disperse and deposit the particles to be examined.
- d. The permeability should be high enough to carry out the filtration within the constraints of equipment size, operating pressure and available time characteristic of good laboratory practice. As an index, it was felt that the structure of the membrane should be such as to obtain a permeability of $10^{-2}\text{ ml/min-cm}^2\text{-psi}$ with the various solutions used in the present particle dispersion study.

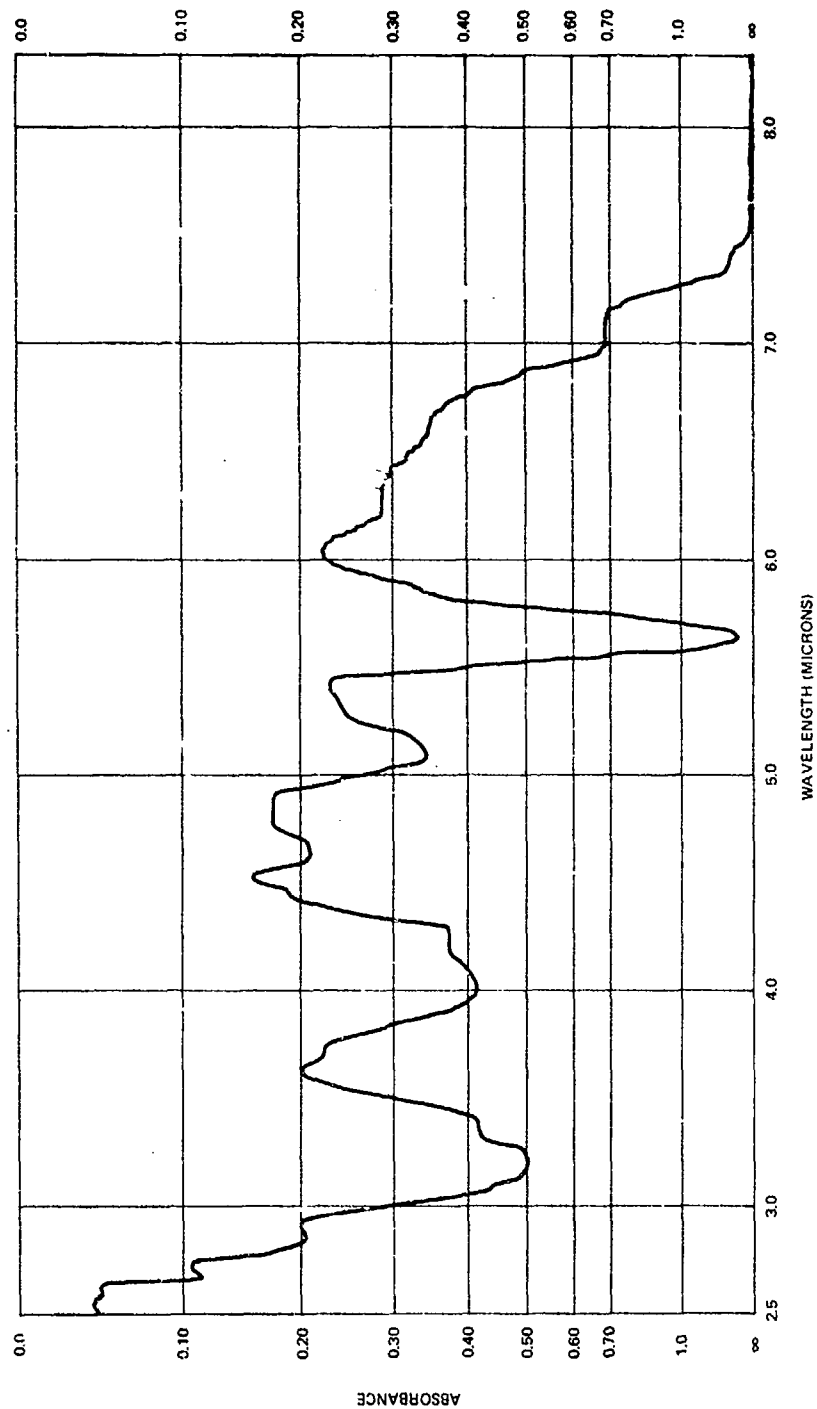


Figure 2-25 INFRARED SPECTRUM OF KRYTOX 157 (COURTESY
E. I. DUPONT de NEMOURS AND CO., INC.)

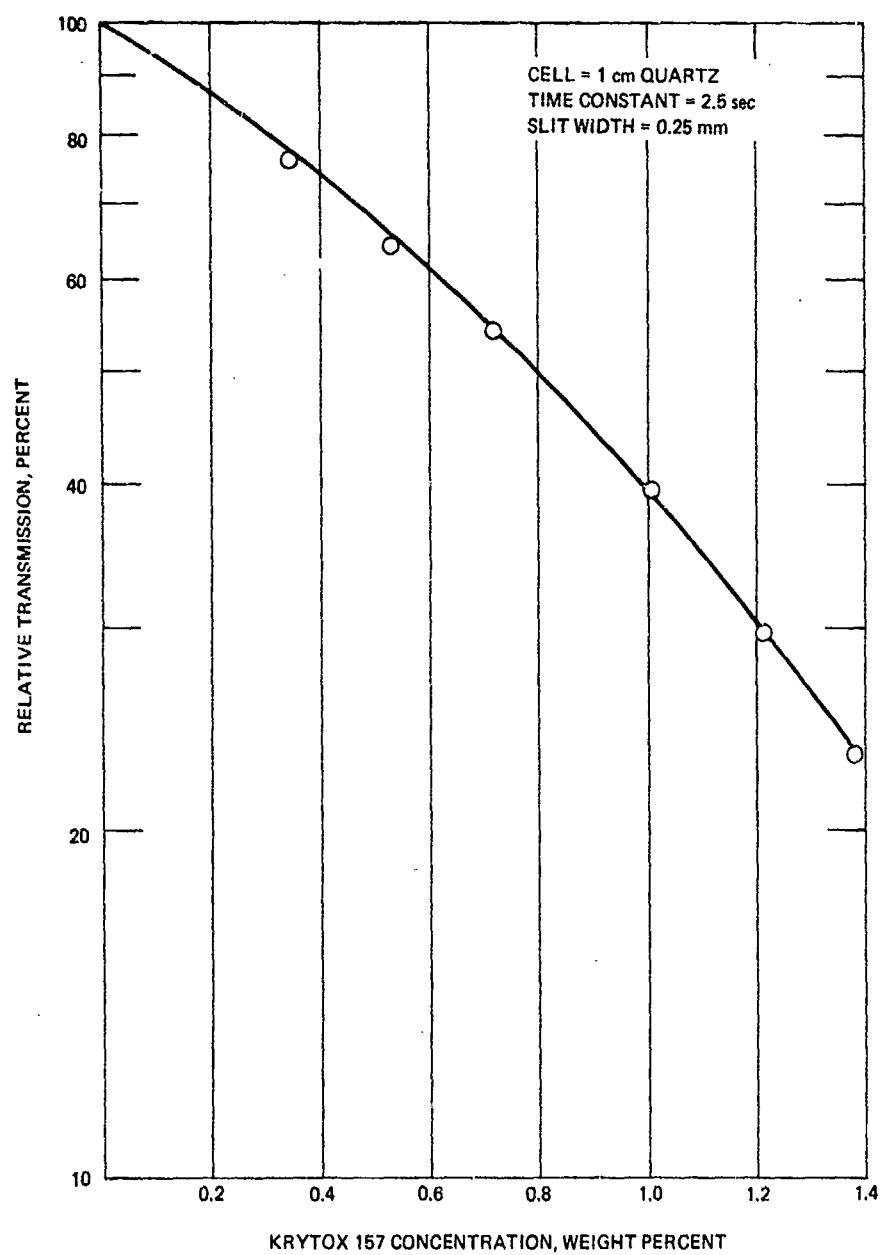


Figure 2-26 INFRARED ABSORBANCE AT 3.18 μm OF FREON
E-3/KRYTOX 157 SOLUTIONS

- e. The membrane should be a stable platform for scanning electron microscopy. It should not decompose when subjected to the intense electron bombardment characteristic of high magnification for the period of time necessary to focus on the particles of interest and to record the information by photography. Ideally the membrane should be able to withstand the effects of 50,000X magnification for 5 minutes or more.
- f. The membrane should be able to accept and be compatible with the conductive metal coatings (typically gold-palladium alloys) used in the preparation of samples for examination under a scanning electron microscope.
- g. The membrane surface should be flat. The membrane should have no contours or features whose relief would interfere with analysis of photomicrographs. This sets a critical requirement on the size of the membrane pores. These pores should be smaller than the limit of resolution of the scanning electron microscope. With existing equipment, this implies a pore size of less than 200Å. The membrane should also be clean, uniform, free of cracks, and gross structural defects.

As no previous studies had been reported in the literature in which perfluorinated liquids were processed with microporous or ultrafiltration membranes, a search was first made among various membrane manufacturers to find suitable candidates of appropriate pore size or molecular weight cutoff which would likely be compatible with perfluorinated liquids. The candidate membranes selected for further study are given in Table 2-7. These materials are representative of all the types of filters available, with the exception of the Nuclepore filters manufactured by General Electric Company. These were not included as candidate filters since the smallest pore size available at the start of this program was 0.1 μm , a value larger than the primary particle size for some of the candidate powders.

Studies in three areas were carried out to provide a basis for selecting the most suitable hydraulic filter: permeability, surfactant retention, and surface smoothness and stability during microscopic examination. Results of these studies are described below. The permeability and retention studies were performed at the outset of the program and led to a preliminary selection of membranes for further study. Roughly midway through the program, leakage of dispersed uranium dioxide through the membranes then being employed and the SEM observation of surface characteristics of the various membranes led to selection of a new material for further studies.

2.5.2 Hydraulic Permeability

Filtration tests were conducted to screen candidate filters. In these tests, the hydraulic permeability, P ($\text{cm}^3/\text{cm}^2\text{-min-psi}$), of a given fluorocarbon liquid or of a solution of Krytox 157 fluorinated surfactant in a fluorocarbon liquid, was measured as a function of time and applied pressure for a number of different commercial membranes.

TABLE 2-7FILTER MEMBRANES INVESTIGATED IN THIS STUDY

<u>Manufacturer</u>	<u>Type</u>	<u>Designation</u>	<u>Nominal Pore Size, μm</u>	<u>Nominal Molecular Weight Cutoff</u>
Millipore Corp.	Millipore Virus Filter	VMWP	0.05	
		VSWP	0.025	
	Pellicon Ultrafiltration Membrane	PSJM		156,000 (95%)
		PSED		35,000 (93%)
		PSAC		13,000 (90%)
Amicon Corp.	Diaflo Ultrafiltration Membrane	XM 300		300,000
		XM 100A		100,000
		XM 50		50,000
		PM 30		30,000
Schleicher & Schuell, Inc.	Selectron Membrane	B 14	0.01	
		O 7	0.01	
Celanese Plastics Co.	Celgard Microporous Propylene Film	2400	0.02 x 0.1 (Ellipsoidal)	

The experimental apparatus consisted of a liquid reservoir fitted with a 13 mm filter holder at its outlet, capable of being pressurized with compressed air. The filter membrane to be tested was first inserted in the filter holder (80 mm² area available for filtration). Prefiltered candidate liquid was then added to the reservoir which was then connected to the compressed air line, causing liquid to flow. The volume of filtrate collected as a function of time was then determined and the hydraulic permeability calculated. Experiments were carried out at different pressure levels (25 psi, 50 psi, 75 psi). Samples of filtrate and feed were saved for analysis of Krytox 157 concentration. Permeability was calculated and plotted as a function of filtration time. To determine long term compatibility, filter membranes were contacted with a given carrier liquid for long periods of time (overnight to two weeks).

The various filter membranes listed in Table 2-7 were contacted with at least one of the following fluorinated liquids: Freon C-51-12, Freon E-3, Fluorinert Liquid FC-43 and Fluorinert Liquid FC-77.

The initial permeability of these different filtration membranes with different carrier liquids are summarized in Table 2-8. Millipore filters MF-VM, MF-VS and Pellicon PSJM were found to be compatible with fluorinated liquids C-51-12, E-3 and FC-43. Some variation in permeability was found with FC-77. Long term (two weeks) interaction of FC-43 with Pellicon PSJM membranes was noted. However, after a short soak (overnight) permeability remained constant to within 20%. Pellicon Filters PSED and PSAC were compatible with C-51-12 and FC-43, but apparently swelled after two weeks contact with Freon E-3. These filters also had a much smaller permeability than the previous filters mentioned.

The various Amicon filters tested all showed undesirable variations in permeability with time. A relaxation effect was noted in all cases, which appears to be a characteristic of these membranes even with water.

The permeability of the S&S Selectron B-14 Filter, which was tested later in the program, was slightly lower than the competitive Millipore VM and VS filters. The hydraulic permeability of the Selectron S&S 0-7 filter was less than 1×10^{-3} ml/min - psi - cm² with Freon E-3, which was considered to be too low a value for the present application. The S&S 0-7 Selectron filter was also unsatisfactory from another standpoint. It was packaged wet (20% methanol) and could only be used wet after solvent exchange (isopropanol, then di-isopropanol ether, then Freon E-3). If the filter was allowed to dry, it wrinkled badly and irreversibly. It was totally unsatisfactory therefore as a substrate for electron microscope determinations which are carried out in a vacuum.

The permeability of the fluorinated liquids through Celgard microporous polypropylene film was very low. In spite of the fact that this film had relatively large ellipsoidal pores (short axis = 200Å, long axis = 500 - 1000Å), the liquids permeated through this material very slowly (less than 10^{-3} ml/cm² - psi - min).

TABLE 2-8

INITIAL PERMEABILITY OF SURFACTANT FREE
FLUORINATED LIQUIDS THROUGH CANDIDATE FILTERS

<u>Filter Membrane</u>	<u>Fluorinated Liquid</u>			
	<u>C-51-12</u>	<u>E-3</u>	<u>FC-43</u>	<u>FC-77</u>
	<u>Permeability (ml/cm²-psi-min) x 10³</u>			
Millipore MF-VM	50	26	20	40*
Millipore MF-VS	60	27	13	43*
Pellicon PSJM	120	44	22	79*
Pellicon PSED	33	16*	18 - 10	49*
Pellicon PSAC	2	3.5	1	12*
Celgard 2400	1	1	1	1
Amicon XM-300	30*	38*	54*	
Amicon XM-100A	8*	8*	1*	1
Amicon XM-50	5.5*	2.3		1.7
Amicon PM-30		No Flow		N.M.
S&S Selectron B-14		18		
S&S Selectron O-7		1		

*Noticeable reduction in P with filtration time or after 2 week soak test.

Blank - Not Tested

On the basis of these studies, it was decided not to use Fluorinert Liquid FC-77 in further characterization work. This liquid appeared to have a noticeable effect on the permeability of the majority of the membranes examined, whereas the other liquids did not. It is possible that there might have been some swelling of the porous matrix in the presence of FC-77.

Millipore VM, VS and Pellicon PSJM appeared to be the most suitable membranes for this work on the basis of hydraulic characteristics, and since they did not retain Krytox 157 to any significant extent as discussed in the subsequent section, these membranes were used during the first phase of the program, especially for partition studies. As discussed below, these membranes were not optimum deposition substrates and also did not have the expected retentivity for very fine particles, especially UO_2 .

2.5.3 Surfactant Retention

Experiments were also carried out to assess the retention of Krytox 157 by the candidate filters from solutions in FC-43 and Freon E-3 perfluorinated liquids. Samples of the feed solutions and filtrates were collected from a series of filtration experiments and were analyzed for Krytox 157 concentration by IR absorbance measurements as described. Surfactant retention was quantitated in terms of the measured rejection, defined by

$$\text{Rejection} = 1 - \frac{\text{concentration in filtrate}}{\text{concentration in feed}}$$

A rejection of zero indicates that surfactant traverses the membrane freely and is not impeded. A rejection of unity, on the other hand, indicates that the membrane is completely impermeable to the surfactant.

Results are presented in Table 2-9 for filtration of FC-43/Krytox 157 and E-3/Krytox 157 solutions. Solute rejection was very close to zero with all membranes except the S&S selectron 9-7 membrane. The other drawbacks of this membrane have already been discussed.

From these results, it was concluded that Krytox 157 was not significantly retained by the remaining candidate filters and that, on the basis of this criterion, these were all suitable for the planned partition and dispersion studies.

2.5.4 Surface Characteristics and Stability for Microscopic Evaluation

In order to assess the suitability of the various candidate filters as a platform support for microscopic examination, scanning electron microphotographs (SEM) were made of the clean filter surfaces. As previously mentioned, SEM work was done under subcontract at Advanced Metals Research, Inc., Burlington, Mass. The instrument used in these studies was an AMR 900 scanning electromicroscope. These initial evaluations were performed at the same time that the partition and early dispersion studies were being carried out. A thin gold/palladium coating, approximately 0.01 μm thick, also was deposited on the surface of each membrane to make the sample conductive.

TABLE 2-9

REJECTION OF KRYTOX 157 BY CANDIDATE FILTERS

<u>Manufacturer</u>	<u>Filter Designation</u>	<u>Measured Rejection</u>
<u>In FC-43 Solution</u>		
Millipore	VMWP	0.01
	VSWP	0.04
	PSJM	0.01
Amicon	XM-100A	0.02
<u>In Freon E-3 Solution</u>		
Millipore	VMWP	0.01
	VSWP	0.01
	PSJM	0.00
Amicon	XM-100A	0.03
Schleicher & Schuel	B-14	0.04
	O-7	0.33

Selected representative photomicrographs of untreated filters as received are shown in Figures 2-27 to 2-31. Several important conclusions were drawn from this work. First, none of the filter substrates used, except the Amicon XM membranes, were considered satisfactory as deposition substrates. The poorest substrates was the Schleicher and Schuell Selection B-14 Filter (Figure 2-27). This filter had a granular structure with a network of pores ranging from 0.1 μm to about 1 μm in diameter. This would mask the system with some particles being caught within the filter and others being camouflaged by the structure of the filter. Furthermore, this filter broke down when the SEM was run at high magnification. At 18000X the filter broke down in less than 1 minute. Even at 4500X, the electron beam had a noticeable effect on the structure within the time needed to focus on the particles ($\sim 1-2$ min). The Millipore VSWP filter behaved in a similar manner, but to a lesser degree. The surface of this filter looked like a flat sheet with many non-contiguous circular holes present. These holes were approximately 0.1 μm in diameter, larger than some of the particles which were expected to be deposited on the filter. The VSWP filters were fairly stable at magnifications up to 4500X, marginally stable at 9000X and unsuitable at 18000X (Figure 2-28). At this magnification, there were significant sample vibrations, believed due to decomposition of the membrane. There was little difference noted in the appearance and behavior of the Pellicon PSED and PSJM filters (Figure 2-29). Both were quite stable under the electron beam. These filters could be exposed to a beam at 18000X for 4 minutes with only a slight change in the surface structure. This is a long enough period of time to allow critical focusing. The major drawback to the Pellicon filters is their surface structure. There is little difference in the appearance of the surface of the Pellicon filters and the Millipore VF filters. Based on the manufacturer's literature, it was presumed that these filters consisted of a thin surface film with an ultrafine structure supported on a normal filter substrate. Based on the (SEM) taken, it appears that this film is either transparent or below the immediate surface of the filter, i.e., somewhere within the bulk of the filter. These results are in agreement with work recently published by Preusser (2-13, 2-14).

Examination of electron micrographs obtained during this study, (Figure 2-30) as well as transmission micrographs examined at Amicon (see below), indicated that Amicon XM membranes have a sponge like open structure with pores ranging from 40Å - 50Å for the XM 50, to about 100Å - 150Å for the XM 300. The XM 100A appears to have pores about 70Å - 80Å in diameter. Scanning electron micrographs at 20,000X of the XM 50 and XM 100A showed very little structural relief. They appeared to be a greyish film with slight undulations and it was barely possible to detect what appeared to be little pinholes, the micropores of the membranes. SEM's of the XM 300 had a similar appearance, but with a much more visible micropore structure.

2.5.5 Final Selection of Filters for Deposition Work

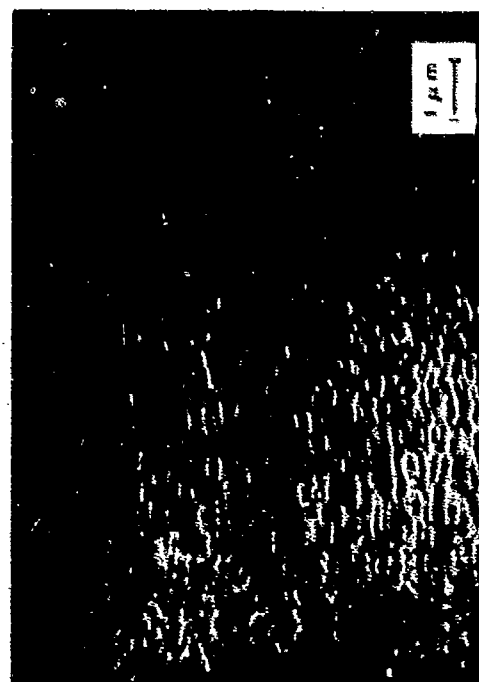
It was earlier mentioned that the Amicon XM membranes failed a number of screening tests in that they exhibited a hydraulic permeability that decreased with time at pressures of 25 psi and above. In view of their superiority for SEM work, these materials were re-evaluated after discussions



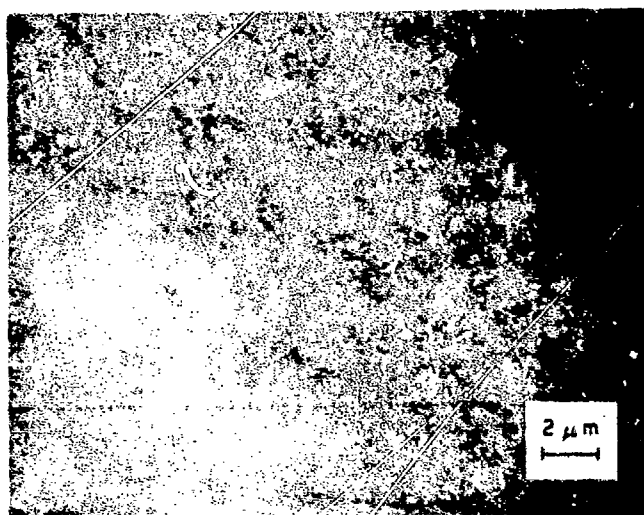
4500X 1:1
FIGURE 2.77 SEM REPRESENTATION OF S85 SELECTED AREA
FILTER, (CENTRAL ZONE PREVIOUSLY EXPOSED FOR 4 MIN
AT 18000X)



9000X 1:1
FIGURE 2.28 SEM REPRESENTATION OF MILLIPORE VS FILTER



4500X 1:1
FIGURE 2.79 SEM REPRESENTATION OF PELLICON PASED
ULTRAFILTER, (CENTRAL ZONE PREVIOUSLY
EXPOSED FOR 4 MIN AT 18000X)



4500X 1:1

Figure 2 30 SEM REPRESENTATION OF AMICON XM-100A
MEMBRANE (CENTER ZONE PREVIOUSLY EXPOSED AT
18000X FOR 4 MIN)

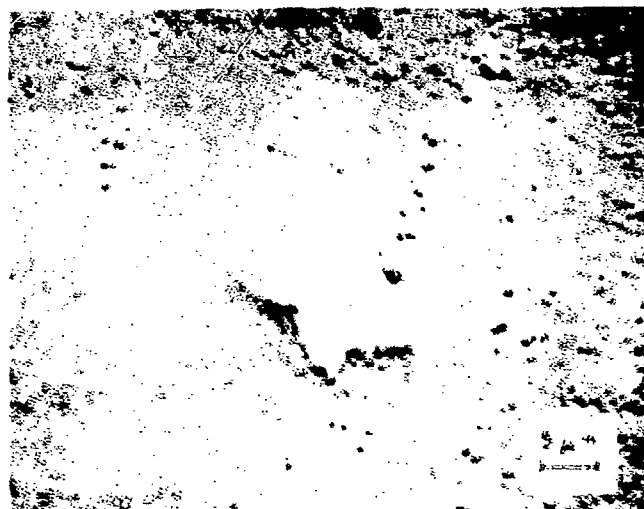


Figure 2 31 SEM REPRESENTATION OF SCRATCHED AMICON
XM-100A MEMBRANE FROM NEW PACKAGE (MEMBRANES
REMOVED BY SLIDING)

63-1283

Reproduced from
Best available copy.

with an Amicon technical representative. The Amicon representative explained that they have found that the XM membranes are best used at what are very low pressures for ultrafiltration work, 10 psi or less (a detail only mentioned in their latest product information catalogue), since the sponge structure of the membrane is fairly fragile. Application of a compressive load, as occurs when one tries to filter a liquid through a membrane supported on a rigid plate, results in compression of the sponge structure and a reduction in the available pore area for flow. Since this collapse is time dependent, the permeability of the membrane will also be time dependent. Bubble pressures for these membranes are low because the sponge like matrix has a low tensile strength and rapidly tears under the applied stress.

The permeability of a 1.04% Krytox 157 solution in Freon E-3 through a 25 mm XM-100A Amicon filter, and retention of Krytox 157 from this solution, were measured at different filtration pressures (4 psi, 8 psi, 14 psi and 20 psi). In all cases the Krytox 157 concentration in the filtrate was not measurably different from the concentration in the feed. However, the permeability varied with applied pressure. At 4 psi, a fairly constant value of $0.11 \text{ ml/cm}^2 \cdot \text{psig} \cdot \text{min}$ was observed for 30 minutes. At 20 psi, the permeability was lower and decreased with time, from an initial value of $8.2 \times 10^{-3} \text{ ml/cm}^2 \cdot \text{psig} \cdot \text{min}$ to $6.7 \times 10^{-4} \text{ ml/cm}^2 \cdot \text{psig} \cdot \text{min}$ at 30 minutes. Operation below 10 psi therefore appeared desirable.

These results confirm the postulated model of the Amicon XM-100A described above. The constant permeability at low pressure and the lack of retention of Krytox 157 indicates that there are no changes in the membrane due to the presence of the fluorinated liquids being used. It was decided to use the Amicon XM-100A membrane in all subsequent work.

The packaging of the Amicon XM-100A proved to be an important detail. Initial lots of 90 mm Amicon XM-100A filters were packaged in Amicon's old-style box. In this box, which had a removable cover, filters were removed by lifting them individually. These filters were usually free of major defects (Figure 2-30). A subsequent lot arrived in a totally different package in which filters were removed by sliding them through a slit in the side of the box. The top microporous surface of these filters invariably had grooves visible to naked eye. As shown in Figure 2-31, these grooves greatly lowered the suitability of the filter for this application. There are visible holes and debris. This lot was returned to the manufacturer in exchange for filters packaged in the old-style containers, and this problem did not present itself again. Since Amicon XM membranes are now being shipped in the new-style box, potential users of the dispersion technique developed in this study should ascertain the absence of grooves and holes in the membrane surface by SEM examination of as-received membranes.

3.0 SURFACTANT PARTITION STUDIES

3.1 Introduction

The object of the surfactant partition studies was to determine the extent and reversibility of adsorption of Krytox 157 on the surface of the candidate powders from Krytox 157/fluorinated liquid solutions. Conditions which favor adsorption are required in order to initially disperse the powders, whereas conditions which favor desorption are required to remove the surfactant from the dispersed, deposited particles. The retention of the finer powders on filter membranes was also investigated as part of these studies.

3.2 Experimental Procedure

3.2.1 Adsorption of Krytox 157 from Solution

The procedure consists of contacting a predetermined weight of a given powder with a fluorinated liquid solution of Krytox 157 of known composition for a sufficiently long period of time to achieve equilibrium. The solid and liquid phases are then separated by ultrafiltration and the residual concentration of Krytox 157 in the liquid is determined. The candidate powders contained particles that were too small to be effectively removed from solution with standard centrifuges. Since the amount and concentration of Krytox 157 initially added, the weight, and thus the surface area, of the powder are known, the concentration measurement also provides the information required to calculate the amount of Krytox 157 adsorbed per unit surface area of the powder. By varying the initial concentration of Krytox 157 and the amount of powder added, it is possible to generate the data required for an adsorption isotherm. In the majority of these tests, 25 mm diameter Millipore ultrafiltration cells (see Figure 3-1) were used as contacting vessels in order to eliminate all in-process transfer operations. The powder and liquid were added to an inverted cell, sealed at the top with a Luer cap. Typically, 0.5 gr to 1.0 gr of powder was added to 15 ml of fluorinated liquid. The fluorinated liquids used were solutions of Krytox 157 in Freon E-3, Freon C-51-12 and FC-43, which contained up to 1.4 weight-percent Krytox 157. A 25 mm filter and the filter support assembly were then inserted into the cell. Millipore VS filters, Pellicon PSJM and Pellicon PSED ultrafilters were used in these tests. After capping the liquid outlet tube with another Luer cap, the sealed ultrafiltration cell was then immersed in a thermostated ultrasonic bath, and subjected to ultrasonic agitation for at least 24 hours. A small Sonolaster 200 ultrasonic bath (shown in Figure 3-2) was used until a larger Branson ATH-58-6 ultrasonic bath, described in the following chapter (see Section 4.3.4) was received. Figure 3-2 shows a cell being placed in the bath.

After 24 hours the cell was removed from the ultrasonic bath, and inverted. The caps then were removed, and the inlet side of the cell was attached to compressed air ($p = 25$ psig) manifold, thus forcing liquid out of the cell into a collection vessel. As shown in Figure 3-3, during filtration the cell was immersed in a constant temperature bath maintained at the same temperature as the ultrasonic bath.

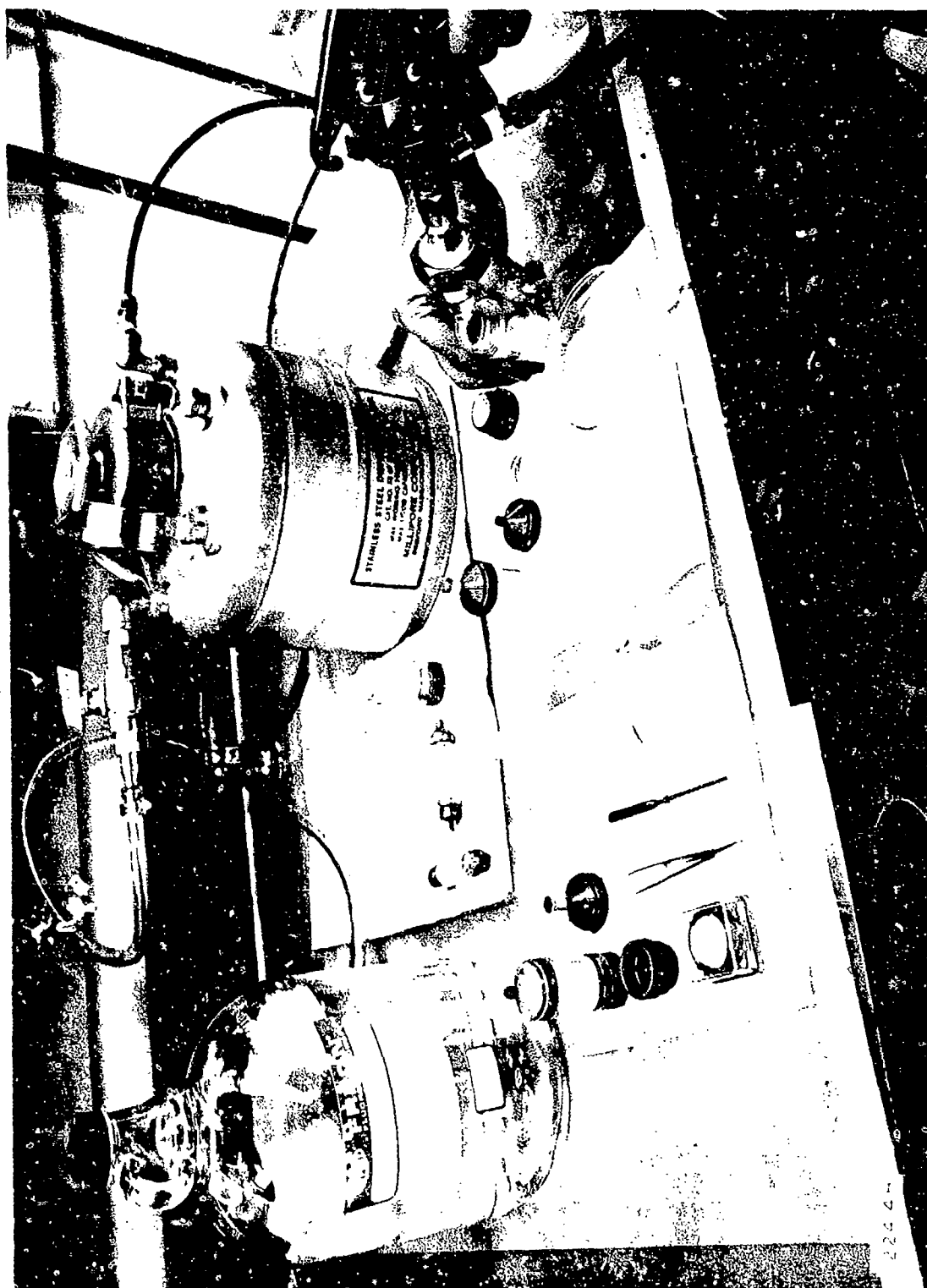


Figure 3-1 25 mm MILLIPORE ULTRAFILTRATION CELL BEING
RINSED IN PREPARATION FOR USE IN ADSORPTION
MEASUREMENTS

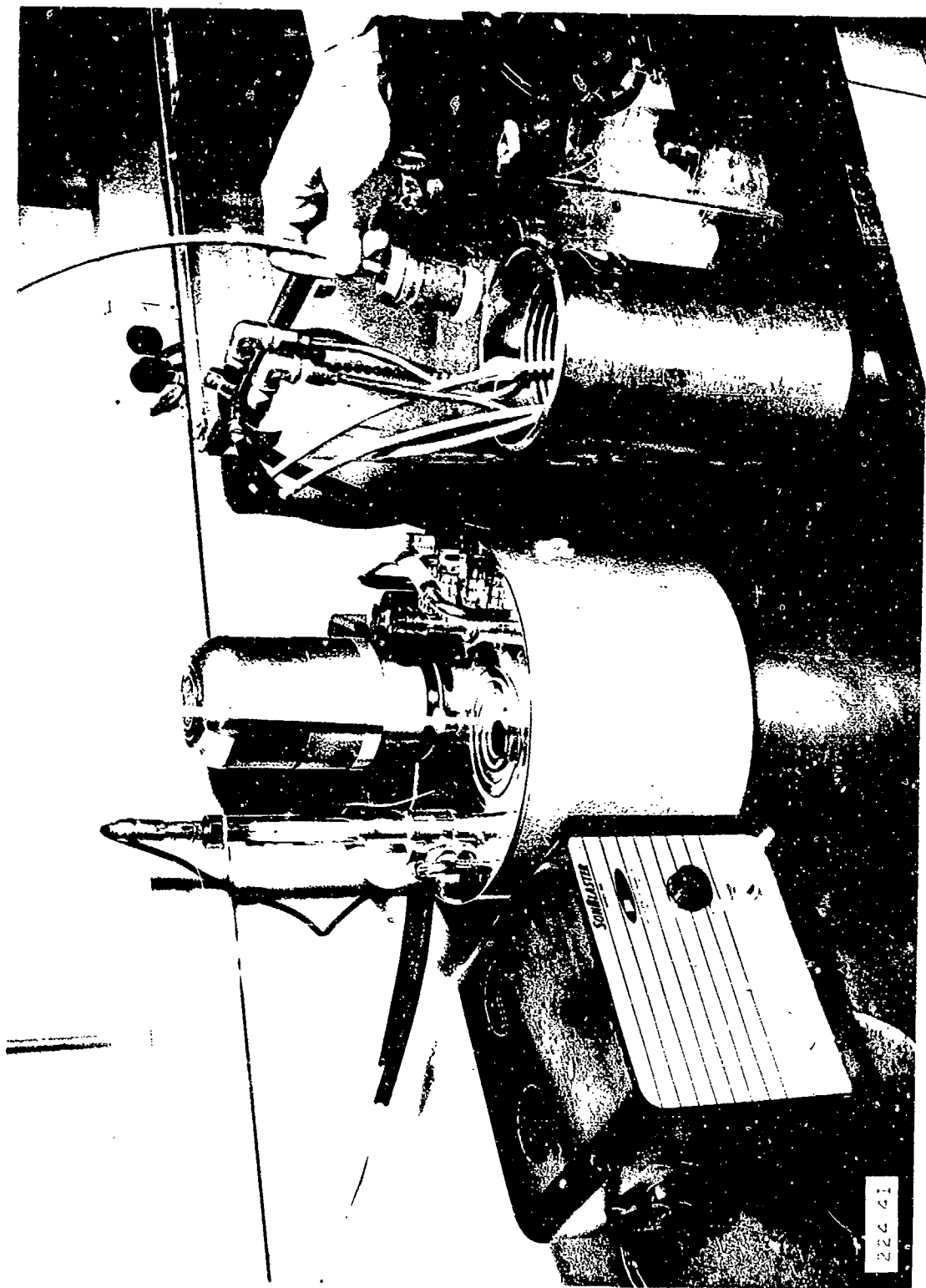


Figure 3-2 ADSORPTION MEASUREMENTS -- SEALED 25 mm.
MILLIPORE FILTRATION CELL BEING INTRODUCED
IN ULTRASONIC BATH (FILTER IS AT TOP OF CELL)

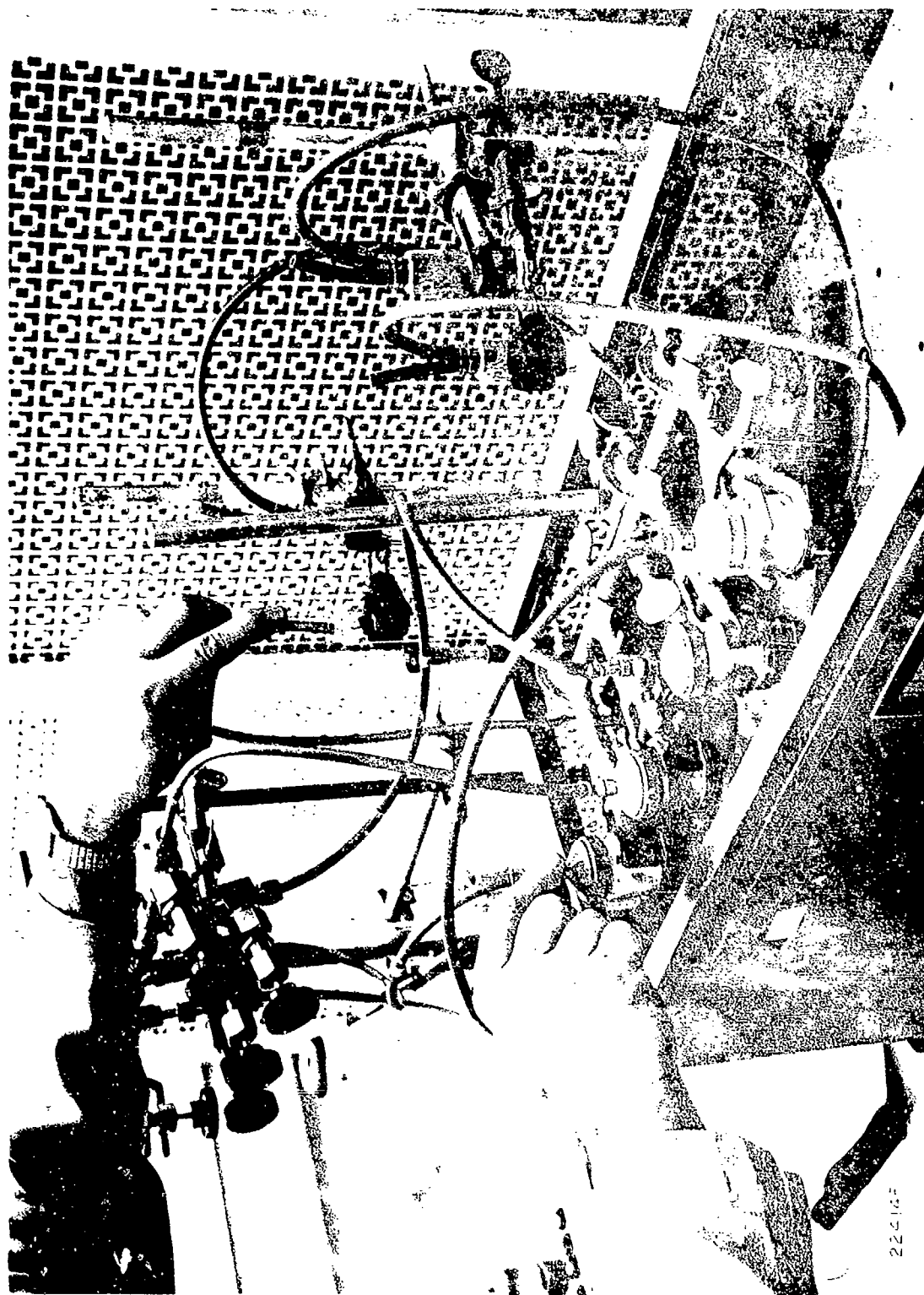


Figure 3-3 ADSORPTION MEASUREMENTS - 25 mm MILLIPORE
ULTRAFILTRATION CELLS IMMERSIED IN CONSTANT
TEMPERATURE BATH FOR FILTRATION OF
FLUORINATED LIQUID. CELL OUTLET
TUBES LEAD TO RECEIVING VESSELS

226147

The residual concentration of Krytox 157 on the filtrate was then measured by infrared analysis, as discussed in the previous chapter.

3.2.2 Adsorption Studies in 90 mm Cell

Additional adsorption studies were carried out in which the particles were separated from the liquid in a Millipore 90 mm Ultrafiltration cell, as shown in Figure 3-4 and Figure 3-5. In these tests, the powder and liquid were initially added to a 50 ml screw cap Oak Centrifuge tube which was then immersed in an ultrasonic bath for 24 hours. The contents of the tube were then transferred to the pre-assembled ultrafiltration cell which was then pressurized to initiate filtration. The filtrate collected was then analyzed for Krytox 157 content.

The principal purpose of using the large cell was to increase surface area available for filtration so as to be able to filter at low pressure (less than 10 psig), required for proper utilization of the Amicon XM-100A membrane. All adsorption data obtained with the 90 mm cell were obtained at ambient temperature, which was approximately 25°C.

3.2.3 Particle Retention

Particle retention characteristics of various filters were examined by preparing dispersions of a given powder in a solution of fluorinated liquid as described above, filtering the suspension through a 90 mm filter in the Millipore 90 mm filtration cell. By analyzing the feed suspension and the filtrate for a characteristic element, a measure of the retention characteristics of a filter was obtained. The retention characteristics of the following filters were examined: Millipore VS, S&S Selectron B14, Pellicon PSJM and PSED, and Amicon XM-100A. The tests were focused on the retention of ENL-1 uranium dioxide dispersed in a 1% Krytox 157-Freon E-3 solution. This was the most severe test of the retention of a filter in that the specific fluorinated solution was the best dispersion medium for UO_2 , which was the finest powder used. Uranium concentration down to 10 ppm was measured by x-ray fluorescence. Limited tests were also carried out with CaF_2 dispersions in the above solution, CaF_2 being the next finest powder examined. In these tests, calcium concentration was measured by atomic adsorption which could detect 0.1 ppm Ca.

3.2.4 Desorption of Krytox 157

Desorption of Krytox 157 was measured in washing experiments. In these tests, a given powder is first dispersed ultrasonically in a given fluorinated liquid that contained a known amount of Krytox 157 HFPO acid. The dispersion is then filtered and the filtrate collected in sequential samples. After removing the dispersing liquid, the deposited powder is washed with pure fluorinated liquid. The resulting filtrate is also collected in sequential samples. The Krytox 157 concentration of the various filtrate samples is measured by I. R. Wash liquid is added and samples collected until the presence of Krytox 157 cannot be detected.

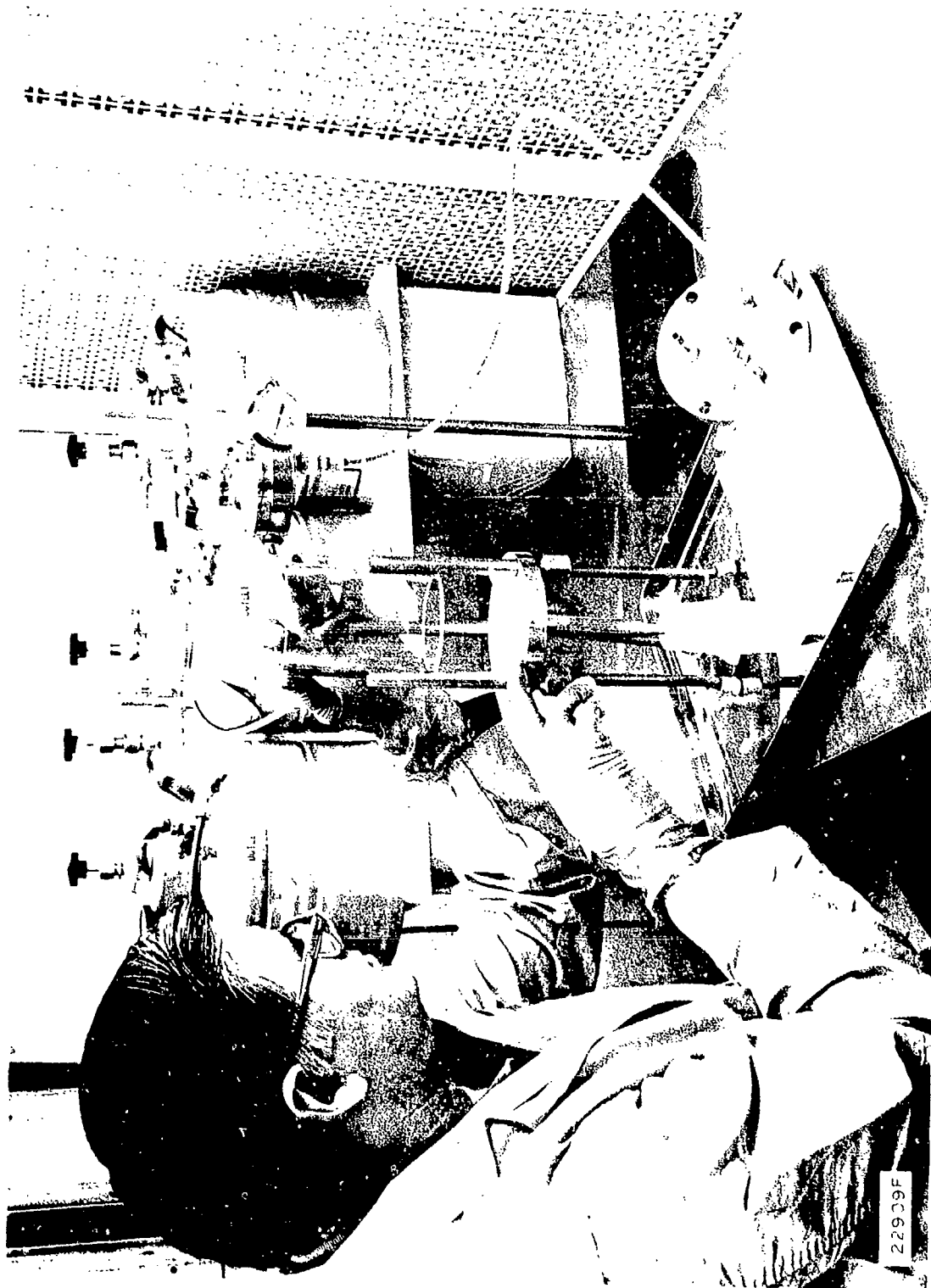
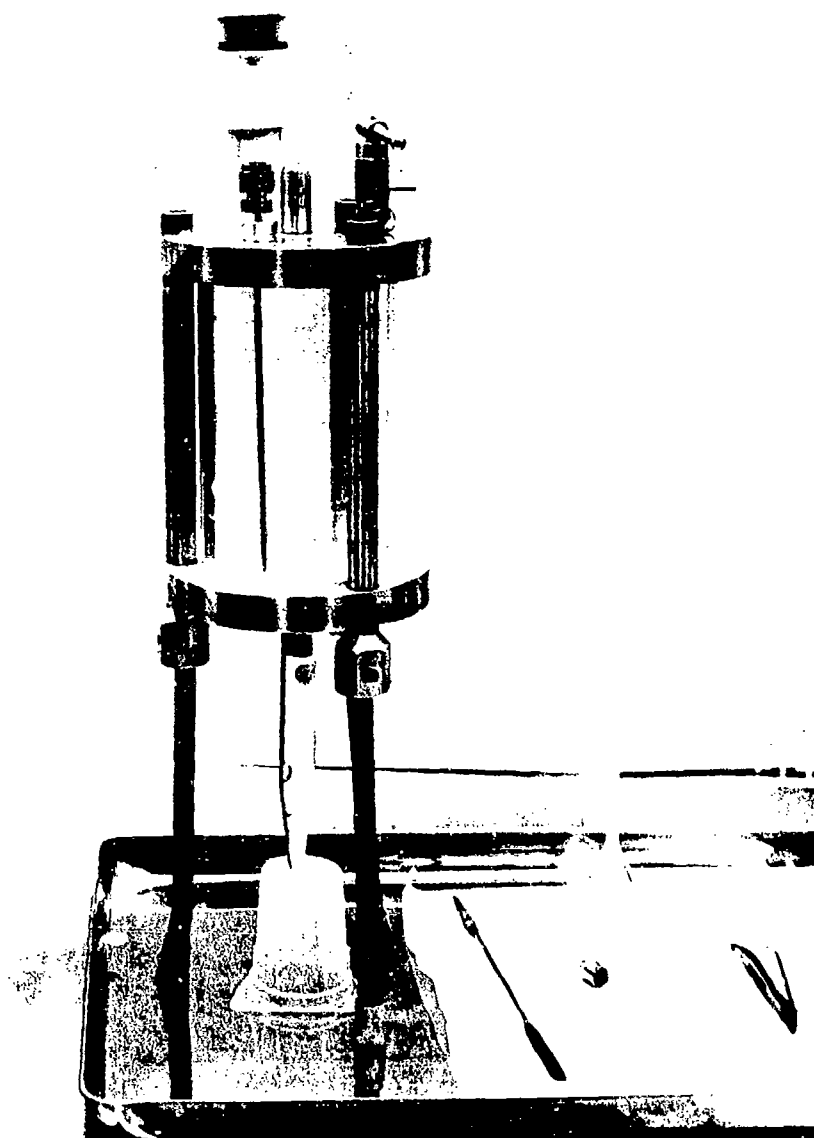


Figure 3-4 ASSEMBLY OF MILLIPORE 90 mm ULTRAFILTRATION
CELL

E-3



22909A

Figure 3-5 MILLIPORE 90 mm ULTRAFILTRATION CELL AFTER
ASSEMBLY FOR A FREON E 3 WASHING RUN

Typically in these washing tests, 1 gram of powder was added to 50 g (25 ml) of a 1% Krytox 157 solution in a tared 50 ml centrifuge tube. The weights of the materials were measured to 0.1 mg on an analytical balance. The feed solutions typically contained about 400 mg of Krytox 157 in either Freon E-3 or FC-43. The suspension was then agitated in an ultrasonic bath for at least 24 hours before filtering and washing.

The tests were all conducted in a 90 mm diameter Millipore ultrafiltration cell. Washing runs were carried out with a variety of filters (Pellicon PSJM, Millipore VS, S&S Selectron B-14, Amicon XM-100A). With filters other than the Amicon XM-100A, poor experimental results were obtained with the finer particle powders, UO_2 and sometimes CaF_2 , due to particle leakage. Test results reported were principally obtained with the Amicon XM-100 filter as the partition membrane. To remove dirt the filters were usually washed before a run with fluorinated liquid free of Krytox 157. Filtrate samples were collected sequentially in graduated 15 ml centrifuge tubes. The volume of a sample varied from 3 ml to 6 ml. For careful determination of the amount of Krytox 157 collected, the filtrate samples were weighed. Because the different fluorinated liquids had different IR adsorption characteristics, the wash liquid and the base of initial dispersion were always the same (e.g. suspensions prepared in a Freon E-3-1% Krytox 157 solutions were always washed with Freon E-3).

The effectiveness of the washing step is determined from a Krytox 157 material balance. For complete washing, the total amount of Krytox 157 collected in the filtrate samples should be equal to the amount of Krytox 157 initially added to the system.

3.3 Experimental Results

3.3.1 Adsorption Measurements

Experiments were carried out in the 25 mm ultrafiltration cells to measure the adsorption of Krytox 157 on each of the four candidate powders (Peerless No. 2 Kaolin, ENL-1 Uranium Dioxide, Sterling MT Carbon Black and Precipitated Calcium Fluoride) from solution in each of three different fluorinated liquids (Freon E-3, FC-43 and Freon C-51-12), at two temperatures: at 25°C and 50°C, for the first two liquids; at 16°C and 22°C for the volatile Freon C-51-12.

Typical results are presented in Figure 3-6. Detailed results are presented in Appendix B. In this figure, the surface concentration of Krytox 157 on Peerless No. 2 Kaolin is plotted against concentration of Krytox 157 in solution, for different fluorinated liquids and at different temperatures. In each instance, the surface coverage of Krytox 157 rapidly rises from zero to a constant value, as the Krytox 157 concentration increases from zero to about 0.2 wt %. A further increase in the liquid concentration of Krytox 157 does not result in a further increase in the surface concentration, indicating saturation.

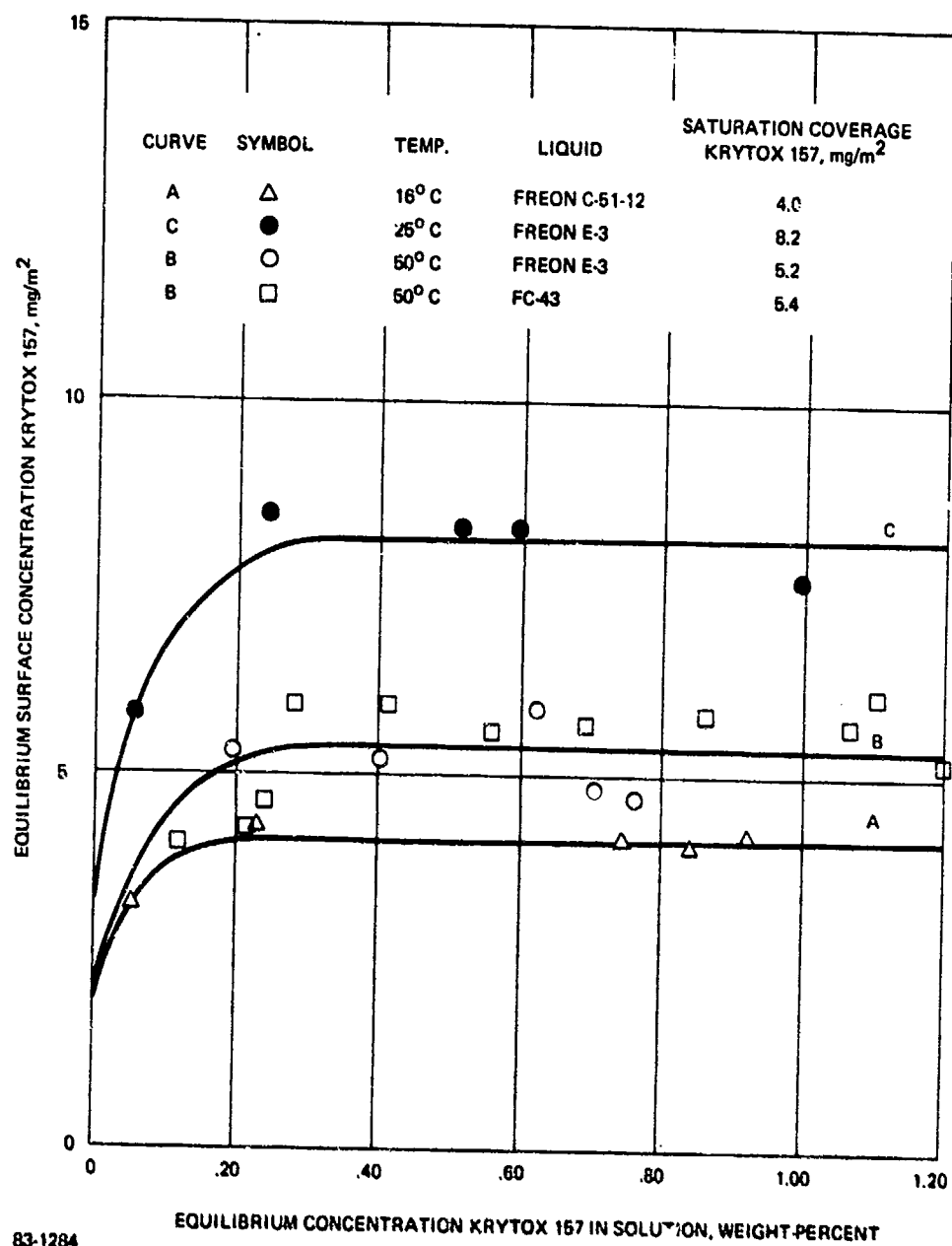


Figure 3-6 ADSORPTION ON KAOLIN OF KRYTOX 157 FROM
FLUORINATED LIQUID SOLUTIONS

The saturation surface coverage is dependent on temperature and on the composition of the carrier liquid. For Freon E-3 solutions the surface coverage at 25°C is higher than at 50°C. Substituting FC-43 for Freon E-3 has no noticeable effect on the adsorption of Krytox 157 on Kaolin. Data for adsorption of Krytox 157 from FC-43 solution at 25°C are omitted from Figure 3-6 for the sake of clarity. There is significantly less adsorption from Freon C-31-12 solutions at 16°C.

Summary results for the various powders obtained in tests are presented in Table 3-1. This table presents the saturation coverage of Krytox 157 absorbed on the different powders examined from various fluorinated solutions at different temperatures. No data are presented for UO_2 powders because leakage of fine particles interfered with the analytical results as further discussed below. Adsorption isotherms similar to the ones presented in Figure 3-6 could be generated.

Adsorption measurements on ENL-1 uranium dioxide powder were sensitive to the filter used to separate the particles from the filtrate subjected to IR analysis. With the Millipore VS, Pellicon PSJM and to a lesser extent Pellicon PSED membrane, the specific surface coverage first increased, reached a maximum, and then decreased with increasing concentration of Krytox 157. This effect was suppressed if the test dispersion was filtered through an Amicon XM-100A ultrafilter. The effect of the membrane on the apparent adsorption of Krytox 157 from Freon E-3 solution on ENL-1 uranium dioxide is shown in Figure 3-7. The apparent decrease in adsorption with increasing concentration is most marked with the Pellicon PSJM membrane, less noticeable with the PSED membrane and suppressed with the Amicon XM-100A ultrafilter.

3.3.2 Particle Retention

It was also observed that the filtrates of runs which showed a suppressed adsorption of Krytox 157 on uranium had a yellow color, characteristic of uranyl compounds. These data correlate with retention data obtained. The retention of ENL-1 dioxide on different filters is presented in Table 3-2. The retention of CaF_2 on Millipore VS and Amicon XM-100A filters is presented in Table 3-3.

3.3.3 Washing Tests

Summary test results of washing experiments on different powders with Freon E-3 and FC-43 are presented in Tables 3-4 and 3-5. From these tests it can be seen that FC-43 is a much more effective wash liquid than Freon E-3. Results for a typical washing test are presented in Figure 3-8 which presents the data for Run W42, the washing of Kaolin with FC-43.

3.4 Discussion of Results

3.4.1 Effects of Partition Filters

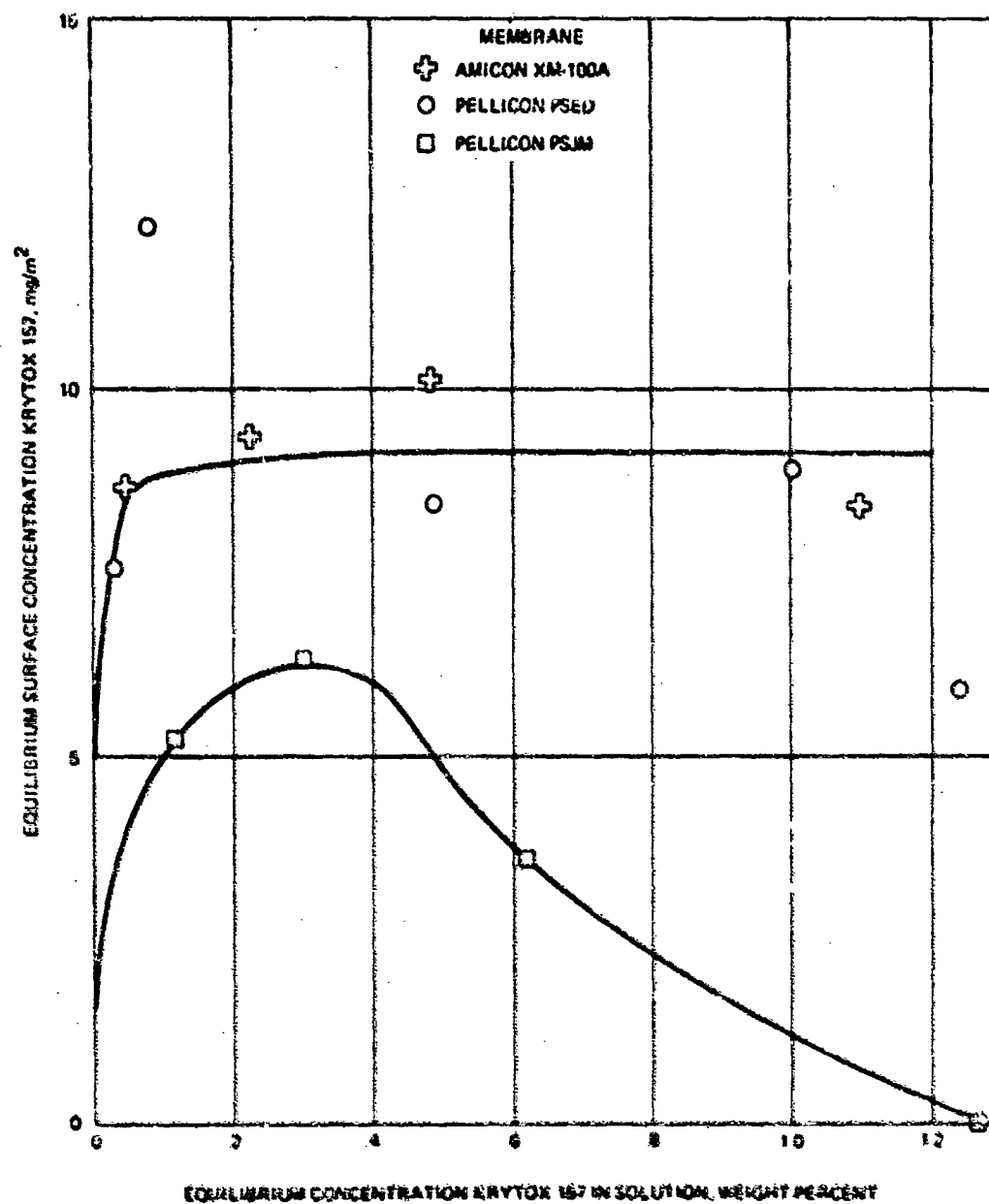
The particle retention characteristics of the filter membranes used to separate the particles from the surrounding liquid can influence the adsorption and washing measurements. Ideally, the filter should completely

TABLE 3-1
APPARENT ADSORPTION OF KRYTOX 157 FROM
FLUORINATED LIQUIDS ON CANDIDATE POWDERS*

Powder		Peerless No. 2 Kaolin	Sterling MT Carbon Black	Precipitated CaF ₂	ENL-1 UO ₂
<u>Liquid</u>	<u>Temp. °C</u>	<u>Saturation Coverage Krytox 157, mg/m²</u>			
FC-43	25	7.8	-	7.9	13.4
FC-43	50	5.4	6.6	9.5	**
Freon E-3	25	8.2	5.6	9.2	**
Freon E-3	50	5.2	3.5	6.5	**
Freon C-51-12	16	4.0	3.2	6.8	**
Freon C-51-12	22	NM	3.2	6.6	**

* Experiments carried out in 25 mm cells.

** No results presented because of interference due to leakage of UO₂ particles past filter membrane.



63-1286

Figure 3-2 EFFECT OF MEMBRANE ON APPARENT ADSORPTION
OF KRYTOX 157 ON ENL-1 URANIUM DIOXIDE FROM
FREON E-3 SOLUTION AT 25°C

TABLE 3-2

RETENTION OF ENL-1 URANIUM DIOXIDE DISPERSIONS ON ULTRAFILTERS

<u>Run No.</u>	<u>Filter</u>	<u>Dispersion Temp °C</u>	<u>C_U in</u>	<u>C_U out ppm</u>	<u>C_U out/C_U in</u>
W-5	B-14	RT	46,000	380	.008
W-1	B-14	50°C	35,600	450	.012
W-10	VSWP	RT	37,000	480	.013
W-12	2 VSWP	RT	36,100	260	.008
W-13	PGED	RT	36,800	280	.008
W-23	XM-100A	RT	35,400	100	.003
W-30	XM-100A	50°C	35,400	60	.002
W-27*	XM-100A	50°C	36,000	220	.006

Dispersion Liquid: 1.12% Krytox 157 in Freon E-3

Dispersion prepared by agitating in ultrasonic bath for 24 hours except for W-27, dispersed with ultrasonic probe.

TABLE 3-3

FILTER RETENTION OF DISPERSED CALCIUM FLUORIDE

<u>Run No.</u>	<u>Filter</u>	<u>Ca in ppm</u>	<u>Ca out ppm</u>	<u>Ca out/Ca in Leakage</u>
W-14	VSWP	21,200	26	.0012
W-24	XM-100A	20,900	14	.0007

Powder dispersed in 1% Krytox 157 - Freon E-3 solution for 24 hours
in ultrasonic bath at 50°C, filtered at room temperature.

TABLE 3-4

RESULTS OF FC-43 WASHING EXPERIMENTS AT AMBIANT WITH AMICON XM-100 FILTER

Run No.	Powder	Weight of Powder, gr W_p	W_{in}	W_{out}	$W_{in} - W_{out}$	$\Delta - W_f^*$	W Adsorbed Initially on Powder	
							mg	mg/m ²
Filter	-	-	460	437	23	0	-	-
W-44	CaF ₂	0.8886	424	379	45	22	56	6.3
W-42	Kaolin	0.9769	426	403	23	-	72	5.9
W-40	UO ₂	0.8275	398	371	27	4	56	11.3
W-35	ST MT	0.9924	430	440	(10)	(33)	91	10.8

* W_f - amount of Krytox 157 retained in blank filter test.

TABLE 3-5

RESULTS OF FREON E-3 WASHING EXPERIMENTS AT AMBIANT

Run No.	Filter	Powder	Weight of Powder, gr W_p	W_{in}	W_{out}	$W_{in} - W_{out}$	$\Delta - W_f^*$	W Adsorbed Initially on Powder	
								mg	mg/m ²
Filter	Amicon XM-100	-	-	464	447	17	0	0	-
W-46	Amicon XM-100	ST MT	1.0225	500	445	55	38	87	10.0
W-15	Millipore VS	ST MT	1.0003	442	386	56	39	63	7.4
W-23	Amicon XM-100	UO ₂	1.0004	482	400	82	65	73	12.2
W-16	Millipore VS	Clay	1.0411	454	342	112	85	96	7.3
W-14A	Millipore VS	CaF ₂	1.0223	455	309	146	129	137	13.2

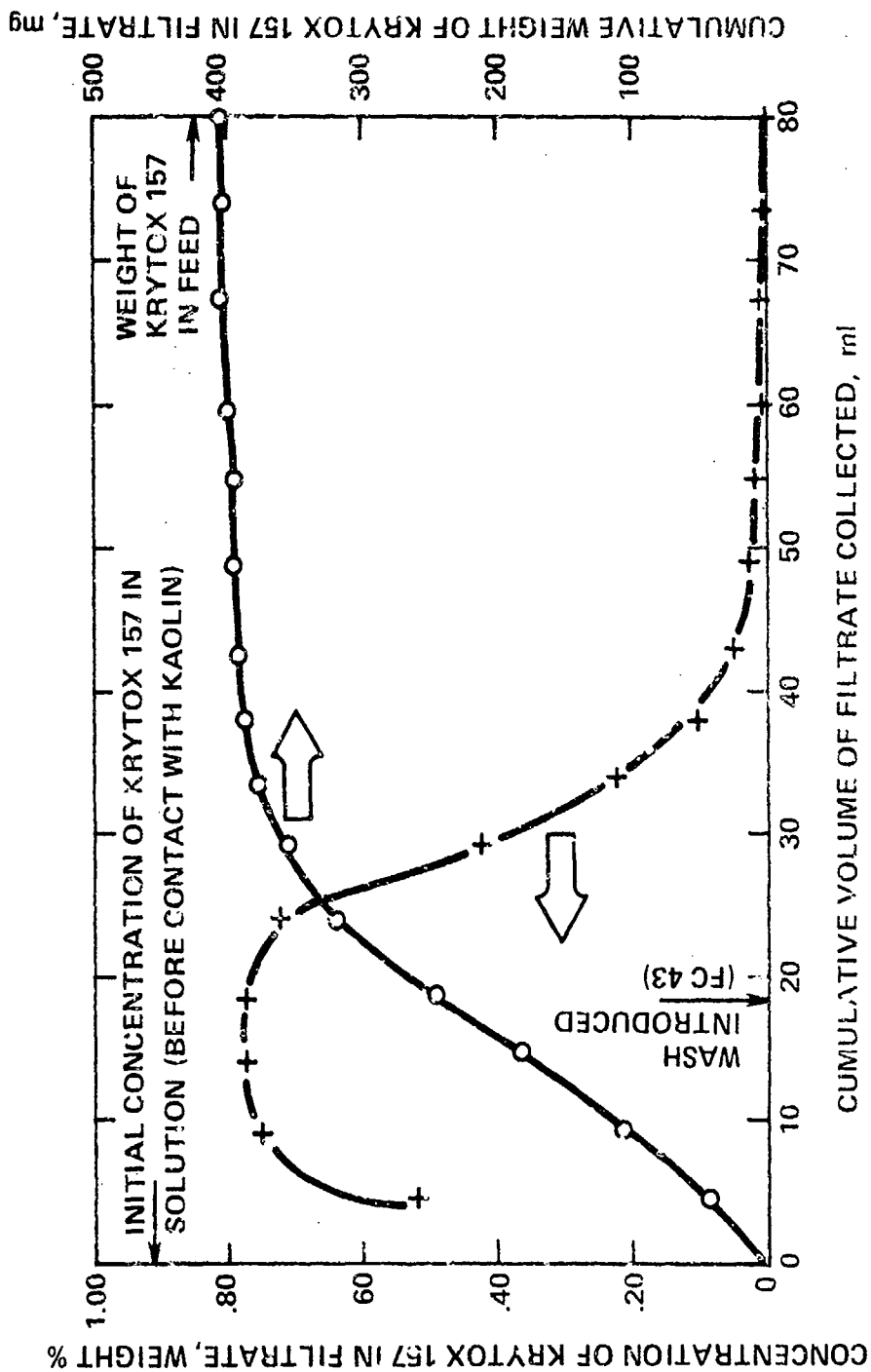


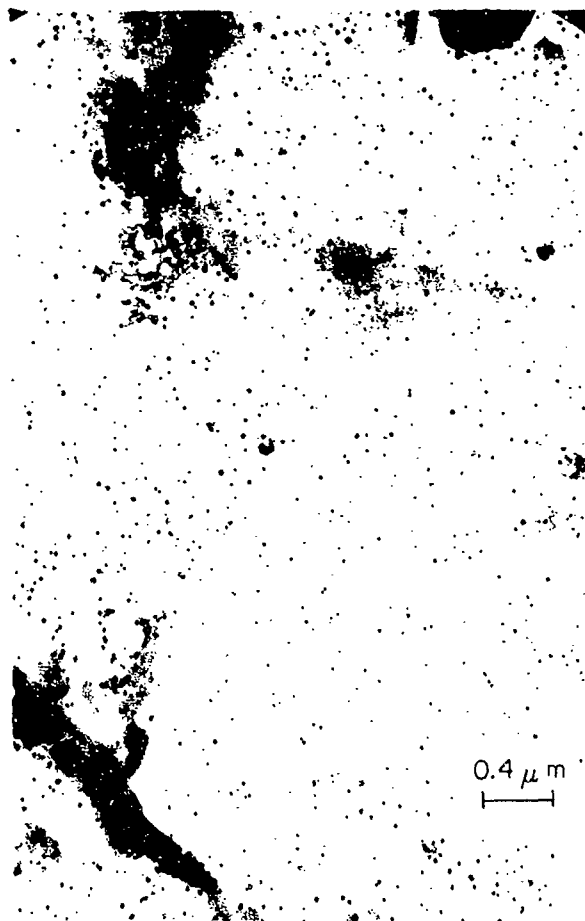
Figure 3-8 FILTRATION AND WASH OF KAOLIN DISPERSION IN
A 1 PERCENT KRYTOX 157/FC-43 SOLUTION THROUGH
FC-43 WET AMICON X/A 100 FILTER
(90 mm DIAMETER)

retain all solid particles. The presence of particles in the filtrate would result in erroneous partition measurements because:

- a. The particles would change the optical characteristics of the filtrate which would influence the IR measurements.
- b. Even if the particles had no optical activity, the apparent surfactant concentration in the filtrate would be higher than the dissolved surfactant concentration because of the surfactant molecules adsorbed on the surface of the particles in suspension.

The reported value of adsorbed surfactant would be too low. Referring to Table 3-2 and 3-3, leakage of UO_2 particles through the partition membranes was a much more significant problem than leakage of calcium fluoride. There was no evidence of leakage of either carbon black or kaolin in the various partition tests and thus these powders were not examined. Calcium fluoride leakage through an XM-100A membrane was 7×10^{-4} . It was approximately twice as high on a Millipore VS filter. Leakage of uranium dioxide particles ranged from 2×10^{-3} to 1.3×10^{-2} depending on the filter and the dispersing conditions. Conditions which favored dispersion of the UO_2 particles (dispersing at 50°C , Freon E-3 as the dispersing liquid, use of the ultrasonic probe, as discussed in more detail in the next chapter), tend to increase particle leakage. The best retention results were obtained with the Amicon XM-100A membrane. Under comparable conditions, UO_2 leakage through an Amicon 100A was then 3×10^{-3} as compared values about 10×10^{-3} for the other membranes tested. As shown in Figure 3-9, the uranium present in the filtrate is due to very fine suspended particles rather than to a dissolved uranyl soap. Some of the uranium in these particles is most probably oxidized to +6 uranium, which would account for the yellowish color of filtrates. Very fine particles less than 100\AA in diameter are clearly shown in this electron micrograph of a UO_2 suspension filtered through a VSWP filter. The particles are smaller than the limit of resolution of the scanning electron microscope used to examine deposited particles (Chapter 5).

Further experiments were carried out to determine if extensive chemical reaction could be occurring, (with negative results - e.g. no reaction). The test consisted in trying to dissolve uranium in a more concentrated solution of Krytox 157 in FC-43 at an elevated temperature. It was through that increasing the temperature and the surfactant concentration and having an excess of surfactant over stoichiometric (two moles of Krytox 157 per mole of UO_2), would favor chemical reaction and accentuate any alteration. In this test, a known amount (0.1145 gr) of ENL-1 uranium dioxide was added to 190 grams of 4.8% weight solution of Krytox 157 in FC-43, in a boiling flask fitted with a reflux condenser. Using a molecular weight of 3500 for Krytox 157, 6.1 moles of Krytox 157 were present per mole of UO_2 . The system was heated to boiling (173°C) and refluxed for six hours. After allowing the flask and its contents to cool overnight to room temperature, the contents were filtered through a tared ultrafiltration cell. To prevent loss of powder the flask was rinsed with fresh FC-43 which was also filtered. Sequential samples of the initial and wash



26000X

Figure 3-9 ELECTRON MICROGRAPH OF SUSPENSION 70
(UO₂ - FC-43 - KRYTOX 157) FILTERED THROUGH
MILLIPORE VSWP FILTER

93-1285

filtrate were collected. The ultrafiltration cell was allowed to dry until it reached a constant weight. The filter cake collected in the filtration was black, like the original uranium oxide. A slight weight gain was observed ($\Delta W = 0.0166$ gr), corresponding to an increase of 15% based on the original powder weight. This weight gain is considered to be adsorbed Krytox 157 and any associated FC-43.

3.4.2 Adsorption Measurements

The results presented indicate that Krytox 157 is adsorbed on the surfaces of all the candidate powders from fluorinated solutions over the range of temperatures examined. The amount of Krytox 157 per unit powder area adsorbed at saturation is approximately 5 mg/m^2 to 10 mg/m^2 . Assuming an average molecular weight of 3500 for Krytox 157, a molecule of this surfactant will cover approximately 18 \AA^2 to 35 \AA^2 . These are not unusual values.

For clay and carbon, adsorption decreases with increasing temperature, the adsorption of CaF_2 appears less sensitive to temperature. Because of experimental difficulties, data obtained with UO_2 at 50°C are questionable so that the effect of temperature could not be determined in these tests. Within the accuracy of the data, it does not appear as though the specific nature of the fluorinated liquid has an effect on the extent of adsorption.

Experimental difficulties which influenced the data included evaporation of fluorinated carrier liquid during test, viz., C-51-12, as well as leakage of fine particles, especially UO_2 through the filters.

Accurate measurements of the adsorption of Krytox 157 on the four different candidate powders were difficult to obtain because of the volatility of Freon C-51-12 at operating temperatures. According to the manufacturer, Freon C-51-12 has a vapor pressure of 5.1 psia at 16°C and 6.5 psia at 22°C . Evaporation of C-51-12 from the filtrates during their collection and during analysis occurred to an observable, however, unknown extent. Simply transferring the solutions from one vessel to another or even into I.R. cells always resulted in some evaporation, even though care was taken to minimize this loss. As a result, the reported adsorption data are believed to be lower than actual data. This is especially true of the data obtained at 22°C . A 10% solvent loss would depress the measured coverage, with the Krytox concentrations and amount of powder used, by 1 mg/m^2 to 3 mg/m^2 . Thus even a small amount of evaporation could greatly influence the measurements.

Leakage of particles was a significant problem with all uranium dioxide measurements, except for the limited data obtained by filtering the samples through Amicon XM-100A membranes. This includes the room temperature data presented in Figure 3-7 as well as the single point adsorption measurements presented in Tables 3-4 and 3-5 obtained as part of washing tests. With this powder, even a small amount of leakage of UO_2 can have a disproportionately large effect on the measured adsorption. Since the particles present in the filtrate have a much higher specific area than those retained on the filter. The particles in the micrograph in Figure 3-9 are smaller than 100 \AA and thus have a specific surface area larger than $60 \text{ m}^2/\text{gr}$, whereas the particles retained by the filter have a specific surface area smaller than $6 \text{ m}^2/\text{gr}$, the specific area of the original feed powder. The presence of 1% of the original powder in the filtrate as particles 100 \AA in diameter or less would decrease the measured surface average by at least 10%, not including their effect on the transmission of light in the cell. The presence of particles would

decrease light transmission to the IR detector, which would indicate a higher Krytox 157 concentration than actually present. This would be given an even lower value for the specific adsorption of Krytox 157 on the powder.

Based on the scattering of the Krytox 157 data, particle leakage was less of a problem with calcium fluoride suspensions, except for samples used to obtain adsorption data at 50°C from Freon E-3 solutions. The adsorption data for this condition are presented in Table B-12 of Appendix B. In this table, results are presented for the filtrates obtained after initial clarification of the liquid through a Pellicon PSED filter, and again after the refiltration through a second PSED filter. Refiltration reduced the measured residual surfactant concentration and increased the surface coverage but did not eliminate the scatter in the data. Samples of the powder dispersed under other conditions showed significantly less scatter especially if they were refiltered.

There was little scatter in the data for the adsorption of Krytox 157 from Freon E-3 solution at 25°C and 50°C on Sterling MT. There was less adsorption at 50°C than at 25°C, which correlates with the dispersion data presented in the following chapter. There is more scatter in the adsorption data from FC-43 solutions. There was apparently little adsorption at 25°C based on the data presented in Table B-8 of Appendix B. These data are believed to be erroneous. These data are in error because there was evidence of carbon leakage through the Millipore filters used to remove the particles from the filtrate. The filtering helped but did not totally eliminate a slight haze. These were also among the initial adsorption measurements made and maximum use was not made of the IR instrument. There could have been an error in analysis as well.

An independent measurement of the adsorption of Krytox 157 on carbon black from FC-43 solution at 25°C was made during one of the washing runs (Run W35). As shown in Table 3-4, 91 mg of Krytox 157 were initially adsorbed on 0.9924 gr of Sterling MT from a Krytox 157 solution. This corresponds to a surface coverage of Krytox 157 of about 10 mg/m².

The easiest adsorption measurements to obtain were those for the adsorption of Krytox 157 on Kaolin, which were described in Section 3.3. There is good agreement between the data obtained for adsorption from FC-43 and Freon E-3 solution at 25°C and 50°C, as obtained in the 25 mm cells. There is even reasonable agreement between these data and the room temperature adsorption measurement present for this powder in Tables 3-4 and 3-5.

3.4.3 Washing Tests

Figure 3-8 presents the results of Run W42, the washing of Kaolin with FC-43. In this figure, the cumulative amount of Krytox 157 collected in the filtrate as well as the concentration of Krytox 157 are presented as a function of the volume of filtrate collected. The first points correspond to the filtration of the dispersion liquid, in which the Krytox 157 in solution is presumably in equilibrium with Krytox 157 adsorbed on the particles. The filtrate concentration should be lower than the feed concentration and constant. As can be seen in

Figure 3-8, this is the case except for the first datum point. The lower Krytox 157 concentration of the filtrate sample is due to the dilution of Krytox 157 containing filtered solution by the Krytox 157 free fluorinated liquid used to rinse the filter, and not to any retention of Krytox 157 by the filter, which was found to be very small (see Section 2.5.3).

The amount of Krytox 157 adsorbed on the Kaolin is obtained from the amount of dispersing liquid and the difference in Krytox 157 concentration between the filtrate at the plateau in Figure 3-8 and the initial Krytox 157 concentration. It is calculated that 72 mg of Krytox 157 are adsorbed by the 0.9769 gr of Kaolin, which has a specific surface area of $12.5 \text{ m}^2/\text{gr}$. This corresponds to a specific adsorption of $5.9 \text{ mg}/\text{m}^2$; which is in general accord with the adsorption results presented in Table 3-1.

The concentration of Krytox 157 drops off rapidly as the first 15 ml of the wash liquid are added. With subsequent additions of wash liquid the Krytox 157 concentration decreases with each sample collected until it is not possible to detect its presence. The first wash samples collected correspond to displacement of bulk liquid held up in the filtration cell by the wash, diluted with some wash liquid. The adsorbed layer around the particles is removed only afterwards. Washing the powder with 65 ml of FC-43 resulted in the recovery of 403 mg of Krytox 157 out of a total of 426 mg. This difference is much smaller than the amount of Krytox 157 adsorbed on the powder. The difference of 23 mg happens to the same value as the difference in the amount of Krytox 157 in the feed and filtrate of the blank run with no powder. Within the accuracy of the experiment, it is concluded that Krytox 157 was removed from the surface of the clay particles.

As shown in Table 3-4, similar results were obtained with the different powders dispersed in 1% FC-43 solutions and then washed with FC-43. In all cases it appears that washing removes the surfactant.

These results are quite different than the results obtained when the powders are first dispersed in a 1% Freon E-3 solution and then washed with Freon E-3. In this instance it appears that the wash does not remove the bulk of the Krytox 157 adsorbed on the particles (see last two columns of Table 3-5). To account for these differences, one can only postulate that there may be differences in solvation of the adsorbed film which results in differences in the stability of the adsorbed layer.

The experimental technique used did not permit the evaluation of the effectiveness of FC-43 washing of dispersions prepared in 1% Krytox/Freon E-3 solutions. The differences in the I.R. adsorption of the two liquids would have interfered with the measurements of Krytox 157 in the filtrates. It is presumed that FC-43 would rapidly displace any residual Freon E-3 when added as a wash.

4.0 POWDER DISPERSION IN FLUORINATED LIQUIDS

4.1 Introduction

The purpose of the dispersion studies was to determine the processing conditions such as time, temperature, and dispersion energy input that result in well dispersed suspensions of the various candidate powders in fluorinated liquids of interest. The process of dispersing a dry powder into a liquid can be visualized as consisting of three stages: wetting of the powder by the liquid, disruption of agglomerates into primary particles, and maintenance of the particles in a dispersed state. These stages overlap in practice since conditions which lead to wetting may also favor dispersion and prevent re-agglomeration.

With the powders presently being studied, it is presumed that maintenance of dispersion will be achieved when there is adsorption of Krytox 157 HFPO acid on the surface of the powder particles and a resulting solvation of the adsorbed surfactant layer. It is also assumed that mechanical energy will be required to disrupt the agglomerates in a reasonable period of time. This energy should be sufficiently high to break down agglomerates held together by relatively weak forces, but not high enough to break the particles themselves. This energy should also be introduced in such a manner as not to result in particle contamination. It should also be amenable to operating on small quantities of material. These constraints limited the means of disruption to ultrasonic techniques which are further discussed below.

4.2 Ultrasonic Dispersion

Prior to carrying out the ultrasonic dispersion phase of this study, a literature survey was carried out in the field of ultrasonic technology. The purpose of this survey was to provide background on the physical basis for the interaction of matter with ultrasonic acoustic energy, the important physical parameters which characterize this interaction, and previous work on ultrasonic dispersion.

Acoustic energy interacts with matter in various ways, and the mechanism of primary importance in any given case depends upon the physical and chemical state of the system and the parameters which characterize the energy(4-1). The latter are the frequency and the power intensity delivered to the material of interest. The frequency is determined by the properties of the transducer. Radiation of acoustic energy follows laws similar to that for light optics. Thus, acoustic energy may be absorbed within a given phase and reflected at phase boundaries. Consequently, the power intensity delivered, for example, to a solid situated within a liquid in an ultrasonic field can be related to the power output of the surrounding transducer(s), only through very complex calculations (and then only for highly idealized geometries) or through direct experimental measurement. The latter can be carried out with a suitably - designed thermocouple probe or a radiation pressure meter. While these techniques are not terribly difficult with proper equipment, the important parameter of delivered power intensity has only rarely been reported in the literature, indicative of the wide chasm between theory and practice in the ultrasonic field.

Several mechanisms are known to operate in ultrasonic fields, including acoustic streaming, cavitation, and production of free radicals. Acoustic streaming results from local instabilities in flow, resulting in circulation patterns over small regions which can generate shear forces at solid surfaces large enough to disrupt weak intermolecular forces. At low frequency (40-500 kHz), large amounts of cavitation energy are present while above about 500 kHz vaporous cavitation may exist but is an insignificant factor until the power intensity level reaches values far in excess of 50 watts/cm². Since most of the ultrasonic irradiating systems commercially available in the past generally delivered a maximum of 10 to 25 watts/cm², it can be safely assumed that in the majority of experiments reported to date, cavitation phenomena had a predominant role only in the lower frequency range. At sufficient power density level and low enough frequency, cavitation bubbles will oscillate and collapse as rarefaction and compression waves pass through liquid media. In addition, hydraulic shock waves are released after collapse of the cavitation bubble. Under adiabatic collapse, instantaneous pressures in the tens of thousands of atmospheres can be obtained⁽⁴⁻²⁾. The magnitude of these effects falls off sharply with increasing frequency.

Studies on the dispersion of solids in the presence of an ultrasonic field are few in number. The earliest studies^(4-3, 4-4) showed qualitatively that colloidal suspensions were formed only when cavitation occurred. More recent work, (e.g., ⁴⁻⁵) however, indicated that optimum dispersion may occur at frequencies in excess of 10³ kHz where there is presumably no cavitation. The effect of non-ionic surfactants on the ultrasonic dispersion of phthalocyanine blue dye in water was the subject of a recent article⁽⁴⁻⁶⁾.

4.3 Experimental Method

4.3.1 Introduction

Given the paucity of applicable quantitative information on the use of ultrasonic energy to disperse powders in a liquid, a series of tests were carried out to determine the effect of sonication on the degree of dispersion of an agglomerated powder suspended in a fluorinated liquid. The goal was to define a set of operating conditions that would result in the complete dispersion of all the candidate powders used in the study, as well as mixtures of these powders, with minimum particle breakage. The ability to disperse uranium dioxide, carbon black, clay, and calcium fluoride would indicate that the technique developed is not sensitive as to the nature of the powder to be dispersed and would most likely be effective with many other powders and dusts.

In order to carry out a meaningful particle dispersion study, the effect of numerous parameters had to be investigated. These included the nature of the powder, powder concentration in the dispersing liquid, the composition of the dispersing liquid, temperature, the characteristics of the ultrasonic energy source and its coupling to the material to be dispersed, sonication time, etc. This study therefore involved a large number of tests which had to be simple and rapid.

The effect of sonolation on the degree of dispersion of a powder processed under a given set of condition was determined as a function time. The influence of different processing parameters were determined by comparing their effect on the kinetics of the dispersion process. The following procedure was used. A constant volume (25 ml) of fluorinated liquid was added to a 50 ml screwcap centrifuge tube that contained a small, known amount of powder. The tube and its contents were then subjected to ultrasonic agitation. Periodically a small sample (typically 20 μ l to 50 μ l) of the contents of the tube were withdrawn for analysis of the size of the suspended particles.

4.3.2 Turbidity Measurements

The purpose of the tests was to obtain a measure of the size distribution of the agglomerates in a given suspension. In order to minimize any alteration of the agglomerate size distribution, the possible methods of analysis were limited to those that could measure the size distribution of suspended objects in a fluorinated liquid directly. The technique had to be rapid, avoid conditions which could alter the size distribution of the suspended material, and be able to operate with a small sample volume. Nephelometry and centrifugal sedimentation met these requirements.

Nephelometry was used as an index of changes in the agglomerate size distribution for the majority of the dispersion tests reported in this section. For a limited number of dispersion tests, the size distribution of the suspended material was also measured by sedimentation in a Joyce Loebel Disc Centrifuge in order to obtain a precise quantitative evaluation of the actual size distribution of the suspended material.

Nephelometry is the measurement of light scattered by particulate matter in suspension. It is commonly used for the detection and quantitation of unwanted particles in liquids, and, with careful application, it may yield valuable information about the state of dispersion of a suspension. The detection and measurement of particulate matter by nephelometry is orders of magnitude more sensitive than measurements by loss of transmitted light. It is a sensitive technique at particulate concentrations of 1 ppm or less.

The use of nephelometry or turbidity in this study is based on the fact that the scattered light is a function of the size distribution and concentration of the particles in suspension. For any given suspension of particulate solid, A, in liquid B, at constant particle concentration, the turbidity measurement with a given optical detection system should be only a function of the size distribution of the particles in suspension. If an agglomerated system is dispersed, the turbidity of the system will change until the dispersion reaches steady state. Thus, the changes in the state of dispersion of a suspension can be readily indexed by turbidity techniques. This technique is especially useful if one wishes to monitor changes in a given suspension with time by removing small aliquots in that the determination may be carried out with small samples. To measure turbidity, samples were withdrawn from the suspension with Eppendorf volumetric pipettes, and diluted with 5.0 ml of the fluorinated liquid used to disperse the powder. The turbidity of the diluted sample was measured in a Model 110 Fluorometer/Nephelometer made by G.K. Turner Associates of Palo Alto, California, in a one square centimeter cuvette. This instrument is described in more detail in Appendix D. These measurements were carried out at constant powder concentrations of 3.2×10^{-3} mg/ml for

suspensions of calcium fluoride and 10^{-3} mg./ml for suspensions of all other powders. The concentrations were chosen to yield turbidity readings on one of the less sensitive scales of the instrument (scale 1 or scale 3) in order to minimize spurious instrument effects. When the concentration of powder in the dispersion sample was varied, the concentration of powder in the final turbidity sample was kept constant by adjusting the volume (typically 20 μ l or 50 μ l) of sample withdrawn from the suspension undergoing sonolation.

The major drawback to this method of analysis is that turbidity measurements are only a relative index of the state of dispersion of a given powder. The relation between turbidity readings and the state of subdivision of the suspension is extremely complex. In order to correlate the size distribution of the suspension, it is necessary to take into account such factors as the refractive indices of the suspended material and of the continuous liquid phase, the wave length of incident light, the ratio of the size of the particles to the wave length of light, and the shape of the particles. Nephelometry does not provide quantitative information on the size distribution of a suspended system because of the complex and non-linear relationship between turbidity and particle size distribution. Such information was obtained in a limited number of tests by sedimentation analysis. This alternate technique suffers from the fact that the experimental procedure is more difficult and it takes longer to obtain the required information. Particle size distribution measurement by sedimentation for particles smaller than 1 μ m requires the use of specialized equipment which was not available for any extensive period of time. In the present studies, where one wished to compare different suspensions of a given particulate material in similar liquids in order to determine the dispersion conditions required to obtain good electron micrographs, the advantages of the turbidity measurements greatly outweighed their disadvantages.

4.3.3 Centrifugal Sedimentation

Sedimentation is another common method of measuring the size distribution of a dispersed system. In a given system the rate of settling of a suspended object is a function of its diameter. While there are several possible methods of sizing particles larger than a few micrometers in diameter, it is extremely difficult to measure the size distribution of smaller particles. The Joyce-Loebl Disc Centrifuge shown in Figure 3-1 is an instrument specifically designed to carry out these measurements. Through the courtesy of Mr. John Swift of the Joyce Loebl Company, access was obtained to a demonstration model for two days. During this time it was possible to characterize a limited number of dispersions by sedimentation as well as by turbidity.

The instrument basically consists of a hollow lucite disk that is rotated at a pre-selected speed (1000-8000 RPM). The disk is partially filled to a radius R_1 with a clear liquid called the spin liquid and a small amount of buffer liquid. The suspension to be analyzed is then introduced into the disk. The particles in the suspension are more dense than the liquids, and the particles will migrate radially outwards. The equation of motion for particles in the sedimentation fluid is Stokes' Law modified for centrifugal action. In a

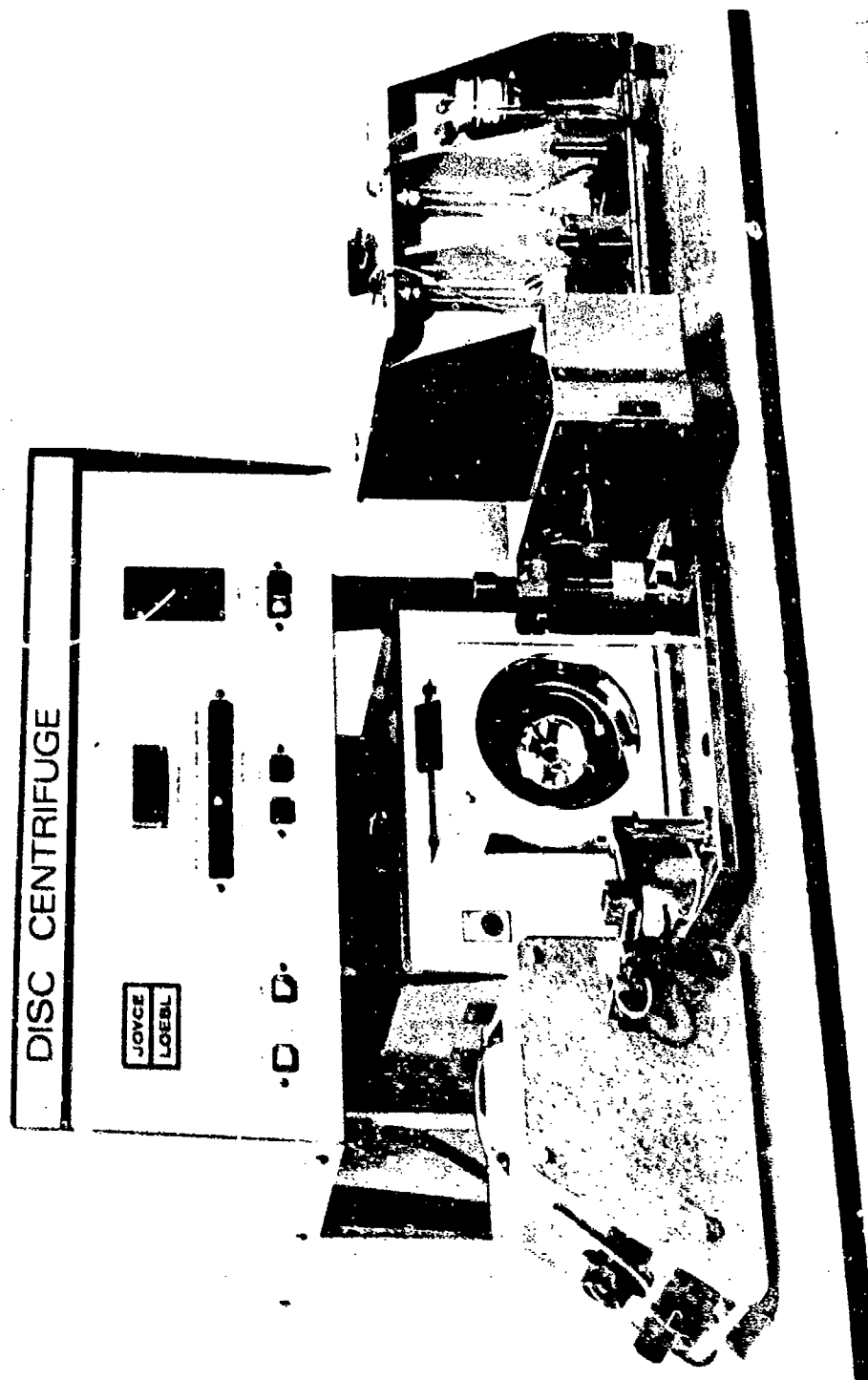


Figure 4 1 JOYCE LOEBEL MK 'II' DISC CENTRIFUGE

period of time, t , a particle of equivalent hydrodynamic diameter, d , will have migrated from a position defined by the radius R_1 to a new position defined by a larger radius, R_2 , according to the following equation:

$$t = \frac{18\eta}{W^2 d^2 (\rho_p - \rho_L)} \ln \frac{R_2}{R_1} \quad (4-1)$$

where

η = viscosity of the spin fluid

W = rotational speed of the disk

ρ_p = density of the particles

ρ_L = density of the spin fluid

This simple relationship is applicable only if the system is hydrodynamically stable, i. e., no "streaming occurs". To eliminate streaming, a small quantity of a buffer liquid is introduced into the annulus of the spin liquid and partially mixed with the spin liquid to establish a narrow density gradient zone instead of the sharp interface which normally exists when the sample suspension is introduced.

The Joyce Loeb Disc Centrifuge is based on the principle that all the parameters in the Stokes equation are either known or precisely measured. The rotation of the disc is exactly controlled by a solid state feedback system to ensure both absolute and rotational disc stability. The sample is introduced into the disc after it has reached constant speed so that transient acceleration effects are eliminated. The settling of the particles within the transparent disc can be observed for instabilities with an automatically synchronized stroboscope. The radius R_2 is defined by the position of a sampling probe or of a photocell detector further discussed below. The radius R_1 is determined by the amount of spin fluid used. The time, t , is the time elapsed after the injection of the sample. The other terms in the above equation, other than d , are properties of the spin fluid (η , ρ_L) and of the particles (ρ_p) which can be measured independently.

With the Joyce Loeb Disc Centrifuge, two types of particle size distribution measurements can be obtained:

- a. Curves of absolute cumulative weight against particle diameter which are obtained by removing and collecting an inner annulus of liquid of external radius R_2 after a preset time with a special sampling probe. The collected fraction will contain all particles smaller than preselected particle diameter D_2 . Quantitative analysis of the cut fraction gives one point of a size distribution curve. An absolute cumulative weight curve is obtained by repeating

the measurement at different preselected sampling times and rotational speed chosen to span the range of particle sizes of interest.

- b. Size distribution curves of comparative frequency against particle size diameter obtained rapidly by the use of a photosedimentometer attachment. Photosedimentometer size distributions are produced by measuring the attenuation of a beam of light passed through the disc cavity at the same radius as the probe final collection point. The attenuated signal is displayed on a chart recorder which produces a curve of light intensity versus time, which is representative of the size distribution of the sample under test. The photosedimentation curves do not give the true particle size distribution curve because the intensity of the transmitted light signal transmitted through the suspension depends on the size as well as the concentration of the particles, i. e., the parameter one wishes to measure affects the measurement. However, the optical trace has the great advantage of providing instantaneous information on the presence of particles of a certain size range in a given suspension. These optical traces can also be used to compare variations in particle distribution in a family of closely related samples. In order to obtain absolute particle size distribution information in this manner, the photosedimentometer traces have to be calibrated against results obtained by using the absolute size distribution technique described above.

4.3.4 Ultrasonic Dispersion Equipment

Two ultrasonic generators were used in the study: an ultrasonic cleaning bath and a high intensity ultrasonic probe.

A first series of tests were carried out in the ultrasonic cleaning system shown in Figure 4-2. The system, made by Branson Instruments Company (Stamford, Connecticut 06904), consisted of an E-Module power supply (Model EMA 30) and a stainless steel transducerized cleaning tank (Model ATH 58-3). The power supply had an output of 450 watts of sonic power at an operating frequency of 40 kHz. The internal dimensions of the tank were 9" x 9" x 7". Ultrasonic power in the tank was distributed over a 40 square inch transducer through approximately 1 gallon of contained working liquid (water). This power level (~ 2 watts/cm²) is sufficient to cause cavitation when the tank is filled with water, as was verified by visual and oral observation. To carry out the dispersion tests in this tank, as shown in Figure 4-2, a test tube rack surrounded by a coil of plastic tubing was placed in the ultrasonic tank. With the rack in place, it was possible to position eight 50 ml centrifuge tubes in the ultrasonic tank. Temperature of the tank contents could be controlled between 35°C and 80°C, either by circulating an ethylene glycol/water mixture from a constant temperature bath through the plastic coil (this was needed to remove heat), or by using 250 watt heaters built into the ultrasonic tank.

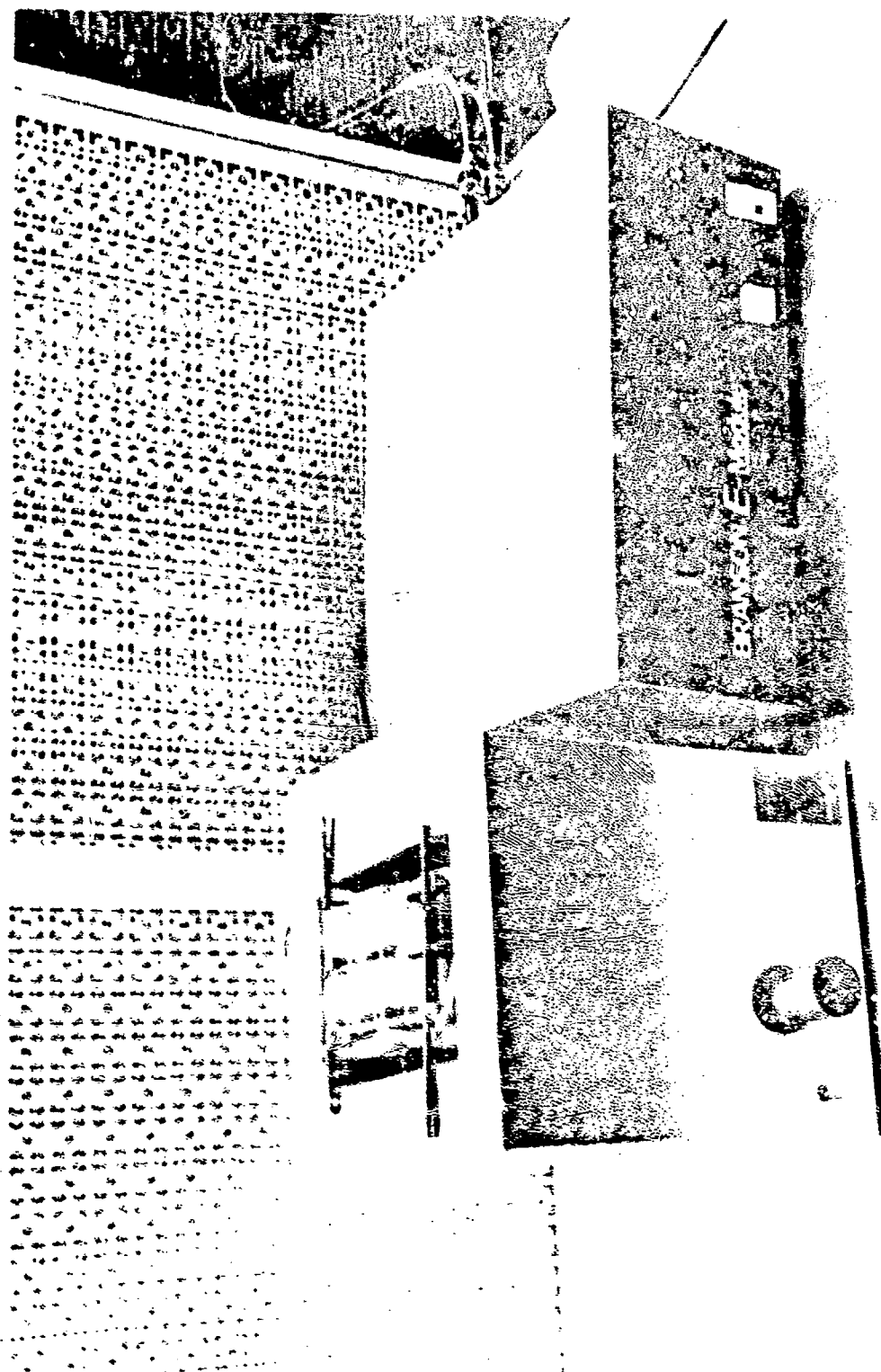


Figure 47 BRANSON L-11 THASONIC BATH AND POWER SUPPLY

In subsequent dispersion tests, the ultrasonic transducer was a Branson Sonifier Model S-75 Ultrasonic Probe (now distributed by Heat Systems Ultrasonics, Inc., Plainview, New York). This instrument has an electrostrictive ceramic transducer operating at 20 kHz. In these tests, the probe was placed inside a 50 ml centrifuge tube that contained the suspension to be dispersed as shown in Figure 4-3. In this figure, the test tube is shown above a jacketted copper cup used to remove heat from the agitated sample. In operation, cooling water was passed through the coils surrounding the cup, the test tube containing the sample was placed in the cup (which also contained some water to promote heat transfer), and the ultrasonic probe was positioned. The sonifier was then turned on and tuned so as to obtain maximum output of sonic energy as indicated by an ammeter on the instrument which was steady to within 10%. Although the sonifier has less than 100 watts output, according to the manufacturer it is possible to obtain a power density of over 80 watts/cm² at the tip of the probe ($A_{pr} = 1.2 \text{ cm}^2$). The average power density throughout the sample tube is less because of the larger cross-sectional area (8 cm²) in the tube and because the acoustic energy is damped in the liquid as the distance from the probe tip increased. It is estimated that the average power density in the tube is of the order of 10 watts/cm² or less. In comparison, the power density of the Branson bath previously used was approximately 2 watts/cm². Since there is circulation and agitation in the tube during sonolation, as shown in Figure 4-4, the dispersion is exposed to much higher power densities with this arrangement than in the bath.

4.4 Experimental Results

The results of various dispersion experiments are presented in this section. These tests include a preliminary series of experiments in which the source of dispersive energy was the ultrasonic bath. Further tests were carried out with the ultrasonic probe as the transducer in which the rate of dispersion was measured by turbidity and by sedimentation.

The appearance of typical suspensions, before (Top Row) and after ultrasonic dispersion (Bottom Row) is shown in Figure 4-5. The carrier liquids are shown for reference.

4.4.1 Dispersion Tests in the Ultrasonic Bath

A first series of tests were carried out in the ultrasonic bath in order to screen the effects of major process parameters, such as composition of the dispersing liquid, temperature, and powder concentration on the rate of dispersion (as measured by turbidity), of various candidate powders and their mixtures. The bath was well suited for these tests since as many as eight samples could be dispersed simultaneously.

The effects of the following parameters were investigated, using turbidity as an index of the degree of dispersion.

a. Position of test samples in ultrasonic bath
(preliminary study).

b. Type of Powder:

Uranium Dioxide, ENL-1
Precipitated Calcium Fluoride
Sterling MT Carbon Black

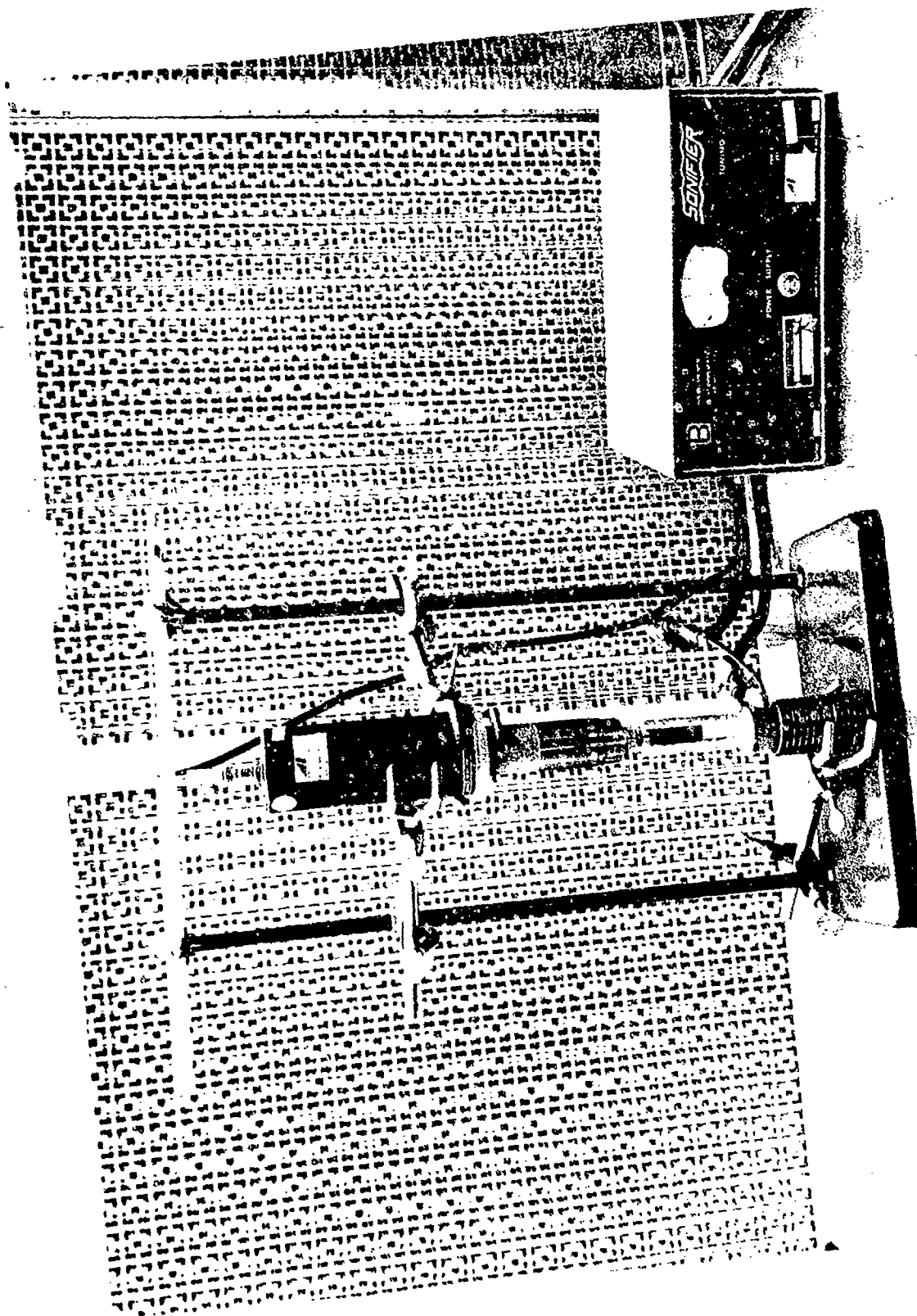


Figure 4-3 SONIFIER PROBE AND POWER SUPPLY PLACED IN
50 ml CENTRIFUGE TUBE

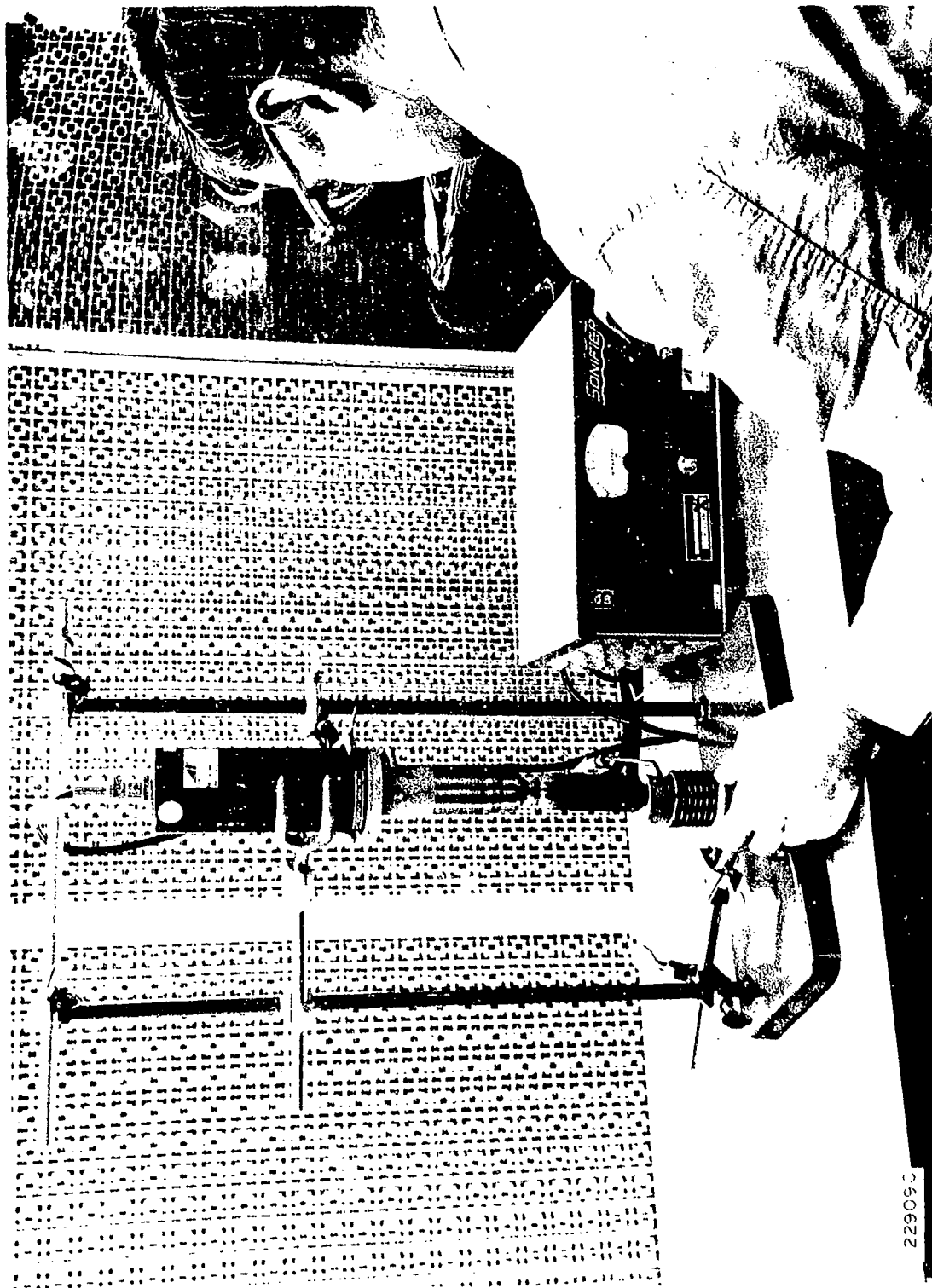


Figure 4-4 STERLING MT CARBON BLACK BEING DISPERSED IN
FLUORINATED LIQUID BY SONIFIER PROBE (SAMPLE
TAKEN OUT OF COOLING JACKET FOR PHOTOGRAPH)

22909C

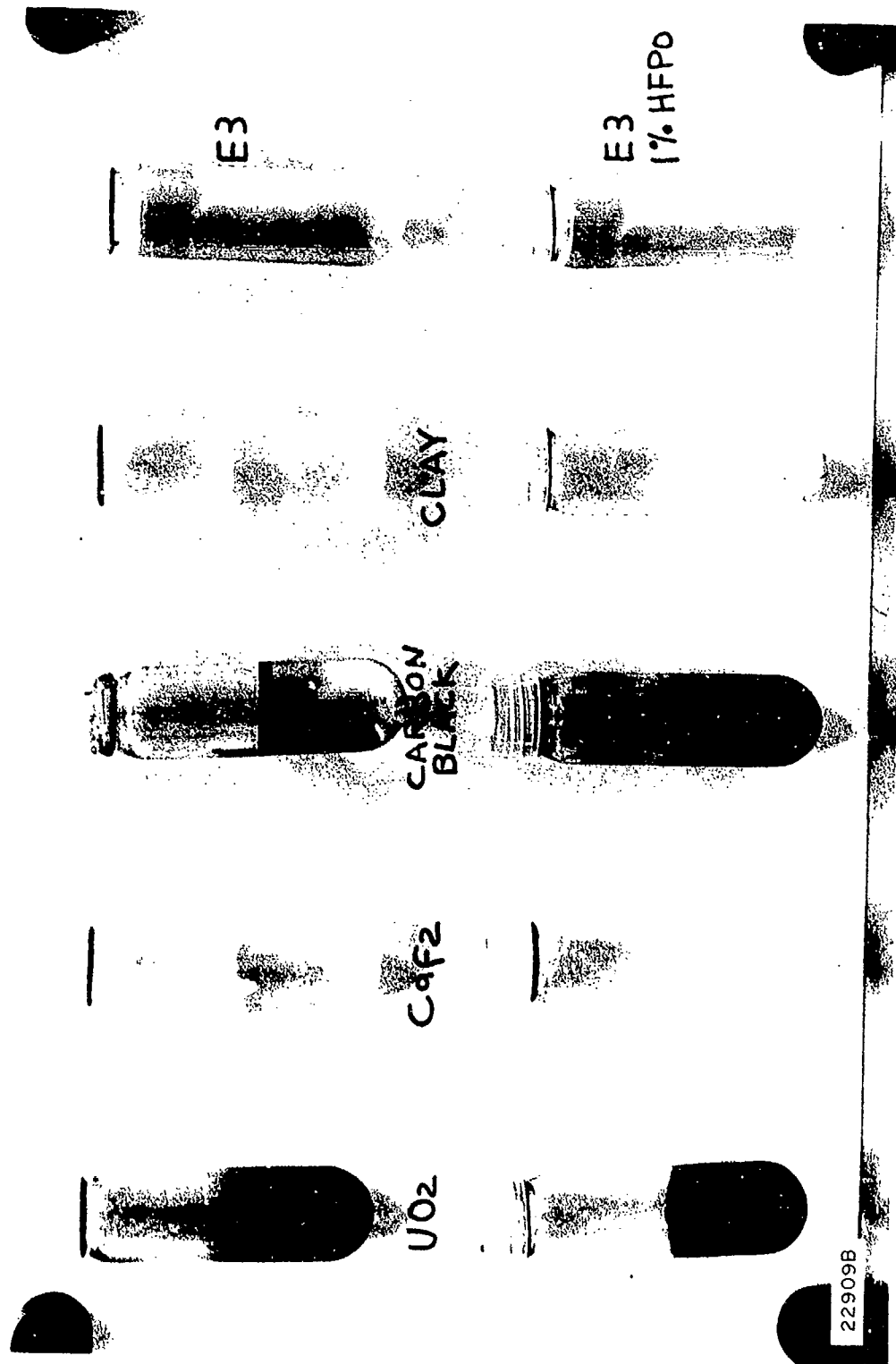


Figure 4-5 SAMPLES OF CANDIDATE POWDERS IN FLUORINATED LIQUIDS BEFORE AND AFTER DISPERSION

Peerless No. 2 Kaolin
Binary Mixtures of Above
Ternary Mixtures of Above
Quaternary Mixture of Above

- c. Powder Concentration: 2 levels at less than 10 mg/ml.
- d. Carrier Liquid: Freon E-3 and FC-43.
- e. Krytox 157 Concentration: 0 to 1.0%.
- f. Temperature: 35°C, 50°C, and 80°C.
- g. Re-dispersion

Test results are summarized in Tables 4-1 to 4-6. The best dispersion results for the various candidate powders were obtained with a 1% solution of Krytox 157 in Freon E-3 at 50°C. These data are also presented in Figures 4-6 to 4-9.

4.4.2 Dispersion Tests with the Ultrasonic Probe

Subsequent series of dispersion tests were run in which the transducer was the S-75 ultrasonic probe. This probe was operated at maximum power output (dial setting of 8). The output current oscillated between 7 amps and 9 amps during a run because of temporal variations in acoustical coupling. The temperature was controlled to a nominal 50°C. It was observed that the temperature in the upper strata of the dispersion near the tip of the probe was 10-15°C higher than near the bottom of the test tube where heat was removed.

Based on the results obtained in the ultrasonic bath, a 1% Krytox 157 solution in Freon E-3 was used as the dispersing liquid in all tests with the ultrasonic probe. Test results with the different candidate powders are presented in Figures 4-6 to 4-9. These include a number of repetitive measurements. As before, the degree of dispersion was measured by turbidity.

The test procedure used with the probe was slightly different than the one used in the bath. First, power to the probe was shut off and the probe lifted out of the sample tube everytime a turbidity sample was removed. Secondly, the probe was never operated unattended. Samples subjected to long dispersion times were irradiated incrementally with intermediate quiescent periods such as nights and week-ends. It was found that the sample undergoing dispersion did not change significantly in turbidity during these periods of rest, e.g., re-agglomeration did not take place. Once a sample was dispersed in the presence of surfactant, it remained dispersed.

4.4.3 Characterization of Dispersions by Sedimentation

A limited number of dispersions were prepared in which the degree of dispersion was examined by sedimentation on the Joyce Loeb Centrifuge and by turbidity. Tests were limited to determining the effects of ultrasonic agitation time, using the sonolator probe, on the size distribution of uranium dioxide and calcium fluoride suspensions in a 1% Krytox 157 -

TABLE 4-1

ULTRASONIC BATH DISPERSION OF URANIUM DIOXIDE POWDER (ENL-1) IN
FLUORINATED LIQUIDS AS INDEXED BY TURBIDITY MEASUREMENTS

Run No.	Temperature °C	Carrier Liquid	Krytox 157 Conc, Wt %	Powder Conc, mg/ml	Length of Run, Min	Turbidity (1) of Diluted Sample (2) for Various Dispersion Times				End of Run
						1 Min	10 Min	100 Min	1000 Min	
D-9	35	Freon E-3	1.0	0.8	3088	8	17	31	48	5
D1-D8 (Mean)	35	Freon E-3	1.0	2.5	> 3000	10	21	34	52	> 64
D-11	35	Freon E-3	0.1	2.5	5745	13	26	38	51	68
D-12	35	Freon E-3		2.5	1210	18	18	14	8	85
D-28	50	Freon E-3	1.0	2.5	1613	14	26	40	53	62
D-32	80	Freon E-3	1.0	2.5	290	18	26	44		48
D-68	80	Freon E-3	1.0	2.5	370	18	26	44		52
D-64	80	Freon E-3	0.1	2.5	385	10	22	41		54
D-60	80	Freon E-3		2.5	415	9	18	35		44
D-36	35	FC-43	1.0	2.5	1399	9	18	27	37	38
D-56	35	FC-43		2.5	312	6	6	6	6	4
D-40	50	FC-43	1.0	2.5	1152	10	21	32	42	42

4-4

1) Scale: 3X

2) Dispersion diluted to 1.0 mg/liter for turbidity measurement.

TABLE 4-2

ULTRASONIC BATH DISPERSION OF PRECIPITATED CALCIUM FLUORIDE IN
FLUORINATED LIQUIDS AS INDEXED BY TURBIDITY MEASUREMENTS

Run No.	Temperature °C	Carrier Liquid	Krytox 157 Conc, Wt %	Powder Conc, mg/ml	Length of Run, Min	Turbidity (1) of Diluted Sample (2) for Various Dispersion Times				End of Run
						1 Min	10 Min	100 Min	1000 Min	
D-24	35	Freon E-3	1.0	3.3	1152	9	16	20	22	21
D-23	35	Freon E-3	1.0	8.0	1102	12	17	22	28	25
D-26	35	Freon E-3	0.1	8.0	4226	12	17	22	28	28
D-27	35	Freon E-3		8.0	942	8	10	12	14	15
D-31	50	Freon E-3	1.0	8.0	1560	12	17	22	28	26
D-35	80	Freon E-3	1.0	8.0	222	12	17	22		23
D-67	80	Freon E-3	0.1	8.0	296	14	17	22		25
D-63	80	Freon E-3		8.0	328	10	10	13		17
D-39	35	FC-43	1.0	8.0	1394	11	13	16	18	17
D-59	35	FC-43		8.0	197	4	6	8		10
D-43	50	FC-43	1.0	8.0	175	9	12	16		15

1) Scale: 3X

2) Dispersion diluted to 3.2 mg/liter for turbidity measurements.

TABLE 4-3

ULTRASONIC DISPERSION OF SHERLING MT CARBON BLACK IN
FLUORINATED LIQUIDS AS INDEXED BY TURBIDITY MEASUREMENTS

Run No.	Temperature °C	Carrier Liquid	Krytox 157 Conc, Wt %	Powder Conc, mg/ml	Length of Run, Min	Turbidity ⁽¹⁾ of Diluted Sample ⁽²⁾ for Various Dispersion Times					End of Run
						1 Min	10 Min	100 Min	1000 Min		
D-19	35	Freon E-3	1.0	0.8	398	30	40	49		55	
D-18	35	Freon E-3	1.0	2.5	356	35	44	53		57	
D-20	35	Freon E-3	0.5	2.5	220	28	36	46		49	
D-21	35	Freon E-3	0.1	2.5	5425	22	29	36	43	48	
D-22	35	Freon E-3		2.5	947	14	21	36		42	
D-30	50	Freon E-3	1.0	2.5	1395	34	44	53	58	60	
D-34	80	Freon E-3	1.0	2.5	209	28	36	45		36	
D-66	80	Freon E-3	0.1	2.5	345	34	40	47		50	
D-62	80	Freon E-3		2.5	315	24	33	42		47	
D-36	35	FC-43	1.0	2.5	1223	30	36	42	48	48	
E-57	35	FC-43		2.5	363	18	22	26		28	
D-42	50	FC-43	1.0	2.5	1365	34	40	47	54	53	

1) Scale: 1X

2) Dispersion diluted to 1.0 mg/liter for turbidity measurements

TABLE 4-4

ULTRASONIC BATH DISPERSION OF NO. 2 KAOLIN IN
FLUORINATED LIQUIDS AS INDEXED BY TURBIDITY MEASUREMENTS

Run No.	Temperature °C	Carrier Liquid	Krytox 157 Conc, wt %	Powder Conc, mg/ml	Length of Run, Min	Turbidity (1) of Diluted Sample for Various Dispersion Times				End of Run
						1 Min	10 Min	100 Min	1000 Min	
D-14	35	Freon E-3	1.0	0.8	1514	17	20	22	25	27
E-13	35	Freon E-3	1.0	2.5	1470	20	22	25	29	31
D-16	35	Freon E-3	0.1	2.5	140	22	22	25		25
D-17	35	Freon E-3		2.5	1305	22	20	19	18	18
D-29	50	Freon E-3	1.0	2.5	1128	31	32	34	35	35
D-33	80	Freon E-3	1.0	2.5	250	24	27	30		32
D-65	80	Freon E-3	0.1	2.5	282	24	27	30		33
D-61	80	Freon E-3		2.5	397	24	27	30		34
D-37	35	FC-43	1.0	2.5	1257	18	19	20	21	20
D-58	35	FC-43		2.5	227	10	10	10		11
D-41	50	FC-43	1.0	2.5	216	21	22	22		21

1) Scale: 3X

2) Dispersion diluted to 1 mg/liter for turbidity measurements.

TABLE 4-5

ULTRASONIC BATH DISPERSION OF BINARY POWDER MIXTURES IN
FLUORINATED LIQUIDS AS INDEXED BY TURBIDITY MEASUREMENTS

Run No.	Powders	Powder Conc, mg/ml	Length of Run, Min	Turbidity ⁽¹⁾ of Diluted Sample ⁽²⁾ for Various Dispersion Times			End of Run
				1 Min	10 Min	100 Min	
BD-46	UO ₂	1.0	411	57	68	80	84
	Sterling MT	1.0					
BD-44	UO ₂	1.0	367	18	29	40	47
	CaF ₂	4.0					
BD-52	UO ₂	1.0	316	12	18	31	39
	CaF ₂	1.0					
BD-45	UO ₂	1.0	339	20	30	45	48
	Kaolin	1.0					
BD-47	Kaolin	1.0	391	23	26	30	32
	CaF ₂	4.0					
BD-53	Kaolin	1.0	397	19	20	22	21
	CaF ₂	1.0					
BD-48	Kaolin	1.0	405	62	75	92	105
	Sterling MT	1.0					

Temperature: 50°C

Liquid: Freon E-3

Krytox 157 Conc: 1.0 wt-percent

1) Scale: $\times 10^3$

2) Dispersion diluted 250 fold for turbidity measurement.

TABLE 4-6

ULTRASONIC BATH DISPERSION OF MULTI-POWDER MIXTURES IN
FLUORINATED LIQUIDS AS INDEXED BY TURBIDITY MEASUREMENTS

Run No.	Powders	Powder Conc, mg/ml	Length of Run, Min	Turbidity ⁽¹⁾ of Diluted Sample ⁽²⁾ for Various Dispersion Times			End of Run
				1 Min	10 Min	100 Min	
TD-49	UO ₂	0.68	385	45	52	63	65
	Sterling MT	0.68					
	Kaolin	0.68					
TD-50	Kaolin	0.68	378	48	54	60	
	CaF ₂	0.68					
	Sterling MT	0.68					
QD-51	UO ₂	0.68	290	46	57	69	77
	Kaolin	0.68					
	Sterling MT	0.68					
	CaF ₂	2.0					

Temperature: 50°C

Liquid: Freon E-3

Krytox 157 Conc: 1.0 wt-percent

1) Scale: XX

2) Dispersion diluted 250 fold for turbidity measurement.

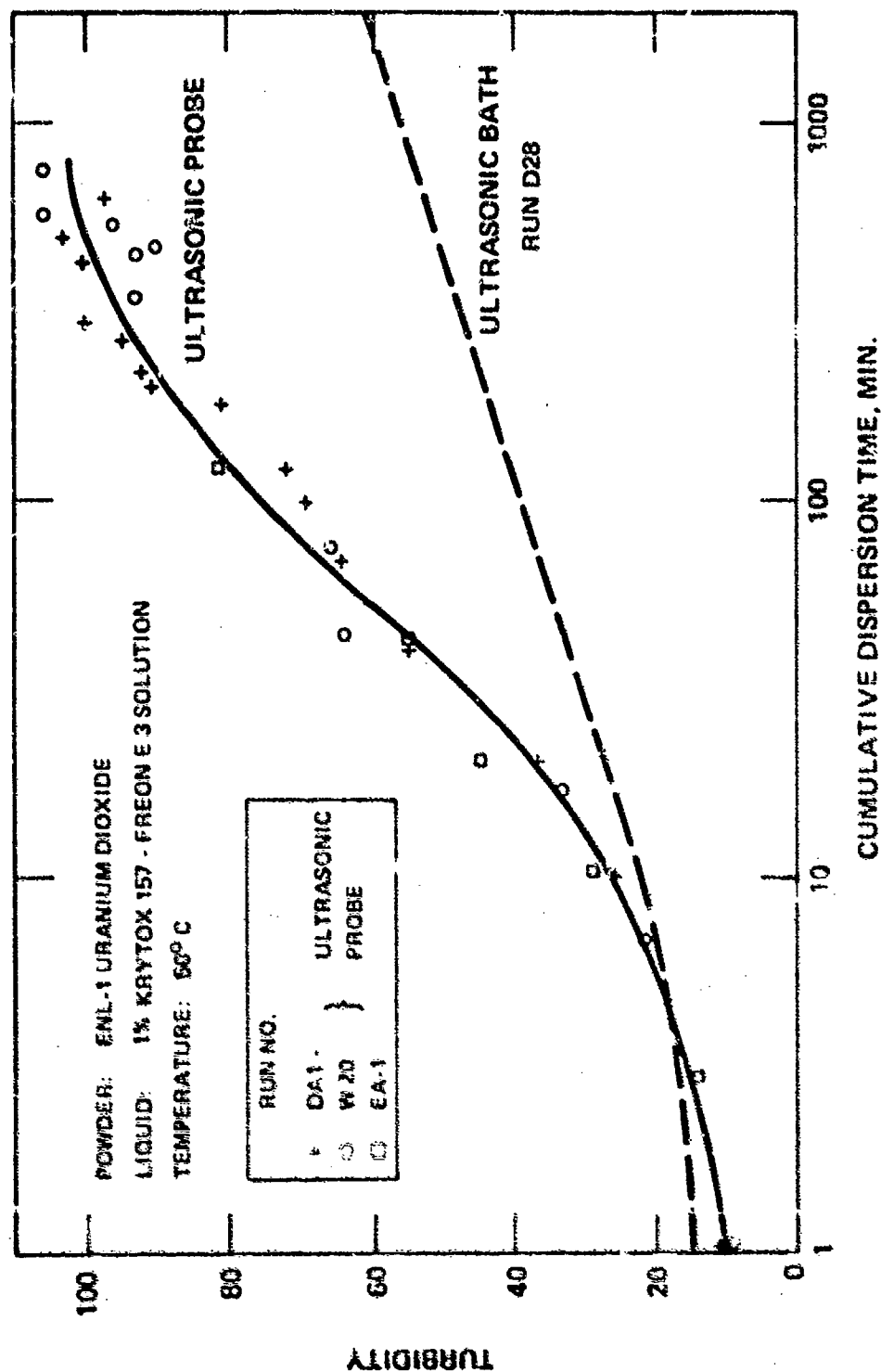


Figure 4-3 ULTRASONIC DISPERSION OF ENL-1 URANIUM DIOXIDE IN FLUORINATED LIQUID

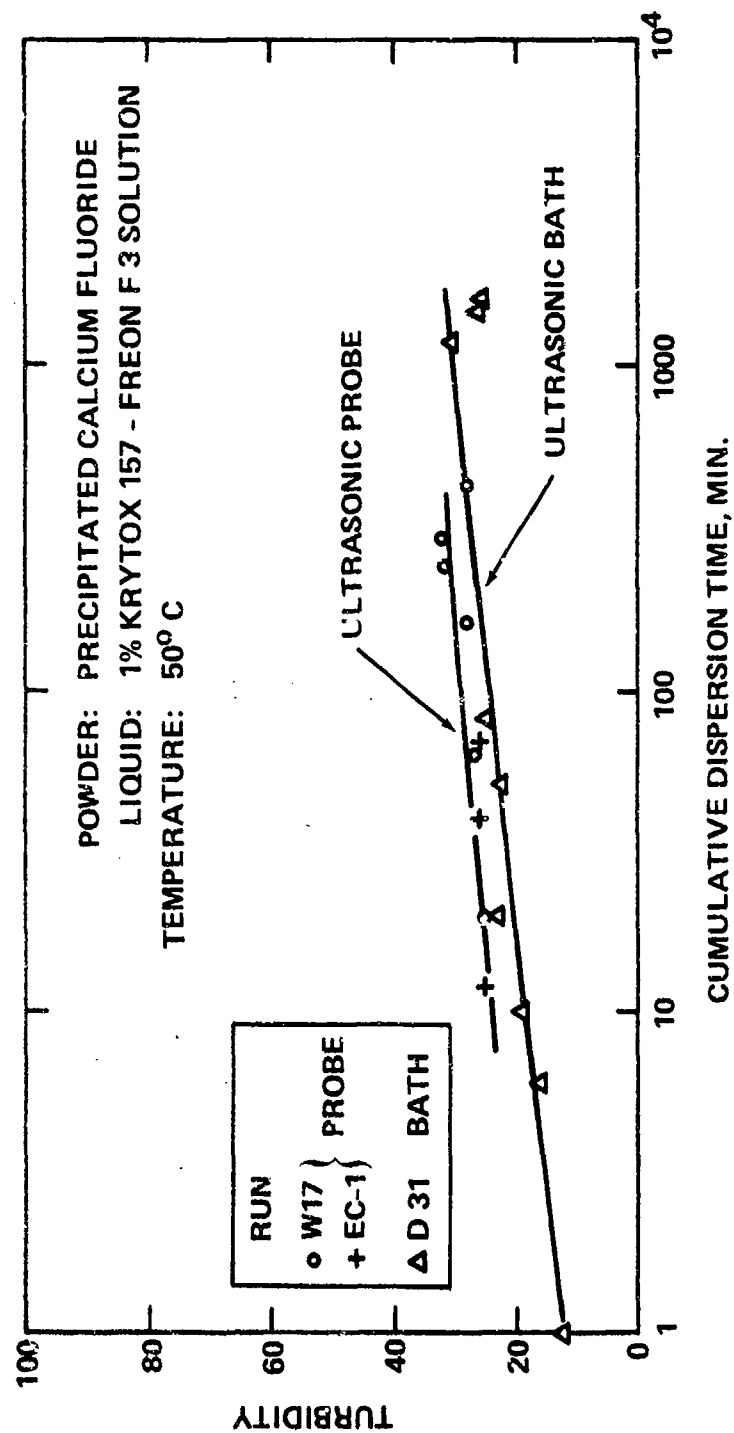


Figure 4-7 ULTRASONIC DISPERSION OF CaF_2 IN FLUORINATED LIQUID

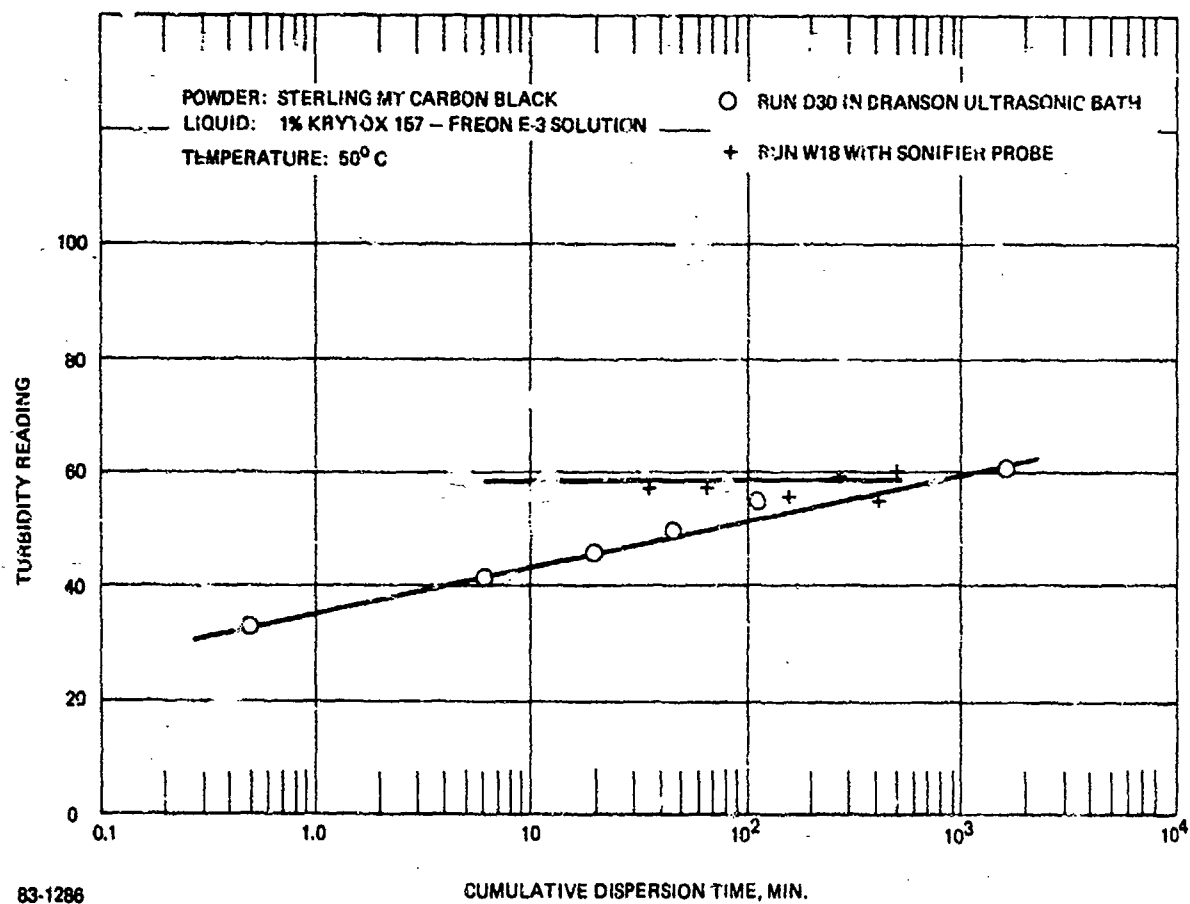
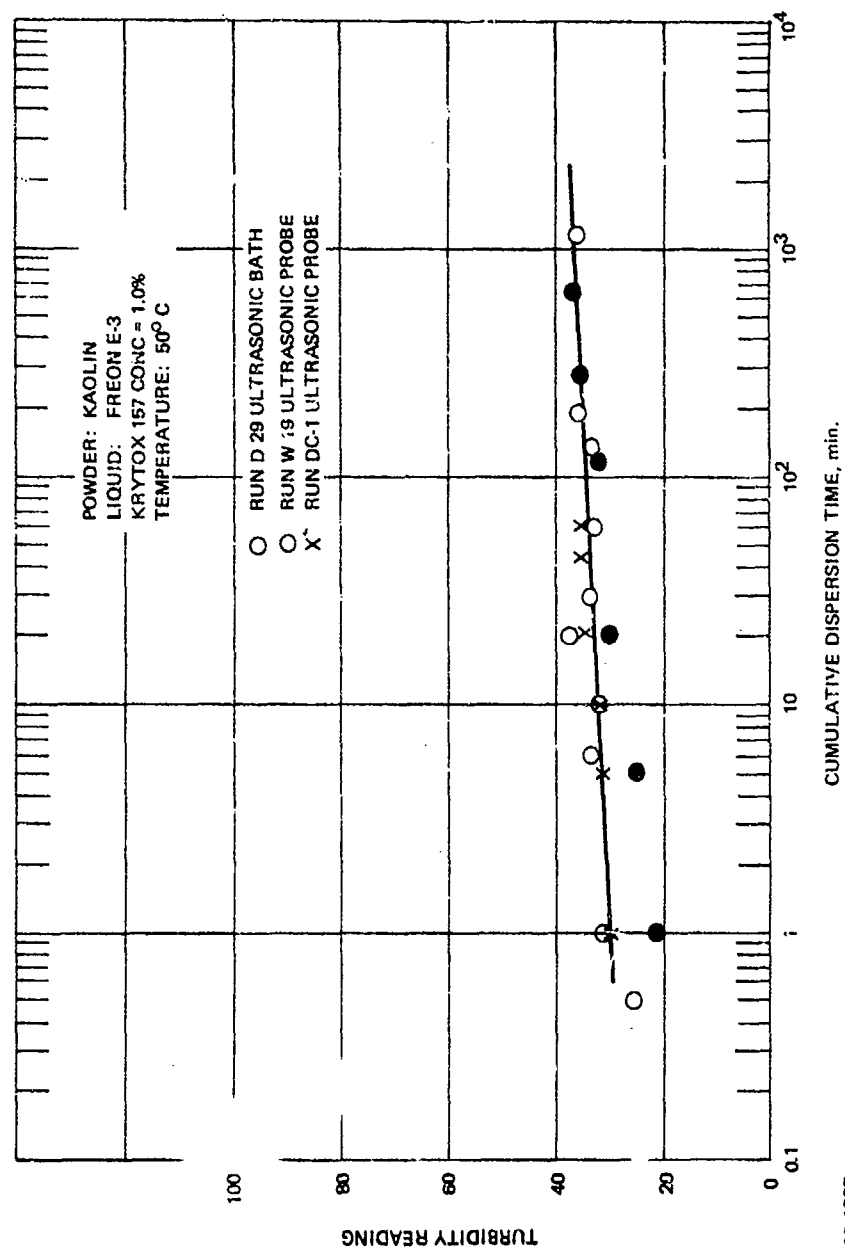


Figure 4-8 ULTRASONIC DISPERSION OF STERLING MT CARBON BLACK IN FLUORINATED LIQUID



Freon E-3 solution. Carbon black and clay were not suited for these experiments, carbon black because its density coincides with those of the fluorinated liquids used, clay because of its unusual particle shape which would make interpretation of the data difficult.

The spin fluid in these tests was a 1% solution of Krytox 157 in FC-43 which had a density of 1.88 gm/cm^3 and a viscosity of 5 cp at 25°C , the operating temperature of the centrifuge. A 1% solution of Krytox 157 in Freon E-3 was used as the buffer liquid. In these tests a 5 ml sample was added to 20 ml of spin fluid and 1.0 ml of buffer liquid, establishing a starting radius, R_1 , of 3.90 cm. The detector and the sampling probe were placed at a radius of 4.82 cm. By varying the speed of the instrument from 1000 RPM to 8000 RPM and operating for various periods of time ranging from 36 seconds (minimum cycle time) to 75 minutes, it was possible to examine the particle size distribution in the range of $0.03 \mu\text{m}$ to over $2 \mu\text{m}$, based on Equation 4-1. This equation was used to calculate equivalent particle diameter from the operational parameters for the systems studied. These results are presented in Figure 4-10.

Uranium Dioxide Suspensions: Two uranium dioxide suspensions, each containing 50 mg of UO_2 /25 ml of solution, were examined on the Joyce Loeb1 instrument. Dispersion EA-1 was prepared and dispersed at the Joyce Loeb1 Applications Laboratory. Samples removed after 3 min, 10 min, 41 min and 106 min of ultrasonic irradiation were examined on the centrifuge. In addition, dispersion DA-1, of similar composition, was examined after it had been exposed to a total of 718 min of irradiation with the ultrasonic probe.

Typical photosedimentation curves are presented in Figure 4-11. These are plots of the signal of the optical detector placed at 4.82 cm radius versus sedimentation time at two operating speeds. The abrupt end of the curve represents removal of the inner annulus of spinning fluid by the sample probe. Photosedimentation curves were obtained for all the uranium dioxide samples. The resulting particle size distribution curves and the corresponding turbidity measurements are presented in Figure 4-12. The measurements for the EA-1 suspension after 106 min dispersion time, and for the DA-1 suspension, were repeated six times at different centrifuge speeds and cycle times and were then sampled in order to generate an absolute particle size distribution curve based on chemical analysis. The optical traces were quite reproducible as shown in Figure 4-13 for suspension DA-1.

These samples were submitted for analysis of uranium content by x-ray fluorescence. Unfortunately, the analytical results were not sufficiently accurate to be used to generate a particle size distribution curve. The reported uranium content ranged from less than 5 ppm (the detection limit) to 30 ppm maximum concentration with an error band of about 20 ppm.

Calcium Fluoride Suspensions: A representative calcium fluoride suspension EC-1 powder containing 200 mg/25 ml fluorinated solution was also prepared, dispersed, and analyzed at Joyce Loeb1. The samples, removed after 12 min, 40 min and 71 min of sonolation were examined by turbidity and sedimentation. Photosedimentation curves were obtained for the

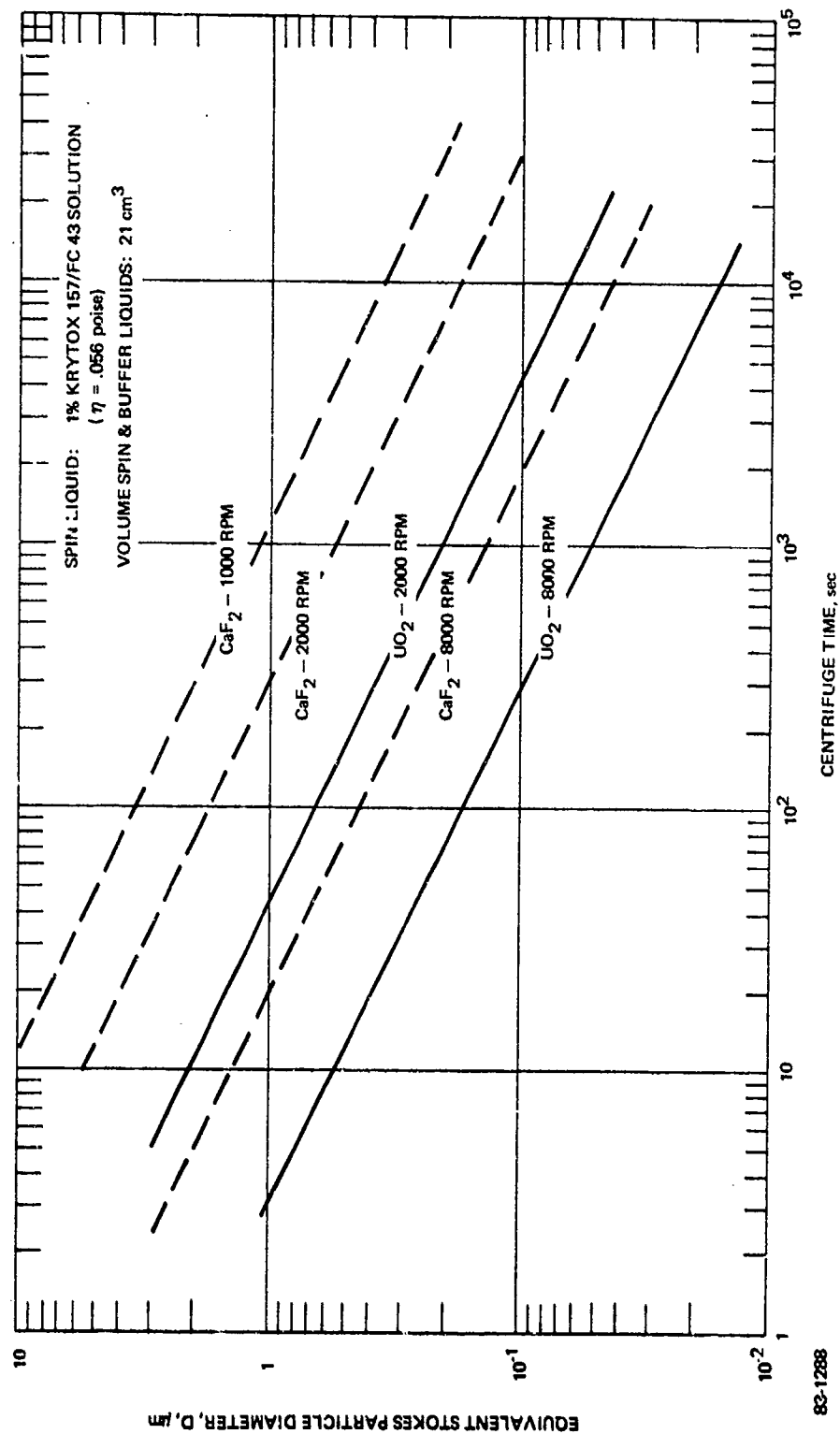


Figure 4-10 CALIBRATION CURVE FOR SEDIMENTATION OF POWDERS IN JOYCE LOEBL MK III CENTRIFUGE

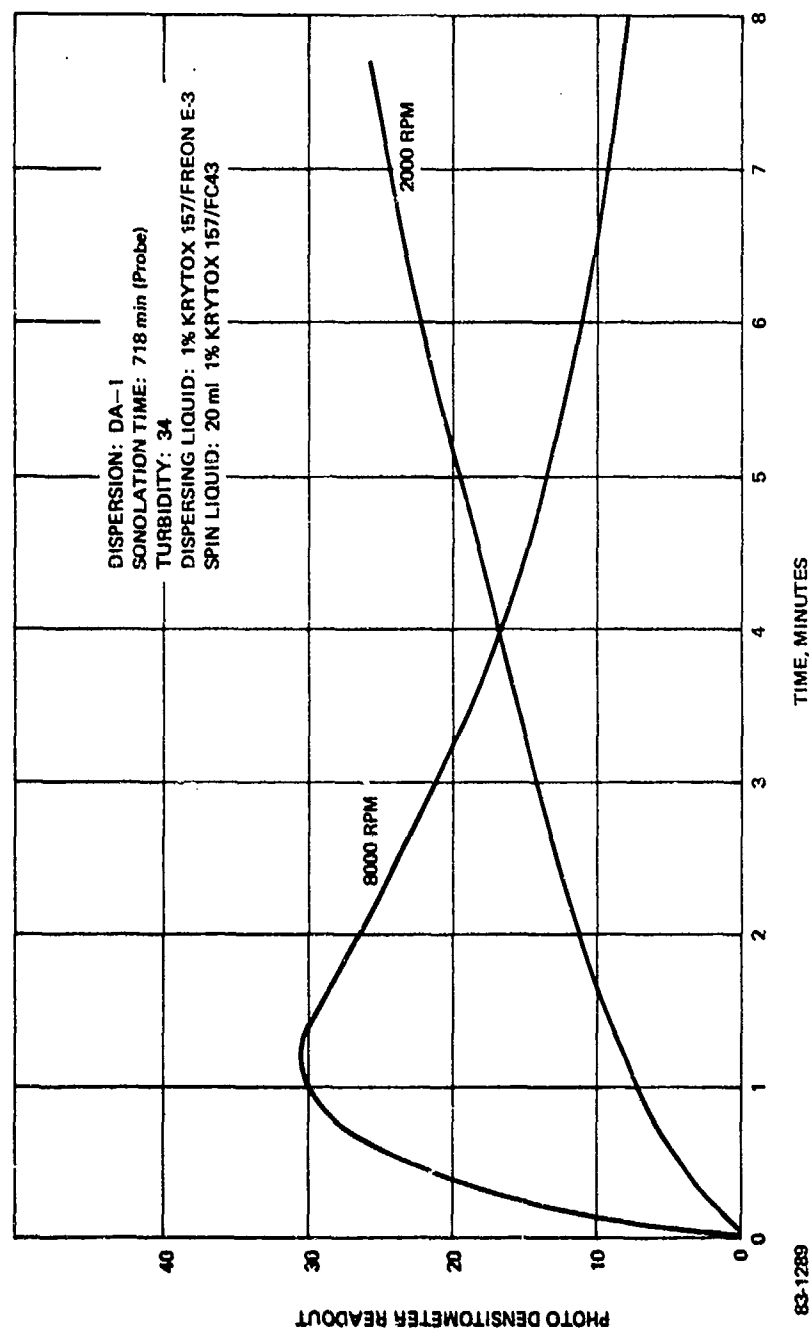


Figure 4-11 PHOTOSEDIMENTATION CURVES FOR UO_2
DISPERSION IN FLUORINATED LIQUID OBTAINED
WITH JOYCE LOEBL CENTRIFUGE

83-1289

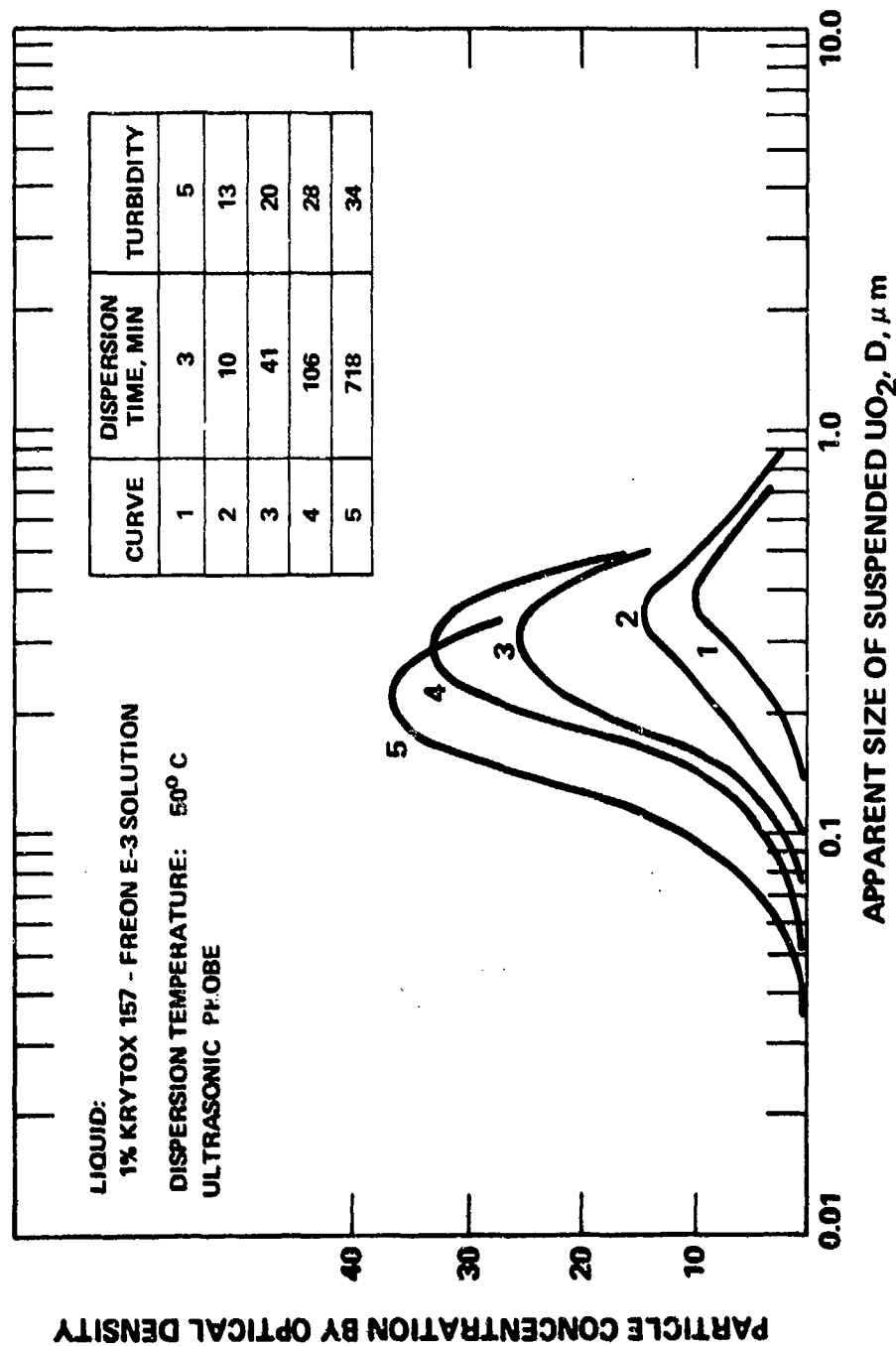


Figure 4-12 EFFECT OF SONOLATION TIME ON SIZE DISTRIBUTION OF UO_2 DISPERSED IN FLUORINATED LIQUID

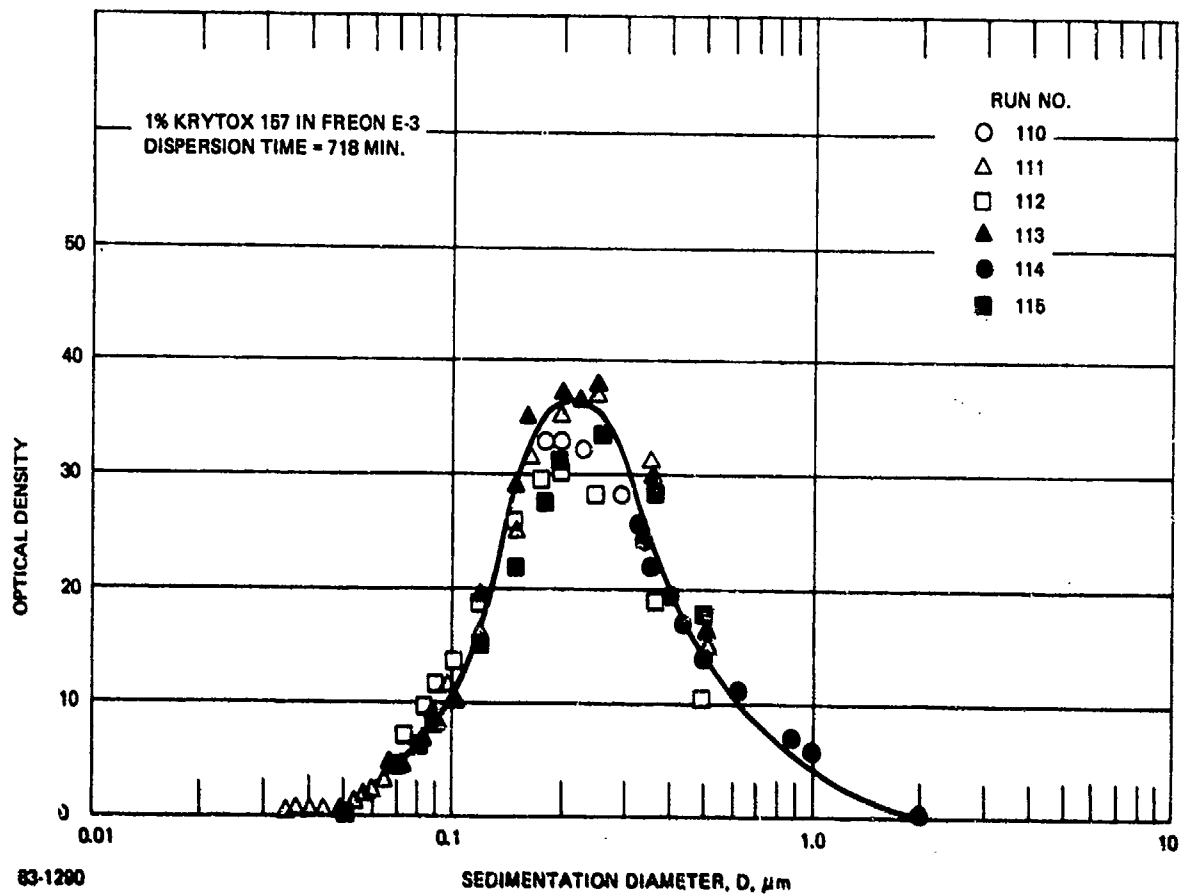


Figure 4-13 REPRODUCIBILITY OF SIZE DISTRIBUTION CURVE
FOR UO_3 DISPERSION

three samples. These results are presented in Figure 4-14. The curve for the 71 min sample is an average of the five photosedimentation curves generated by the samples used to develop an absolute particle size distribution curve. The samples removed were analyzed for calcium by atomic adsorption. These results are presented in Table 4-7. The resulting particle size distribution curve is plotted on log normal paper in Figure 4-15. According to these results the dispersion has a geometric weight average diameter of 0.22 μm with a geometric standard deviation of 2.3.

4.5 Discussion of Results

4.5.1 Correlation of Turbidity with Size of Suspended Material

In general it was observed that the turbidity of irradiated suspension increased with increasing sonolation time. After sufficient time, the turbidity of a given suspension attained a constant value. The results presented in Figures 4-12 and 4-14, for uranium dioxide and calcium fluoride dispersions, show a correlation between the turbidity of a suspension and the size distribution of suspended material. For a given powder, a higher turbidity index is commensurate with a smaller average size of the suspended material.

Large changes in the turbidity index indicate a significant change in the size distribution, as noted with the results for uranium dioxide presented in Figure 4-12. Conversely, if the turbidity of a sonolated suspension attains a constant value that does not change significantly with further sonolation time, it can be presumed that there is no significant change in the distribution of the suspended material. It is noted for calcium fluoride, as shown in Figure 4-14, that both the optical size distribution curves and the turbidity measurements do not change markedly with further sonolation time. Furthermore, the results presented in Figure 4-15 indicate that the calcium fluoride suspension analyzed was well dispersed. Since the data plot as a straight line on log-probability paper, the material in suspension has a log normal size distribution. Kapteyn's law⁽⁴⁻⁷⁾ can thus be used to calculate other average particle diameters. According to this law, if the basic distribution (of particle diameter d ; for instance) is log normal with mean u and standard deviation σ , then the j th moment distribution is again log normal with the same standard deviation σ and mean u , such that

$$\ln u_j = \ln u + j \ln^2 \sigma \quad (4-2)$$

Accordingly a value for the arithmetic volume/surface mean particle diameter, \bar{d}_{vs} , can be estimated from Figure 4-15 by the following equation:

$$\ln \bar{d}_{vs} = \ln \bar{d}_{wg} - 0.5 \ln^2 \sigma_g \quad (4-3)$$

where

\bar{d}_{wg} = geometric diameter by weight

σ_g = standard deviation of \bar{d}_{wg}

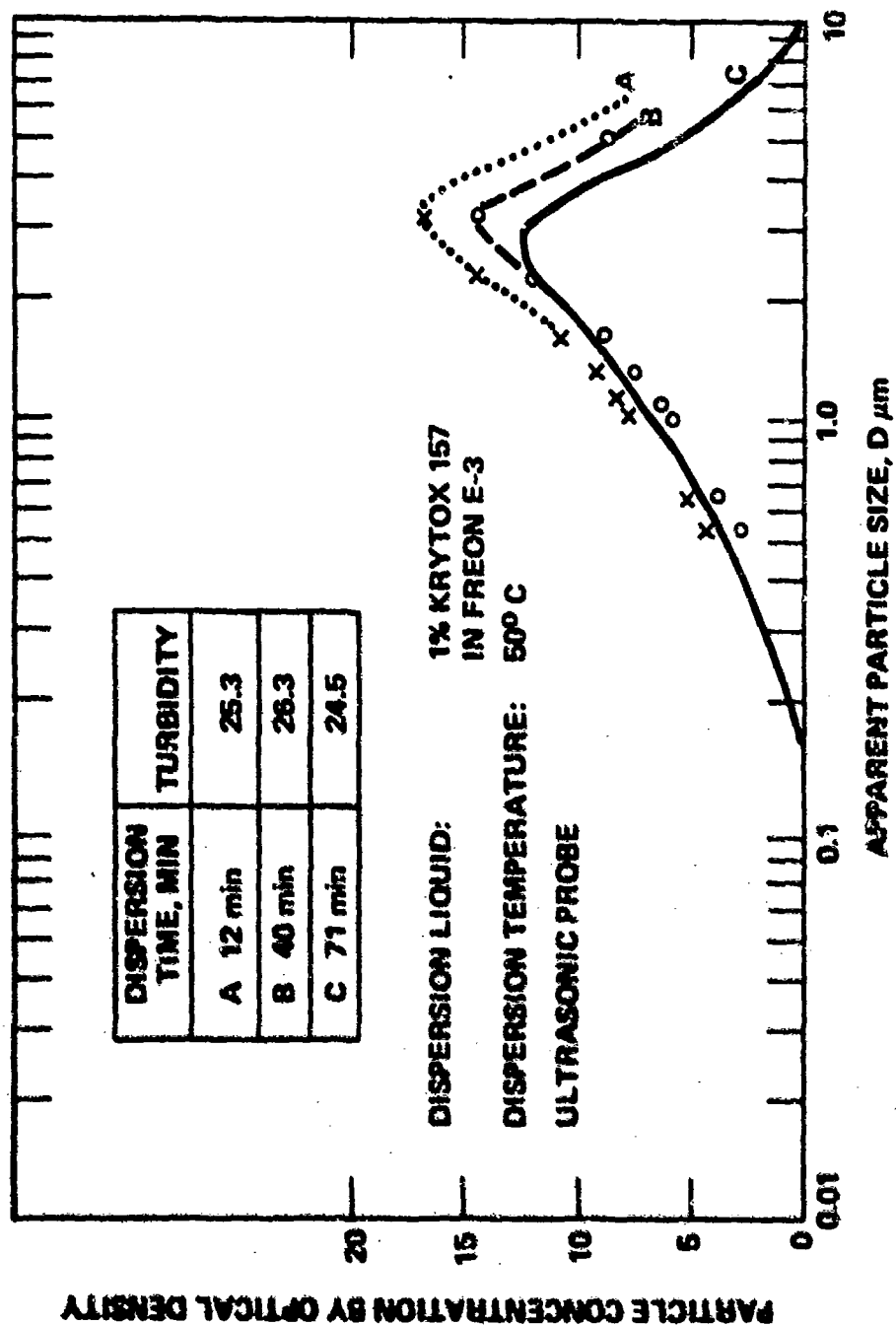


Figure 4-14 EFFECT OF SONOLATION TIME ON SIZE DISTRIBUTION OF CaF_2 DISPERSED IN FLUORINATED LIQUID

TABLE 4-7

PARTICLE SIZE DISTRIBUTION OF CaF_2 DISPERSION IN 1%
KRYTOX-FREON E-3 SOLUTION BY SEDIMENTATION ANALYSIS

Sample No.	122	123	124	125	126
Centrifuge Speed, RPM	2000	8000	2000	8000	1000
Length of Run, in Centrifuge, Secs	1200	1200	400	240	90
Equivalent CaF_2 Particle Diameter, D, μm	0.52	0.13	0.90	0.29	3.8
Volume of Undersize Sample, ml	20.5	17.8	15.5	17.5	16.8
Calcium Concentration in Undersize Sample ppm (w/v)	89	28	130	86	155
Calcium Content of Undersize Sample, mg	1.83	0.50	2.01	1.50	2.60
Calcium Content in Feed Sample, mg	←————— 2.16 —————→				
Weight Fraction Particles Smaller than D	0.85	0.23	0.93	0.70	1.00

Dispersion No. EC-1

Dispersion Time: 71 min

Turbidity: 24.5

CaF_2 Content: 202.1 mg CaF_2 / 41.5201 gr/solution = 8.42 mg CaF_2 /ml = 4.32 mg Ca/ml

Sample Size: 0.5 ml

Buffer: 1.0 ml 1% Krytox 157-Freon E-3 Solution

Spin Liquid: 20 ml 1% Krytox 157-FC-43 Solution

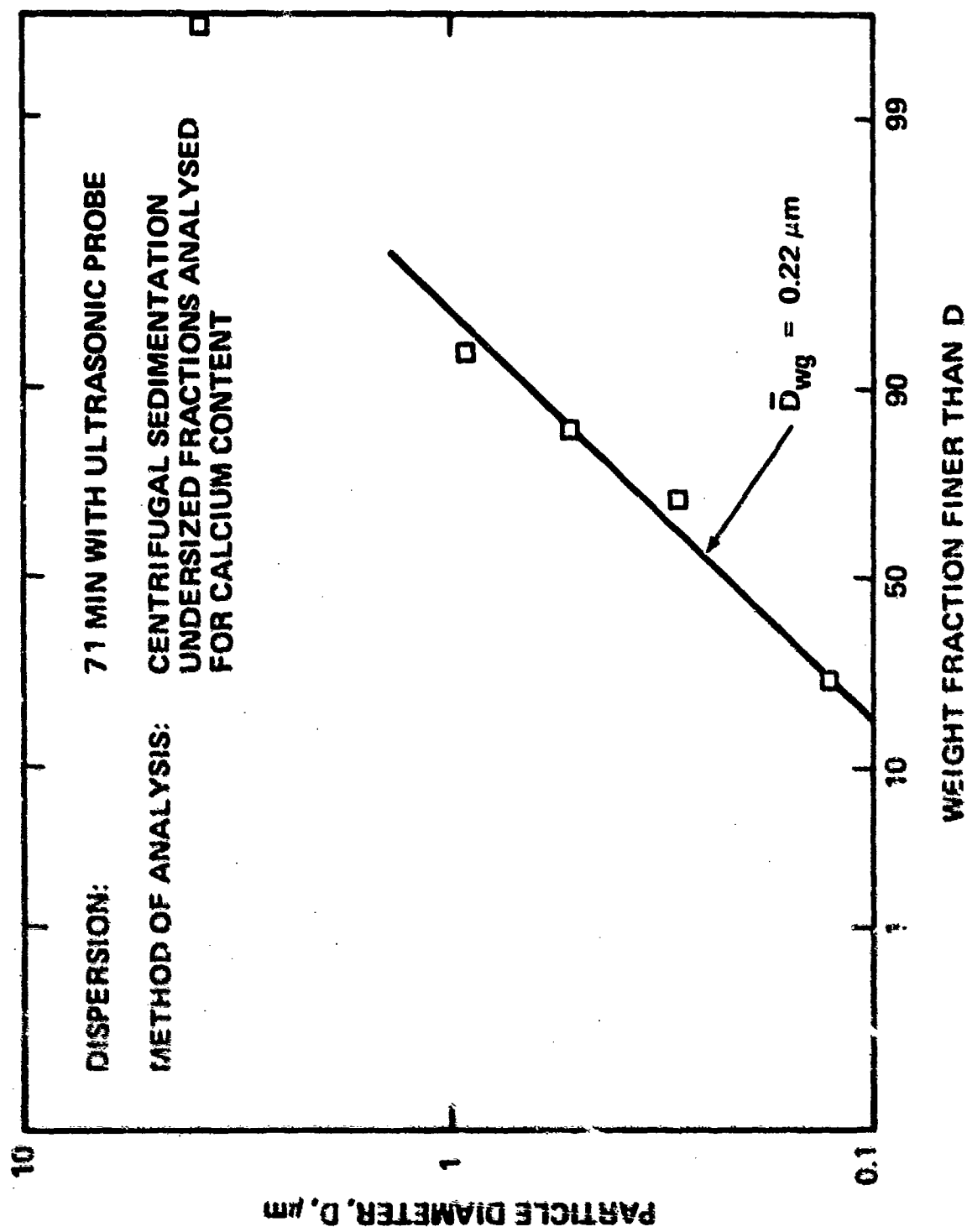


Figure 4-15 PARTICLE SIZE DISTRIBUTION OF CALCIUM
FLUORIDE DISPERSED IN A 1 PERCENT
KRYTOX 157 - FREON E-3 SOLUTION

From Figure 4-15, $\bar{d}_{wg} = 0.22 \mu\text{m}$ and $\sigma_g = 2.3$ so that $\bar{d}_{vs} = 0.16 \mu\text{m}$. This estimate of \bar{d}_{vs} does not differ significantly from the value of $0.19 \mu\text{m}$ obtained by B.E.T. measurements for the equivalent spherical particle diameter of the ultimate calcium fluoride particles (see Table 2-1), which is also a volume to surface mean particle diameter. The implication of these results is that the calcium fluoride suspension analyzed was completely dispersed and that the resulting primary particles were not significantly reduced from their true size. The objects in suspension were essentially ultimate CaF_2 particles rather than agglomerates of these particles.

4.5.2 Effect of Process Parameters on Particle Dispersion

The results of the dispersion studies based on the turbidity measurements are summarized in Table 4-8. The rate of increase of turbidity, or the rate of dispersion of each suspension prepared, and the time needed to attain a constant turbidity were found to be influenced by the following parameters:

- a. Composition of the Dispersing Liquid: Solutions of Krytox 157 in Freon E-3 are much more effective media for dispersion than solutions of Krytox 157 in FC-43. With both liquids, there is little or no dispersion in the absence of Krytox 157.
- b. Ultrasonic Power Intensity: Increasing the ultrasonic power intensity increases both the rate and extent of the dispersion process, especially as the size of the ultimate particle decreases.
- c. Size of the Ultimate Particles: The smaller the size of the ultimate particles in the agglomerate or conglomerate, the more difficult it becomes to disperse these particles. The most difficult powder to disperse was ENL-1 uranium dioxide which was the finest particle sized powder studied. This powder contained a large fraction of particles smaller than $0.1 \mu\text{m}$, with particles as small as $0.04 \mu\text{m}$ being definitely present.
- d. Time: The rate of dispersion decreases with increasing sonolation time. At a low power density (e. g. in the ultrasonic bath), when dispersion occurred it was noted that the turbidity of the suspensions increased as the log of the time of ultrasonic irradiation. Even though some of the tests carried out lasted over 5400 minutes (90 hours), it was not possible to determine from the turbidity data whether the system had reached a steady state in which the size distribution of the suspended material did not change further with time. At high power density (e. g. with the ultrasonic probe), all the powders ultimately reached a steady state value of turbidity. The time required to attain the plateau increased with decreasing particle size. It took approximately 600 min to attain a constant turbidity index with ENL-1 UO_2 dispersions.

TABLE 4-8
SUMMARY RESULTS OF DISPERSION STUDIES BASED ON TURBIDITY MEASUREMENTS

PARAMETER	KRYTOX 157 CONCENTRATION	CARRIER LIQUID	TEMPERATURE	ULTRASONIC TRANSDUCER*	DISPERSION TIME REQUIRED TO ATTAIN CONSTANT TURBIDITY READING
Range Studied	0 - 1.0 wt. %	Freon E-3 or FC43	35-80°C	Ultrasonic Bath (low power density) vs. Ultrasonic Probe (high power density)	Ultrasonic Probe Ultrasonic Bath
UEL-1 Uranium Dioxide	Turbidity is significantly lower when no Krytox 157 is added. No noticeable effect between 0.1% and 1% Krytox 157 in Freon E-3	Turbidity higher with Freon E-3 than with FC43 solutions	Turbidity increases with increasing temperature	Little difference in turbidity up to 10 min. dispersion time. Beyond 10 min., turbidity increases much more rapidly with probe than with bath.	Not attained in 3000 min.
Calcium Fluoride	Same as UO ₂	Same as UO ₂	No effect of temperature observed	More rapid dispersion with probe than with bath	~200 min. >1000 min.
Peerless No. 2 Kaolin	At 35°C, same as UO ₂ At 80°C, no effect of Krytox 157 concentration	Same as UO ₂	Maximum turbidity at 50°C	No noticeable difference	~10 min.
Sterling MT Carbon Black	At 35°C, increases with increasing Krytox 157 concentration. At 80°C, no effect of Krytox 157 concentration	Same as UO ₂	In Freon E-3, turbidity lower at 80°C than at 50°C or 35°C, where measurements did not differ significantly. In FC43, turbidity is higher at 50°C than at 35°C.	More rapid dispersion with probe than with bath	~20 min. >100 min.

*50 mg Powder in 25 ml 1% Krytox 157 - Freon E-3 Solution at 50°C.

The dispersion tests with the probe could be interrupted without noticeable reagglomeration taking place. It was noted that powders once dispersed always stayed dispersed. The reported sonolation time for a given run was the cumulative time of a series of separate runs on one sample.

- e. Temperature: The effect of temperature on the rate of dispersion depends on the composition of the particles to be dispersed. All the powders studied could be effectively dispersed at 35°C or 50°C. Increasing the temperature to 80°C had an adverse effect on the dispersion of kaolin and carbon black.
- f. Particle Concentration: There was no noticeable effect of particle concentration at the concentration levels examined.
- g. Mixtures of Powders: Mixtures of powders did not behave in a significantly different manner than individual powders.

4.5.3 Postulated Dispersion Mechanism

These results can be explained in terms of a simple model which considers that an agglomerate or conglomerate is broken into smaller agglomerates and/or individual particles if stresses of sonic origin exceed the strength of the agglomerate. The dispersion process is enhanced by the presence of Krytox 157, which adsorbs at the surface of the particles.

The adsorbed Krytox 157 reduces attractive particle-to-particle forces in the agglomerate, thus facilitating agglomerate breakdown and also prevents dispersed particles from reagglomerating after they have been liberated from an agglomerated matrix. It is assumed and substantiated by our results that there is not sufficient ultrasonic energy to break primary bonds, i.e. reduce the size of the ultimate particles.

It is not possible to precisely define either the cohesive or disruptive forces acting on a sonolated agglomerate because there are too many unknown parameters. However, it is possible to obtain an order of magnitude estimate of the effectiveness of the dispersion process by considering:

- a. The crushing strength of an agglomerate as a useful index of the resistance of an agglomerate to dispersion, and
- b. the product of the mass of an agglomerate times the acceleration amplitude due to the propagation of sound through the dispersion liquid as a measure of the forces which could result in dispersion.

According to Hertz⁽⁴⁻⁸⁾ the crushing strength of a brittle sphere can be expressed by the following equation:

$$P = \left[\left(\frac{3}{1-2v} \right) \left(\frac{\sigma}{0.615} \right) \right]^3 \frac{D^2}{E} \quad (4-4)$$

where

P = applied compressive load at failure

D = sphere diameter

E = modulus of elasticity

v = Poisson's ratio

σ = maximum tensile stress in the sphere due to the applied compressive load

Kaiser⁽⁴⁻⁹⁾ combined the above equation with Rumpf's expression⁽⁴⁻¹⁰⁾ for the tensile strength of an agglomerate:

$$\sigma_Z = \left(\frac{9}{8} \right) \left(\frac{1-\epsilon}{\epsilon} \right) \left(\frac{H}{d^2} \right) \quad (4-5)$$

where

σ_Z = tensile strength of an agglomerate

ϵ = volume fraction voids

d = diameter of ultimate particles

H = mean particle to particle bonding force

to obtain the following expression for the crushing strength of a spherical agglomerate:

$$P = \left[\left(\frac{3}{1-2v} \right) \left(\frac{9}{8} \right) \left(\frac{1-\epsilon}{0.615\epsilon} \right) \left(\frac{H}{d^2} \right) \right]^3 \frac{D^2}{E} \quad (4-6)$$

$$P = \left[\left(\frac{5.5}{1-2v} \right) \left(\frac{1-\epsilon}{\epsilon} \right) \left(\frac{H}{d^2} \right) \right]^3 \frac{D^2}{E} \quad (4-7)$$

If the particles adhere because of secondary valence forces, then H can be expressed by Equation 1-1.

$$H = \frac{Bd}{36a^3} \quad (4-8)$$

where

a = particle to particle surface separation distance.

B = Lifschitz constant

so that

$$P = \left[\left(\frac{5.5}{1-2\nu} \right) \left(\frac{1-\epsilon}{\epsilon} \right) \left(\frac{B}{36a^3d} \right) \right]^3 \frac{D^2}{E^2} \quad (4-9)$$

The disruptive forces on an agglomerate are considered to be proportional to an inertial force F_i , defined by the following equation:

$$F_i = m\Gamma \quad (4-10)$$

where m is the mass of the agglomerate and Γ is the acceleration amplitude due to the application of acoustic energy through the medium of propagation. The acceleration is given by the following equation:

$$\Gamma = 2\pi f \sqrt{\frac{2I}{\rho_m c}} \quad (4-11)$$

where

c = velocity of sound in the medium

f = vibration frequency

I = applied ultrasonic energy/unit area

ρ_m = density of the propagation medium

The mass of an agglomerate is simply:

$$m = \frac{\pi D^3}{6} \rho_p (1-\epsilon) \quad (4-13)$$

where ρ_p is the density of the particles.

According to the above, agglomerates will be dispersed in an ultrasonic bath as long as:

$$\Gamma > \frac{P}{m} \quad (4-14)$$

or after substituting and cancelling terms:

$$2 \pi f \sqrt{\frac{2I}{\rho_m c}} > \left[\left(\frac{5.5}{1-2v} \right) \left(\frac{B}{36a^3 d} \right) \right]^3 \left(\frac{(1-\epsilon)^2}{\epsilon^3} \right) \left(\frac{6}{\rho_p \pi D E^2} \right) \quad (4-15)$$

The above predicts that it becomes more difficult to disperse an agglomerated powder with an ultrasonic source as:

- a. The size of the agglomerates, D, decreases. For a given powder, the largest agglomerates will disappear first with smaller agglomerates being progressively more difficult to disperse. The rate of dispersion will decrease with time.
- b. The volume fraction voids decreases. Everything else being equal, open structured agglomerates will be easier to disperse than compacted agglomerates. This parameter was not investigated in this study. The effect of compaction on the dispersibility of pigments is a well known phenomenon in the paint industry⁽⁴⁻¹¹⁾.
- c. The size of the primary particles, d, decreases. As the size of the ultimate particles decreases significantly, more power input will be required. Such an effect was clearly noted in this study. The powder with the largest particles (kaolin) was the easiest to disperse and the one with the smallest particles (ENL-1 uranium dioxide) was the most difficult to disperse.
- d. The distance between particles decreases. The term (B/a^3) increases to the third power. This is a measure of the secondary valence forces between the particles. The ability to disperse a powder in a surfactant solution reflects this effect. Since the dispersibility varies inversely as the ninth power of a, according to this model, this is a dominating effect. Immersing a powder in a wetting liquid increases particle to particle separation. Immersing the powder in a solution of a surfactant which can adsorb on the surface of the particles and form a thick solvated layer increases a even more. A solution of Krytox 157 in Freon E-3 was a much more effective dispersing medium then a solution of Krytox 157 in FC-43.

This reflects the possibility that the surfactant is more firmly bound to the particle surface in Freon E-3 than in FC-43, as discussed in the previous chapter. The solvated layer around a particle is most probably thicker in Freon E-3 than in FC-43. The thickness of a Freon E-3 solvated film of Krytox 157 is estimated to be 75Å. This estimate is based on values at 30°C of the thickness of Freon E-3 solvated films of HFPO hexamer acid (30Å) and HFPO decamer acid (45Å) reported in a previous study⁽⁴⁻¹²⁾. The effect of temperature on the dispersion process reflects the stability of the stabilizing film. The lowered dispersibility of kaolin and carbon black at 80°C is most probably due to the desorption of Krytox 157 from the surface of these powders at that temperature. The sensitivity of dispersion of Sterling MT to the Krytox 157 concentration reflects the adsorption characteristics of Krytox 157 on this powder.

According to the above expression, there is a critical acoustic acceleration threshold required to overcome the forces holding particles together in an agglomerate. The results obtained with the uranium dioxide dispersions are a striking indication that this is so. The acoustic acceleration in the ultrasonic bath was insufficient to disrupt UO₂ agglomerates below a certain size. Increasing the acoustic acceleration by using the probe resulted in a significant improvement in the degree of dispersion.

Numerical values of Γ for Freon E-3 suspensions in the ultrasonic bath and in the ultrasonic probe can be estimated from the properties of Freon E-3 listed in Table 2-3 and from information provided by the manufacturer of the ultrasonic sources. In the ultrasonic bath, for which $f = 40 \text{ KHz}$ and $I \sim 2 \text{ watts/cm}^2$, Γ is approximately equal to $4.5 \times 10^6 \text{ cm/sec}^2$, or 4500 times the acceleration due to gravity. When the probe is used, the power density decreases with increasing distance from the tip. The maximum acceleration level which controls the dispersion process, corresponds to the maximum power density which is estimated to be 80 watts/cm^2 . With this source, for which $f = 20 \text{ KHz}$, Γ_{max} is approximately 10^7 cm/sec^2 or 10^4 times gravity.

4.5.4 Conditions for Powder Dispersions

Based on the above measurements, it is concluded that the candidate powders are best dispersed when suspended in a 1% solution of Krytox 157 in Freon E-3 at 50°C. The ultrasonic probe is a better transducer than the bath. With this source of acoustic energy, the powders should be sonolated for at least 600 min to disperse powders as small as the ENL-1 uranium dioxide. Measuring the turbidity of the suspension is a useful method of monitoring the dispersion process.

The scope of the present dispersion study was limited by the characteristics of available ultrasonic sources. The results obtained indicated that it is possible to disperse a powder sample in a reasonable period of time. The dispersion process may be significantly improved however. The time required to disperse a fine powder may be significantly reduced by using acoustic

transducers optimized for this application. Increasing the frequency and power density should significantly improve the rate of dispersion. Mathieu-Sicaud and Levavasseur⁽⁴⁻⁵⁾ have indicated that barium sulphate particles 0.1 μm in diameter, are most easily dispersed in water when a transducer oscillating at 10^3 KHz is used. The use of a variable frequency generator may improve the dispersion process of a random powder. With such equipment it would also be possible to carry out more focused experiments which would lead to better scientific understanding of ultrasonic dispersion.

5.0 PARTICLE DEPOSITION STUDIES

Information obtained from each of the previous studies was integrated in the particle deposition studies which are the culmination of the program. During this phase of the program, samples of the candidate powders and their mixtures dispersed in a fluorinated liquid were deposited on an ultrafiltration membrane which was then washed and dried. The deposited powder samples were all examined by scanning electron microscopy. The micrographs were examined visually and with an automated particle counter to obtain qualitative and quantitative information on the degree and quality of dispersion of the deposited samples. In addition, selected samples were submitted for elemental analysis, using either an electron probe microanalyzer or a non-dispersive x-ray analyzer.

5.1 Basic Method of Sample Preparation

The basic preparative procedure used consisted of the following steps:

- a. Preparation of a primary concentrated dispersion.
- b. Preparation of a dilute secondary dispersion with a desired particle concentration.
- c. Ultrafiltration of the dilute secondary dispersion.
- d. Washing of the particles deposited on the ultrafiltration membrane.
- e. Drying of the membrane.

5.1.1 Preparation of Primary Particle Dispersions

The experimental procedure described in Section 4.4.2 was used to prepare the primary dispersions. A known weight of powder (usually 50 mg or 60 mg) was added to 25 ml of a 1% Krytox 157 - Freon E-3 solution in a water cooled 50 ml polycarbonate centrifuge tube. The mixture was then sonolated with the S-75 ultrasonic probe. Periodically, the sonolation process was interrupted and the probe temporarily withdrawn in order to remove one or more aliquot samples of the dispersion.

These aliquots, which ranged from 10 μ l to as much as 350 μ l in volume, were then diluted with additional 1% Krytox 157 - Freon E-3 solution to form the secondary dispersions used to prepare the deposited samples. Initially, one of these aliquot samples was also used to measure the turbidity of the suspensions with the Turner fluorometer, as described in Section 4.3.2. The fluorometer became inoperative mid-way during the course of these studies. Turbidity measurements were thus not obtained for all runs. Fortunately, turbidity measurements as well as limited centrifugal sedimented measurements were at least obtained for the critical uranium oxide dispersion studied in this phase (sample series DA-1). These measurements were already discussed in Section 4.5.

5.1.2 Secondary Particle Dispersions

A secondary dispersion was prepared by adding an aliquot of the primary dispersion to 25 ml of 1% Krytox 157 - Freon E-3 solution, contained in a 50 ml screwcap polycarbonate centrifuge tube. The tube and its contents were then placed in the Branson Ultrasonic Bath until the suspension was to be filtered. The temperature of the bath was 50°C. The ultrasonic bath was used to insure good mixing and dispersion of the aliquot in the bulk fluorinated liquid, but at a much lower power intensity level than in the probe.

Secondary dispersions were used for a number of reasons. First, it was possible to prepare many samples from a given master batch. The effect of sonolation time on a given primary dispersion could thus be monitored. The amount of powder deposited on the filter could be controlled by the size of the aliquot sample; the greater the volume of the sample removed, the larger the surface concentration of particles deposited on the filter membrane. The effect of powder loading after a given period of ultrasonic agitation could thus be monitored. The volume of the diluent liquid was not critical and was chosen for convenience. With this volume, the initial height of liquid in the cell was 7 mm. A further advantage of using secondary dispersions was that these could be stored in the ultrasonic bath for a given period of time since only one 90 mm filtration system was available. A number of samples could be withdrawn simultaneously and kept in limbo until they could be filtered. Finally, dilution of the dispersion prepared with the probe minimized cross-sample contamination, as further discussed in Section 5.3.

5.1.3 Particle Deposition

After being well mixed in the ultrasonic bath, the secondary dispersions were filtered through an ultrafiltration membrane in a 90 mm Millipore Laboratory Ultrafiltration cell. This is the same cell that was used in the washing studies as described in Section 3.2 and shown in Figures 3-5 and 3-6. Based on the results and experience obtained in the previous phases of the study, Amicon's XM-100A ultrafiltration membrane was the deposition membrane of choice in this phase of the program.

After the membrane was placed in the cell and the cell assembled (as shown in Figure 3-6), the dispersion was added to the cell through a funnel consisting of the body of a 30 ml disposable plastic syringe attached to the cell's retentate port. The latter was a tube with a Luer fitting leading to the bottom of the cell through which liquids may be added or withdrawn. The syringe body was removed and replaced with a Luer cap. The cell was then pressurized to approximately 1 psig (± 0.3 psig) with compressed air and the dispersion filtered. The particles were deposited on the membrane, and the dispersion liquid was collected in a receptacle below the cell. This initial deposition step usually took between 10 min and 20 min to carry out, depending on the filtration pressure and the effective permeability of the actual membrane used. The permeabilities of the various membranes to the dilute dispersions were within 30% of 0.1 ml/cm² - psig - min, the initial permeability of XM-100A membrane to a 1% Krytox 157 - Freon E-3 solution, as reported in Section 2.5.5.

5.1.4 Washing of Deposited Particles

The particles were washed first with FC-43 and then with Freon C-51-12. After the initial dispersion liquid was removed, the air line leading to the cell was shut off and the pressure in the system relieved. After removing the cap, 25 ml of FC-43 was added to the cell directly through the retentate port, with a plastic syringe. As before, the syringe was removed, the cap replaced, and the cell repressurized. The FC-43 wash liquid filtered through the membrane, displacing the residual dispersion medium and removing Krytox 157 from the deposited material.

The amount of FC-43 wash liquid used was based on the results of the washing experiments presented in Section 3.3. It was shown that in the absence of powder, essentially all the Krytox 157 was removed by the first 15 ml of FC-43 wash liquid from a filter previously exposed to 25 ml of a 1% Krytox 157 - FC-43 solution. If the solution contained 1.0 gr of powder, the bulk of the Krytox 157 was removed by the first 15 ml of FC-43 wash, and by the time 60 ml of wash liquid was used, Krytox 157 could not be detected in the effluent. In the deposition studies under consideration in this section, the amount of powder deposited normally varied from 0.02 mg to 0.4 mg (with one run containing 0.7 mg of powder). In all these runs, the amount of powder was less than 0.1% of the amount of powder used in the washing tests. It was considered that the washing characteristics of the deposited particle/filter system would be essentially those of the blank filter, in that essentially all the Krytox 157 would be removed by the first 15 ml of wash FC-43. An extra 10 ml were used as a margin of safety.

After the FC-43 wash liquid had filtered through, the deposited material was then washed with 25 ml of Freon C-51-12 repeating the above procedure. The reason for using a Freon C-51-12 wash was to displace a non-volatile liquid, FC-43, with a very volatile one. It will be recalled that Freon C-51-12 which boils at 45°C, evaporates readily under ambient conditions. It has a vapor pressure of about 0.5 atm at 25°C and a low heat of vaporization (about 21 cal/grm (2-6)). The amount of C-51-12 was not considered critical as long as it displaced FC-43. The volume of wash C-51-12 was arbitrarily chosen to be equal to the volume of FC-43 used in the initial washing step.

The washing of the deposited particles with FC-43 was the slowest filtration step because of the lower permeability of FC-43 through the XM-100A membrane. It normally took twice as long to filter the FC-43 wash (20 min - 40 min) as it did to filter the initial secondary dispersion. The effective permeability of FC-43 in these tests was about 0.05 ml/min-psi-cm². Washing with C-51-12 was very rapid, occurring within 2 to 5 min. This corresponds to an effective permeability for C-51-12 of about 0.5 ml/min-psi-cm² in this system.

5.1.5 Drying of the Membrane

At the end of the wash cycle the particles are deposited on a filter wet with C-51-12 which had to be removed. Air pressure to the cell was first raised to 10 psig. This resulted in the immediate initial removal of 2-3 ml of liquid C-51-12. The air stream also contained C-51-12 vapor. The presence of the vapor was easily detected by visual observation. Air was allowed to pass through the filter until C-51-12 vapor could not be detected (usually about 5 min). At this point, the air supply was shut off, the pressure lowered and the cell disassembled. The filtration membrane was then transferred, glossy side up, to the bottom half of a 100 mm plastic Petri dish and allowed to stand over night at the rear of the laminar flow hood which is described in a subsequent section. The following morning, the filter was covered with the top half of the Petri dish. The covered container which contained the prepared sample was then labelled and sealed with plastic tape.

5.2 Other Methods of Sample Preparation

The majority of powder samples which were examined were prepared according to the procedure outlined above. A number of samples were also prepared in which specific steps in the procedure were varied. These included alternate methods of preparing secondary dispersions and alternate washing methods as well as preliminary experiments with other membranes as filter substrates.

In a series of tests, secondary dispersions of samples obtained from the same primary dispersion were prepared by three different dispersion techniques: dispersion in the ultrasonic bath as described before, dispersion with the ultrasonic probe, and dispersion by simply shaking the dispersion by hand.

A number of alternate washing procedures were also tried with samples deposited on XM-100A membranes. These included no washing at all, washing of "sandwiched" particles and "pousse-cafe" washing. The alternate methods were examined as possible means of avoiding horizontal flow of wash liquid on the membrane.

In the sandwich technique, the particles were deposited by filtering a secondary dispersion on a XM-100A membrane, as outlined in Section 5.1.3. The ultrafiltration cell was then opened and a second XM-100A membrane was placed on top of the first membrane. The top membrane was placed upside down so that the particles were sandwiched between two ultrafiltration films. The cell was then reassembled. The filter assembly was then washed with FC-43 and C-51-12 and air dried in the manner described in Sections 5.1.4 and 5.1.5. The washing time was, however, slower because of the greater hydraulic resistance of two membranes. The particles were sandwiched between the two filters which could be peeled apart and examined individually.

The "pousse-cafe" washing technique involved the layering of the wash liquid above the secondary dispersion. Since the density of FC-43 ($\rho = 1.88 \text{ gr/cm}^3$) is greater than the density of the 1% Krytox 157 - Freon E-3 solution used as the dispersion medium ($\rho = 1.73 \text{ gr/cm}^3$), an alternate to FC-43 was required. Freon E-1, which has a relatively low density of

1.54 gr/cm³ for a fluorinated liquid and is also volatile (B. P. 40.3°C), was used as the wash liquid. Freon E-1 is the lowest molecular weight homologue of Freon E-3.

Preliminary deposition tests with and without washing were also carried out with other 90 mm diameter filters as substrates. These included the PSIM and PSED Pellicon ultrafilters, the Millipore VSWP filter and the S&S B14 filter.

5.3 Precautions Taken to Prevent Sample Contamination

A difficulty encountered in trying to prepare samples of carefully selected dust (e.g. particles of interest) is the ubiquitous presence of unwanted dust particles in the atmosphere. By using a number of simple precautions, sample contamination by unwanted foreign particles proved to be no problem, even though the work was performed in a standard industrial laboratory, not a special clean room. The following precautions were taken:

- a. All key preparation steps were carried out in a Horizontal Flow Clean Bench (made by Pure Aire Corp. of America) shown in Figure 5-1. This laminar flow work station is rated to deliver Class 100 (Federal Spec. 209) performance.
- b. All the liquids used in the study that came into contact with the powders during any sample preparation step were filtered just before use. Compressed air was filtered through a 90 mm filter.
- c. All the pieces of equipment that would come into contact with either the powders or dispersions of these powders were first carefully cleaned by standard methods to remove gross contaminants and then were always rinsed with filtered 1% Krytox 157 - Freon E-3 solution, with some mechanical or (if possible), ultrasonic agitation. Particular care was taken to clean the glossy side of the ultrafilters on which the particles were deposited, the polycarbonate centrifuge tubes used to prepare and contain the dispersions, and the ultrasonic probe. The ultrasonic probe, which came into contact with all the dispersions that were prepared, was cleaned after each run by first rinsing it with 1% Krytox 157 solution in Freon E-3, then cleaning the probe ultrasonically (i.e. turning it on) with 25 ml of clean 1% Krytox 157 - Freon E-3 solution in 50 ml test tube (e.g. a blank run), and finally rinsing the probe again with more 1% Krytox 157 - Freon E-3 solution after sonication was stopped and it was removed from its cleaning bath.
- d. Even with the precautions outlined above, it was not possible to completely clean the ultrasonic probe. To prevent any significant level of cross contamination of powder samples from the probe, particles of interest were first dispersed

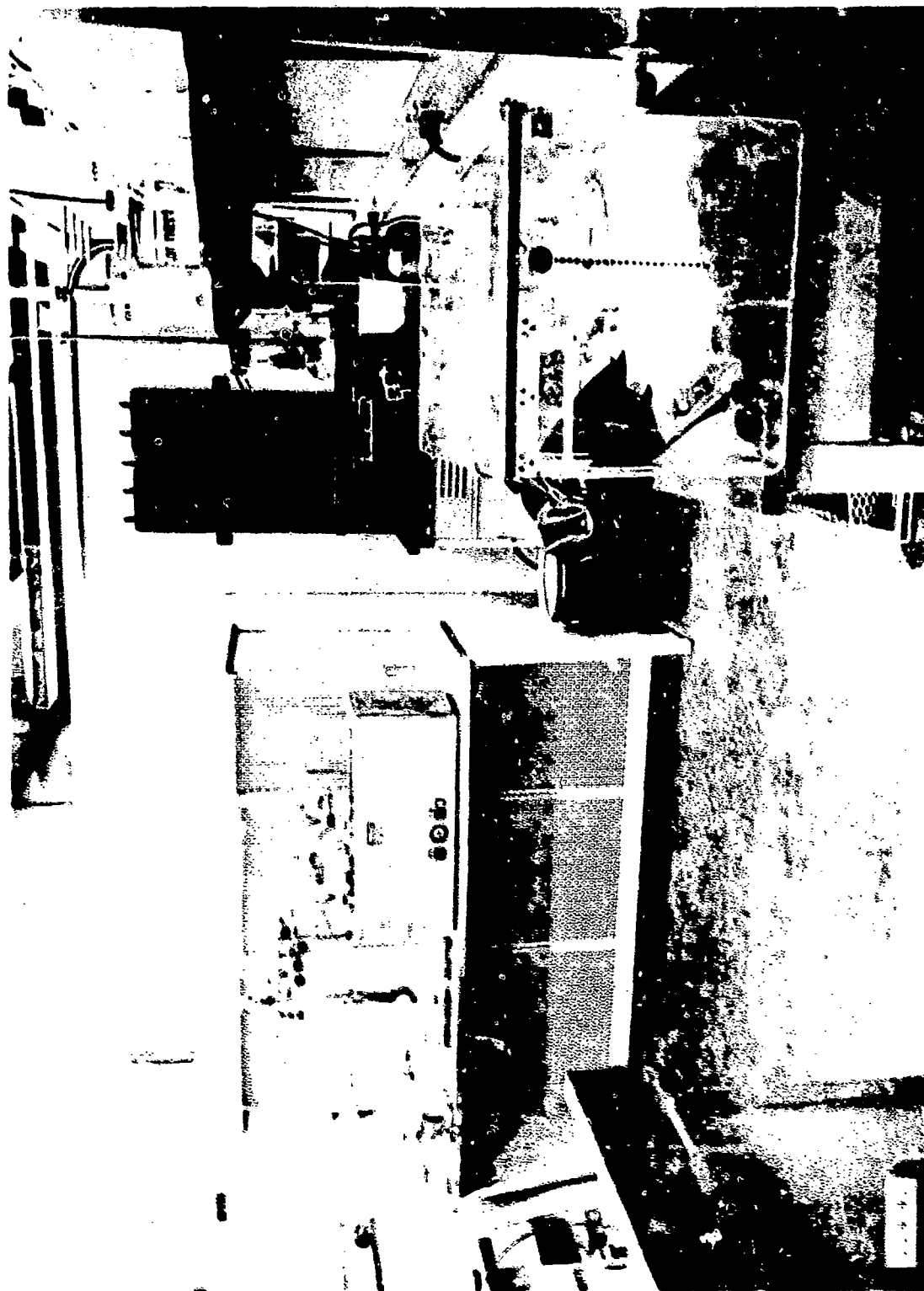


Figure 5-1 LAMINAR FLOW BENCH USED IN STUDIES

with the probe in a 1% Krytox 157 - Freon E-3 solution at a high solids concentration and then diluted with clean 1% Krytox 157 - Freon E-3 solution, as previously described.

- e. All samples of powder deposited on the ultrafilters were kept in 100 mm plastic petri dishes which were normally covered and stored in standard 1 lb coffee cans filled with a polyethylene cover. This humble container proved to be the best storage vessel that we found for the deposited samples. It has the proper geometry, it is rigid, it is air tight when capped, but yet it can be easily opened and is of a convenient size.

5.4 Examination of Deposited Particles

The samples prepared at Avco were taken to Advanced Metals Research, Inc., (AMR) for S.E.M. examination and microchemical analysis.

5.4.1 S.E.M. Examination

A small segment approximately 0.5 cm x 0.5 cm, was cut from each filter with a scalpel. The shape of these segments was varied for identification. Up to five different segments were then mounted on a sample knob and coated with a thin gold-palladium film to make them conductive. Scanning electron micrographs were then taken on the AMR 900 high resolution scanning electron microscope. Each sample was usually examined by photomicrography at increasing magnification levels, typically 450X, 4500X and 18000X. This range of magnification was sufficient to examine the extent of agglomeration in the sample and identify individual particles with satisfactory resolution. A low magnification micrograph of a typical segment is shown in Figure 5-2.

The photomicrographs were 4 x 5 in Polaroid 3000 prints. There was no distortion in the magnification in the horizontal axis of the photograph (5 in side). Because of the tilt angle of sample holder with reference to the electron beam, magnification along the vertical axis of the photograph (4 in side) was less than true magnification by a factor equal to the sine of the tilt angle. The tilt angle was approximately 45°.

The photomicrographs were labelled and then filed. They were subsequently examined at Avco with a Millipore *MC Particle Measurement and Computer System. With this device, the total number of particles in the photograph, the length mean particle diameter, \bar{D}_L , and the fractional surface coverage of the particles were measured. \bar{D}_L was measured along the horizontal axis (5 in side) of the photomicrograph where the magnification was accurately known. Because of the distortion in the other axis, measurement of \bar{D}_A , the surface mean particle diameter, would not have been meaningful. However, this does not apply to fractional surface coverage measurements since the projected image of surface coverage is independent of the angle of projection.



Figure S-2 FILTER SAMPLE IN SCANNING ELECTRON
MICROGRAPH

63-1291

5.4.2 Analysis of Individual Particles

The AMR microscope had a Princeton Gamma Tech (PGT) x-ray element analyzer accessory. This non-dispersive x-ray probe was used to obtain the elemental analysis of selected individual particles viewed by the microscope. With this device the x-ray spectra of various elements of $Z \geq 9$ in the sample are accumulated and displayed in a manner which permits rapid elemental identification.

5.4.3 Electron Microprobe Analysis

The average composition of various deposited samples was also obtained. A number of deposited samples were examined with a Norelco AMR/3 electron probe microanalyzer. Small segments of the ultrafiltration filter were cut out and coated with a light carbon deposit. A blank XM-100A filter was included in the samples studied.

After preliminary tests with focused beam of high intensity, the samples were examined with a 15 KV non-focused beam, approximately $200 \mu\text{m}$ in diameter. Because it was possible to place as many as 15 different samples in the instrument at one time, by setting the spectrometer to analyze for one element at a time, it was possible to analyze the samples very quickly.

Two spots of a given sample were examined for uranium (uranium dioxide), aluminum (Kaolin), calcium (calcium fluoride), fluorine (for residual organic fluorine and calcium fluoride) and carbon (for Sterling MT carbon black). Reference materials used for each of these elements were uranium metal, aluminum metal, calcium carbonate, lithium fluoride and graphite, respectively. Because of the carbon coating used in the sample preparation and because the filter is an organic polymer, the carbon measurements were made by difference, correcting for the carbon content of the blank filter. An additional correction is also required for the carbon content associated with residual dispersing media, which can be estimated from fluorine measurements, in the absence of calcium fluoride in the samples.

5.5 Experimental Results

5.5.1 Introduction

Deposited samples of each of the following powders were prepared and analyzed: ENL-1 Uranium Dioxide, Sterling MT Carbon Black, Peerless No. 2 Kaolin, Calcium Fluoride; five equal weight binary mixtures (UO_2 /Carbon Black, Kaolin/Carbon Black, CaF_2 /Carbon Black, UO_2 /Kaolin, UO_2 / CaF_2); two equal weight ternary mixtures (UO_2 /Carbon Black/ CaF_2 and UO_2 /Carbon Black/Kaolin), and one equal weight quaternary mixture of these powders.

The results are presented in selected scanning electron micrographs and in the tables which follow. Information relating to sample preparation, dispersion time, turbidity readings (where measured), powder loading, and expected surface coverage, (based on the powder content of the secondary dispersion and specific cross-sectional area of the deposited powder as discussed at the end of Appendix C), is presented for each powder or mixture in a specific table, as are the quantitative results obtained from the various

photomicrographs at different magnification levels. The results of microchemical analysis are summarized separately. Only limited turbidity data are reported because malfunction of the equipment precluded measurement of turbidity at the end of the test program.

All the data presented in these tables were obtained with washed powder samples deposited on Amicon XM-100A ultrafiltration membranes. It was not possible to examine unwashed samples deposited on the XM-100A membranes because these did not accept the gold/palladium coating. In the SEM, these samples accumulated charge and thus could not be examined. No quantitative data are presented for samples deposited on the other filters used as substrates because of the significantly lower quality of the results and the resulting difficulties in data interpretation.

Dispersions with a single powder component were made with powders that were not subjected to any pretreatment. In these runs, the primary dispersion normally contained 50 mg of powder in 25 ml of dispersing liquids, except for a few CaF_2 dispersions which contained 200 mg CaF_2 in 125 ml fluorinated liquid. Dispersions of binary, ternary, and quaternary mixtures were made with powders that were agitated dry for 6 hours as described in Section 2.2.3. In these tests the primary dispersions contained 60 mg of total powder weight per 25 ml of dispersing liquid. The binary mixtures contained 30 mg of each of two powders, the ternary mixtures contained 20 mg of each of three powders and the quaternary mixture contained 15 mg of each of the four candidate powders.

5.5.2 SEM Examination of Deposited Samples

The experimental runs carried out are summarized in Table 5-1, which lists the various powders examined and the corresponding tables (Table 5-2 to 5-13), and figures (Figures 5-3 to 5-56). Samples were prepared in the standard manner described above except as specifically noted. All figures refer to scanning electron photomicrographs except where noted.

5.5.3 Analysis of Individual Particles

For a selected number of samples, individual particles were also examined with the PGT x-ray analyzer. These measurements were performed on the same filter fraction as the SEM results presented in the previous section, but a month later. The photomicrographs represent a different region of the sample.

Figure 5-57 is a photomicrograph of sample FQ1-10. It was probed at points A, B and C. The corresponding spectra are presented in Figures 5-58 and 5-59. There is a common chlorine peak for all points examined. Point B is an area devoid of particles. The resulting spectrum is due to the composition of the XM-100A membrane. It indicates a high chlorine concentration, and the manufacturer was called to confirm this finding. According to Amicon, chlorine-containing material is used in the manufacture of the XM-100A membrane and analysis of the membrane would indicate the presence of chlorine. In addition to chlorine, the spectrum shown for A shows that the particle contains Al, Si and Au. The particle in question is evidently gold coated Kaolin. The spectrum for Point C shows peaks for Au, Cl and Ca; this would correspond to the presence of a small gold coated calcium fluoride particle.

TABLE 5-1

SUMMARY OF DEPOSITED SAMPLES EXAMINED BY SEM

<u>Powder</u>	<u>Table</u>	<u>Figures*</u>	<u>Comments</u>
UO ₂	5-2	5-3 to 5-13	Runs DAL-1 to DAL-17 prepared in standard manner. Runs DAL-18S to DAL-21S are sandwich runs. Figures 5-3 and 5-4 are macro-photographs of filters on which powder samples were deposited.
Sterling MT Carbon Black	5-3	5-14- to 5-20	
Calcium Fluoride	5-4	5-21 to 5-24	
Peerless No. 2 Kaolin	5-5	5-25 to 5-28	
Carbon Black/Kaolin Binary Mixture	5-6	5-29 to 5-34	
UO ₂ /Carbon Black Binary Mixture	5-7	5-35 to 5-41	The method of agitating the secondary dispersion was varied with samples FBL-8 and FBL-9. For sample FBL-8, the secondary dispersion was prepared by shaking the aliquot of primary dispersion with diluent fluorinated liquid. For sample FBL-9, the ultrasonic probe was used to prepare the secondary dispersion. The secondary dispersion was sonolated for 20 minutes with the probe. The reference is sample FBL-10 which was prepared in the standard manner. The secondary dispersion was sonolated in the bath for 50 min before filtration.
CaF ₂ /Carbon Black Binary Mixture	5-8	5-42	
UO ₂ /CaF ₂ Binary Mixture	5-9	5-43	
UC ₂ /Kaolin Binary Mixture	5-10	5-44	
UO ₂ /CaF ₂ /Carbon Black Ternary Mixture	5-11	5-45	
UO ₂ /Kaolin/Carbon Black Ternary Mixture	5-12	5-46	
UO ₂ /Kaolin/CaF ₂ / Carbon Black Quarternary Mixture	5-13	5-47 to 5-56	Run FQ1-10 prepared by "pousse cafe" wash method with Freon E-1 as wash liquid.

*Figures are scanning electron photomicrographs unless otherwise specified.

TABLE 5-2

DEPOSITION AND SEM EXAMINATION OF ENL-1 URANIUM DIOXIDE ON AMICON XM-100A ULTRAFILTER

Sample No.	UO ₂ Powder	DAL-1	DAL-2	DAL-3	DAL-4	DAL-5	DAL-6	DAL-7	DAL-8	DAL-9	DAL-10	DAL-11	DAL-12	DAL-13	DAL-14	DAL-15	DAL-16	DAL-17
Dispersion: Mass, mds.	-	1	10	40	100	120	270	400	415	415	503	503	503	610	678	678	678	678
Turbidity Index	11	26.2	54.5	69.0	72	95	MM	MM	10.0	100	105	105	105	95	75	1X	100	100
Aliquot Volume, μ l	200	200	200	200	350	700	400	400	200	50	200	200	200	50	200	50	20	10
Powder Weight on Filter, μ g	400	400	400	400	400	400	700	400	400	100	100	400	400	100	400	100	40	20
Powder Loading, μ g/cm ²	10.4	10.4	10.4	10.4	10.4	18.2	10.4	10.4	10.4	2.6	2.6	10.4	10.4	2.6	1.4	1.4	2.6	0.5
Surface Coverage, %	45.6	15.6	15.6	15.6	15.6	27.4	15.6	15.6	15.6	3.9	3.9	3.9	15.6	3.9	15.6	3.9	1.5	0.8
Magnification 450X																		
Number of Particles	77	351	MM	435	523	663	651	517	758	562	234	484	617	490	484	170	296	27
Length Average Particle Diameter, \bar{L}_p , μ m	26	1.77	1.44	1.60	2.87	1.51	1.53	1.53	1.57	1.35	1.70	1.38	5.98	1.48	1.82	1.14	1.19	1.31
Measured $\frac{1}{2}$ Surface Covered	29	3.2	3.6	4.5	12.1	5.4	3.7	6.5	3.4	1.0	3.0	3.0	25.6	3.7	3.5	1.8	0.6	0.15
Magnification 6500X																		
Number of Particles	44	106	MM	520	473	573	1003	1186	1014	955	715	1299	257	714	1000	1030	423	167
Length Average Particle Diameter, \bar{L}_p , μ m	1.7	.32	.25	.26	.31	.33	.24	.24	.384	.22	.24	.250	.81	.39	.27	.254	.231	.19
Measured $\frac{1}{2}$ Surface Covered	28	2.7	9.1	8.5	14.1	21.6	16.6	24.2	11.3	4.1	1.1	1.1	29.1	16.4	15.5	16.1	5.2	0.8
Magnification 16500X																		
Number of Particles	10	10	107	109	122	272	348	332	301	170	3.1	178	78	253	238	151	19	36
Length Average Particle Diameter, \bar{L}_p , μ m	.18	.18	.16	.16	.18	.17	.181	.22	.22	.21	.12	.23	.10	.16	.12	.12	.11	.10
Measured $\frac{1}{2}$ Surface Covered	0.9	0.9	9.2	14.0	25.0	26.1	25.0	14.0	14.0	14.0	17.4	27.0	2.0	16.2	1.3	1.0	0.5	1.2

Table 5-2 (cont.)

Sample No.	DAI-18*	DAI-18*	DAI-18*
Dispersion: Filter, etc.	678	100	100
Turbidity Index	100	100	100
Aliquot Volume, ml	100	100	100
Powder Weight on Filter, mg	200	100	20
Powder Loading, mg/cm ²	5.2	2.0	0.1
Surface Coverage, %	7.8	3.9	0.6
Magnification 450X	Top Filter	Top Filter	Bottom Filter
Number of Particles	102	102	102
Length Average Particle Diameter, \bar{L}_p , μ m	1.57	1.57	1.57
Measured % Surface Covered	1.3	1.3	11.0
Magnification 1500X	432	15	330
Number of Particles	0.32	0.21	0.2
Length Average Particle Diameter, \bar{L}_p , μ m	15.8	10.0	22.2
Measured % Surface Covered			
Magnification 1500X	501	152	150
Number of Particles	0.11	0.12	0.1
Length Average Particle Diameter, \bar{L}_p , μ m	1.1	1.1	1.1
Measured % Surface Covered			

*% dwtch 80's

TABLE 5-3
DEPOSITION AND SEM EXAMINATION OF STERILIZED MC CARBON BLACK ON AMICON XM-100A TRANSMITTER

Sample No.	Sterling MC Powder	DEL-1	DEL-2	DEL-3	DEL-4	DEL-5	FL-1	FL-2	FL-3	FL-4
Dispersion Time, Min.		1	10	54	83	180	210	210	210	210
Turbidity		←			NY					
Aliquot Volume, μ l	No Pre-treatment on Tape	50	50	50	50	50	10	20	50	100
Powder Weight on Filter, μ g		100	100	146	100	100	20	40	100	200
Powder Loading, μ g/cm ²		2.6	2.6	2.6	2.6	2.6	0.5	1.0	2.6	5.2
Surface Coverage, %		5.5	5.5	5.5	5.5	5.5	1.1	2.1	5.5	10.9
<u>Magnification 1500X</u>										
Number of Particles	98	751	602	415	454	425	98	290	460	890
Length Average Particle Diameter, \bar{D}_L , μ m	9.3	1.33	1.26	1.26	1.26	1.25	1.06	1.15	1.13	1.55
Comments Surface Covered, %	13.6	9.1	3.9	3.0	2.6	2.5	0.4	1.4	2.2	6.5
<u>Magnification 1500X</u>										
Number of Particles	1208	181	297	295	183	270	90	101	182	366
Length Average Particle Diameter, \bar{D}_L , μ m	1.4	0.50	0.44	0.48	0.55	0.44	0.24	0.354	0.21	0.54
Comments Surface Covered, %	40	8.2	9.8	9.4	4.6	8.5	1.3	2.6	7.2	16.4
<u>Magnification 1500X</u>										
Number of Particles	85	96	92	92	78	33	25	21	15	124
Length Average Particle Diameter, \bar{D}_L , μ m	1.96	0.146	0.22	0.22	0.16	0.31	0.10	0.24	0.44	-
Comments Surface Covered, %	12.6	7.2	11.7	11.7	7.3	8.9	1.6	3.8	5.6	-

TABLE 5-4

DEPOSITION AND SEM EXAMINATION OF PRECIPITATED CALCIUM FLUORIDE ON AMICON XM-100A ULTRAFILTER

Sample No.	CaF ₂	DDL-1	DDL-2	DDL-3	DDL-4	DDL-5	EC-1	F3-1	F3-2	F3-3	F3-4
Dispersion Time, Min.		1	10	30	60	63	71	360	360	360	360
Turbidity		8	15	NM	NM	NM	26	NM	NM	NM	NM
Aliquot Volume, μ l	No Pretreatment on Tape	10	10	10	10	20	10	10	20	50	100
Powder Weight on Filter, μ g		80	80	80	80	160	80	20	40	100	200
Powder Loading, μ g/cm ²		2.1	2.1	2.1	2.1	4.2	2.1	0.5	1.0	2.5	5.2
Surface Coverage, %		5.9	5.3	5.3	5.3	10.3	5.3	1.3	2.5	6.3	13.0
<u>Magnification 4500X</u>											
Number of Particles	209	105	156	157	90	248	75	54	38	102	94
Length Average Particle Diameter, \bar{D}_L , μ m	9.2	1.69	1.41	1.36	1.36	1.40	1.49	1.10	1.66	1.22	2.00
Measured Surface Coverage, %	27.3	1.3	0.9	1.2	0.6	1.6	0.6	0.2	0.3	0.5	1.2
<u>Magnification 4500X</u>											
Number of Particles	3	101	272/416	375	155	561	313	294	151	237	397
Length Average Particle Diameter, \bar{D}_L , μ m	6.1	.28	.22-/.34	.23	.22	.26	.22	.31	.17	.25	0.24
Measured Surface Coverage, %	52.2	1.7	3.2/9.4	4.9	1.9	9.4	4.1	6.0	1.2	3.6	5.4
<u>Magnification 18000X</u>											
Number of Particles		12	15/16	164/54	54	113	65/46	193	40	75	100
Length Average Particle Diameter, \bar{D}_L , μ m		.22	.15-/.12	.15-/.15	.14	.22	.15/.097	0.098	.086	.13	.12
Measured Surface Coverage, %		1.9	0.6/1.2	10.5/2.6	4.0	7.5	1.4/1.6	5.8	1.0	5.0	5.5

TABLE 5-5

DEPOSITION AND SEM EXAMINATION OF PFERLESS NO. 2 KAOLIN ON AMICON XM-100A ULTRAFILTER

Sample No.	Kaolin Powder							
Dispersion Time, Min.	DCL-1	DCL-2	DCL-3	DCL-4	F2-1	F2-2	F2-3	F2-4
Turbidity	1.0	10	30	60	180	180	180	180
Aliquot Volume, μ l	30	32	32	36	NM	NM	NM	NM
Powder Weight on Filter, μ g	50	50	50	50	10	20	50	100
Powder Loading, μ g/cm ²	100	100	100	100	20	40	100	200
Kaolin Surface Coverage, %	2.6	2.6	2.6	2.6	0.5	1.0	2.6	5.2
	16.2	16.2	16.2	16.2	3.1	6.3	16.2	32.5
Magnification 450X								
Number of Particles	214	238	216	257	NM	71	158	298
Length Average Particle Diameter, \bar{D}_L , μ m	11.8	2.12	2.50	1.75	1.60/1.45	2.50	1.53	2.52
Measured Surface Coverage, %	31.8	3.1	4.8	2.8	0.3/0.4	0.8	1.2	4.3
Magnification 4500X								
Number of Particles	81	59	176	NM	91	206	308	266
Length Average Particle Diameter, \bar{D}_L , μ m	0.40	0.44	0.35		.23	.28	.270	.370
Measured Surface Coverage, %	3.8	2.3	5.1		1.1	5.5	6.6	9.4
Magnification 18000X								
Number of Particles	9	NM	NM	NM	44	69	62	NM
Length Average Particle Diameter, \bar{D}_L , μ m	.144				.13	.16	.270	
Measured Surface Coverage, %	.5				12.5	4.7	12.2	

TABLE 5-6

DEPOSITION AND SEM EVALUATION OF KAOLIN/CARBON BLACK HEAVY MIXTURE

Sample No.	FB3-1	FB3-2	FB3-3	FB3-4	FB3-5	FB3-6	FB3-7
Dispersing Time, min	1	10	50	130	130	130	130
Aliquot Volume, μ l	50	50	50	10	20	50	100
Weight Carbon Black on Filter, μ g	60	60	60	12	24	60	120
Loading Carbon Black on Filter, μ g/cm ²	1.6	1.6	1.6	0.3	0.6	1.6	3.2
Carbon Black Surface Coverage %	3.3	3.3	3.3	0.65	1.3	3.3	6.6
Weight Kaolin on Filter, μ g	60	60	60	12	24	60	120
Loading Kaolin on Filter, μ g/cm ²	1.6	1.6	1.6	0.3	0.6	1.6	3.2
Kaolin Surface Coverage %	9.7	9.7	9.7	2.0	3.9	9.7	19.4
Total Surface Coverage %	13.0	13.0	13.0	2.6	5.2	13.0	26.0
<u>Magnification 4500X</u>							
Number of Particles	509	526	801	272	408	707	942
Length Average Particle Diameter, \bar{D}_L , μ m	1.49	1.67	1.82	1.18	1.17	1.32	1.48
Comments Surface Coverage %	4.0	4.2	7.3	1.4	2.0	4.5	6.7
<u>Magnification 4500X</u>							
Number of Particles	123	77	121	122	122	201	178
Length Average Particle Diameter, \bar{D}_L , μ m	0.55	0.72	0.66	0.31	0.34	0.46	0.45
Comments Surface Coverage %	5.7	5.7	7.5	3.4	3.5	7.9	6.1
<u>Magnification 18000X</u>							
Number of Particles	16	29	39	27	5	37	30
Length Average Particle Diameter, \bar{D}_L , μ m	0.37	0.42	0.21	0.17	.08 / .15	.27	.29
Comments Surface Coverage %	5.3	37.0	.0	2.3	2.5 / 1.6	7.1	6.8

TABLE V5-7
DEPOSITION AND SEM EXAMINATION OF UO₂/CARBON BLACK BINARY MIXTURE

Sample No.	FEL-1	FEL-2	FEL-3	FEL-4	FEL-5	FEL-6	FEL-7	FEL-8	FEL-9	FEL-10	FEL-11
Dispersion Time, Min.	1	10	100	133	133	133	133	578	578	578	578
Aliquot Volume, μ l	50	50	50	10	20	50	100	10	10	10	20
Weight UO ₂ on Filter, μ g	60	60	60	12	24	60	120	12	12	12	24
Loading UO ₂ on Filter, μ g/cm ²	1.6	1.6	1.6	0.3	0.6	1.6	3.2	0.3	0.3	0.3	0.6
UO ₂ Surface Coverage, %	2.4	2.4	2.4	0.9	0.9	2.4	4.8	0.5	0.5	0.5	0.9
Weight C Black on Filter, μ g	60	60	60	12	24	60	120	12	12	12	24
Loading C Black on Filter, μ g/cm ²	1.6	1.6	1.6	0.3	0.6	1.6	3.2	0.3	0.3	0.3	0.6
C Black Surface Coverage, %	3.4	3.4	3.4	0.6	1.2	3.4	6.8	0.6	0.6	0.6	1.2
Total Surface Coverage, %	5.8	5.8	5.8	1.1	2.1	5.8	11.6	1.1	1.1	1.1	2.1
<u>Magnification 4500X</u>											
Number of Particles	167	868	748	343	562	1150	898	114	283	228	266
Length Average Particle Diameter, \bar{D}_L , μ m	9.2	1.65	1.42	1.48	1.27	2.12	1.51	1.45	1.74	1.13	1.05
Measured Surface Coverage, %	20.0	8.0	5.7	2.7	3.5	12.5	6.8	17	2.7	1.0	1.1
<u>Magnification 4500X</u>											
Number of Particles	12	193	160	169	12/73	113	234/140	45	284	117	112
Length Average Particle Diameter, \bar{D}_L , μ m	4.8	.32	.464	.304	2.46/.48	.74	.34/.86	.40	.40	.27	0.31
Measured Surface Coverage, %	41.0	5.8	6.4	3.6	1.5/3.4	8.9	6.3/9.8	17	7.5	1.9	2.4
<u>Magnification 18000X</u>											
Number of Particles	6	10	3	11/15	1	17	1109	14	23	56	11
Length Average Particle Diameter, \bar{D}_L , μ m	.218	.256	.61	.25/.13	1 x 3	.19	.054	.27	.16	.10	.28
Measured Surface Coverage, %	0.9	1.6	0.9	.7/.9	1.6	11.9	1.6	2.8	1.2	1.6	1.8

TABLE 5-8

DEPOSITION AND SEM EXAMINATION OF CaF_2 /CARBON BLACK BINARY MIXTURE

Sample No.	FB2-2	FB2-1	FB2-2	FB2-3	FB2-4	FB2-5	FB2-6	FB2-7
Dispersing Time, min		1	10	100	130	130	130	130
Aliquot Volume, μl		50	50	50	10	20	50	100
Weight CaF_2 on Filter, μg	No Treatment on Tape	60	60	60	12	24	60	120
Loading CaF_2 on Filter, $\mu\text{g}/\text{cm}^2$		1.6	1.6	1.6	0.3	0.6	1.6	3.6
CaF_2 Surface Coverage %		4.0	4.0	4.0	0.8	1.5	4.0	8.0
Weight Carbon Black on Filter, μg		60	60	60	12	24	60	120
Loading Carbon Black on Filter, $\mu\text{g}/\text{cm}^2$		1.6	1.6	1.6	0.3	0.6	1.6	3.6
Carbon Black Surface Coverage %		3.3	3.3	3.3	0.5	1.3	3.3	6.5
Total Surface Coverage %		7.3	7.3	7.3	1.5	2.8	7.3	14.5
Magnification 450X								
Number of Particles		1142	724	687	315	544	1238	889
Length Average Particle Diameter, \bar{D}_L , μm		1.48	1.65	2.37	1.20	1.21	1.60	1.36
Measured Surface Coverage %		6.0	6.1	11.5	1.1	2.55	9.7	5.7
Magnification 4500X								
Number of Particles		88	147	62	98	31	173	3291
Length Average Particle Diameter, \bar{D}_L , μm		.73	.52	.64	.30	.29	.41	.42
Measured Surface Coverage %		5.8	6.1	3.9	2.0	8.6	5.9	5.9
Magnification 18000X								
Number of Particles		23	28	12	9	49	19	112
Length Average Particle Diameter, \bar{D}_L , μm		.200	.312	1.20	.48	.22	.18	.43
Measured Surface Coverage %		2.5	7.4	15.9	5.5	12.5	4.7	12.5

TABLE 5-9
DEPOSITION AND SEM EXAMINATION OF UO_2/CaF_2 BINARY MIXTURE

Sample No.	FBP-4	FB4-1	FB4-2	FB4-3	FB4-4	FB4-5	FB4-6	FB4-7
Dispersing Time, Min.		1	10	100	130	130	130	130
Aliquot Volume, μ l	No Treatment on Tape	50	50	50	10	20	50	100
Weight UO_2 on Filter, μ g		60	60	60	10	20	50	100
Loading UO_2 on Filter, μ g/cm ²		1.6	1.6	1.6	0.3	0.6	1.6	3.2
UO_2 Surface Coverage %		2.4	2.4	2.4	0.5	0.9	2.4	4.8
Weight CaF_2 on Filter, μ g		60	60	60	12	24	60	120
Loading CaF_2 on Filter, μ g/cm ²		2.7	2.7	2.7	0.6	1.1	2.7	5.3
CaF_2 Surface Coverage %		6.8	6.8	6.8	1.5	2.8	6.8	13.2
Total Surface Coverage %		9.4	9.4	9.4	2.0	3.7	9.4	18.0
<u>Magnification 4500X</u>								
Number of Particles		277	165	525	157	165	235	378
Length Average Particle Diameter, \bar{D}_L , μ m		1.38	1.30	1.51	1.26	1.45	1.40	1.33
Measured Surface Coverage %		1.8	1.0	3.9	0.9	1.2	1.5	2.5
<u>Magnification 4500X</u>								
Number of Particles	17	404	372	487	375	391	588	695
Length Average Particle Diameter, \bar{D}_L , μ m	11.9	0.22	0.23	0.32	0.23	0.23	0.27	0.30
Measured Surface Coverage %	43	5.1	4.5	9.6	4.5	4.6	6.2	12.6
<u>Magnification 18000X</u>								
Number of Particles		114	195	32	25	85	110	13
Length Average Particle Diameter, \bar{D}_L , μ m		.13	.13	.15	.14	.10	.14	.17
Measured Surface Coverage %		6.3	9.9	1.9	0.9	3.4	8.0	8.2

TABLE 5-10

DEPOSITION AND SEM EXAMINATION OF UO_2 /KAOLIN BINARY MIXTURE

Sample No.	FB5-1	FB5-2	FB5-3	FB5-4	FB5-5	FB5-6	FB5-7
Dispersing Time, Min.	1	10	100	130	130	130	130
Aliquot Volume, μ l	50	50	50	10	20	50	100
Weight UO_2 on Filter, μ g	60	60	60	12	24	60	120
Loading UO_2 on Filter, μ g/cm ²	1.6	1.6	1.6	0.3	0.6	1.6	3.2
UO_2 Surface Coverage %	2.4	2.4	2.4	0.5	0.9	2.4	4.8
Weight Kaolin on Filter, μ g	60	60	60	12	24	60	120
Loading Kaolin on Filter, μ g/cm ²	1.6	1.6	1.6	0.3	0.6	1.6	3.2
Kaolin Surface Coverage %	9.7	9.7	9.7	2.0	3.9	9.7	19.4
Total Surface Coverage %	12.1	12.1	12.1	2.5	4.8	12.1	24.2
<u>Magnification 4500X</u>							
Number of Particles	260	194	317	54	205	260	462
Length Average Particle Diameter, \bar{D}_L , μ m	1.78	1.48	1.52	1.31	1.34	1.42	1.43
Measured Surface Coverage %	2.3	1.2	2.4	0.4	1.3	1.8	3.2
<u>Magnification 4500X</u>							
Number of Particles					122	155	222
Length Average Particle Diameter, \bar{D}_L , μ m					0.26	0.22	0.19
Measured Surface Coverage %					2.3	3.1	4.4
<u>Magnification 18000X</u>							
Number of Particles					21	24	27
Length Average Particle Diameter, \bar{D}_L , μ m					1.0 / 0.1	0.8	0.91
Measured Surface Coverage %					3 / 1.1	1.1	1.2

TABLE 5-11

REDUCTION AND NEW REDUCTION OF $\text{NO}_2/\text{O}_2/\text{C}$ (CARBON MASS) TEMPERATURE

Sample No.	FI-1	FI-2	FI-3	FI-4	FI-5	FI-6	FI-7
Operating time, min.	1	10	100	130	130	130	130
Aluminum volume, μm^3	50	50	50	10	20	50	100
Weight NO_2 on filter, μg	40	40	40	8	1	40	80
Limiting NO_2 on filter, $\mu\text{g}/\text{cm}^2$	1.0	1.0	1.0	0.2	0.4	1.0	2.1
NO_2 surface coverage %	1.5	1.5	1.5	0.3	0.6	1.5	3.1
Weight surface black on filter, μg	40	40	40	8	1	40	80
Limiting surface black on filter, $\mu\text{g}/\text{cm}^2$	1.0	1.0	1.0	0.2	0.4	1.0	2.1
Surface black, surface coverage	2.5	2.5	2.5	0.4	0.4	2.5	4.4
Weight of NO_2 on filter, μg	40	40	40	8	1	40	80
Limiting of NO_2 on filter, $\mu\text{g}/\text{cm}^2$	1.0	1.0	1.0	0.2	0.4	1.0	2.1
Gas, surface coverage	2.5	2.5	2.5	0.5	1.0	2.5	5.3
Peak surface coverage	6.2	6.2	6.2	1.2	2.5	6.2	12.8
Weight surface black	40	394	403	281	422	470	717
Weight of particles	40	1.54	2.0	1.1	1.2	1.32	1.33
Limiting surface particle diameter, \bar{D}_p , μm	40	2.1	4	1.1	2.2	2.0	1.8
Surface coverage	40	2.1	4	1.1	2.2	2.0	1.8
Weight surface black	40	394	403	281	422	470	717
Weight of particles	40	1.54	2.0	1.1	1.2	1.32	1.33
Limiting surface particle diameter, \bar{D}_p , μm	40	2.1	4	1.1	2.2	2.0	1.8
Surface coverage	40	2.1	4	1.1	2.2	2.0	1.8
Weight surface black	40	394	403	281	422	470	717
Weight of particles	40	1.54	2.0	1.1	1.2	1.32	1.33
Limiting surface particle diameter, \bar{D}_p , μm	40	2.1	4	1.1	2.2	2.0	1.8
Surface coverage	40	2.1	4	1.1	2.2	2.0	1.8

TABLE 5-12
DEPOSITION AND SEM EXAMINATION OF (UO₂/CARBON BLACK/KAOLIN) TERNARY MIXTURE

Sample No.	FT2-1	FT2-2	FT2-3	FT2-4	FT2-5	FT2-6	FT2-7
Dispersing Time, Min.	1	10	100	130	130	130	130
Aliquot Volume, μ l	50	50	50	10	20	50	100
Weight UO ₂ on Filter, μ g	40	40	40	8	16	40	80
Loading UO ₂ on Filter, μ g/cm ²	1.0	1.0	1.0	0.2	0.4	1.0	2.1
UO ₂ Surface Coverage %	1.5	1.5	1.0	0.3	0.6	1.5	3.2
Weight Carbon Black on Filter, μ g	40	40	40	8	16	40	80
Loading Carbon Black on Filter, μ g/cm ²	1.0	1.0	1.0	0.2	0.4	1.0	2.1
Carbon Black Surface Coverage %	2.2	2.2	2.2	0.4	0.9	2.2	4.4
Weight Kaolin on Filter, μ g	40	40	40	8	16	40	80
Loading Kaolin on Filter, μ g/cm ²	1.0	1.0	1.0	0.2	0.4	1.0	2.1
Kaolin Surface Coverage %	9.7	9.7	9.7	1.9	3.9	9.7	19.5
Total Surface Coverage %	13.4	13.4	13.4	2.6	5.4	13.4	27.1
Magnification 450X							
Number of Particles	760	823	268	353	1454	622	1014
Length Average Particle Diameter, \bar{D}_L , μ m	1.64	1.56	1.43	1.67	1.18	1.50	1.90
Measured Surface Coverage %	6.3	6.5	1.9	2.4	2.2	4.4	9.5
Magnification 4500X							
Number of Particles	107	285	1.4	377	322	256	40
Length Average Particle Diameter, \bar{D}_L , μ m	0.66	0.38	0.35	0.39	0.23	0.57	1.22
Measured Surface Coverage %	5.9	8.5	4.1	9.9	4.7	9.8	6.8
Magnification 18000X							
Number of Particles	37	18	5	34	19	34	294
Length Average Particle Diameter, \bar{D}_L , μ m	0.27	0.24	0.27	0.33	0.24	0.28	0.16
Measured Surface Coverage %	5.8	8.0	0.9	4.7	2.9	5.9	15.0

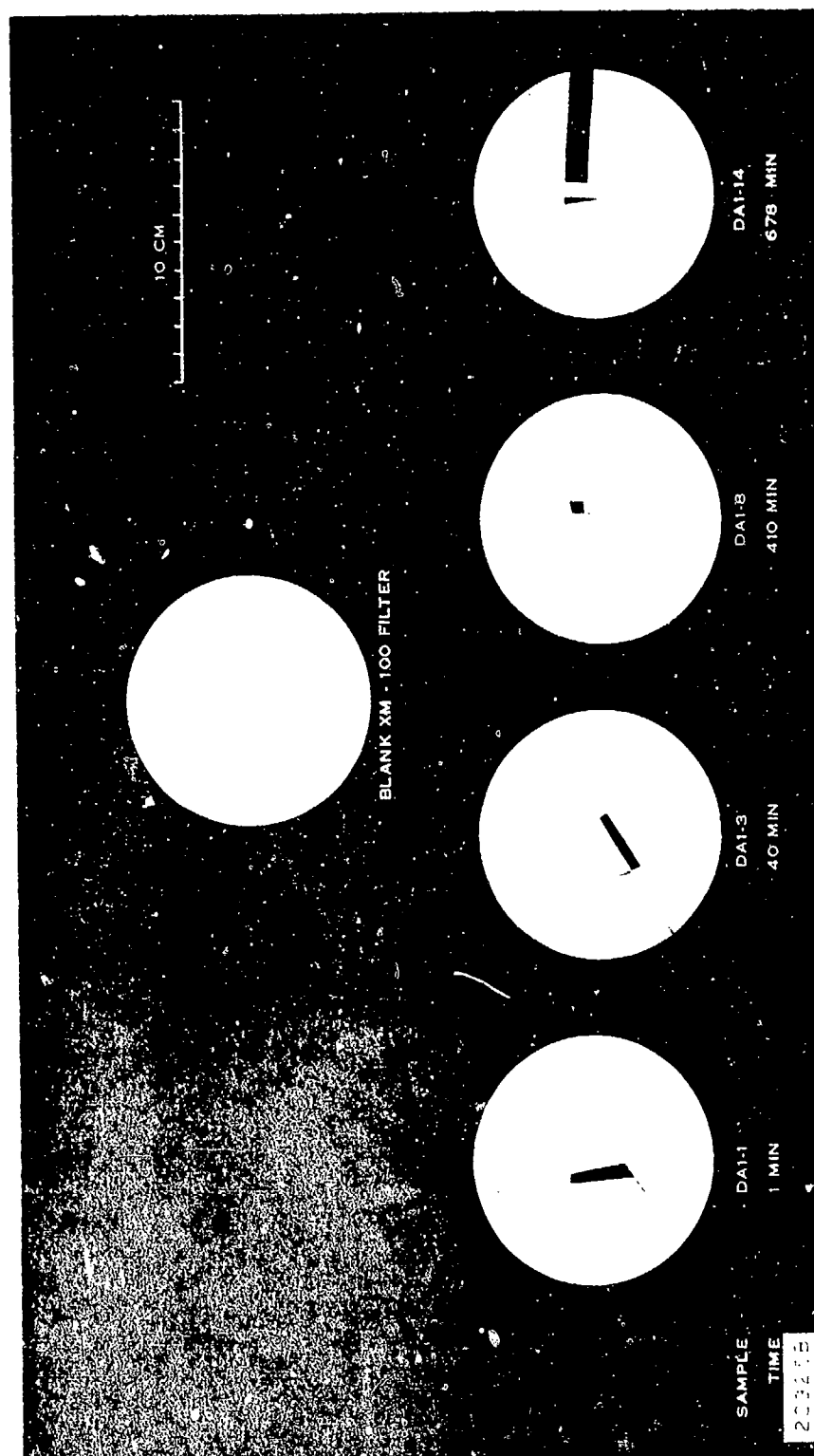


Figure 5-3 EFFECT OF SONOLATION TIME ON APPEARANCE OF
DISPERSED ENL-1 URANIUM DIOXIDE POWDER DEPOSITED
ON XM-100 ULTRAFILTER (POWDER LOADING = $10 \mu\text{g}/\text{cm}^2$)

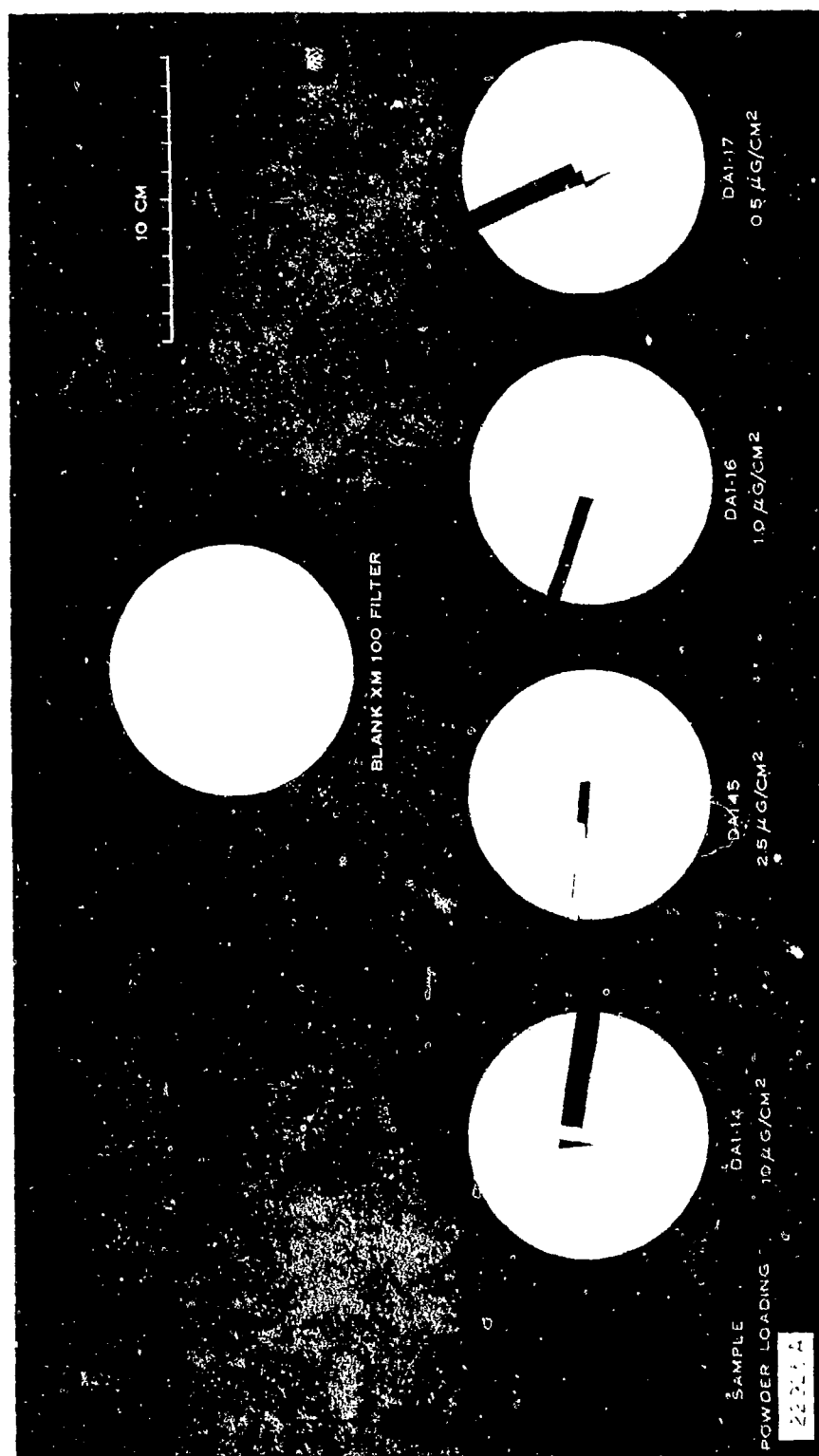


Figure 5-4 EFFECT OF POWDER LOADING ON APPEARANCE OF
DISPERSED ENL-1 URANIUM DIOXIDE POWDER DEPOSITED
ON XM 100 ULTRAFILTER (SONOLATION TIME 678 MIN)

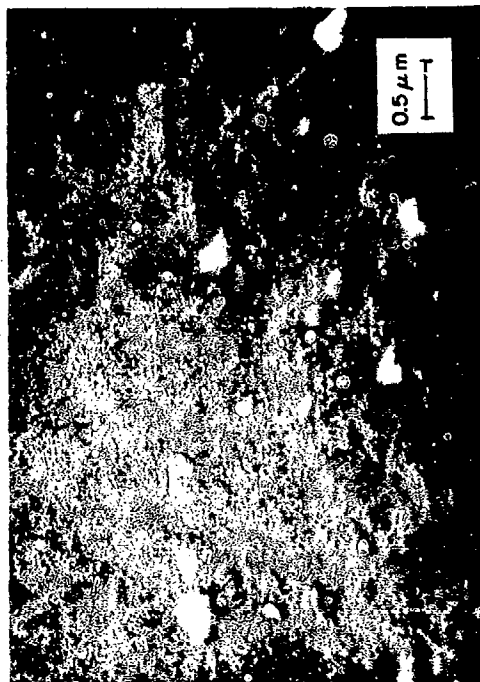


Figure 5-5 SEM PHOTOMICROGRAPH OF DEPOSITED UO_2
SAMPLE DA1-1

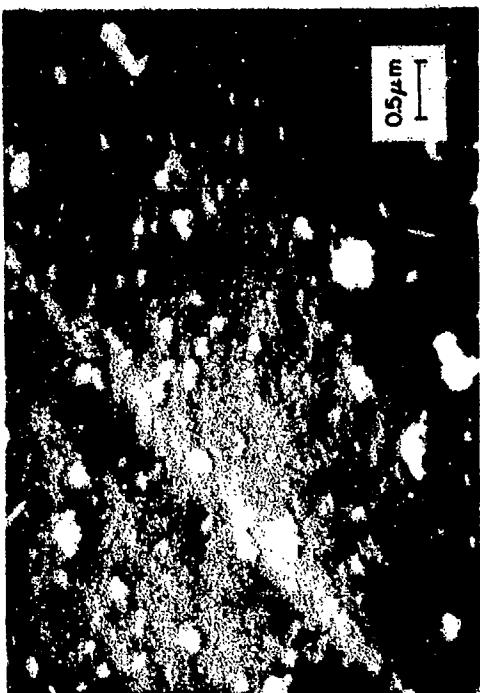


Figure 5-6 SEM PHOTOMICROGRAPH OF DEPOSITED UO_2
SAMPLE DA1-3

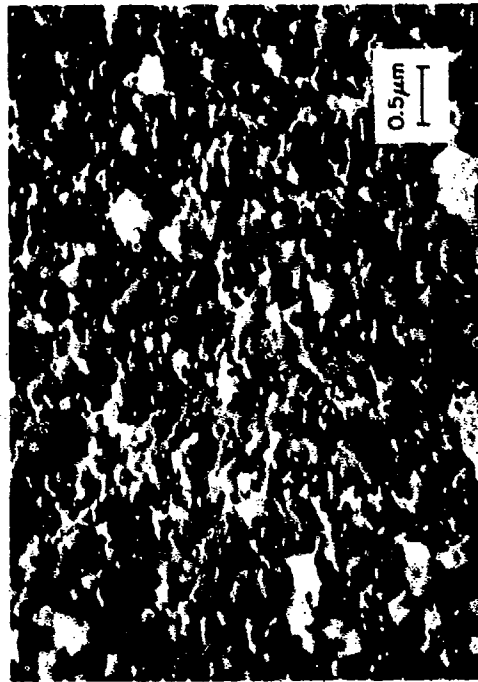
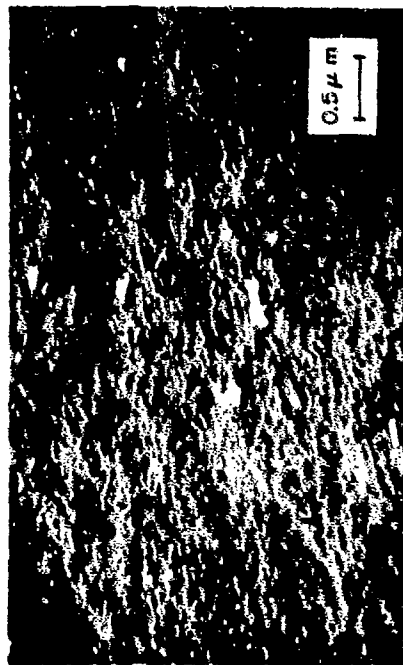


Figure 5-7 SEM PHOTOMICROGRAPH OF DEPOSITED UO_2
SAMPLE DA1-8



Figure 5-8 SEM PHOTOMICROGRAPH OF DEPOSITED UO_2
SAMPLE DA1-14

Reproduced from
best available copy.



SEM PHOTOMICROGRAPH OF DEPOSITED UO_2
SAMPLE DA1-14

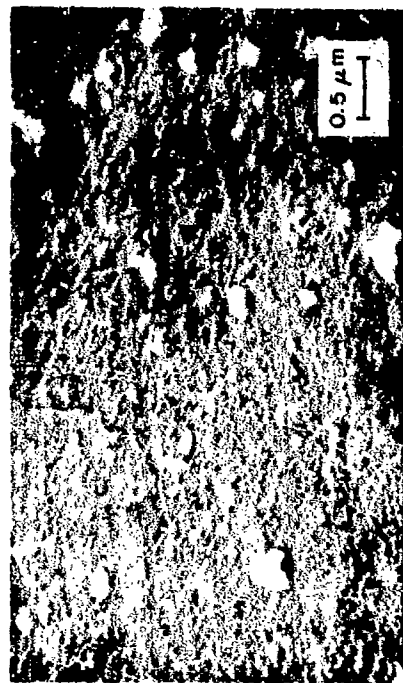
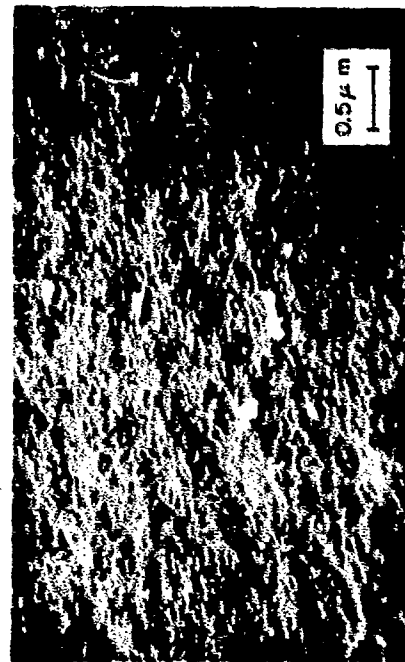


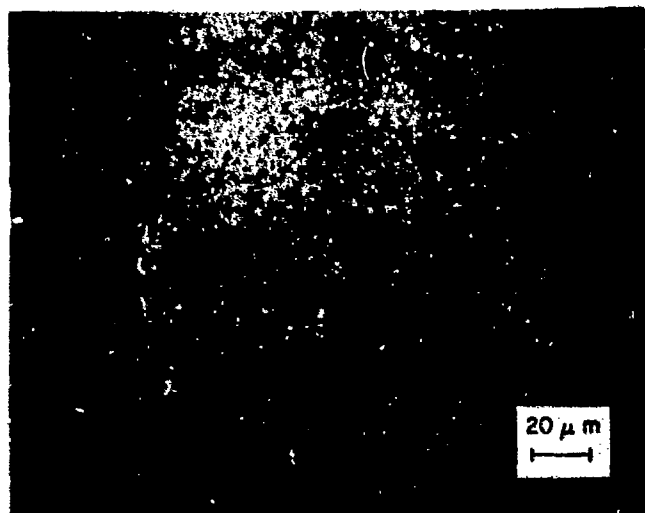
Figure 5-9 SEM PHOTOMICROGRAPH OF DEPOSITED UO_2
SAMPLE DA1-15



SEM PHOTOMICROGRAPH OF DEPOSITED UO_2
SAMPLE DA1-16

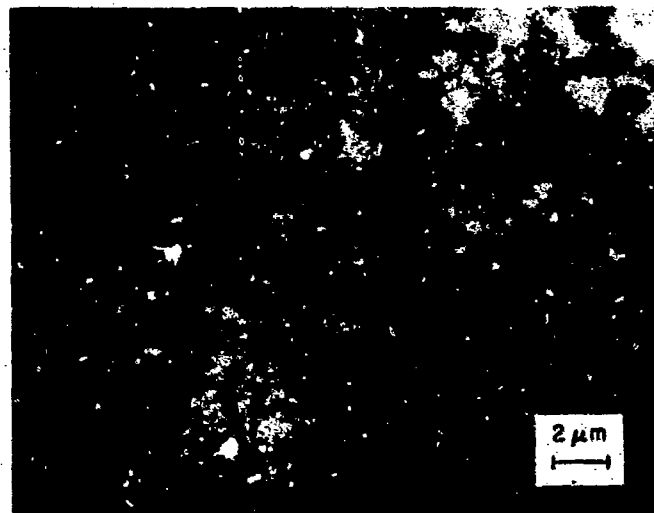


Figure 5-10 SEM PHOTOMICROGRAPH OF DEPOSITED UO_2
SAMPLE DA1-17



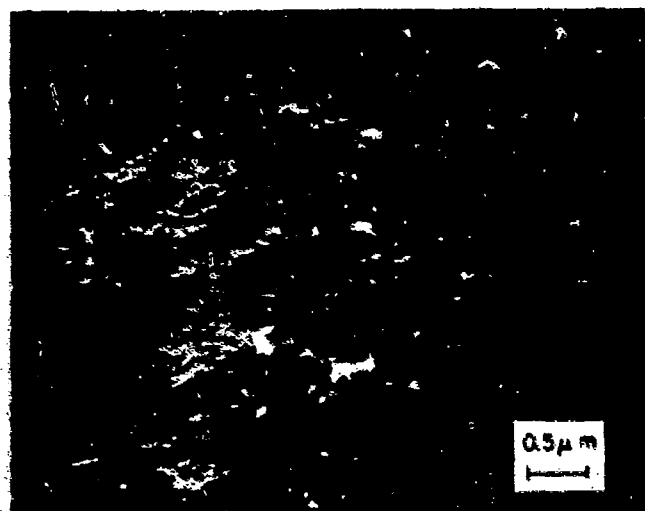
450X 1:1

Figure 5-11 SEM PHOTOMICROGRAPH OF DEPOSITED UO_2
SAMPLE DA1-16



4500X 1:1

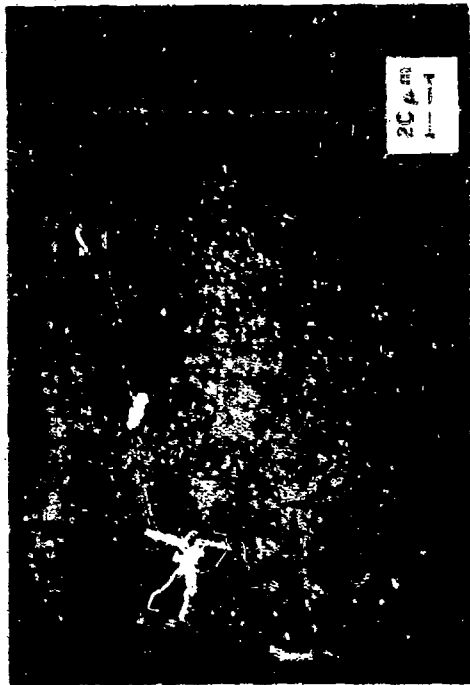
Figure 5-12 SEM PHOTOMICROGRAPH OF DEPOSITED UO_2
SAMPLE DA1-16



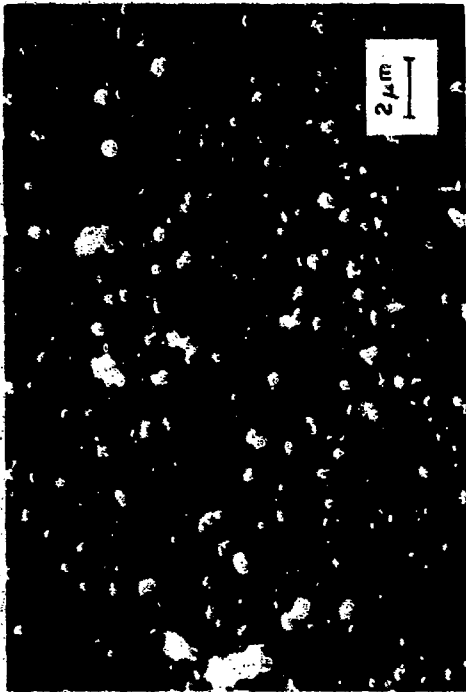
18000X 1:1

Figure 5-13 SEM PHOTOMICROGRAPH OF DEPOSITED UO_2
SAMPLE DA1-16

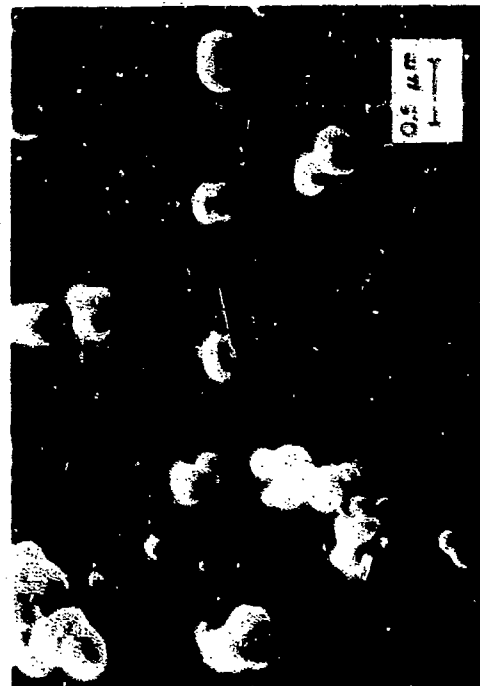
1-1295



450X 1:1
Figure 5-14 SEM PHOTOMICROGRAPH OF DEPOSITED CARBON
BLACK SAMPLE F1-3



4500X 1:1
Figure 5-15 SEM PHOTOMICROGRAPH OF DEPOSITED CARBON
BLACK SAMPLE F1-3



1800X 1:1
Figure 5-16 SEM PHOTOMICROGRAPH OF DEPOSITED CARBON
BLACK SAMPLE F1-3

83-1298

Reproduced from
best available copy.

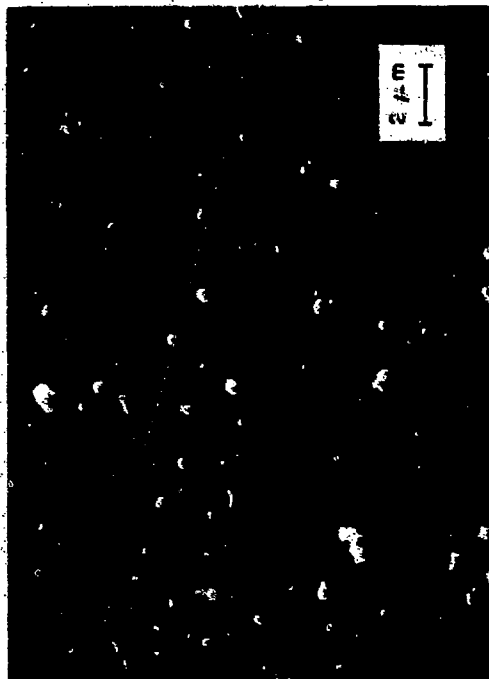


Figure 5-18 SEM PHOTOMICROGRAPH OF DEPOSITED CARBON
BLACK SAMPLE F1-2

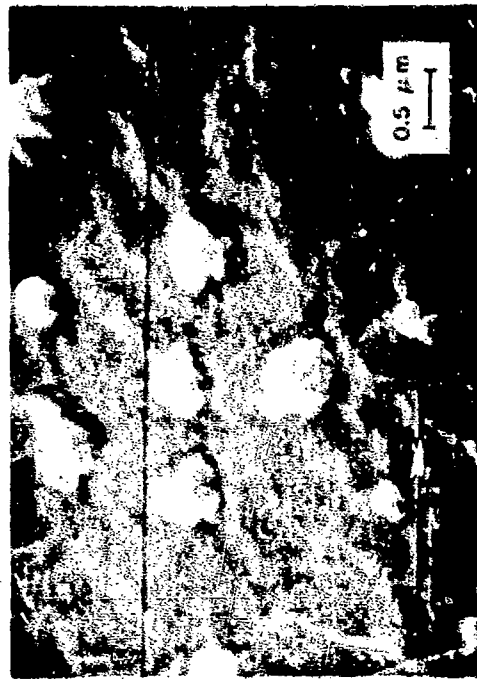


Figure 5-20 SEM PHOTOMICROGRAPH OF DEPOSITED CARBON
BLACK SAMPLE B1-1

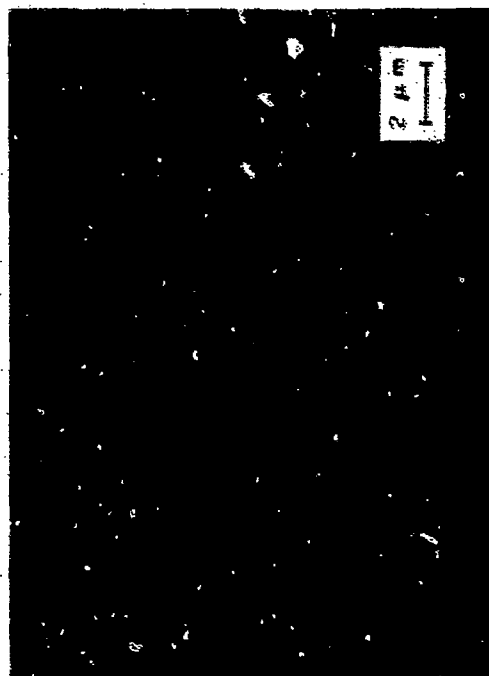


Figure 5-17 SEM PHOTOMICROGRAPH OF DEPOSITED CARBON
BLACK SAMPLE F1-1

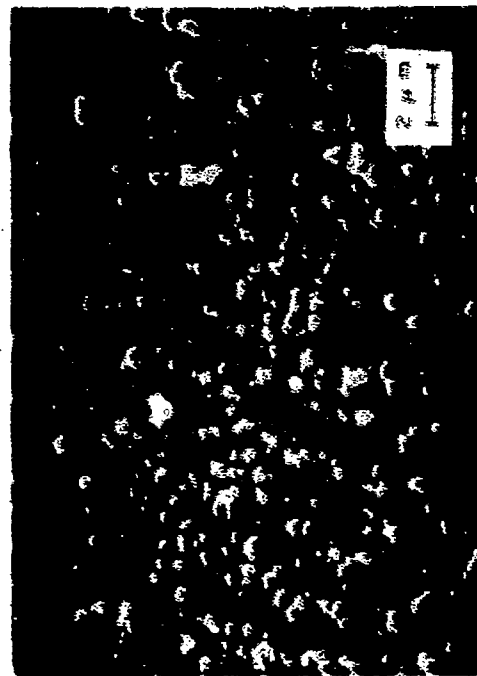


Figure 5-19 SEM PHOTOMICROGRAPH OF DEPOSITED CARBON
BLACK SAMPLE F1-4



Figure 5-21 SEM PHOTOMICROGRAPH OF DEPOSITED CaF_2
SAMPLE F3-1

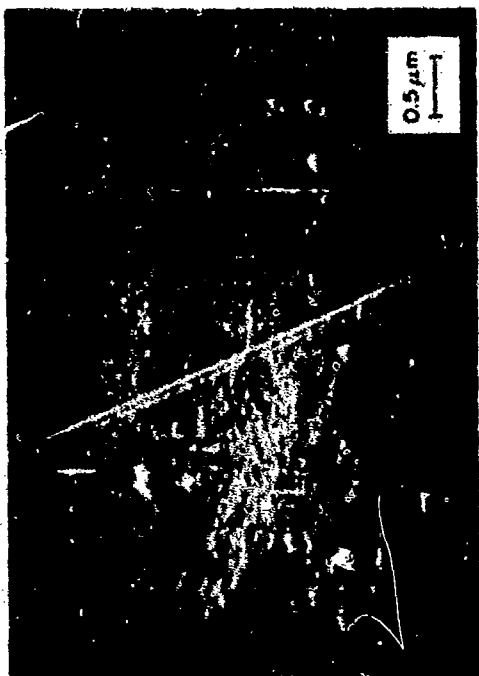


Figure 5-22 SEM PHOTOMICROGRAPH OF DEPOSITED CaF_2
SAMPLE F3-2

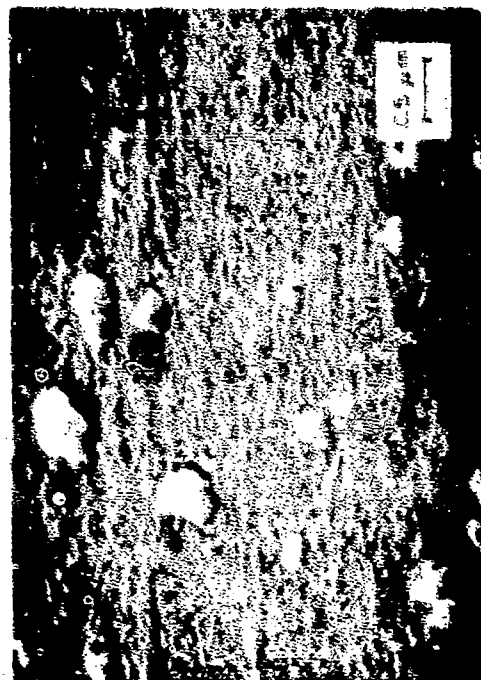


Figure 5-23 SEM PHOTOMICROGRAPH OF DEPOSITED CaF_2
SAMPLE F3-3

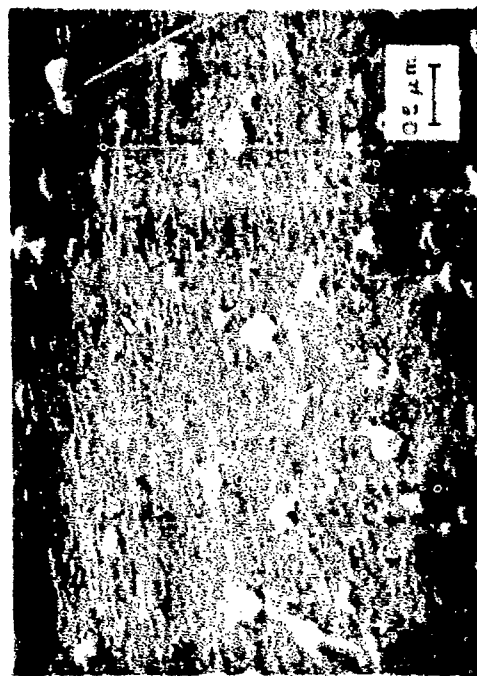


Figure 5-24 SEM PHOTOMICROGRAPH OF DEPOSITED CaF_2
SAMPLE F3-4

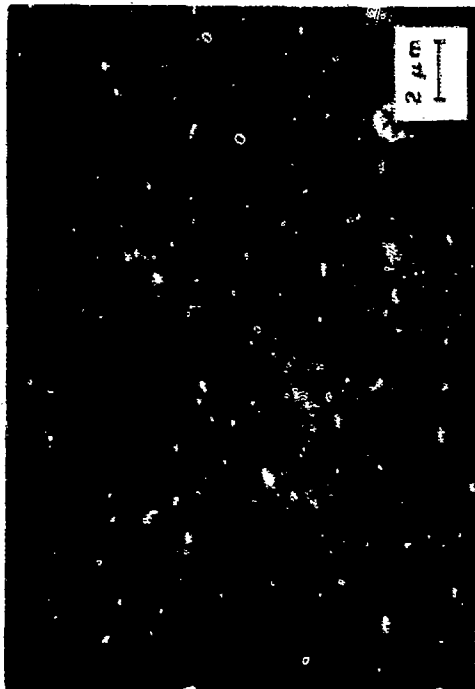


Figure 5-25 SEM PHOTOMICROGRAPH OF DEPOSITED KAOLIN
SAMPLE F2.1

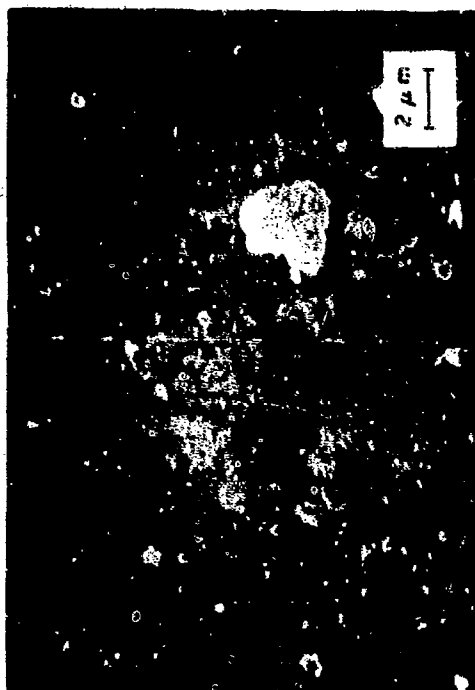


Figure 5-26 SEM PHOTOMICROGRAPH OF DEPOSITED KAOLIN
SAMPLE F2.2

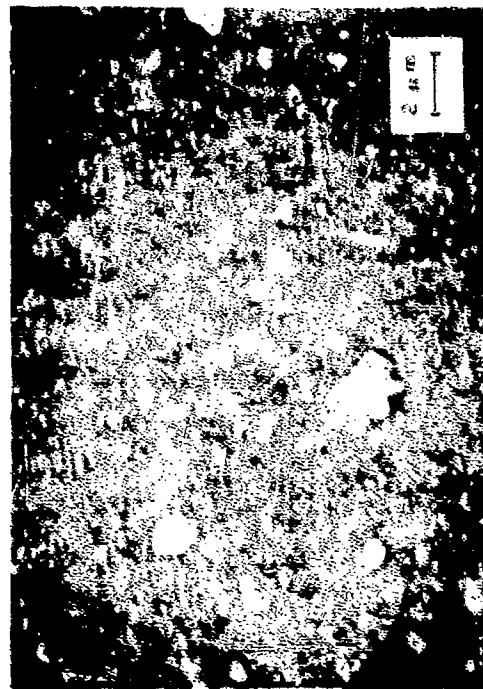
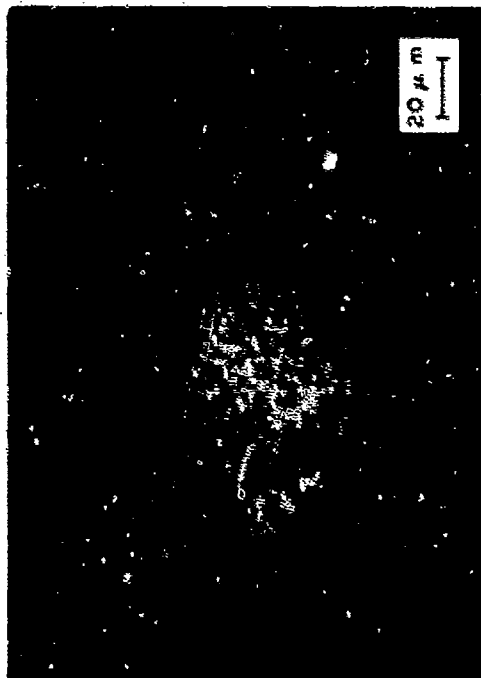


Figure 5-27 SEM PHOTOMICROGRAPH OF DEPOSITED KAOLIN
SAMPLE F2.3



Figure 5-28 SEM PHOTOMICROGRAPH OF DEPOSITED KAOLIN
SAMPLE F2.4



450X 1:1
Figure 5-20 SEM PHOTOMICROGRAPH OF BINARY (KAOLIN-CARBON BLACK) SAMPLE FB3-4



4500X 1:1
Figure 5-30 SEM PHOTOMICROGRAPH OF BINARY (KAOLIN-CARBON BLACK) SAMPLE FB3-4



18,000X 1:1
Figure 5-21 SEM PHOTOMICROGRAPH OF BINARY (KAOLIN-CARBON BLACK) SAMPLE FB3-4



Figure 5-12 SEM PHOTOMICROGRAPH OF BINARY KAOLIN-CARBON BLACK) SAMPLE FB3-2



Figure 5-13 SEM PHOTOMICROGRAPH OF BINARY KAOLIN-CARBON BLACK) SAMPLE FB3-5

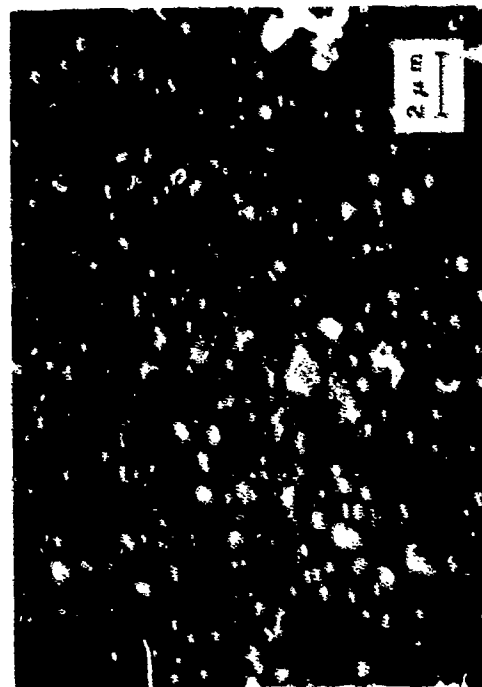
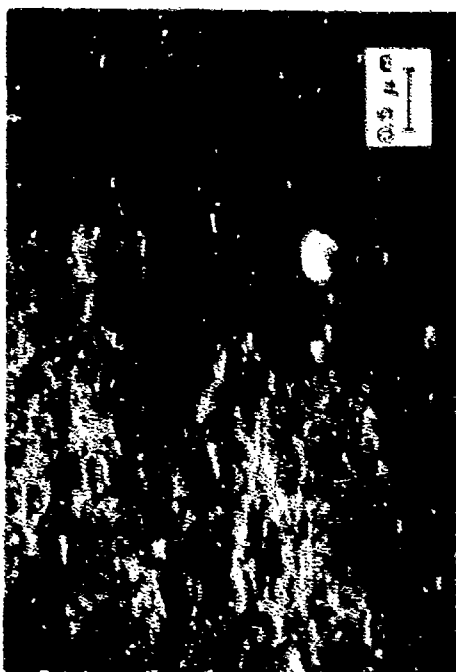


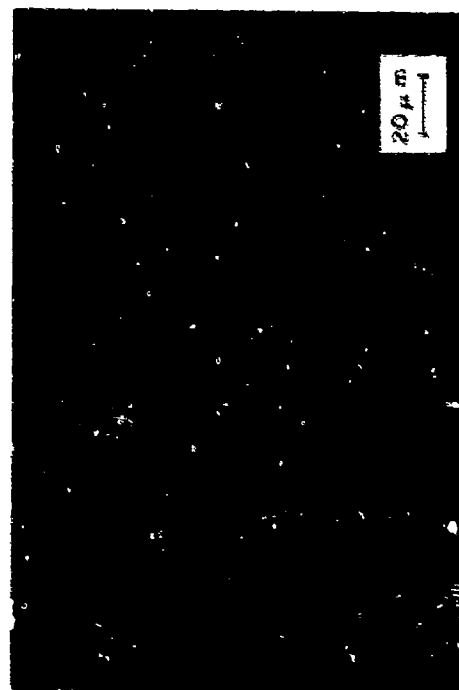
Figure 5-14 SEM PHOTOMICROGRAPH OF BINARY KAOLIN-CARBON BLACK) SAMPLE FB3-6



450X 1:1
Figure 5-15 SEM PHOTOMICROGRAPH OF BINARY UO_2 -
CARBON BLACK(S) SAMPLE FBI-10



4500X 1:1
Figure 5-36 SEM PHOTOMICROGRAPH OF BINARY
 UO_2 -CARBON BLACK(S) SAMPLE FBI-10



12000X 1:1
Figure 5-37 SEM PHOTOMICROGRAPH OF BINARY
 UO_2 -CARBON BLACK(S) SAMPLE FBI-10

Reproduced from
best available copy.



Figure 5-39 SEM PHOTOMICROGRAPH OF BINARY
(UO₂-CARBON BLACK) SAMPLE FB1-11

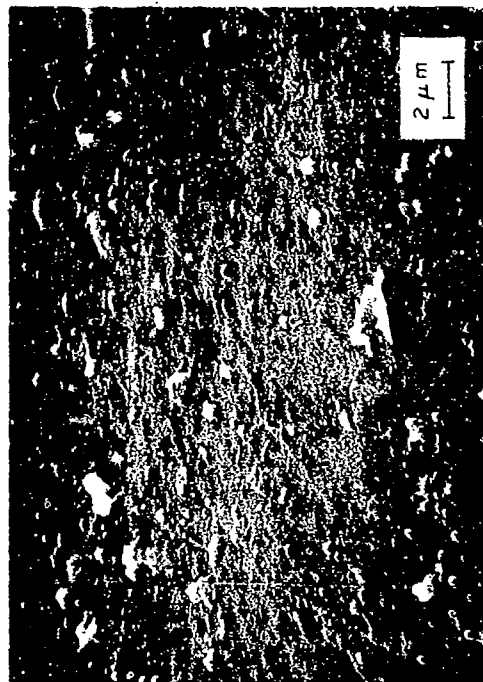


Figure 5-41 SEM PHOTOMICROGRAPH OF BINARY
(UO₂-CARBON BLACK) SAMPLE FB1-9

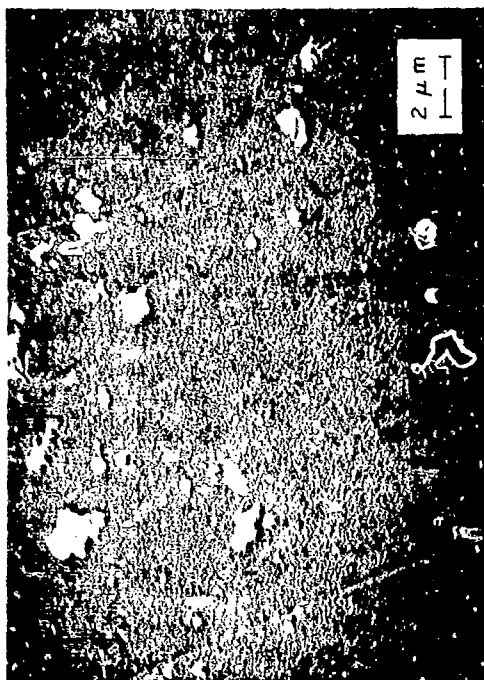


Figure 5-38 SEM PHOTOMICROGRAPH OF BINARY
(UO₂-CARBON BLACK) SAMPLE FB1-4

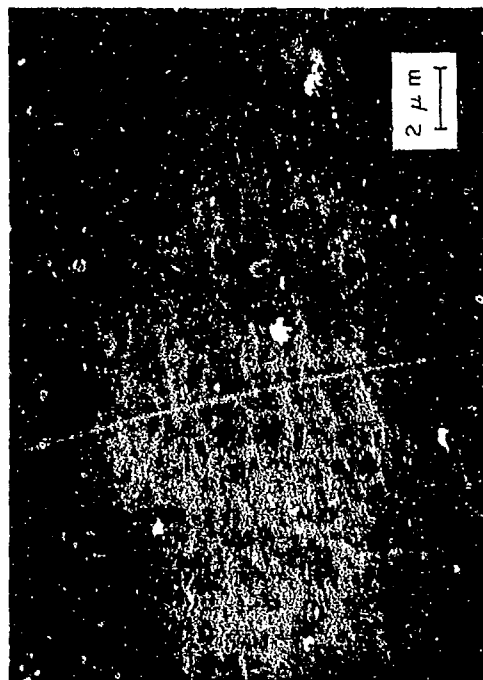


Figure 5-40 SEM PHOTOMICROGRAPH OF BINARY
(UO₂-CARBON BLACK) SAMPLE FB1-8



Figure 5-42 SEM PHOTOMICROGRAPH OF BINARY
(CaF_2 -CARBON) SAMPLE FB2-4

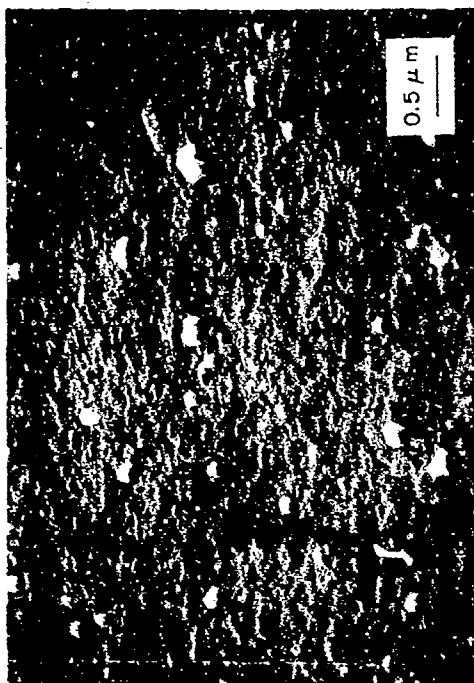


Figure 5-43 SEM PHOTOMICROGRAPH OF BINARY
(CaF_2 - UO_2) SAMPLE FB4-4

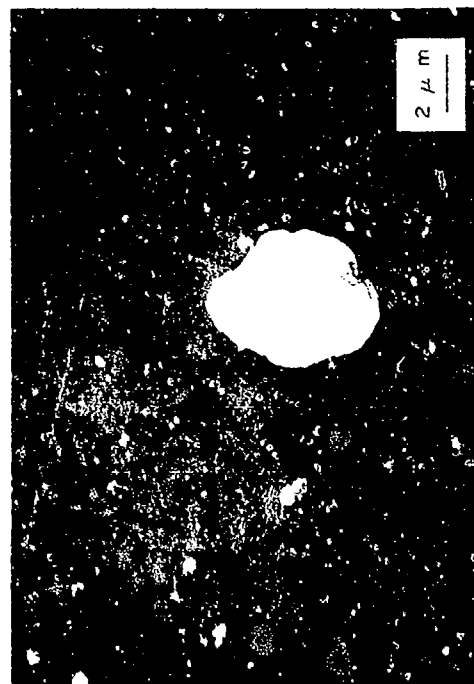


Figure 5-44 SEM PHOTOMICROGRAPH OF BINARY
(KAOLIN- UO_2) SAMPLE FB5-5

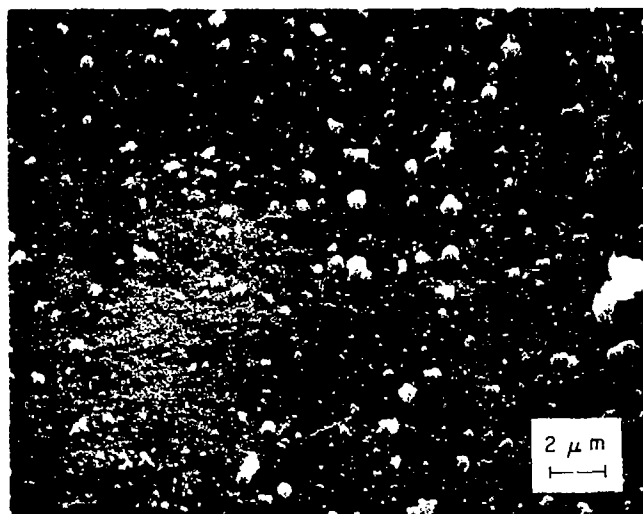


Figure 5-45 SEM PHOTOMICROGRAPH OF TERNARY
(UO_2 -CARBON BLACK- CaF_2) SAMPLE FT1-5

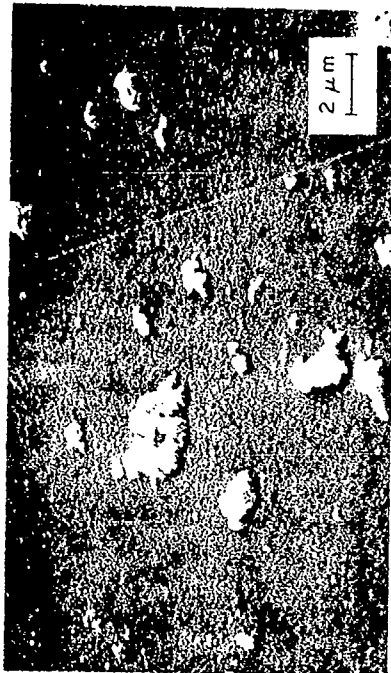


Figure 5-46 SEM PHOTOMICROGRAPH OF TERNARY
(UO_2 -CARBON BLACK-KAOLIN) SAMPLE FT2-5

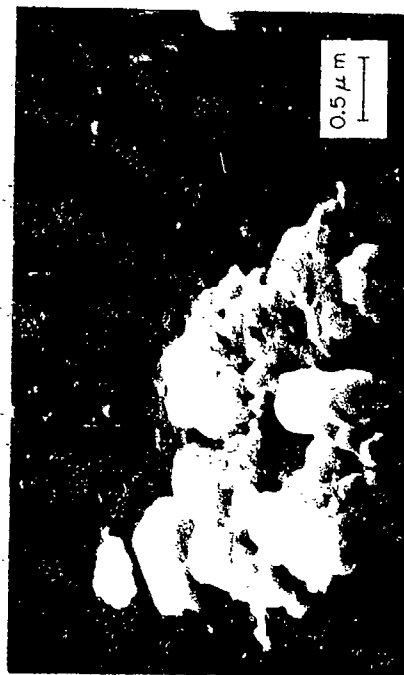
83 - 1304



450X 1:1
Figure 5-47 SEM PHOTOMICROGRAPH OF QUATERNARY
SAMPLE FQ1-3



4500X 1:1
Figure 5-48 SEM PHOTOMICROGRAPH OF QUATERNARY
SAMPLE FQ1-3



18000X 1:1
Figure 5-49 SEM PHOTOMICROGRAPH OF QUATERNARY
SAMPLE FQ1-3

83-1305



450X 1:1
Figure 5-50 SEM PHOTOMICROGRAPH OF QUARTERNARY
SAMPLE FQ1-8



4500X 1:1
Figure 5-51 SEM PHOTOMICROGRAPH OF QUARTERNARY
SAMPLE FQ1-8



18000X 1:1
Figure 5-52 SEM PHOTOMICROGRAPH OF QUARTERNARY
SAMPLE FQ1-8

83-1306

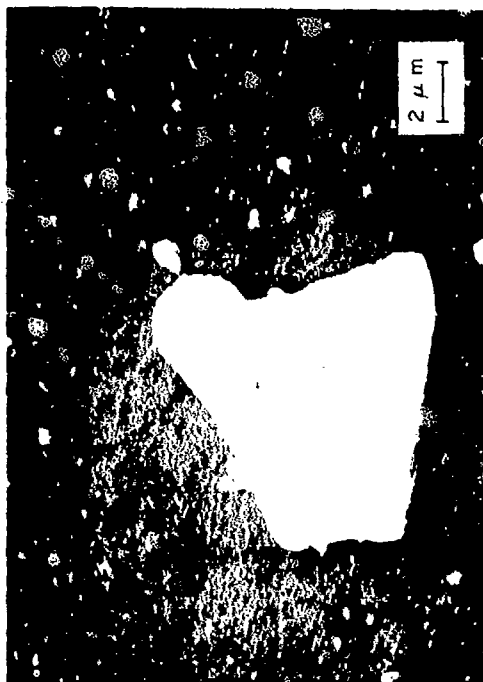


Figure 5-53 SEM PHOTOMICROGRAPH OF QUATERNARY
SAMPLE FQ1-4, SHOWING A LARGE KAOLIN PARTICLE



Figure 5-55 SEM PHOTOMICROGRAPH OF QUATERNARY
POWDER SAMPLE FQ1-10

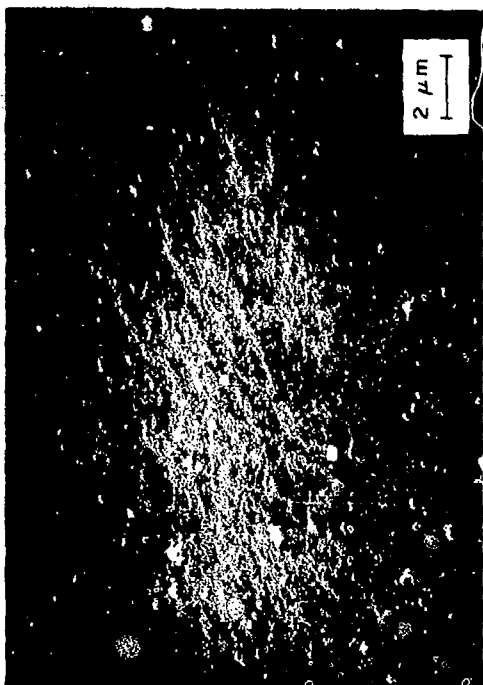


Figure 5-54 SEM PHOTOMICROGRAPH OF QUATERNARY
SAMPLE FQ1-9

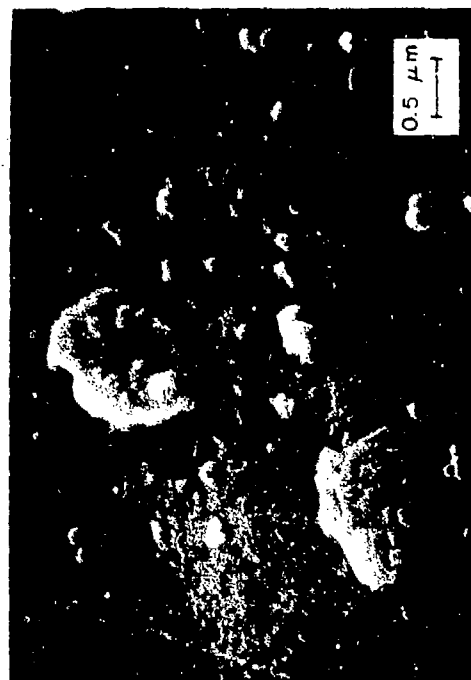


Figure 5-56 SEM PHOTOMICROGRAPH OF QUATERNARY
SAMPLE FQ1-10

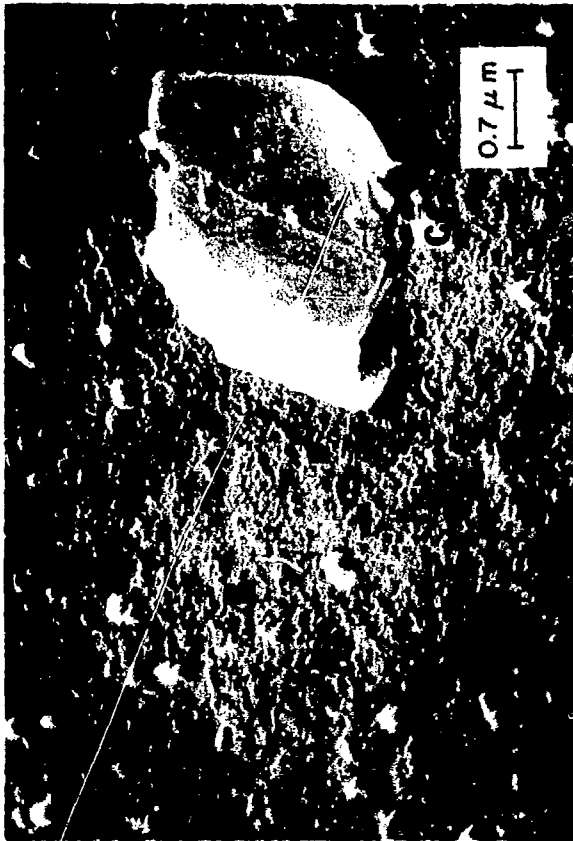
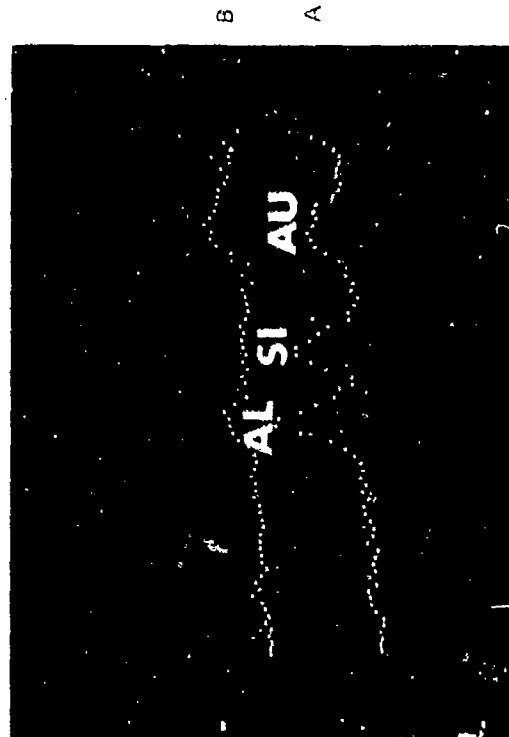
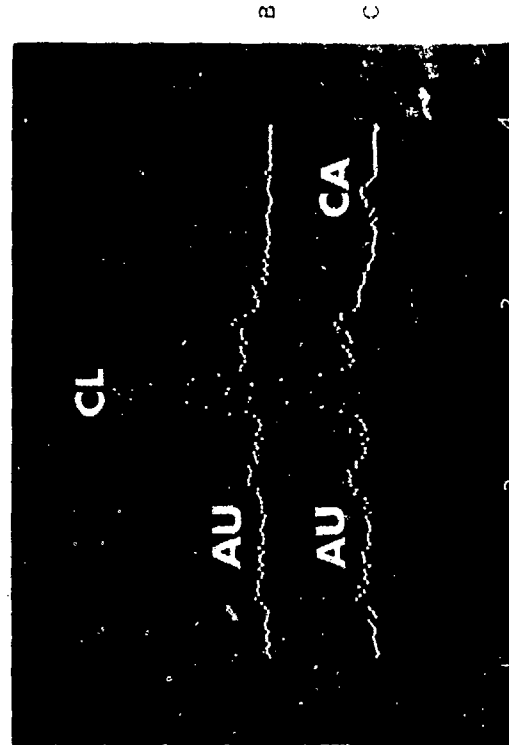


Figure 5-57 SEM PHOTOMICROGRAPH OF QUARTERNARY
DEPOSITED SAMPLE FQ1-10



KEY

Figure 5-58 BACKGROUND SPECTRUM OF GOLD COATED
FILTER AT SPOT B, FIGURE 5-57 SHOWING
CHARACTERISTIC Au AND Cl PEAKS AND
SPECTRUM OF PARTICLE A (KAOLIN)
SHOWING CHARACTERISTIC Au, Al
AND Si PEAKS



KEY

Figure 5-59 BACKGROUND SPECTRUM OF GOLD COATED
FILTER AT SPOT C, FIGURE 5-57, AND SPECTRUM
OF PARTICLE C (CaF₂) SHOWING
CHARACTERISTIC Au AND
Ca PEAKS

Figure 5-60 is a photomicrograph of sample FQ1-8, which contains a large clay particle. The corresponding spectrum is shown in Figure 5-61.

Figure 5-62 is a photomicrograph of sample FB5-4. This sample contains uranium dioxide and Kaolin particles. The sample was probed at Points D and E. The particle at Point D is Kaolin, the particle at Point E is uranium dioxide (Figures 5-63 and 5-64).

5.5.4 Electron Microprobe Analysis

The results of electron microprobe analysis of different deposited samples are presented in Table 5-14. These measurements were made with a defocused, 200 μm diameter, 15 KV electron beam. The beam current was 0.1 micro amp under these conditions. It was noted that sample FQ1-10 had greater tendency to accumulate charges than the other samples. Beams of higher intensity resulted in wrinkling or destruction of the XM-100A filter substrate as shown in Table 5-15. The bracketed values in the first column represent the error due to variations in background intensity level.

5.6 Discussion of Results

5.6.1 Introduction

The goal of the proposed sample preparation method is to transform an agglomerated powder into discrete primary particles that are uniformly deposited on a suitable filter surface and that can then be used for subsequent analysis. The success of the technique requires that:

- a. The substrate used is stable and does not interfere with the analytical measurements.
- b. The agglomerated powder mixture in the fluorinated liquid is completely dispersed into primary particles before deposition.
- c. The particles do not re-agglomerate during deposition or washing.
- d. The particles are uniformly deposited on the filter and once deposited, are not disturbed by subsequent treatment such as washing.
- e. There is minimal contamination of the deposited particles due to the presence of any residual dispersing liquid or the introduction of foreign materials.

The results presented in the previous section will be discussed within the context of the above requirements. Other points to be discussed include the apparent variation in average particle size of a given sample with the scale of magnification, the statistical limitations of the present study, and some qualitative comments on specific scanning electron photomicrographs.

Reproduced from
best available copy.

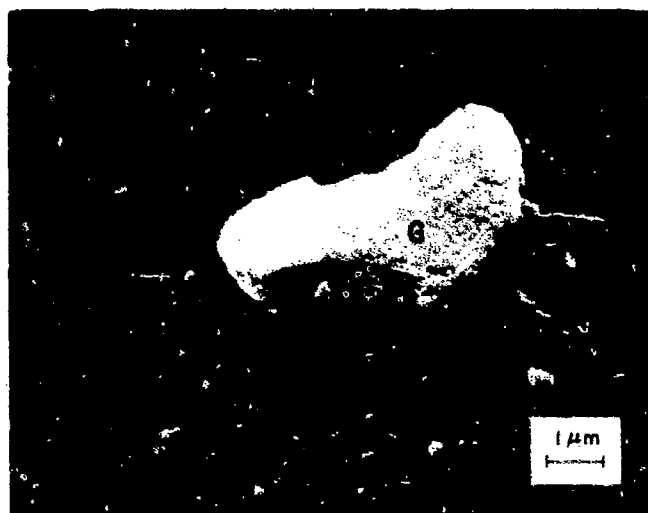
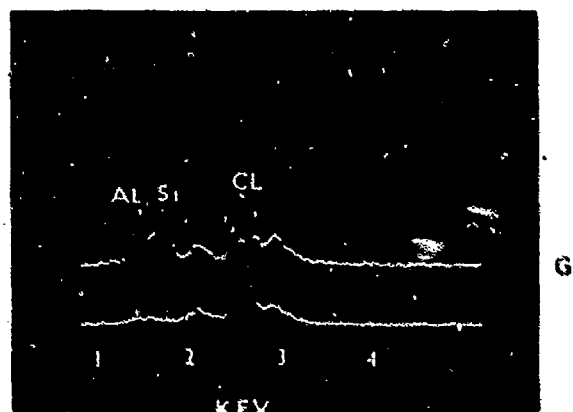


Figure 5-60. PHOTOMICROGRAPH OF GOLD COATED KAOLIN
PARTICLE FROM QUATERNARY SAMPLE FO1-8



KEY

Figure 5-61. SPECTRUM FOR THIS GOLD COATED KAOLIN
PARTICLE, SHOWING CHARACTERISTIC AL, Si, AND Au
PEAKS, AND CL PEAK DUE TO FILTER

83-1309

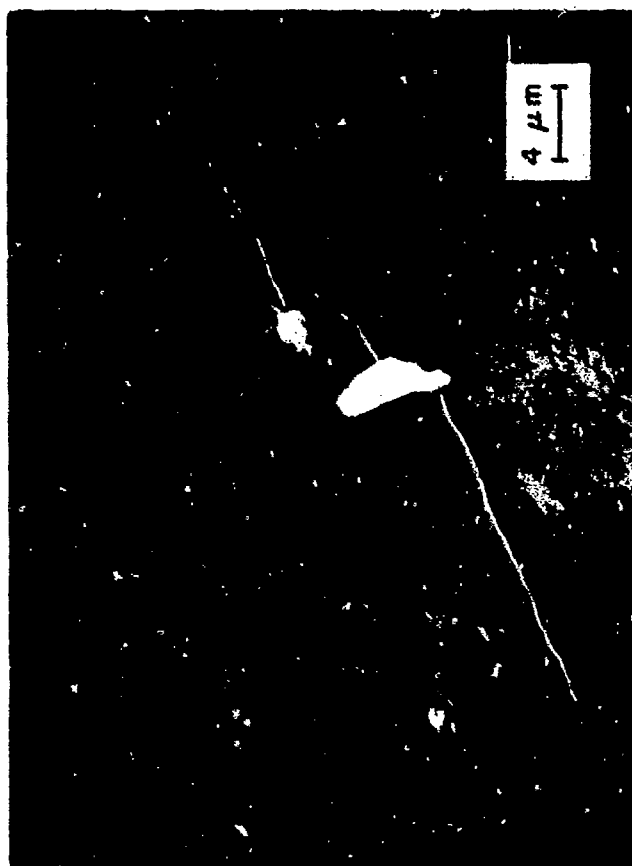


Figure 5-62 SEM PHOTOMICROGRAPH OF KAOLIN PARTICLE
AND ENL-1 UO_2 AGGLOMERATE FROM SAMPLE F85-4



Figure 5-63 SPECTRUM OF GOLD COATED KAOLIN PARTICLE D
SHOWING CHARACTERISTIC AL, SI AND AU PEAKS

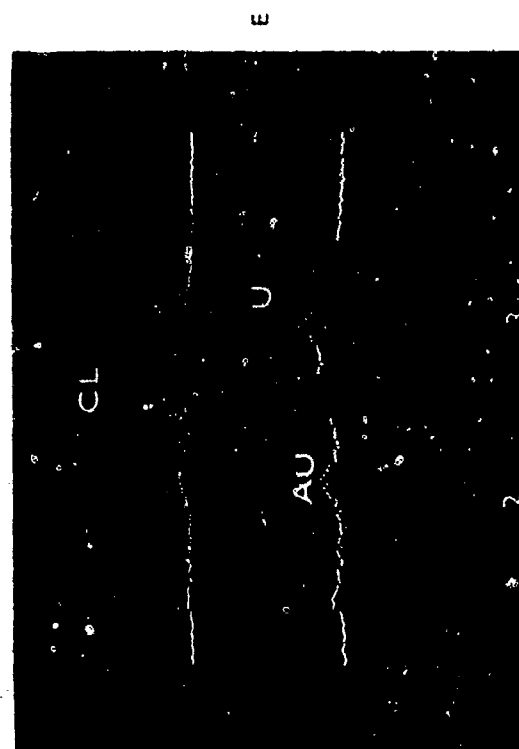


Figure 5-64 SPECTRUM OF GOLD COATED UO_2 AGGLOMERATE
SHOWING CHARACTERISTIC AU AND U PEAKS

4-12-5-14

TABLE OF ELEMENTAL ANALYSIS

Blank 100-4
FALCON

Sample No. EL-1 EL-2 EL-3 EL-4 EL-5 EL-6 EL-7 EL-8 EL-9 EL-10 EL-11 EL-12 EL-13 EL-14 EL-15 EL-16 EL-17 EL-18 EL-19 EL-20 EL-21 EL-22 EL-23 EL-24 EL-25 EL-26 EL-27 EL-28 EL-29 EL-30 EL-31 EL-32 EL-33 EL-34 EL-35 EL-36 EL-37 EL-38 EL-39 EL-40 EL-41 EL-42 EL-43 EL-44 EL-45 EL-46 EL-47 EL-48 EL-49 EL-50 EL-51 EL-52 EL-53 EL-54 EL-55 EL-56 EL-57 EL-58 EL-59 EL-60 EL-61 EL-62 EL-63 EL-64 EL-65 EL-66 EL-67 EL-68 EL-69 EL-70 EL-71 EL-72 EL-73 EL-74 EL-75 EL-76 EL-77 EL-78 EL-79 EL-80 EL-81 EL-82 EL-83 EL-84 EL-85 EL-86 EL-87 EL-88 EL-89 EL-90 EL-91 EL-92 EL-93 EL-94 EL-95 EL-96 EL-97 EL-98 EL-99 EL-100

Sample No.

Loading CO_2 , $\mu\text{g}/\text{cm}^2$

Loading H_2 , $\mu\text{g}/\text{cm}^2$

Weight O in Sample Area, μg

Loading O_2 , $\mu\text{g}/\text{cm}^2$

Loading O_2 , $\mu\text{g}/\text{cm}^2$

Loading CO_2 , $\mu\text{g}/\text{cm}^2$

Weight O in Sample Area, μg

Loading CO_2 , $\mu\text{g}/\text{cm}^2$

Loading H_2 , $\mu\text{g}/\text{cm}^2$

Weight O in Sample Area, μg

Loading CO_2 , $\mu\text{g}/\text{cm}^2$

Weight O in Sample Area, μg

Loading CO_2 , $\mu\text{g}/\text{cm}^2$

Weight O in Sample Area, μg

Loading CO_2 , $\mu\text{g}/\text{cm}^2$

Weight O in Sample Area, μg

Loading CO_2 , $\mu\text{g}/\text{cm}^2$

Weight O in Sample Area, μg

Loading CO_2 , $\mu\text{g}/\text{cm}^2$

Weight O in Sample Area, μg

Loading CO_2 , $\mu\text{g}/\text{cm}^2$

Weight O in Sample Area, μg

Loading CO_2 , $\mu\text{g}/\text{cm}^2$

Weight O in Sample Area, μg

Loading CO_2 , $\mu\text{g}/\text{cm}^2$

Weight O in Sample Area, μg

Loading CO_2 , $\mu\text{g}/\text{cm}^2$

Weight O in Sample Area, μg

Loading CO_2 , $\mu\text{g}/\text{cm}^2$

Weight O in Sample Area, μg

Loading CO_2 , $\mu\text{g}/\text{cm}^2$

Weight O in Sample Area, μg

Loading CO_2 , $\mu\text{g}/\text{cm}^2$

Weight O in Sample Area, μg

Loading CO_2 , $\mu\text{g}/\text{cm}^2$

Weight O in Sample Area, μg

Weighted Average CO_2 = $\frac{\sum \text{Loading } \text{CO}_2 \times \text{Weight}}{\sum \text{Weight}}$ = 2.9

Weighted Average H_2 = $\frac{\sum \text{Loading } \text{H}_2 \times \text{Weight}}{\sum \text{Weight}}$ = 1.9

TABLE 5-15

EFFECT OF ELECTRON PROBE INTENSITY ON AMICON XM-100A ULTRAFILTER

<u>Beam Voltage</u> <u>KV</u>	<u>Beam Current</u> <u>μ amp</u>	<u>Beam Diameter</u> <u>μm</u>	<u>Results</u>
30	0.3	25	Hole in Filter
25	0.3	200	Hole in Filter
20	0.2	200	Marginal Wrinkling of Filter
15	0.1	25	Filter Unstable
15	0.1	200	No Destruction of Filter Noted

5.6.2 Suitability of the XM-100A Ultrafilter as a Deposition Substrate

The Amicon XM-100A ultrafiltration membrane is considered to be superior, for the purposes of this study, to any other ultrafiltration membranes that are presently commercially available. The XM-100A membrane is very stable in a scanning electron microscope. A given deposited particle can be examined at magnifications as high as 45000X for many minutes without noticeable decomposition of the membrane. For purposes of comparison, Figure 5-65 presents an electron micrograph of clay particles deposited from a 1% Krytox - Freon E-3 solution on a VS Millipore filter after examination at 18000X. The filter around the target particle has been destroyed.

The pores of the XM-100A membrane are sufficiently small to be unobservable at the magnifications used in this study. In SEM microscopy of properly prepared samples, the Amicon XM-100A membrane appears as a blank dark grey background that has no relief. This greatly facilitates the examination of individual particle and the measurement of particle size distribution curves. There was no interference in the measurement of particle distribution with the Millipore μ MC system due to surface structure of the XM-100A membrane. This was not the case with other membranes examined (Pellicon Ultrafilters, Millipore VS, S&S Selection B-14) where signals from the structure of the membrane interfered with signals from the deposited particles.

A further advantage of the XM-100A membrane is that all observable particles will be retained on the surface of the membrane as shown in Figure 5-67. This is in significant contrast to the other membranes examined, even the competitive Pellicon Ultrafilters. Figure 5-66 is an electron micrograph of UO_2 particles deposited from a 1% Krytox 157 - Freon E-3 solution on a Pellicon PSJM filter, at a nominal powder loading of $1 \mu\text{g}/\text{cm}^2$. The pores at the surface of the membrane are larger than some of the particles retained.

It is to be further noted that the gold-palladium coating on sample QD1-10, which was washed with Freon E-1, had a different appearance than the gold-palladium coating of samples washed in the normal manner. The coating appeared to be much lighter. While the sample could be examined in the SEM, it was difficult to obtain high contrast images because the sample had a tendency to accumulate a charge. As shown in Table 5-14, this sample had a much higher residual fluorine content than any of the other samples examined.

For the majority of the deposited samples, the gold-palladium coating was applied just prior to their examination by SEM. Most of the micrographs were taken within one or two days after the samples were coated.

The micrographs shown in Figures 5-57, 5-60, and 5-62 were taken approximately two months after the samples were coated. The original coated samples, which were stored in a dessicator, were re-examined in the SEM in order to photograph samples in which individual particles were simultaneously being analyzed by PGT non-dispersive x-ray probe. These samples were much more difficult to examine in the SEM. After a few minutes in the microscope, each sample had a tendency to accumulate charge which made it difficult to keep the sample in focus for a long period of time. Cracks



Figure 5-65 SEM PHOTOGRAPH OF EAGLE PARTICLES
DEPOSITED ON MILLIPORE VS FILTER NOYE WEARDOWN
OF FILTER DUE SEM ELECTRON BEAM (PRELIMINARY
SAMPLE 100 6)

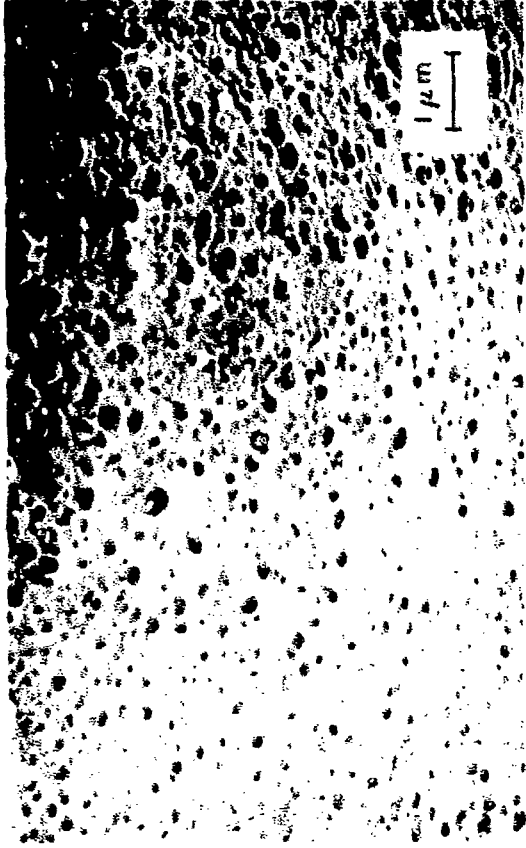


Figure 5-66 SEM PHOTOGRAPH OF ENL-1 UO_2 PARTICLES
DEPOSITED ON PELLICON PSJM ULTRAFILTER
(PRELIMINARY SAMPLE D-28)

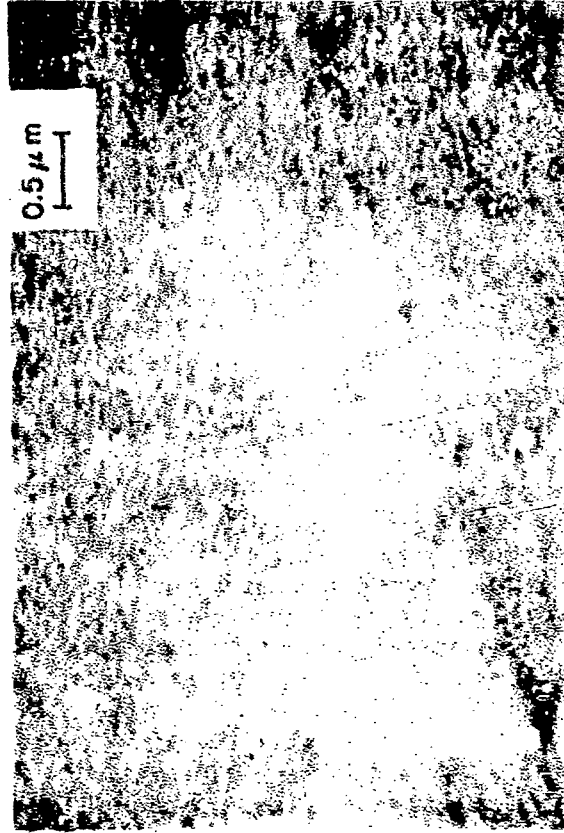


Figure 5-67 SEM PHOTOGRAPH OF ENL-1 UO_2 PARTICLES
DEPOSITED ON AMICON XM100A ULTRAFILTER
(SAMPLE DA1-17)

Reproduced from
best available copy

were also observed to form in the sample substrate under these conditions (see Figure 5-62). The above deterioration of the sample is believed due to alterations, such as oxidation of the gold-palladium film thus rendering it less conductive, during the few months that transpired between the initial coating of the sample and examination in the microscope.

The elapsed time between sample preparation on the filter and deposition of the gold-palladium coating is not believed to have an effect on the quality of the photographs. It took much longer to prepare the deposited powder samples at Avco than it took to examine them at AMR. In order to efficiently use AMR's facilities, samples were prepared and accumulated until there were a sufficient number such that their examination would require at least one working day. The time between preparation and examination varied between 2 and 20 days.

The occurrence of the defects noted above was totally independent of the use of the non-dispersive x-ray probe. During the initial series of electron micrographs, a few samples were also examined with the PGT probe which was observed to have no effect on the sample. During the final series of tests, on aged samples, deterioration occurred after a few minutes at high magnification whether or not the x-ray probe was used. Fortunately the sample was stable enough to perform meaningful measurements.

A key conclusion from the results is that samples deposited on an XM-100A can be examined for elemental composition by a non-dispersive x-ray probe. The only interference due to the filter is a very noticeable chlorine peak which results from the composition of the filter itself. This chlorine peak did not interfere with measurement and interpretation of the spectrum of the deposited inorganic particles. In each case the spectrum expected of the characteristic elements was observed.

The Amicon XM-100A membrane could also be used as a substrate for electron microprobe work by using low energy density levels, as shown in Table 5-15. It was necessary to work with a defocused beam of relatively low energy. Use of high intensity focused beams resulted in the destruction of the filter. This places limitations on the size of the sample that can be examined and the sensitivity of the measurement for elements such as uranium. In order to overcome these limitations, the substrate must be made more resistant to thermal degradation. This could be readily accomplished on blank membranes by using different coatings (for example, aluminum, possibly gold), or heavier coatings of these materials or possibly carbon, which would protect and dissipate heat away from the point of the filter surface being examined. Another possibility would be to use a different ultrafiltration membrane than XM-100A as a deposition substrate. For reasons already mentioned, there are not many suitable candidate materials. The only possible alternative to the XM-100A membrane is a new ultrafilter, type SM, presently undergoing development at Amicon, which should be commercially available by summer, 1973.

Examination of electron micrographs taken by Amicon, of development samples of the Type SM membrane, indicated that this material had the same general structural characteristics as the type XM membrane and would thus be expected to offer the advantages of the type XM membrane as discussed above. A key difference is the composition of the membrane. Amicon's representative disclosed that the surface of the type SM membrane was made with polymers that had a melting point a few hundred degrees higher than the materials used to make the type XM membrane. The type SM membrane should thus be even more stable than the type XM membrane. It is recommended that the suitability of these membranes for the present application be examined when they become commercially available.

5.6.3 Effect of Scale of Measurement on Apparent Size of Deposited Particles

The average apparent particle size of a given powder sample as determined by examination of scanning electron micrographs, decreased with increasing magnification of the micrograph. This variation is due to the bias introduced by the microscope and the automatic particle counter. At any magnification, a particle has to have an image at least 0.5 mm in diameter on the photomicrograph to be seen and measured. Particles with smaller images will escape detection. Similarly, it will not be possible to size a particle whose image is larger than the photomicrograph which is 11.5 cm long. At any magnification it is possible to measure particles only within a certain size range. With these constraints at 450X, it is possible to examine particles ranging in size from about 0.6 μm to 220 μm . At 4500X, the range of examination is about 0.06 μm to 22 μm . At 18000X, the range is about 0.02 μm (the resolution of the microscope) to 5 μm . The upper limit of the size range is reduced by at least a factor of ten if the micrographs are used to obtain particle size distribution measurements which require the presence of many particles on the photographs.

The BET spherical average diameters of the ultimate particles of the powders examined in this study ranged from 0.09 μm to 0.39 μm . It was observed microscopically that these mainly ranged in size from 0.05 μm to 0.5 μm . Kaolin contained some larger particles while UO_2 contained some smaller particles. These conclusions are based on examination of the various photomicrographs as well as other tests (e.g. sedimentation studies).

With the powders of interest, the micrographs at 450X do not give any information regarding the ultimate particle size. These micrographs can only be used to determine the presence of large agglomerates and major variations in the appearance of the deposited sample. For nearly all the samples examined that did not contain Kaolin, the average apparent size measured at 450X was less than 1.6 μm . This corresponds to one length unit in automatic particle size measurements. The average apparent particle size at 450X of the Kaolin containing samples was larger because of the presence of large Kaolin particles.

Micrographs taken at 4500X yielded the maximum amount of information on the state of dispersion of the powders of interest. There was a good matching of size range. It was possible to examine a reasonably large number of particles and still detect the majority of the individual particles and the presence of small agglomerates.

Micrographs taken at 18000X were mainly used to obtain details as to the size and structure of particles and agglomerates. At this magnification, the sample under examination is too small to be representative of the sample population. This is especially true of deposited powder mixtures containing Kaolin. This is well brought in Figure 5-44.

5.6.4 Degree of Dispersion of Deposited Powders

All runs for which the deposited powder sample was dispersed for only a short period of time were badly agglomerated because the particles in suspension were still agglomerated before deposition. As discussed in the previous section, there is a minimum time of sonolation needed to attain a high level of dispersion. Minimum sonolation times required to satisfactorily disperse the powders were about 10 minutes for Kaolin, 30 minutes for carbon black, 100 minutes for calcium fluoride, and over 400 minutes for uranium dioxide. All deposited samples which contained a given powder and which were sonolated for a shorter period of time than the minimum cited above were invariably agglomerated.

For all the powders and powder mixtures examined, it was noted that deposited samples which contained a high powder loading were always more agglomerated than those with low powder loadings. This was true even with samples which came from the same primary batch after long sonolation times sufficient to apparently completely disperse the suspensoid. The average particle size of material deposited on a filter increased as the amount of powder in the sample increased, as shown in Figure 5-68. In this figure the abscissa is the fraction of the surface covered by powder, \bar{K}_t , and the ordinate is the ratio of the length average particle diameter, \bar{D}_L , to the B.E.T. equivalent particle diameter, \bar{d}_{vs} . The points represent experimental values of \bar{K}_t , and \bar{D}_L obtained from electron micrographs at 4500X. The data for UO_2 include runs DA1-7 to DA1-17, listed in Table 5-2; for carbon black, all runs listed in Table 5-3 except run DB1-1; for calcium fluoride, all runs in Table 5-4 except run DD1-1; and for kaolin, all runs listed in Table 5-5 except runs DC1-1 and DC1-2. Data were not presented for runs in which there were indications that initial dispersion had not taken place.

The specific surface area measured by nitrogen adsorption, A_s , is a good measure of the average size of the ultimate particles for a given powder and is independent of the degree of agglomeration. This average size, \bar{d}_{vs} , can be expressed as

$$\bar{d}_{vs} = \frac{\beta}{A_s \rho} \quad (5-1)$$

where ρ is the density of the particles and β is a shape factor. Values of β and the interpretation of \bar{d}_{vs} for different simple geometries are presented in Table 5-16. Accurate values of A_s and ρ can be obtained with agglomerated powders. The only assumption required to determine a value of \bar{d}_{vs} concerns the shape of the particles. Such information can be obtained from micrographs of agglomerated powders, such as the ones shown in Section 2.2. Sterling MT carbon black consists of particles that are clearly spheres. Uranium dioxide and calcium fluoride particles appear to be irregular polyhedrons, which were considered to be quasi-spherical in shape.

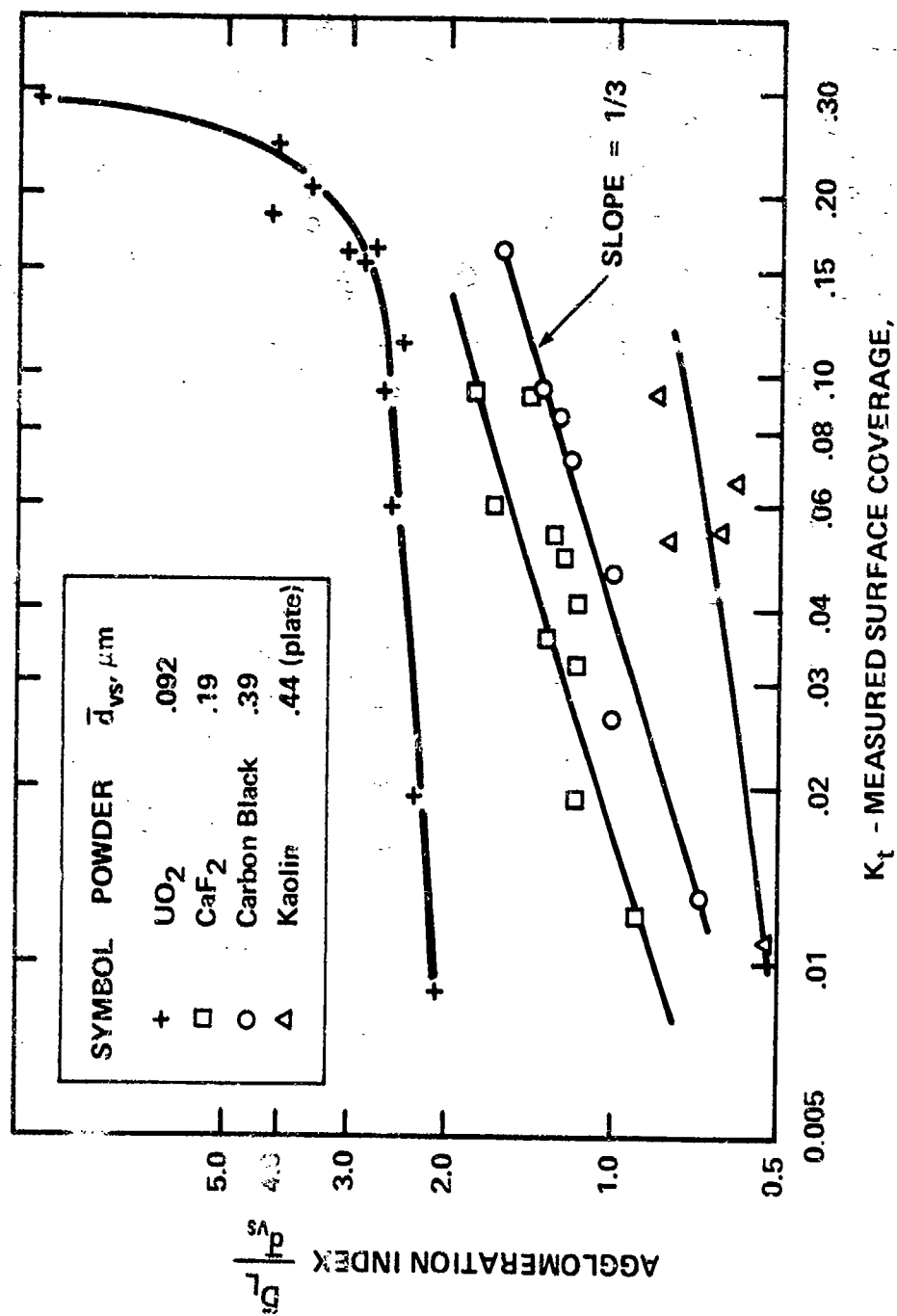


Figure 5-68 EFFECT OF POWDER LOADING ON APPARENT SIZE OF DEPOSITED PARTICLES

TABLE 5-16

EFFECT OF PARTICLE SHAPE ON INTERPRETATION OF \bar{d}_{vs}

<u>Particle Shape</u>	<u>Surface Area</u>	<u>Weight</u>	<u>Specific Surface Area, A_s</u>	<u>β</u>	<u>\bar{d}_{vs}</u>
Sphere	πD^2	$\rho \frac{\pi D^3}{6}$	$6/\rho D$	6	D
Cube	$6 a^2$	ρa^3	$6/\rho a$	6	a
Flat Plate (a, b > c)	2ab	ρabc	$2/\rho c$	2	c

The particles of kaolin are thin, squarish platelets with a large aspect ratio. In Figure 5-68, for the first three powders (UO_2 , CaF_2 and Carbon Black), \bar{D}_L/\bar{d}_{vs} is the ratio of mean agglomerate diameter to the equivalent spherical particle diameter. For clay, \bar{D}_L/\bar{d}_{vs} represents the ratio of agglomerate diameter to the average length of kaolin platelet. In calculating this dimension it was assumed that kaolin had an average aspect ratio of about 7:1 (aspect ratio = length/thickness) which, while arbitrary, appeared to be realistic for this material.

The results presented in Figure 5-68 can be summarized as follows:

- a. The average size of the deposited powder increases with increasing surface coverage of the powder.
- b. For any given surface concentration, the degree of agglomeration increases with decreasing particle size. For all powders except UO_2 , \bar{D}_L is smaller than the BET particle diameter at apparent surface loading of 0.02 or less. For UO_2 , \bar{D}_L is twice the BET particle diameter at a surface loading of 0.008, the lowest value examined.
- c. For carbon black and calcium fluoride samples (\bar{D}_L/\bar{d}_{vs}) appears to increase as $K_t^{1/3}$ over an order of magnitude variation in K_t . For uranium oxide, (\bar{D}_L/\bar{d}_{vs}) initially increases as $K_t^{0.1}$ over the range $0.08 \leq K_t \leq 0.10$ and then very rapidly with increasing K_t for values of $K_t \geq 0.15$. For kaolin, (\bar{D}_L/\bar{d}_{vs}) also increases with K_t , apparently at a value intermediate between those found for UO_2 and the other two powders. The few data points for kaolin are sufficiently scattered to prevent more precise definition of the slope of the line.
- d. Values of $\bar{D}_L/\bar{d}_{vs} < 1$ are noted for clay and one point each for carbon black and CaF_2 . This reflects the meaning and accuracy with which this ratio can be obtained, rather than breakage of primary particles. The measurements of A_s were accurate to within $\pm 6\%$. The absolute value of \bar{d}_{vs} depends on the shape assumed and is therefore subject to systematic error. In the case of the powders other than kaolin, the shape assumed is not critical, since the shape factor is same for a cube as it is for sphere. It is important for kaolin, however, because it is highly anisotropic. With the assumptions chosen, $\bar{d}_{vs} = \bar{a} = 0.44 \mu\text{m}$. This value of \bar{d}_{vs} is more than twice the equivalent spherical diameter for this powder which is $0.18 \mu\text{m}$. The true value of \bar{d}_{vs} for this powder may well be between these two values.

Another factor which influences the numerical value of the agglomeration index is the fact that \bar{D}_L is a length mean agglomerate diameter, i.e.

$$\bar{D}_L = \frac{\sum n_i D_i}{\sum n_i} \quad (5-2)$$

whereas \bar{d}_{vs} is a volume to surface mean diameter

$$\bar{d}_{vs} = \frac{\sum n_i d_i^3}{\sum n_i d_i^2} \quad (5-3)$$

\bar{D}_L is a first moment average whereas \bar{d}_{vs} is a higher moment average of order 2.5. A more correct agglomerate index would have been either the ratio of \bar{D}_L/\bar{d}_L or of $\bar{D}_{vs}/\bar{d}_{vs}$. It was not possible to obtain \bar{D}_{vs} or a measure of the standard deviation in the size of the deposited powder from the electron micrographs, since the Millipore π MC particle size analyzer available at Avco did not have the attachment needed to measure particle size distribution and deviations about the mean. With the exception of CaF_2 , the size distribution of the ultimate particles was not known either so that \bar{d}_L could not be calculated. For CaF_2 , a value of \bar{d}_L can be calculated, using Kapteyn's transformation (5-1), from the values of \bar{d}_{wg} and σ_g obtained from the sedimentation data presented in Figure 4-15.

$$\ln \bar{d}_L = \ln \bar{d}_{wg} - 2.5 \ln^2 \sigma_g$$

since $\bar{d}_{wg} = 0.22 \mu\text{m}$ and $\sigma_g = 2.3$, $\bar{d}_L = 0.04 \mu\text{m}$. For this powder

$$\frac{\bar{D}_L}{\bar{d}_L} \approx 4 \frac{\bar{D}_L}{\bar{d}_{vs}}$$

A similar correction could also be applied to the other powders.

The experimental observations discussed above can best be explained in terms of particle reagglomeration, on or near the filter surface, during the FC-43 washing step. The physical picture is as follows. It is assumed that the secondary dispersion of particles in 1% Krytox 157 - Freon E-3 contains no agglomerates, only primary particles. The particles do not interact or flocculate because each particle is surrounded by an adsorbed solvated layer of Krytox 157. As the suspension is filtered, the particles are concentrated on or near the surface of the ultrafiltration membrane. At the end of the initial filtration step, not all the 1% Krytox 157 - Freon E-3 solution is removed. The region near the filter surface may be viewed as a thin liquid film in which the particles are suspended. These particles are not stationary, but are subject to Brownian motion and are free to move laterally across the filter or vertically throughout the height of the film. This will result in particle/particle collision as well as collisions with the filter. As in the dispersion before filtering, the particles (and all the other solid surfaces) are coated with a solvated film of adsorbed Krytox 157 which presents agglomeration.

An excess of wash liquid, FC-43 is now introduced and forced past the particles through the ultrafiltration membrane as shown in Figure 5-69. The film of the initial dispersing medium bathing the particles is first displaced. Krytox 157 then desorbs from the surface of the ultrafiltration membrane the particles adhering to the membrane as a result of the same forces responsible for the formation of the initial agglomerate. In practice, there can also be reagglomeration due to interparticle contact as a result of Brownian motion in the liquid volume near the membrane surface.

According to the calculations in Appendix C,

$$\frac{\bar{D}}{\bar{d}} = \frac{1}{(1-\epsilon)} \left(1 + \frac{16 vt K_o}{\bar{d}} \right)^{1/3} \quad (5-4)$$

or

$$\frac{\bar{D}}{\bar{d}} = \left[\frac{1}{(1-\epsilon)} \right]^{1/3} \left[1 + vt \left(\frac{\bar{D}}{\bar{d}} \right) (1-\epsilon) 16 \left(\frac{K_t}{\bar{d}} \right) \right]^{1/3} \quad (5-5)$$

In the above equations:

\bar{D} = agglomerate average diameter

\bar{d} = particle average diameter

ϵ = volume fraction voids in the agglomerate

v = superficial velocity of wash liquid

t = effective time of washing

K_o = surface coverage of dispersed particles

K_t = surface coverage of agglomerated particles

Equations 5-4 and 5-5 are equivalent. In equation 5-4, \bar{D}/\bar{d} is expressed in terms of K_o , the surface coverage which would be obtained if the deposited sample were completely dispersed. In equation 5-5, \bar{D}/\bar{d} is expressed in terms of K_t , the actual surface coverage which presumes the presence of agglomerates. In the limit, as $\bar{D}/\bar{d} \rightarrow 1$, $K_t \rightarrow K_o$.

Two terms in the above equations, ϵ and vt , are not amenable to experimental observation, which is a limitation in trying to apply these equations numerically to the data obtained. In the limit, at $K_t \rightarrow K_o$, $\epsilon \rightarrow 0$. The product, vt , has dimensions of volume of wash liquid/unit area of filter surface. The effective time of wash, or corresponding volume of wash during which the particles are subject to reagglomeration, is not known.

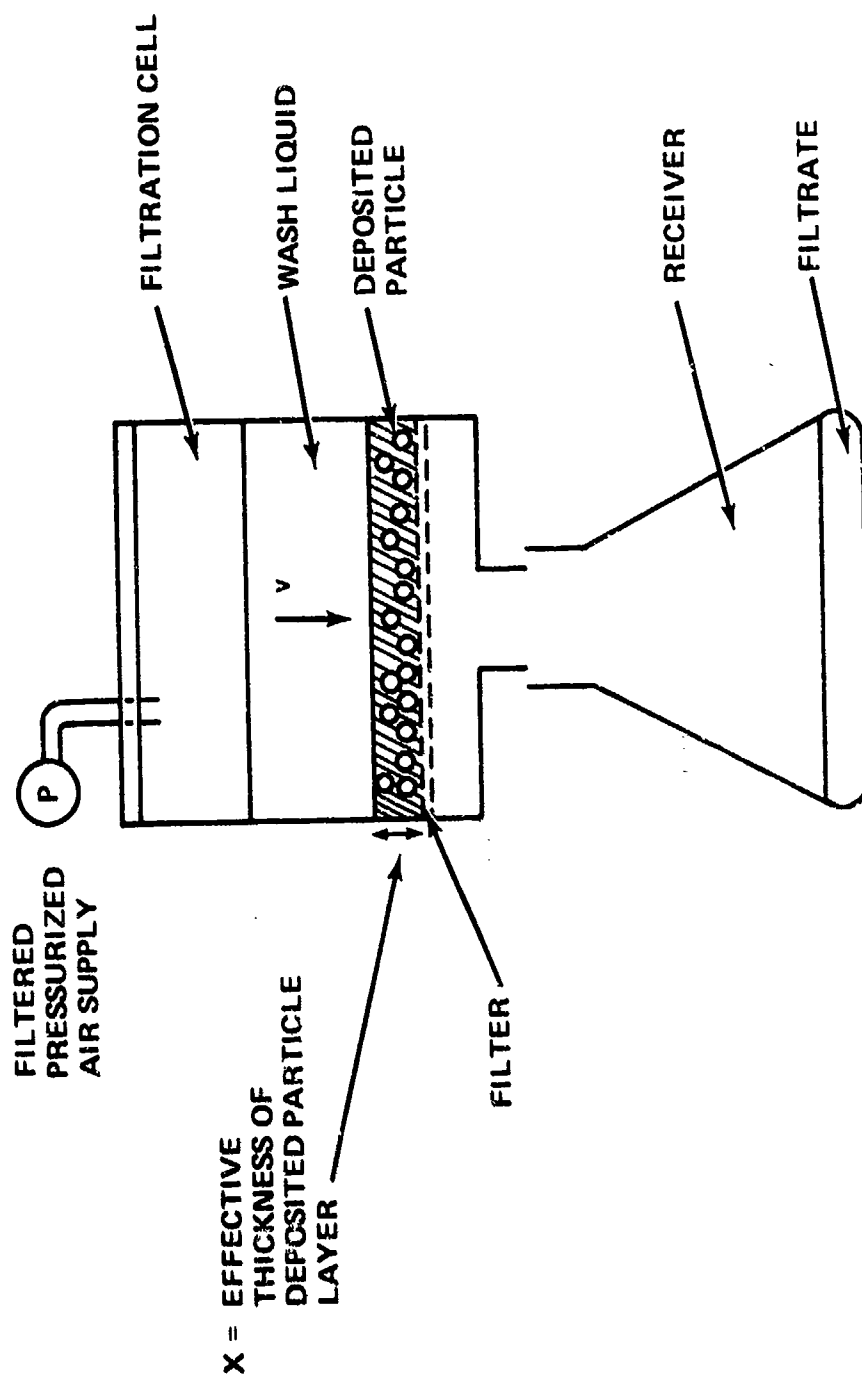


Figure 5-69 SCHEMATIC DIAGRAM OF DEPOSITED PARTICLES DURING WASHING

The most conservative assumption is to assume that the particles are free to reaggregate during the complete wash cycle. In this case, the term vt is equal to the volume of wash liquid divided by the filter area of 37 cm^2 since all the surfactant is apparently removed during the 25 ml FC-43 wash, the corresponding value of $vt \approx 25 \text{ cm}^3 / 37 \text{ cm}^2 \approx 0.7 \text{ cm}$. Another limitation in the theory developed is that the presence of the filter and collisions of the particles with the filter are not taken into account in the above equations. Particles which collide with the membranes will adhere to it as a result of the same forces responsible for agglomerate formation, so that the filter surface acts as a particle sink which removes particles from suspension and prevents their further interaction with particles in the bulk. This could effectively limit t to very short periods of time.

Equation 5-4 can be used to develop a criterion for the powder loading that may be deposited on a filter with minimal reagglomeration, $\bar{D}/\bar{d} \rightarrow 1$, $d(\bar{D}/\bar{d})/dt \rightarrow 0$ and $\epsilon \rightarrow 0$, i.e., there is virtually no change in agglomeration size with time. If $\bar{D}/\bar{d} = 1$, then $16 VtK_o/\bar{d} \ll 1$, so that equation 5-4 may be rewritten as:

$$\frac{\bar{D}}{\bar{d}} = 1 + \frac{16 vt K_o}{3\bar{d}} + \dots \quad (5-6)$$

and

$$\frac{d(\frac{\bar{D}}{\bar{d}})}{dt} = \frac{16 v K_o}{3\bar{d}} + \dots \quad (5-7)$$

An order-of-magnitude criterion for minimal reagglomeration is that the particle loading be such that $16 v K_o/3\bar{d} \ll 1$. This suggests definition of a "critical" surface coverage, K_o^* ,

$$K_o^* = \frac{3\bar{d}}{16 v} \quad (5-8)$$

Minimization of reagglomeration requires $K_o \ll K_o^*$. Values of K_o^* are presented in Table 5-17 for each of the candidate powders. From the permeability of FC-43 ($0.05 \text{ ml/min} - \text{psig} - \text{cm}^2$), and for an operating pressure of 1 ps.g, a constant value of $v \approx 8.3 \times 10^{-4} \text{ cm/sec}$ was used in these calculations. The corresponding values of critical powder loading, W^* ($\mu\text{g/cm}^2$), are also presented in Table 5-17, where $W^* = a K_o^*/A_s$, where A_s is the specific surface area of the powder and a is a shape factor, as outlined in more detail in Appendix C. These calculations are based on the assumption that $\bar{d} = d_{vs}$ which may give a high estimate for K_o^* and W^* .

From the values calculated in Table 5-17, it can be seen that the minimum powder loadings used in the experiments were close to the values of W^* . In order to have obtained samples with minimal agglomeration, surface loadings lower by one order of magnitude should have been used in the deposition studies.

TABLE 5-17

CRITICAL SURFACE LOADING OF CANDIDATE POWDERS

<u>Powder</u>	$\bar{d}_{vs}, \text{ cm}$ ($\times 10^{+5}$)	$A_s \text{ cm}^2/\text{gr}$	a^*	K_o^*	W_c^* ugm/cm^2
ENL UO_2	0.92	6.0×10^4	4	2.1×10^{-3}	0.14
CaF_2	1.9	10.1×10^4	4	4.3×10^{-3}	0.17
Sterling MT Carbon Black	3.9	8.5×10^4	4	8.8×10^{-3}	0.41
Peerless No. 2 Clay	4.4	12.5×10^4	2	10×10^{-3}	0.16

$$*K_o = \frac{3 \bar{d}_{vs}}{16 v} \approx 2.27 \times 10^2 \bar{d}_{vs} \quad W_o = \frac{a K_o}{A_s}$$

v = superficial velocity of wash liquid $\approx 8.3 \times 10^{-4} \text{ cm/sec.}$

a = shape factor defined in Table C-1.

The actual minimum powder loading used for each of the powders in these studies was $W_m = 0.5 \mu\text{g}/\text{cm}^2$. This value of W_m is higher than W^* for UO_2 , CaF_2 and clay, and approximately equal to W^* for carbon black. It is interesting to note that the UO_2 and CaF_2 samples at this loading were much more agglomerated than the carbon black and clay samples. Kaolin was quite well dispersed even though it had a low value of W^* . This may reflect the very different shape of the Kaolin particles which makes the interpretation of d_{vs} , and thus Ko^* , difficult. Further experimentation is still required at lower powder loadings to determine the maximum value that should be used so as to insure minimum reagglomeration of an arbitrary sample. For the worst case in these studies, namely uranium dioxide, an upper-bound estimate of the maximum powder loading would be $0.1 \mu\text{g}/\text{cm}^2$. A more conservative estimate would assume that $W = 0.05 W^*$.

5.6.5 Comparison of Agglomerated and Conglomerated Mixtures

Samples prepared from mixed powders were similar to samples prepared from a single powder component. In order to obtain a good deposited sample from a multicomponent powder mixture, it is necessary that each individual component in the mixture be well dispersed during the dispersion process. For example, all multicomponent mixtures containing uranium dioxide and ultrasonically dispersed for less than 600 minutes were agglomerated. Usually, well-dispersed deposited samples were observed with those mixtures which were subjected to a sufficiently long dispersion time (viz samples FQ1-8, FB1-10).

As with individual powders discussed above, reagglomeration became more significant as powder loading on the deposited sample increased. No attempt was made to calculate critical loading values for multicomponent powder mixtures. This is a much more complex problem than the analysis of reagglomeration of similar particles. However, it is expected that Mueller's extension (5-3) of the Smoluchowski (5-2) theory to polydisperse colloidal suspensions should be applicable. It is well established that, in a flocculating colloidal sol, the rate of coagulation of small particles in the presence of large particles is greater than the rate of coagulation the small particles alone. Consequently, the critical loading for a multicomponent mixture is probably smaller than the values calculated for the individual powders (Table 5-17).

An interesting observation is that there was significantly less conglomeration than agglomeration in deposited samples prepared from multicomponent powders. In trying to assess the effectiveness of dispersion of a single powder, it is difficult to differentiate between an agglomerate and an aggregate. For example are the carbon black particles in Figure 5-16 aggregates or agglomerates? This confusion does not occur with conglomerated powders that are physically mixed together. Individual particles of two different powders can only be associated by secondary valence forces. They cannot be aggregated. For example, in Figures 5-30 and 5-33, there are no Kaolin-Carbon Black conglomerates. In both these photomicrographs there are a few double and triplet carbon black particles which could be either aggregates or

agglomerates. The latter were probably present before the washing and deposition steps. Similarly, in Figures 5-35 and 5-36 there are no UO_2 -carbon black conglomerates, even though some of the UO_2 and carbon particles appear agglomerated (or is it aggregated?).

5.6.6 Elemental Composition of Deposited Samples

Results of elemental analysis by electron microprobe on selected samples are presented in Table 5-14. With the exception of Run FQ1-10, there is good agreement between the reported value of the surface concentration of aluminum and the expected value in those samples containing Peerless No. 2 Clay (aluminum assay of 20.7 wt %). With the exception of Run FQ1-10, there is also good agreement between reported values of Ca surface coverage and expected Ca surface coverage. While uranium is detected only in those samples where uranium dioxide was deposited, there is poor agreement between the expected and measured values of uranium. There is little correlation between the reported values of carbon surface coverage and the expected values based on the deposited sample composition.

The concentration of a given element in a sample was calculated according to the following equation:

$$C_A = a_A \left(\frac{I_{SA} - I_{BA}}{I_{OA}} \right) \quad (5-9)$$

where

C_A = concentration of element A in sample, mg/cm²

I_{SA} = radiation intensity of sample

I_{BA} = background radiation intensity due to filter

I_{OA} = radiation intensity of reference material

a_A = proportionality factor ≈ 1

Values of I_{OA} and I_{BA} are presented in Table 5-18.

TABLE 5-18
FACTORS FOR ELECTRON MICROPROBE MEASUREMENTS

Element	C	S	Al	Ca	U
Reference Material	Graphite	SiF	Al Metal	CaCO_3	U Metal
I_{SA} Ref., counts/min.	530	1260	1500	705	130
I_{BA} , counts/min.	530	1200	1500	1400	130
I_{BA}^* , counts/min.	530 \pm 5	6.3 \pm 0.3	1.9 \pm 0.7	1.6 \pm 0.2	0.8 \pm 0.2
Range of I_{SA}	50-150	10.5-37.5	0.7-1.2	1.1-2.4	0.5-13.2

*Chart recorder, Androm IV-10A Membrane.

For Al and Ca in which $I_{SA} \gg I_{BA}$, there is good agreement between the measured and expected values of Ca. These results indicated that the samples tested were uniformly deposited.

The lack of quantitative agreement for uranium is due mainly to the low sensitivity for uranium of the electron microprobe with a 15 KV beam rather than to gross deviation in sample uniformity. As noted in the table, pure uranium has a count rate of only 132 count/min which is only about twenty times higher than the background count rate.

The poor correlation between expected and measured values of carbon is due to the high background signal for this element. The background reflects the deposited carbon used to prepare the sample as well as carbon in the polymer matrix of the Amicon XM-100A membrane.

Sample FQ1-10 is different from the other samples in that it was prepared with a "pousse-cafe" wash. This sample should be uniformly deposited. The high Al content and low Ca content would reflect local inhomogeneities due to the presence of a large Kaolinite particle in one of two examined samples which would bias the measurements. The measured fluorine content for this sample was $16 \mu\text{g}/\text{cm}^2$ which is much higher than for any of the other samples which were washed with FC-43 and Freon C-51-12 (these had an average fluorine background of $2.9 \mu\text{g}/\text{cm}^2$). The net amount of carbon on this sample was also very high. This is an indication that there was more residual fluorocarbon in this sample. Freon E-1 is not as effective a washing agent as FC-43 and Freon C-51-12.

The range of residual fluorine content in the sample for runs not containing calcium fluoride ranged from $1.8 \mu\text{g}/\text{cm}^2$ to $4.1 \mu\text{g}/\text{cm}^2$, a twofold variation. This is significantly less than the range of powder loading, which was varied twenty-fold, and indicates that the majority of the residual fluorocarbon must have been associated with the filter rather than with the particles. There are two possible explanations for this. It is most likely that not all the Krytox 157 was removed with 25 ml of FC-43. Doubling the amount of wash FC-43 should result in a further lowering of residual fluorine content by an order of magnitude. Another possibility might be the presence of trace amounts of Freon C-51-12 or Freon E-1 wash liquid in the filter structure because of capillary condensation in spite of the high volatility of these liquids. This does not appear likely since Freon E-1 is more volatile than Freon C-51-12 and yet sample FQ1-10 had a higher residual fluoride content.

3.6.7 Further Evaluation of Uniformity of a Deposited Sample

In addition to elemental analysis, the uniformity of a deposited sample was assessed by:

- a. Examining the filter on which the powder was deposited by eye and noting any variations in the shading or hue of the filter due to the deposited powder. This technique was limited to samples which contained high concentrations of a deeply colored powder (VO_2 or carbon black) and to gross inhomogeneities. It also required well dispersed samples as shown in

Figures 5-3 and 5-4. There is a correlation between the color of the deposit on the filter and the photomicrographs shown in Figures 5-5 to 5-13.

- b. Examining electron micrographs of the deposited sample. A measure of the degree of uniformity of the sample could be obtained by examining many different areas of a filter under a microscope and comparing the variation in the observed values of the surface coverage, K_t , obtained from different photomicrographs.

A measure of the degree of sample uniformity can also be obtained by comparing the experimentally observed value of surface coverage, K_t , in a given photomicrograph to the expected value (based on powder content), which would be obtained, if the particles were completely dispersed and uniformly deposited. The limitations of this measurement are:

- a. The visibility of the particles in the micrograph. If the particles are much smaller than the limit of resolution of the photomicrograph the apparent measured surface coverage will be too low. As previously discussed, photomicrographs at 4500X would provide the best measure of K_t .
- b. The degree of agglomeration of the deposited sample. Since $K_t = K_0 (\bar{d}/\bar{D} \epsilon)$, K_t may be different than K_0 even if the sample is uniformly deposited, if it significantly agglomerated. For well dispersed samples where $\bar{D}/\bar{d} \rightarrow 1$ and $\epsilon \rightarrow ()$, K_t may be equal to K_0 . For agglomerated samples, with values of $\bar{D}/\bar{d} > 1$, K_t may be larger or smaller than K_0 depending on the value of ϵ . If $\epsilon \rightarrow 0$, $K < K_0$ since $\bar{d}/\bar{D} < 1$. However if $\epsilon \rightarrow 1$, as would occur with an open structured agglomerate, then K_t could be larger than K_0 .

Examination of Tables 5-2 to 5-5 for deposition tests with individual powders, indicates that for most of the runs, especially the final test samples after a long dispersion time indicated that the ratio $K_t/K_{exp} < 1.5$. For uranium, for runs DA1-14 to DA1-17, K_t increases with increasing powder as expected. There are discrepancies for some of the earlier runs in particular DA1-1 and DA1-10, DA1-11 and DA1-12. These results will be discussed later. For carbon black (Table 5-3) there is excellent agreement. For runs F1-1 to F1-14 $K_t/K_{exp} < 1.5$.

There is also good agreement for calcium fluoride (Table 5-4) except for run F3-1 where K_t is large. The values of K_t are lower than K_0 for clay based on \bar{d}_{vs} . This reflects the assumptions used in arriving at \bar{d}_{vs} (i.e., flat plate with an aspect ratio of 7:1) and the assumption that the clay particles shall lie flat on the filter.

For the powder mixtures (Tables 5-6 to 5-13) there is general agreement between K_t and K_o (the total surface coverage of the individual deposited powders). With the exception of the runs containing Kaolin, and samples FB1-8 and FB1-9, where secondary dispersion was prepared by shaking and with the probe.

There can be significant variations in sample uniformity if the powder is not well dispersed in the suspension being filtered. Sample DA1-1 (UO_2 dispersed for one minute only) is an example of a sample where the initial particles (following dispersion) are not well dispersed. There is still significant gross agglomeration. Any deposited material is probably present as scattered lumps of agglomerated powder. There is also the possibility with this sample that, because the material was not well dispersed in the primary dispersion, the aliquot withdrawn from the dispersion was not a representative sample. Sample FB1-8 is representative of a sample where the secondary dispersion, prepared by shaking by hand, was most probably not uniform. K_t and \bar{D}_L were both higher for sample FB1-8 than for sample FB1-10 prepared in the standard way. High values of K_t and \bar{D}_L were also found for sample FB1-9, where the secondary dispersion was prepared with the ultrasonic probe. As can be clearly seen in Figure 5-41, this is due to contamination of the sample by residual material adhering to the ultrasonic probe. Therefore, if one wishes to use a probe with a dilute sample, special care has to be taken to assure its complete cleanliness.

There can also be significant variations in sample uniformity if the sample is disturbed during the washing step. This can occur if great care is not taken in introducing the wash liquid. As shown in Figure 5-70, liquids are introduced into the filtration cell through a cannula which extends from the top of the cell to within a few millimeters above the filter surface. The main disadvantage of adding wash liquid to the cell via this cannula is that wash liquid is added from a point source and flows horizontally across the bottom of the cell, e.g. the filter on which the particles are deposited. If the wash liquid is added quickly, a wave front is formed, within a height approximately equal to the distance between the tip of the cannula and the filter surface. The horizontal velocity of the liquid traversing the filter is not small. Assuming a height of 3 mm, the wash liquid added at a rate of 1 ml/sec will have a velocity of about 0.5 cm/sec at a point 1 cm from the outlet of the cannula. This wave can disturb the deposited particles. Particles will be removed from the filter region near the cannula, where liquid velocity is higher, and be deposited near the far wall of the cell (in relation to the cannula) as the horizontal velocity of the liquid decreases and approaches zero.

This phenomenon was observed quite clearly with run DA1-11. The FC-43 wash was added quickly. The wave front of the wash was visibly darker as it moved across the filter and previously deposited particles were being picked up. About 5 mm from the cell wall, the velocity of the wash decreased perceptibly and resulted in the formation of a dark line of material on the filter. A direct analogy is an ocean wave picking up and redepositing sand on a beach. Figure 5-71 shows a photomicrograph taken at the center of the filter sample, and Figure 5-72 is a photomicrograph taken at the edge region where the line of dark material was formed, resulting in a local region with a high particle loading. The degree of reagglomeration in this zone is significantly higher than in the central region for reasons already discussed in Section 5.6.4.

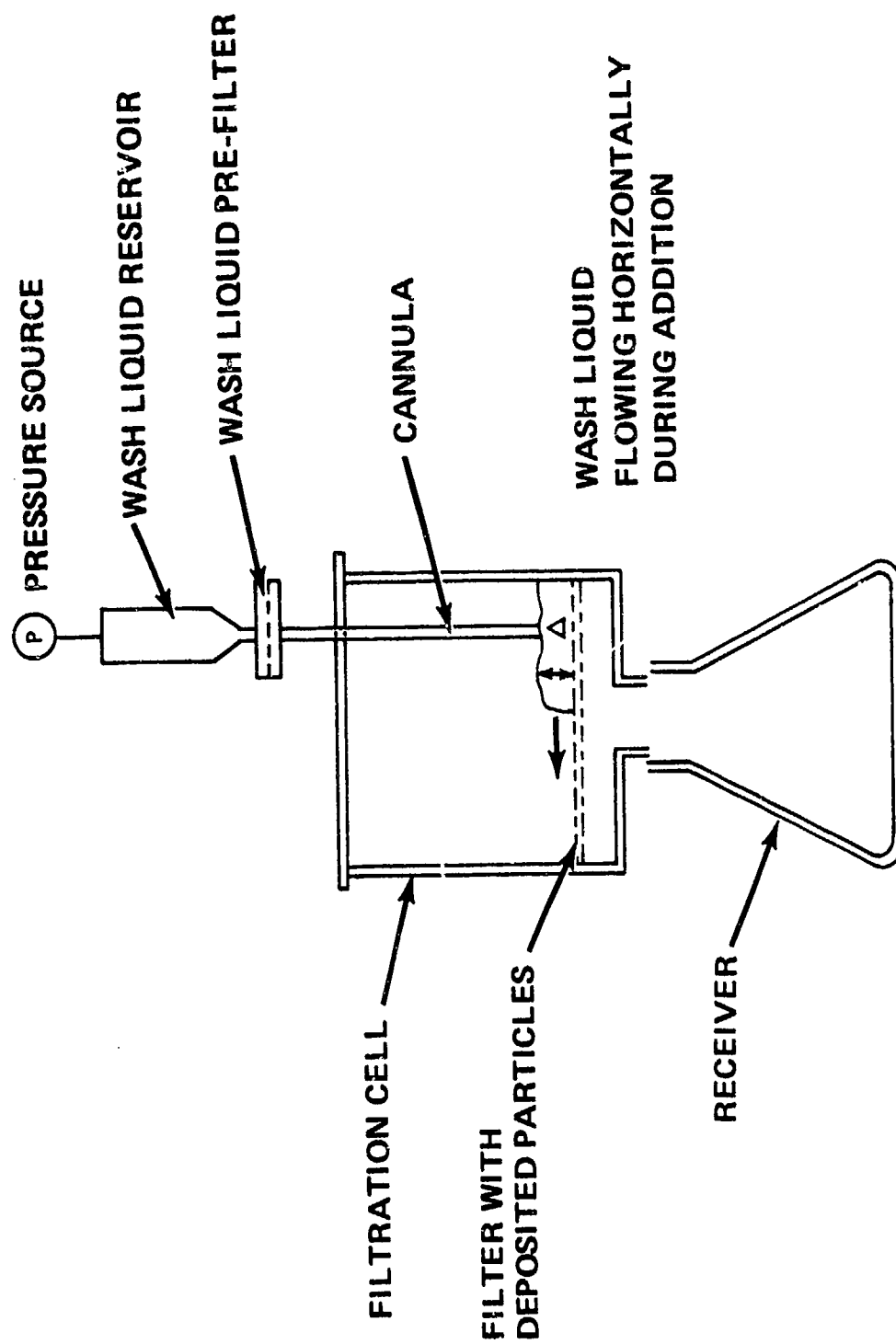


Figure 5-70 ADDITION OF WASH LIQUID TO DEPOSITED PARTICLES

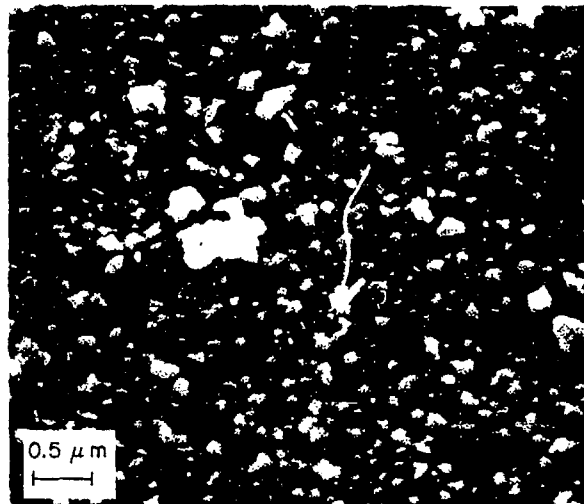


Figure 5-71 SEM PHOTOMICROGRAPH OF DEPOSITED UO_2
SAMPLE DA1-11 (NEAR CENTER OF FILTER)

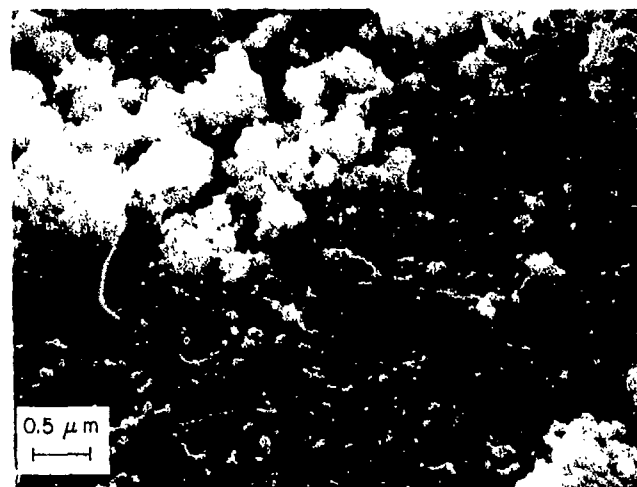


Figure 5-72 SEM PHOTOMICROGRAPH OF DEPOSITED UO_2
SAMPLE DA1-11 (NEAR EDGE OF FILTER)

83-1312

To circumvent this problem, the wash liquid has to be introduced in such a manner that it has a minimum horizontal velocity relative to the particles deposited on the filter. One way of accomplishing this is to add the wash liquid very slowly in dropwise fashion. This was the procedure used for the bulk of the runs presented in the study. Based on the results obtained, it appears that this is a satisfactory way of proceeding, even though the wash liquid still has a finite horizontal velocity. The sandwich and the "pousse cafe" techniques were conceived as two alternate methods of completely eliminating the problem.

In the sandwich runs, the wash liquid would flow horizontally across the top filter which would act as a diffuser. The wash liquid would only flow vertically past the particles deposited between the two filters. The sandwich method was not satisfactory because:

- a. The filters did not separate cleanly when pulled apart. Part of the surface layer of one filter sometimes remained attached to the other filter, thus masking the particles deposited in the region.
- b. From electron micrographs, it was observed that the deposited particles did not adhere preferentially or uniformly to one or the other filter. The samples did not appear as uniform as those obtained with direct but careful addition of the wash liquid.
- c. The technique was slow. Because of the increase in hydraulic resistance of two filters in series, the time needed to filter the wash was much greater than by drop-wise addition. Furthermore, two filters doubles the time needed for analysis of the sample.

This method was abandoned after the preliminary tests presented in Table 5-2.

In the "pousse-cafe" wash technique, the wash liquid is layered above the dispersion before the particles are deposited. This also prevents the problem of wash liquid flowing horizontally past deposited particles. This method was only tried on one sample at the end of the program, Sample FQ1-10. The deposited sample appeared to be quite uniform in photomicrographs. However, because it is a multicomponent sample, it is hard to quantify the results. The major drawback of this method was the high residual fluorine content of the deposited material as discussed in the previous section. This occurred because Freon E-1, which has a density of 1.54 gm/cm^3 , was used as the wash liquid.

Since the density of FC-43 ($\rho = 1.88 \text{ gm/cm}^3$) is higher than the density of a 1% Krytox 157 - Freon E-3 solution ($\rho = 1.73 \text{ gr/cm}^3$) used to disperse the particles, FC-43 could not be layered directly above the suspension before deposition. The following subterfuges might result in improved washing:

a. Pousse Cafe Wash with Freon E-1 Buffer Layer

The concept is to introduce the dispersion into the cell and then float on this dispersion a layer of Freon E-1 or other fluorinated liquid of lower density than the dispersion. Pressure is applied to the cell and the particles are deposited while the dispersion is filtered. FC-43 is

slowly added to the floating wash liquid after the particles are deposited. The low density wash liquid acts as a diffuser for the FC-43. After sufficient FC-43 has been added to result in an effective wash, but before it has been completely filtered, Freon E-1 or Freon C-51-12 is layered above the FC-43. The final addition displaces the non-volatile FC-43 with volatile liquid which is readily dried.

b. Upward Flow During Washing

Another way of eliminating the motion of wash liquid across the interface would be to deposit the particles on the filter as before. After the particles were deposited, the cell would be turned upside down so that the filter is now at the top of the cell. The FC-43 wash would be introduced at the bottom of the cell and pumped upward against the filter. After a sufficient amount of FC-43 was made to flow past the particles to remove the bulk of the residual Krytox 157, and thus obtain particle adherence to the filter, the ultrafiltration cell, filled with FC-43, would be returned to its original position (the filter is now at the bottom of the cell). The remaining FC-43 in the cell would be filtered through the membrane. A low density volatile wash liquid would be added on top of the FC-43 layer as before.

The second approach appears as though it would be more cumbersome than the first. It would also be limited to dispersion containing submicron particles. At an applied pressure of 1 psi, the superficial velocity of FC-43 through an Amicon XM-100A membrane is approximately 10^{-3} cm/sec. This is equal to the terminal settling velocity of a 3 μ m uranium dioxide particle in the liquid due to the acceleration of gravity. Suspensions containing larger particles could not be filtered unless the filtering pressure were increased. This would present other drawback with the XM-100A membrane, as discussed in Section 2.5.5.

6.0 SUMMARY, CONCLUSIONS AND RECOMMENDATIONS

6.1 Summary

6.1.1 Technical Problem

Often the analysis of particles released to the environment from industrial facilities is hindered because these particles are combined with others in the form of agglomerates or conglomerates. If the particle(s) of interest are small in comparison to the others as is usually the case, useful and necessary information will be lost due to a present lack of capability for selectively analyzing single particles within an agglomerate/conglomerate.

The "spontaneous" agglomeration/conglomeration of finely divided solids (below 1 micrometer in size) is believed to be essentially due to secondary valence forces or Van der Waal forces. These forces have a universal character and have to be taken into account with any finely dispersed system of solid particles, irrespective of the composition of the solid materials or of surrounding fluid phase. While there are no obvious techniques of dispersing sub-micron particles in the gas phase, it is standard technology to disperse sub-micron particles in liquid systems which contain surface active agents.

The requirement that the suspension method developed must disperse the agglomerated materials into separate particles without physical or chemical changes places stringent limitations on the choice of liquids that can be used to disperse the particles. The components of the candidate liquid dispersing mixtures must, therefore, neither react nor combine irreversibly with any particle in the matrix. Ideal candidate materials are the fluorinated hydrocarbon liquids, which are stable, chemically inert, and furthermore, not found in nature so that the presence of any residual material is readily detectable. It has been demonstrated that colloidal dispersions can be prepared in these inert media by using poly (hexafluoropropylene oxide) carboxylic acids as a stabilizing agent.

The objective of this program was to develop to a routine procedure the capability for using a perfluorinated surfactant as an agent in bringing about the dispersion of particles in an agglomerate/conglomerate. The dispersion would be of such a nature as to allow subsequent analytical measurements to be made on the separated particles. As a result of the advent of new instrumentation which potentially permits chemical analysis of particles much smaller than 1 micrometer in diameter, and because such particles are usually present as agglomerates, emphasis was directed toward developing a capability for dispersion of agglomerates/conglomerates comprised of particles in the size range of 0.005 to 5 micrometers released to the environment from industrial facilities.

The goals of the program were to develop a dispersion technique that had the following desirable characteristics:

- a. No physical or chemical change in original particles due the dispersion process (mandatory).
- b. No sample loss.

- c. Complete dispersion (100% efficiency).
- d. No reagglomeration of dispersed particles.
- e. Final state of each individual dispersed particle compatible with analysis by various techniques (electron microprobe, scanning and transmission electron microscopes, ion microprobe, mass spectrometer, etc.).

6.1.2 General Methodology

The great ease with which fine powders can be dispersed in a liquid phase as compared to the gas phase formed the basis of the approach which is outlined in Figure 6-1. The agglomerated matrix is first dispersed in a fluorinated organic liquid which is unlikely to dissolve or react irreversibly with any of the solid particles that form the matrix. The dispersed solid particles in suspension are then partitioned from the liquid phase by filtration, using a filtering membrane such as an ultrafilter, that has pores smaller than the smallest particles in suspension. By making the concentration of particles small enough and the area of the filter large enough for a given volume of suspension, the particles will be separated from each other on a statistical basis when deposited on the filter. After removing the residual dispersing liquid adhering to the particles on the filter, by evaporation for example, a system of dry, isolated solid particles is obtained on the filter membrane. These particles can then be examined individually.

The purpose of the investigation was to develop this sample preparation technique, and demonstrate that it could be used as a routine procedure of preparing agglomerated/conglomerated powders for analysis, using commercially available materials and equipment.

6.1.3 Technical Results

The experimental investigations were carried out with the four powders described in Table 6-1. These powders are considered to be representative of many classes of sub-micron particles found in the atmosphere. The properties and function of the fluorinated liquids used in the study are listed in Table 6-2.

The principal factors investigated were:

- a. Solid/liquid interaction.
- b. Powder dispersion.
- c. Choice of ultrafiltration membrane.
- d. Deposition and characterization of dispersed particles.

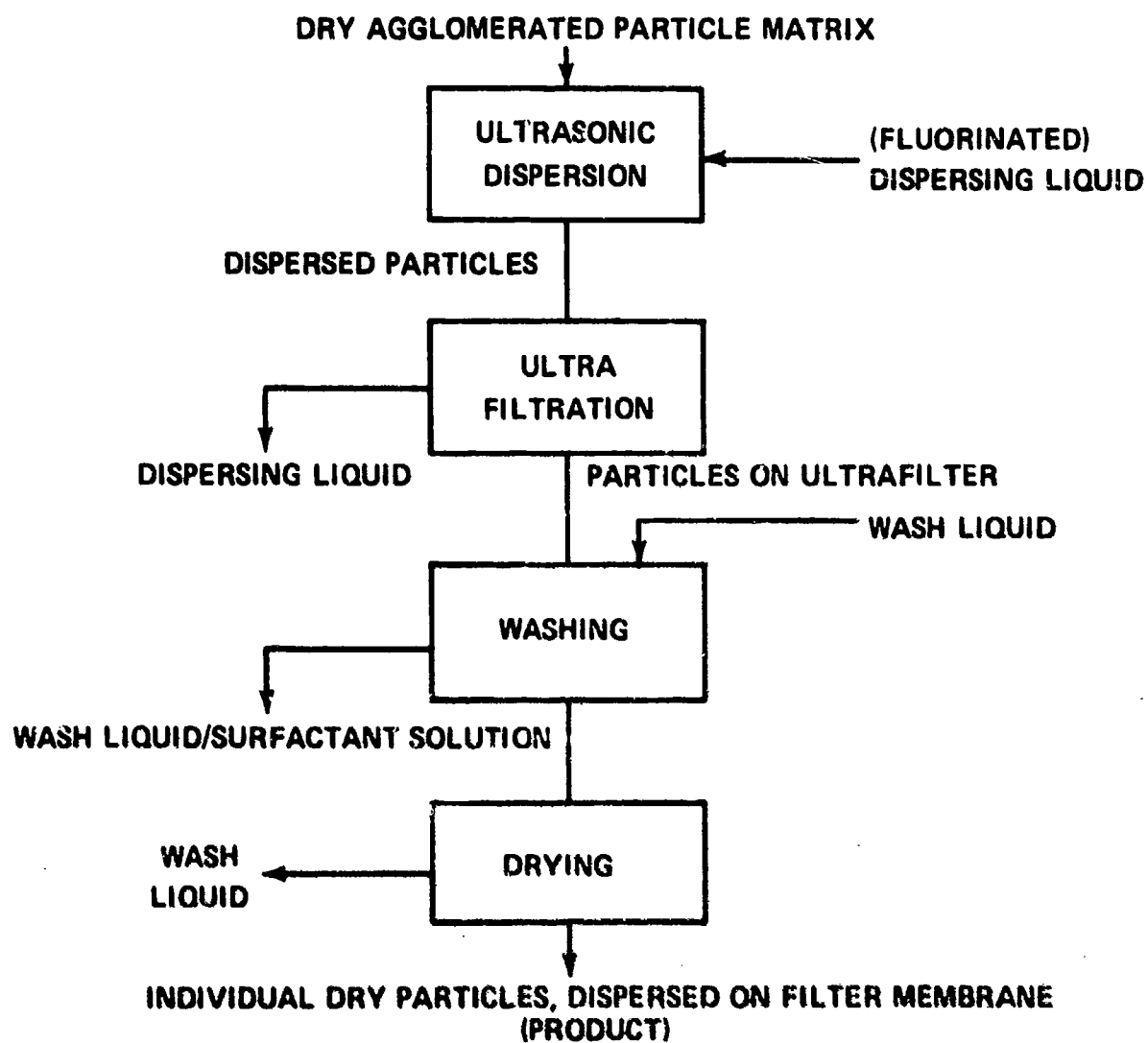


Figure 6-1 MATERIAL FLOW DIAGRAM FOR AVCO
DISPERSION TECHNIQUE

TABLE 6-1
POWDERS USED IN STUDY

POWDER	URANIUM DIOXIDE	CALCIUM FLUORIDE	CARBON BLACK	KAOLIN
DESIGNATION	ENL-1	PRECIPITATED, USP	STERLING MT	PEERLESS NO. 2
SOURCE	ELDORADO NUCLEAR	J. T. BAKER	CABOT	R.T. VANDERBILT
SPECIFIC SURFACE AREA, BY BET, M ² /GR	6.0	10.1	8.5	12.5
PARTICLE SHAPE	~ SPHERICAL	~ SPHERICAL	SPHERE	PLATE
PARTICLE DENSITY, GR/CM ³	10.9	3.18	1.8	2.60
BET EQUIVALENT PARTICLE SIZE, μ M	0.092	0.19	0.39	0.44*

*PLATE

TABLE 6-2

PRINCIPAL FLUORINATED LIQUIDS USED IN STUDY

Liquid	Krytox 157	Freon E-3	FC-43	Freon C-51-12
Manufacturer	Dupont	Dupont	3M	Dupont
Chemical Formula	$\begin{array}{c} \text{CF}_3 \\ \\ \text{F}(\text{CF}_2\text{CF}_2\text{O})_n\text{CF}_3\text{COOH} \\ n \approx 15-20 \end{array}$	$\begin{array}{c} \text{CF}_3 \\ \\ \text{F}(\text{CF}_2\text{CF}_2\text{O})_3\text{CF}_3\text{CH} \end{array}$	$(\text{C}_4\text{F}_9)_3\text{N}$	C_6F_6
Density at 25°C, gr/cm^3	1.89	1.72	1.88	1.7
Viscosity at 25°C, CP	1700	2.37	5.53	0.98
Boiling Point, °C	Very High	152	174	45
Use in Program	Dispersing Agent	Dispersing Liquid	Primary Wash Liquid	Secondary Wash Liquid

Solid-Liquid Interaction: Determine the extent and reversibility of the interaction of fluorinated chemical compounds that could be used in the process with various powder samples of interest. While solid/liquid interaction is required in order to disperse the powder, this interaction has to be reversible in order to prevent contamination of the prepared particles by these fluorinated agents which might interfere with their subsequent analysis.

It was found that Krytox 157 was adsorbed on the surface of all the candidate powders. Depending on the powder and temperature, the amount of Krytox 157 adsorbed per unit area of powder at saturation ranged from about 5 mg/m² to 10 mg/m². Surface saturation was attained at bulk liquid Krytox 157 concentrations of less than 0.5% weight-percent. Adsorbed Krytox 157 was effectively removed from the surface of the particles by washing with FC-43 fluorinated liquid.

Powder Dispersion: Determine the processing conditions such as time, temperature, and dispersion energy input that result in well dispersed suspension of agglomerated/conglomerated powders in fluorinated liquids of interest.

The effect of two ultrasonic transducers on the dispersion of candidate powders and their mixtures in various fluorinated liquids (Freon E-3 and FC-43) was studied as a function of irradiation time (up to 5400 min), at different temperatures (35° - 80°C), surfactant concentration (0 - 1.0% by weight in carrier liquid) and powder concentrations (0.8 to 8.0 mg/ml). The two ultrasonic generators used on this study were a Branson E ultrasonic cleaning bath irradiating at 40 KHz, with a power density of 2 watts/cm²; and a Branson Sonifier Model S-75 ultrasonic probe, irradiating at 20 KHz, with a maximum powder density of over 80 watts/cm². In these tests, the size of the suspended solids (e.g., the degree of dispersion) was monitored as a function of dispersion time, principally by measuring the turbidity of aliquots diluted to a constant powder concentration. Additional data on suspensoid size distribution was obtained by centrifugal sedimentation.

It was found that the candidate powders could be ultrasonically dispersed in fluorinated solutions of Krytox 157. The principal results were as follows:

Composition of the Dispersing Liquid: Solutions of Krytox 157 in Freon E-3 are much more effective media for dispersion than solutions of Krytox 157 in FC-43. With both liquids, there is little or no dispersion in the absence of Krytox 157. A one weight percent Krytox 157/Freon E-3 solution effectively dispersed all the candidate powders and their mixtures.

Ultrasonic Power Intensity: Increasing the ultrasonic power intensity increases both the rate and extent of the dispersion process, especially as the size of the ultimate particle decreases. The powders were much more effectively dispersed with the ultrasonic probe than with the ultrasonic bath.

Time: The rate of dispersion decreases with increasing sonolation time, indicating that the dispersion process depends on the size of the agglomerates present.

Size of the Ultimate Particles: The smaller the size of the ultimate particles in the agglomerate or conglomerate, the more difficult it becomes to disperse these particles. The most difficult powder to disperse was ENL-1 uranium dioxide which was the finest particle sized powder studied. This powder contained a large fraction of particles smaller than 0.1 μm , with particles as small as 0.04 μm being definitely present. It took approximately 600 min to disperse this powder with the ultrasonic probe. It was not dispersed after 5400 min in the ultrasonic bath.

Temperature: The effect of temperature on the rate of dispersion depends on the composition of the particles to be dispersed. All the powders studied could be effectively dispersed at 35°C or 50°C. Increasing the temperature to 80°C had an adverse effect on the dispersion of kaolin and carbon black.

Particle Concentration: There was no noticeable effect of particle concentration at the concentration levels examined.

Mixture of Powders: Mixtures of powders did not behave in a significantly different manner than individual powders.

Re-agglomeration: It was noted that powders once dispersed stayed dispersed. The dispersion tests with the probe could be interrupted without noticeable re-agglomeration taking place.

These results can be explained in terms of a simple model which considers that an agglomerate or conglomerate is broken into smaller agglomerates and/or individual particles if stresses of sonic origin exceed the strength of the agglomerate. The dispersion process is enhanced by the presence of Krytox 157, which adsorbs at the surface of the particles. The adsorbed Krytox 157 reduces attractive particle-to-particle forces in the agglomerate, thus facilitating agglomerate breakdown and also prevents dispersed particles from re-agglomerating after they have been liberated from an agglomerated matrix. It appears from the results that there is not sufficient ultrasonic energy to break primary bonds, i.e., reduce the size of the ultimate particles.

Ultrafilters: Determine which commercially available ultra-filtration membranes can be used in this technique. Desirable filter characteristics include retention of the smallest particles of interest, inertness in fluorinated liquid media used to prepare the powder samples, high permeability and stability, and lack of interference with different methods of analysis.

The major manufacturers of the ultrafiltration membranes were contacted. Of the many membranes available, twelve commercial membranes were selected for further study. The Amicon XM-100A ultrafiltration membrane is considered to be superior to any other ultrafiltration membranes that are presently commercially available. The XM-100A membrane is very stable in a scanning electron microscope. A given deposited particle can be examined at magnifications as high as 45000X for many minutes without noticeable decomposition of the membrane. The pores of the XM-100A membrane are sufficiently small to be unobservable at the magnifications used in this study. In SEM examination of properly prepared samples, the Amicon XM-100A membrane appears as a blank dark grey background that has no relief with all observable particles retained on the surface of the membrane. This greatly facilitates the examination of individual particles and the measurement of particle size distribution curves.

Samples deposited on an XM-100A can be examined for elemental composition by a non-dispersive x-ray probe. The only interference due to the filter is a very noticeable chlorine peak due to the composition of the filter itself. This chlorine peak did not interfere with interpretation of the spectra of the deposited inorganic particles studied. The Amicon XM-100A membrane could also be used as a substrate for electron microprobe work by using a defocused 15 Kv electron beam. Use of high intensity focused beams resulted in the destruction of the filter.

The Amicon XM-100A membrane was stable when brought in contact with the fluorinated liquids used to disperse the particles. It showed negligible retention for Krytox 157, the dispersing agent used in these studies. The hydraulic permeability of the fluorinated liquids through this membrane was sufficiently high (~ 0.1 ml/min - cm²-psig) to permit rapid filtration at filtration pressures of less than 10 psig-the maximum operating pressure for this membrane.

The minimum size of particle retained by this membrane is estimated to be equal to the pore size of the membrane which is approximately 0.007 μ m. Smaller particles could be captured by using finer pored membranes, but at the expense of a lower hydraulic permeability and increased retention of Krytox 157 micelles, which would interfere with the sample preparation technique and the subsequent measurements.

Deposition and Characterization of Dispersed Particles:

Utilizing the information obtained as described above, determine the conditions required to provide well-dispersed particles on a stable substrate. Demonstrate the effectiveness of the method by suitable comparative analyses of a variety of prepared samples and of the initial powders.

Information obtained from each of the previous studies was integrated in the particle deposition studies which are the culmination of the program. During this phase of the program, samples of the candidate powders and their mixtures dispersed in a fluorinated liquid were deposited on an ultrafiltration membrane which was then washed and dried. The effects of dispersion time and powder loading on the filter were systematically investigated. The deposited powder samples were all examined by scanning electron microscopy. The micrographs were examined visually and with an automated particle counter to obtain qualitative and quantitative information on the degree and quality of dispersion of the deposited samples. In addition, the elemental composition of selected samples was determined, using either an electron probe microanalyzer or a non-dispersive x-ray element analyzer.

6.1.4 Preparative Method Developed

The basic preparative procedure developed consists of the following steps:

- a. Preparation of a primary concentrated dispersion: The powder sample, typically 50 mg or less, is dispersed ultrasonically in a centrifuge tube containing 25 ml of a 1% Krytox 157 - Freon E-3 solution at 50°C. It is recommended that a high intensity probe, such as a Sonifier, be used to carry out the dispersion and that the dispersion process be monitored with a nephelometer.

In order to insure complete dispersion, the sample should be sonolated until no further change in turbidity is observed, which could require in excess of 600 min.

- b. Preparation of a dilute secondary dispersion with a desired particle concentration: An aliquot sample of the above dispersion is removed and diluted with an additional 25 ml of 1% Krytox 157 - Freon E-3 solution. It is necessary that diluted samples be well mixed. The size of the aliquot is adjusted to obtain a particle loading on the deposition filter of $1 \mu\text{g}/\text{cm}^2$ or less, depending on the particle size.
- c. Ultrafiltration of the dilute secondary dispersion: The secondary dispersion is filtered through an Amicon XM-100A ultrafiltration membrane at an applied pressure of about 1 psig, resulting in the deposition of particles larger than $0.007 \mu\text{m}$ on the membrane.
- d. Washing and Drying of Deposited Particles: About 25 ml of fluorinated liquid FC-43 are slowly added to the cell and allowed to permeate past the deposited particles to remove the dispersing medium and adsorbed surfactant. About 25 ml of a very volatile fluorinated liquid, Freon C-Freon C-51-12, are then added to remove the non-volatile FC-43. The Freon C-51-12 wet filter is easily air dried.

The product is an assembly of individual particles deposited on a flat laboratory filter. Individual particles or sub-assemblies of particles can be readily examined on this filter by a variety of microanalytical tools.

6.2 Conclusions

The major goals of the program have been met in that a preparative procedure has been developed which will permit normally agglomerated or conglomerated particles less than $1 \mu\text{m}$ in size, down to at least $0.02 \mu\text{m}$ in size, (which is the limit of resolution of a scanning electron microscope) to be analyzed individually.

The method requires that the agglomerates be initially well dispersed and deposited at a low surface concentration. Just as the analysis of individual particles becomes increasingly more difficult to perform with decreasing particle size, the method of preparation becomes more difficult as the size of the particles decreases. As the size of particles decreases, the acoustic energy required for dispersion increases and the permissible surface concentration of deposited particles decreases. With very small ($< .01 \mu\text{m}$), particle retention becomes a problem.

6.3 Recommended Further Research

The preparative procedure was tested with known samples only. The technique should now be applied to samples of natural origin. Within the scope of the present program, it was not possible to carry out any detailed, indepth analysis of the deposited samples. This should be performed to obtain a sound statistical basis of deposited sample uniformity.

The preparative technique and the quality of the samples may be improved by:

- a. Examining the suitability of the Amicon SM ultrafiltration membrane when it becomes commercially available. This membrane, which is presently under development, would be more resistant to high energy beams than the Amicon XM-100A membrane, while still retaining the other desirable characteristics of the latter.
- b. Examine the effect of improved ultrasonic dispersion equipment. The time required for dispersion, especially of small particles less than $0.1 \mu\text{m}$ in size, could be significantly reduced by developing an ultrasonic transducer optimized for this application.
- c. Examine deposition of low particle loadings: The degree of re-agglomeration decreases markedly with powder loading, but so does the number of particles per unit area. In these studies the minimum loading examined was $0.5 \mu\text{g}/\text{cm}^2$. Examinations of samples with a lower powder loading is believed warranted, especially if the sample contains a significant concentration of particles smaller than $0.1 \mu\text{m}$ in size.

7.0 LIST OF REFERENCES

Chapter 1

- 1-1 Davies, R., et al, "Sub-Micron Separation and Data", I.I.T. Research Institute, Chicago, Illinois, Report No. IITRI-C-6239-A005-1, Contract No. F-33657-71-C-0859, AD 739197, 31 October 1971.
- 1-2 Meissner, H.P., et al, I & EC Process Design and Development, 3, 197-201 (1964).
- 1-3 Rumpf, H., Chem. Ing. Tech., 30, 144 (1958).
- 1-4 Rumpf, H., "Strength of Granules and Agglomerates", 379-418, Agglomeration, Knepper, W.A., Editor, Interscience Publishers, New York, 1962.
- 1-5 Van der Waals, J.D., Dissertation, Leyden (Netherlands) 1873.
- 1-6 Kallmann, H., and Willstatter, H., Naturwissenschaften, 20, 959 (1932).
- 1-7 London, F., Z. Physik, 63, 245, (1930).
- 1-8 Lifschitz, E.M., J. Exp. Theor. Physik USSR, 29, 94 (1954).
- 1-9 DeJongh, J.G.V., "Measurement of Retarded Van der Waals Forces", Doctoral Dissertation, Utrecht Univ. (Netherlands) 1958).
- 1-10 Verwey, E.J.W., and Overbeek, J. Th.G. "Theory of the Stability of Lyophobic Colloids", p. 4, Elsevier Publishing Company, Amsterdam, 1948.
- 1-11 Mackor, E.L., J. Colloid Science, 6, 492 (1951).

Chapter 2

- 2-1 Medalia, A.I. and Heckman, F.A., J. Colloid and Interface Sci., 36 173 (1971).
- 2-2 Medalia, A.I., J. Colloid and Interface Sci., 24 393 (1967).
- 2-3 Meissner, H.P., et al, I & EC Process Design and Development, 5, 10-14 (1966).
- 2-4 Noge, Y., et al, Fed. Proc., 29 (5) 1802 (1970).
- 2-5 E.I. duPont de Nemours & Co., Inc., "Freon" Products Division, "Freon" E Series Fluorocarbons", Technical Bulletin EL-8B, Wilmington, Del., 1967.
- 2-6 E.I. duPont de Nemours & Co., Inc., "Freon" Products Division, "Freon C-51-12 Fluorocarbon", Technical Bulletin EL-13, Wilmington, Del., 1967.
- 2-7 3M Company Chemical Division "3M Brand Inert Fluorochemical Liquids" St. Paul, Minn. 1965.

Chapter 2 (Continued)

- 2-8 3M Company Chemical Division, St. Paul, Minn., "Personal Communication", February, 1973.
- 2-9 MacKenzie, J.S., Allied Chemical Corp., Buffalo, New York, "Personal Communication", December, 1971.
- 2-10 Kaiser, R., and Rosensweig, R.E., "Study of Ferromagnetic Liquid", NASA CR 1407, August, 1969.
- 2-11 Anon, "Physical Properties of Chemical Compounds", p. 12, Advances in Chemistry Series No. 15, American Chemical Society, Washington, D.C., June, 1955.
- 2-12 Lawson, N. D., E. I. DuPont de Nemours and Co., Inc., Wilmington, Del., Personal Communication, July 13, 1971.
- 2-13 Preusser, H. J., Kolloid Z. u. Z. Polymere, 250, 133-141 (1972).
- 2-14 Preusser, H. J., Kolloid Z. u. Z. Polymere, 250, 579-583 (1972).

Chapter 3

None

Chapter 4

- 4-1. Fry, W.J. and F. Dunn, "Ultrasound" Analysis and Experimental Materials in Biological Research, in Physical Techniques in Biological Research, Vol. IV, Special Methods, Mastuk Ed. Academic Press, New York, 1962, p. 265.
- 4-2. Boucher, R.M.G., Brit. Chem. Eng., 15, 363 (1970).
- 4-3. Sollner, K., Trans. Farr. Soc., 34, 1170 (1938).
- 4-4. Sollner, K., Chem. Revs., 34, 371 (1944).
- 4-5. Mathieu - Sicaud, A. and G. Levavasseur, Compt. Rendus., 227 (3), 196 (1948).
- 4-6. Nukina, K., et al, Kolloid-Z.u.Z. Polymere, 250, 116 (1972).
- 4-7. Herdan, G., "Small Particle Statistics", 2nd Edition, p. 85, Butterworths, London, 1960.
- 4-8. Hertz, H., J. Reine Angew. Math., p. 92 (1881).
- 4-9. Kaiser, R., "Agglomeration of Zinc Oxide Powder", ScD Thesis, M.I.T., Cambridge, Mass., 1962.
- 4-10. Rumpf, H., Chem. Ing. Tech., 30, 144 (1958).
- 4-11. Patton, T.C., "Paint Flow and Pigment Dispersion", Chapter 7, Interscience Publishers, New York, 1964.
- 4-12. Kaiser, P., and Rosensweig, R.E., "Study of Ferromagnetic Liquid", NASA CR 1407, August, 1969.

Chapter 5

- 5-1. Herdan, G., loc. cit Ref. 4-7.
- 5-2. Kruyt, H.R., Editor, "Colloid Science", Volume I, Chapter VII,
"Kinetics of Flocculation" by THG Overbeck, p. 278-283, Elsevier
Publishing Company, Amsterdam, 1952.
- 5-3. Kruyt, H.R., ibid., p. 286-288.

APPENDIX A

Standard Avco Method of
Preparation of Powder Support Films

General techniques using parlodian and evaporated carbon support films^(A-1) have been used for the various powders.

1. A large petri dish (~15 to 20 cm diameter), fitted with a drain tube and tap, is filled with distilled water.
2. A large circle of fine wire gauze (about 100 mesh/in) is placed on the bottom of the dish.
3. Any number of grids are placed on the wire gauze.
4. Two drops of a 4% solution of parlodian in amyl acetate are allowed to fall on the surface at the center of the dish from a dropping pipette.
5. When the solvent has evaporated to leave a solid film, it is removed from the surface with a needle; its purpose is to clean the water surface.
6. A second film is now formed in the same way and this can be mounted on grids. Neither film will reach the edge of the dish because, as the parlodian solution moves across the water surface, it sweeps a layer of contaminant molecules from the center to the edge. This layer eventually becomes resistant to compression, preventing further expansion of the parlodian film.
7. When the second film is solid, the tap is opened and the surface layer allowed to slowly settle onto the grids.
8. The petri dish is partly covered and the wire gauze and grid allowed to dry in place.
9. Each plastic film is broken with a fine needle point at the grid O.D., then the coated grids can be picked up.

This method permits the coating of a large number of grids in one operation and films are of relatively uniform thickness and unbroken over the whole area of the grid.

An alternate technique which produces extremely uniform plastic films consists of filling a clear glass dish (~20 cm diameter) with distilled water. The surface of the water can be cleaned by placing a drop or two of 4% solution of parlodian on the water, then lifting the film while collecting the dust particles. Place another drop of parlodian on the water surface and allow to dry to thin plastic film. When dry, grids are placed on selected areas of the film containing best dispersion and thinness. With a round-hole loop, center and pick up a grid with film while cutting film at C.D. of loop. Invert and place on specimen peg driers.

Carbon is evaporated onto the plastic films prepared by either of the above techniques. These carbon-parlodion support films are generally used as is; however, the parlodion can be dissolved with amyl acetate after the powder is dispersed on the film.

Powder Dispersion

The various powders are mixed with ethyl alcohol until a slightly cloudy solution exists. The solutions are ultrasonically dispersed (~5 min in ultrasonic vibrator) and a sample immediately taken with an eye dropper. One drop is placed on a carbon-parlodion support film and allowed to dry under cover. Several specimens were made to insure random sampling of each powder. The samples are then placed in the electron microscope and photographed.

Reference

A-1. Drummond, D.G., J. Roy. Micr. Soc., 70, 1 (1950).

APPENDIX B

ADSORPTION OF KRYTOX 157 FROM
FLUORINATED SOLUTIONS ON CANDIDATE POWDERS

TABLE B-1
ADSORPTION DATA
FIRELESS NO. 2 CLAY (12.5 m²/gr) - FREON E-3 - KRYTOX 157 SYSTEM

Test No.	Powder Weight (Grams)	Surface Area m ²	Weight of Solution (Grams)	Initial Surf Conc In Liquid Wt %	Final Surf Conc In Liquid Wt %	Initial Amt Surf In Liquid (Grams)	Final Amt Surf In Liquid (Grams)	Amt Surf Adsorbed (Grams)	Surf Adsorbed, mg/m ²
187	1.1116	16.5	17.1512	1.38	0.59	0.2367	0.1012	0.1355	8.26
188	1.1403	14.2	17.1932	0.524	0.053	0.0918	0.0091	0.0827	5.82
189	0.9176	11.5	17.1508	1.00	0.51	0.1715	0.0875	0.0840	8.29
190	0.8733	5.94	17.1470	0.534	0.24	0.0915	0.0412	0.0503	8.47
204	0.7096	8.82	17.1712	1.38	0.99	0.2361	0.1700	0.0669	7.59

Contact Time: 7 1/2 hours in 40 Waz Branson Ultrasonic Bath

Temperature: 25°C

Samples Filtered through: Pollicon Ultrafiltration Membrane PSM.

TABLE E-2

ADSORPTION DATA

PERMILES NO. 2 CLAY (12.5 m^2/gr) - FREON E-3 - KRYTOX 157 SYSTEM

Test No.	Powder Weight (Grams)	Surface Area m^2	Weight of Solution (Grams)	Initial Sur: Conc In Liquid Wt %	Final Surf Conc In Liquid Wt %	Initial Amt Surf In Liquid (Grams)	Final Amt Surf In Liquid (Grams)	Amt Surf Adsorbed (Grams)	Surf Adsorbed mg/m^2
215	0.6100	7.63	17.0945	0.423	0.19	0.0721	0.0316	0.0405	5.31
216	0.7922	9.82	17.583	0.695	0.40	0.1191	0.0681	0.0510	5.20
217	0.8042	10.60	17.1763	1.00	0.70	0.1718	0.1207	0.0511	4.84
218	1.0923	13.73	17.1590	1.09	0.62	0.1870	0.1064	0.0806	5.90
219	1.2870	16.00	17.1172	1.20	0.76	0.2054	0.1301	0.0753	4.71

Contact Time: 24 Hours in 40 KHz Branson Ultrasonic Bath

Temperature: 50°C

Samples Filtered Twice through Pollicon Ultrafiltration Membrane PSM

TABLE B-3

ADSORPTION DATA

PEARLESS NO. 2 CLAY (12.5 m²/gm) - FC-43 - KRYTOX 157 SYSTEM

Test No.	Powder Weight (Grams)	Surface Area (m ²)	Weight of Solution (Grams)	Final Surfactant Conc. In Liquid Weight %	Initial		Final Amount		Surfactant Adsorbed mg/m ²
					Amt In Liquid (Grams)	Surfactant In Liquid (Grams)	Surfactant Adsorbed (Grams)	Amount Adsorbed (Grams)	
72	3.8739	47.2	37.0631	0.12	0.371	0.044	0.327	5.25	
71	3.0895	38.5	37.7046	0.28	0.377	0.106	0.271	7.05	
60	2.0853	26.1	37.3600	0.50	0.374	0.187	0.187	7.20	
59	1.5030	18.8	36.2803	0.57	0.363	0.207	0.156	8.31	
58	1.1580	14.4	37.2211	0.66	0.372	0.246	0.126	8.77	

Initial Krytox 157 Concentration: 1.007% by Weight

Temperature: 25°C

Contact Time: > 24 Hours in Sonoblaster 200 Ultrasonic Bath

Samples filtered through Millipore VS Ultrafilters.

TABLE B-4
 ADSORPTION DATA
 PEERLESS NO. 2 CLAY ($12.5 \text{ m}^2/\text{gm}$) - FC43-KRYTOX 157 SYSTEM

Test No.	Powder Weight (Grams)	Surface Area m^2	Weight of Solution (Grams)	Initial Surf Conc In Liquid Wt %	Final Surf Conc In Liquid Wt %	Initial Amt Surf In Liquid (Grams)	Final Amt Surf In Liquid (Grams)	Amt Surf Adsorbed (Grams)	Surf Adsorbed/ mg/m^2
82A	0.7814	9.75	18.7770	0.44	0.22	0.0826	0.0413	0.0413	4.23
83A	0.3967	5.00	18.6093	0.44	0.28	0.0819	0.0521	0.0298	5.96
101A	1.1926	14.87	18.6931	0.44	0.12	0.0322	0.0224	0.0598	4.02
102A	0.6469	8.12	18.6912	0.44	0.24	0.0822	0.0448	0.0374	4.60
109A	1.1411	14.26	18.4799	0.99	0.56	0.1830	0.1035	0.0795	5.58
110A	0.7680	9.60	18.2752	0.99	0.69	0.1809	0.1261	0.0548	5.70
119A	0.4289	5.36	18.3645	1.03	0.86	0.1892	0.1579	0.0313	5.85
120A	1.5405	19.25	18.4411	1.03	0.41	0.1899	0.0756	0.1143	5.95
132	0.3940	4.93	18.6051	1.26	1.10	0.2344	0.2047	0.0297	6.04

Temperature: 50°C

Contact Time: 24 Hours Before Filtration in Sonoblaster 200 Ultrasonic Bath.

Samples Filtered Through Pellicon PSJM Ultrafiltration Membrane.

TABLE B-5
ADSORPTION DATA
PEERLESS NO. 2 CLAY ($12.5 \text{ m}^2/\text{gr}$) - FREON C-51-12 - KRYTOX 157 SYSTEM

Test No.	Temp °C	Powder Weight (Grams)	Surface Area m^2	Weight of Solution (Grams)	Initial Surf Conc In Liquid Wt %	Final Surf Conc In Liquid Wt %	Initial Amt Surf In Liquid (Grams)	Final Amt Surf In Liquid (Grams)	Amt Surf Adsorbed (Grams)	Surf Adsorbed/ mg/m^2
135	16	0.4409	5.51	16.6473	1.06	0.920	0.1765	0.1532	0.0233	4.21
36	16	0.7219	9.02	16.6378	1.06	0.840	0.1763	0.1398	0.0365	4.04
137	16	1.0060	12.60	16.6040	1.06	0.745	0.1759	0.1237	0.0525	4.17
144	16	1.4377	18.00	16.6466	0.40	0.050	0.0666	0.0083	0.0583	3.24
145	16	0.5422	6.78	16.6493	0.40	0.225	0.0666	0.0375	0.0291	4.29

Contact Time: 24 Hours in 40 Khz Branson Ultrasonic Bath.
Samples Filtered through Feliicon PSJM Ultrafilter Membrane.

TABLE B-6

ADSORPTION DATA

STERLING MT CARBON BLACK ($8.5 \text{ m}^2/\text{gr}$) - FREON E-3 - KRYTOX 157 SYSTEM

Test No.	Powder Weight (Grams)	Surface Area m^2	Weight of Solution (Grams)	Initial Surf Conc In Liquid Wt %	Final Surf Conc In Liquid Wt %	Initial Amt Surf In Liquid (Grams)	Final Amt Surf In Liquid (Grams)	Amt Surf Adsorbed (Grams)	Surf Adsorbed/ mg/m^2
191	1.2677	10.8	16.9985	1.38	1.03	0.2346	0.1751	0.0595	5.51
193	1.0301	8.76	7.1616	0.543	0.26	0.0932	0.0446	0.0486	5.55
194	0.7439	6.32	17.0068	1.21	1.02	0.2058	0.1735	0.0323	5.11
205	0.7405	6.29	16.4252	1.00	0.78	0.1643	0.1281	0.0362	5.78
207	0.7014	5.96	14.9174	0.717	0.48	0.1070	0.0716	0.0354	5.94

Contact Time: 24 Hours in 40 KHz Branson Ultrasonic Bath.

Temperature: 25°C

Samples Filtered through Pellicon Ultrafiltration Membrane PSJM.

TABLE B-7

ADSORPTION DATA

STERLING MT CARBON BLACK ($8.5 \text{ m}^2/\text{gr}$) - FREON E-3 - KRYTOX 157 SYSTEM

Test No.	Powder Weight (Grams)	Surface Area m^2	Weight of Solution (Grams)	Initial Surf Conc In Liquid Wt %	Final Surf Conc In Liquid Wt %	Initial Amt Surf In Liquid (Grams)	Final Amt Surf In Liquid (Grams)	Amt Surf Adsorbed (Grams)	Surf Adsorbed mg/m^2
240	0.5478	4.66	17.6957	0.42	0.34	0.0749	0.0598	0.0151	3.24
241	0.6550	5.57	17.1133	0.70	0.58	0.1189	0.0993	0.0196	3.52
242	0.8164	6.94	17.1235	1.00	0.79	0.1712	0.1358	0.0354	5.10
243	1.0623	9.03	17.1079	1.09	0.92	0.1865	0.1579	0.0286	3.17
244	1.1915	10.10	17.1285	1.20	0.97	0.2055	0.1656	0.0399	3.94

B-8

Contact Time: 24 Hours in 40 Khz Branson Ultrasonic Bath

Temperature: 50°C

Samples Filtered Twice through Pellicon Ultrafiltration Membrane PSJM

TABLE B-8
ADSORPTION DATA
STERLING MT CARBON BLACK ($8.5 \text{ m}^2/\text{gm}$) - FC43 - KRYTOX 157 SYSTEM

Test No.	Powder Weight (Grams)	Surface Area (m^2)	Weight of Solution (Grams)	Final Surfactant Conc. In Liquid Weight %	Initial Amt. Surfactant In Liquid (Grams)	Final Amount Surfactant In Liquid (Grams)	Amount Surfactant Adsorbed (Grams)	Surfactant Adsorbed mg/m^2
68	2.1075	18.24	37.3644	0.94	0.377	0.354	0.023	1.3
67	1.4090	11.90	37.2351	1.04	0.376	0.391	(0.015)	
66	0.8881	6.98	37.4520	1.14	0.378	0.430	(0.058)	
46	0.4804	4.09	37.0763	1.04	0.374	0.389	(0.015)	
47	0.3782	2.87	37.3207	0.98	0.376	0.368	0.008	2.8

Initial Krytox 157 Concentration: 1.01% by Weight

Temperature: 25°C

Contact Time: > 24 Hours in Sonoblaster 200 Ultrasonic Bath

Samples filtered through Millipore VS Ultrafilters.

TABLE B-9
ADSORPTION DATA
STERLING MF (8.5 m²/gm) - FC43-KRYTOX 157 SYSTEM

Test No.	Powder Weight (Grams)	Surface Area m ²	Weight of Solution (Grams)	Initial Surf Conc In Liquid Wt %	Final Surf Conc In Liquid Wt %	Initial Amt Surf In Liquid (Grams)	Final Amt Surf In Liquid (Grams)	Amt Surf Adsorbed (Grams)	Surf Adsorbed/ m ² /gm
99A	0.4719	4.01	18.6453	0.44	0.28	0.0820	0.0522	0.0298	7.40
100A	1.1570	9.94	18.6909	0.44	0.19	0.0822	0.0355	0.0467	4.70
105	0.7078	6.02	18.6926	0.44	0.28	0.0822	0.0524	0.0298	4.95
106	0.9580	8.14	18.6959	0.44	0.21	0.0823	0.0393	0.0430	5.28
113A	0.7639	6.49	18.4502	0.99	0.66	0.1827	0.1218	0.0609	9.28
114A	0.9866	8.31	18.3821	0.99	0.62	0.1820	0.1140	0.0680	8.20

Temperature: 50°C

Contact Time: 24 Hours Before Filtration on 40 KHz Branson Ultrasonic Bath.

Samples Filtered Through Pellicon PSJM Ultrafilter Membrane

TABLE B-10

ADSORPTION DATA

STERLING MT (8.5 m²/gr) - FREON C-51-12 - KRYTOX 157 SYSTEM

Test No.	Temp °C	Powder Weight (Grams)	Surface Area m ²	Weight of Solution (Grams)	Initial Surf Conc In Liquid Wt %	Final Surf Conc In Liquid Wt %	Initial Amt Surf In Liquid (Grams)	Final Amt Surf In Liquid (Grams)	Amt Surf Adsorbed (Grams)	Surf Adsorbed/ mg/m ²
162	16	1.1931	10.1	16.6709	0.51	0.22	0.0842	0.0348	0.0494	4.87
163	16	0.3717	3.16	16.5639	0.51	0.44	0.0836	0.0728	0.0108	3.42
164	16	0.9531	8.10	16.6100	1.02	0.74	0.1699	0.1229	0.0470	5.80
165	16	0.4374	3.72	16.6728	1.02	1.00	0.1705	0.1667	0.0038	1.02
179*	22	0.5289	4.50	16.6539	1.11	1.05	0.7848	0.1748	0.0100	2.22
180*	22	0.7624	6.50	16.6500	1.35	1.30	0.2247	0.2165	0.0082	1.27

Contact Time: 24 Hours in Sonoblastar 200 Ultrasonic Bath or Branson 40 Khz Ultrasonic Bath(*).
 Samples Filtered through Pellicon PSM Ultrafilter Membrane.

TABLE B-11
ADSORPTION DATA
PRECIPITATED CALCIUM FLUORIDE ($10.1 \text{ m}^2/\text{g}$) - FREON E-3 - KRYTOX 157 SYSTEM

Test No.	Powder Weight (Grams)	Surface Area cm^2	Weight of Solution (Grams)	Initial Surf Conc In Liquid Wt %	Final Surf Conc In Liquid Wt %	Initial Amt Surf In Liquid (Grams)	Final Amt Surf In Liquid (Grams)	Amt Surf Adsorbed (Grams)	Surf Adsorbed/ mg/m^2
195	1.0137	10.2	19.1586	1.21	0.70	0.2076	0.1201	0.0875	8.57
196	1.0243	10.3	16.8862	0.717	0.32	0.1211	0.0540	0.0671	6.51
197	0.5667	5.72	17.2154	0.717	0.43	0.1234	0.0740	0.0494	8.63
198	0.7533	8.01	17.1878	1.21	0.68	0.2080	0.1169	0.0911	11.4
206	0.9454	9.55	15.5608	1.00	0.55	0.1556	0.0856	0.0700	7.33
228	0.5550	5.61	17.1463	1.409	1.08	0.2416	0.1852	0.0564	10.1
228*	0.5550	5.61	17.1463	1.409	1.02	0.2416	0.1749	0.0667	11.9

Contact Time: 24 Hours in 40 KHz Branson Ultrasonic Bath

Temperature: 25°C

Sampler Filtered through Pellicon Ultrafiltration Membrane PSM.

*Refiltered through Pellicon Ultrafiltration Membrane PSED.

TABLE B-12
ABSORPTION DATA
PRECIPITATED CALCIUM FLUORIDE (10.1 m²/gr) - FREON E-3 - KRYTOX 157 SYSTEM

Test No.	Powder Weight (Grams)	Surface Area m ²	Weight of Solution (Grams)	Initial Sur: Conc In Liquid Wt %	Final Sur: Conc In Liquid Wt %	Initial Amt Surf In Liquid (Grams)	Final Amt Surf In Liquid (Grams)	Amt Surf Adsorbed (Grams)	Surf Adsorbed mg/m ²
245 (1)	0.7490	7.57	17.0387	0.42	0.30	0.0723	0.0504	0.0219	2.89
245 (2)	0.7490	7.57	17.0387	0.42	0.24	0.0723	0.0402	0.0321	4.24
246	0.8196	8.48	17.2030	0.70	0.47	0.1196	0.0800	0.0396	4.67
246R	0.8194	8.48	17.2030	0.70	0.36	0.1196	0.0621	0.0575	6.78
247	0.9430	9.52	17.1263	1.00	0.56	0.1713	0.0956	0.0757	7.94
247R	0.9430	9.52	17.1263	1.00	0.42	0.1713	0.0719	0.0994	10.44
248	1.1463	11.60	17.1234	1.09	0.92	0.1866	0.1575	0.0291	2.51
248R	1.1463	11.60	17.1234	1.09	0.66	0.1866	0.1036	0.0736	6.35
249	1.3307	13.40	16.4715	1.20	0.87	0.1977	0.1436	0.0541	4.02
249R	1.3307	13.40	16.5715	1.20	0.82	0.1977	0.1347	0.0630	4.69

~ Contact Time: 24 Hours in 40 Mhz Branson Ultrasonic Bath

Temperature: 50°C

(1) Samples Filtered Once through Pellicon Ultrafiltration Membrane PSED

(2) Samples Filtered Twice through Pellicon Ultrafiltration Membrane PSED

TABLE B-13
ADSORPTION DATA
PRECIPITATED CALCIUM FLUORIDE (10.1 μ^2 /gm) - FC43-KRYTOX 157 SYSTEM

Test No.	Powder Weight (Grams)	Surface Area μ^2	Weight of Solution (Grams)	Initial Surf Conc In Liquid Wt %	Final Surf Conc In Liquid Wt %	Initial Amt Surf In Liquid (Grams)	Final Amt Surf In Liquid (Grams)	Amt Surf Adsorbed (Grams)	Surf Adsorbed/ mg/m^2
88A	0.7364	7.63	18.6439	0.44	0.09	0.0820	0.0168	0.0652	8.55
101A	1.2206	12.32	18.7066	0.44	0.082	0.0823	0.0153	0.0670	5.44
104A	0.6134	6.19	18.7006	0.44	0.14	0.0823	0.0262	0.0561	9.06
111A	1.4576	14.72	18.2608	0.99	0.18	0.1308	0.0329	0.1479	10.0
112A	0.8333	8.47	18.2028	0.99	0.52	0.1802	0.0947	0.0855	10.1
113A	1.2058	12.12	18.1363	1.03	0.37	0.1868	0.0671	0.1197	9.88

Temperature: 50°C

Contact Time: 24 Hours Before Filtration In Branson 40 KHz Ultrasonic Bath.

Samples Filtered Through Pellicon P30M Ultrafilter Membrane

TABLE B-14

ADSORPTION DATA

PRECIPITATED CALCIUM FLUORIDE ($10.1 \text{ m}^2/\text{gr}$) - FREON C-51-12 - KRYTOX 157 SYSTEM

Test No.	Temp °C	Powder Weight (Grams)	Surface Area m^2	Weight of Solution (Grams)	Initial Surf Conc: In Liquid Wt %	Final Surf Conc In Liquid Wt %	Initial Amt Surf In Liquid (Grams)	Final Amt Surf In Liquid (Grams)	Amt Surf Adsorbed (Grams)	Surf Adsorbed/ mg/m^2
149	16	1.5106	15.50	16.5833	0.40	0.02	0.0671	0.0033	0.0638	4.12
150	16	0.5637	5.69	16.5423	0.40	0.20	0.0669	0.0323	0.0346	6.08
151	16	0.8735	2.73	16.6189	0.40	0.29	0.0673	0.0482	0.0191	6.87
157	16	1.1232	11.30	16.6100	1.02	0.51	0.1699	0.0839	0.0860	7.61
160	16	1.0146	10.20	16.5609	0.50	0.13	0.0828	0.0215	0.0613	6.25
161	16	0.3359	3.39	16.6071	0.50	0.35	0.0830	0.0581	0.0249	7.35
177*	22	0.4893	4.94	16.6432	1.11	0.94	0.1847	0.1569	0.0278	5.62
178*	22	1.5216	15.40	16.6308	1.11	0.39	0.1846	0.0657	0.1189	7.72
184*	22	0.9155	9.25	16.6231	1.41	1.06	0.2094	0.1732	0.0361	6.61
185*	22	1.3188	13.50	15.5578	1.41	0.77	0.2194	0.1195	0.0999	6.40

Contact Time: 24 Hours in Sonobath 200 Ultrasonic Bath or Branson 40 KHz Ultrasonic Bath (*).

Samples Filtered through Pallison P33M Ultrafilter Membrane.

TABLE B-15

ADSORPTION DATA

PRECIPITATED CALCIUM FLUORIDE (10.1 m²/gm) - FC43 - KRYTOX 157 SYSTEM

Test No.	Powder Weight (Grams)	Surface Area (m ²)	Weight of Solution (Grams)	Final Surfactant Conc. in Liquid Weight %	Initial Amt. Surfactant In Liquid (Grams)	Final Amount Surfactant In Liquid (Grams)	Amount Surfactant Adsorbed (Grams)	Surfactant Adsorbed mg/m ²
75	4.0735	41.4	36.8714	0.26	0.369	0.097	0.272	6.68
74	2.9396	29.6	37.4530	0.39	0.375	0.146	0.229	7.74
57	2.1277	21.4	37.2589	0.64	0.373	0.240	0.133	6.21
56	1.7230	17.4	37.8223	0.78	0.378	0.216	0.162	9.31
55	1.2736	12.9	37.2935	0.74	0.373	0.277	0.096	7.44
37	0.6412	6.50	37.4327	0.83	0.374	0.310	0.064	9.84

Initial Krytox 157 Concentration: 1.007% by Weight

Temperature: 25°C

Contact Time: > 24 Hours in Sonoblaster 200 Ultrasonic Bath

Samples filtered through Millipore VS ultrafilter.

TABLE B-16

ADSORPTION DATA

URANIUM DIOXIDE ENL-1 (6.9 m²/g) - FREON E-3 - KRYTOX 157 SYSTEM

Test No.	Powder Weight (Grams)	Surface Area m ²	Weight of Solution (Grams)	Initial		Final		Amt Surf Adsorbed (Grams)	Final Amt Surf In Liquid (Grams)	Amt Surf Adsorbed (Grams)	Surf Adsorbed/mg/m ²
				Surf Conc In Liquid Wt %	Surf Conc In Liquid Wt %	Surf Conc In Liquid Wt %	Surf Conc In Liquid Wt %				
NA 1	0.4654	2.73	39.0024	1.10	1.04	1.04	1.04	0.0234	0.4026	0.0234	8.4
NA 4	0.4460	2.68	45.9779	0.55	0.49	0.49	0.49	0.0270	0.2259	0.0270	10.1
NA 5	0.4992	3.00	42.9800	0.29	0.23	0.23	0.23	0.0279	0.0980	0.0279	9.3
NA 6	0.5059	3.03	43.4197	0.11	0.05	0.05	0.05	0.0261	0.3217	0.0261	8.6

Exhaust Conditions: 24 hrs in 40 kHz Branson Ultrasonic Bath at 50°C.

Samples filtered through 90 mm Amicon XM-100A Ultrafiltration Membrane.

TABLE B-17
ADSORPTION DATA
URANIUM DIOXIDE ENL-1 ($6.0 \text{ m}^2/\text{gr}$) - FREON E-3 - KRYTOX 157 SYSTEM

Test No.	Powder Weight (Grams)	Surface Area m^2	Weight of Solution (Grams)	Initial Surf Conc In Liquid Wt %	Final Surf Conc In Liquid Wt %	Initial Amt Surf In Liquid (Grams)	Final Amt Surf In Liquid (Grams)	Amt Surf Adsorbed (Grams)	Surf Adsorbed/ m^2/m
199	1.2192	7.32	17.1681	0.346	0.025	0.0594	0.0043	0.0551	7.53
200	1.0602	6.36	17.1491	0.534	0.08	0.0916	0.0137	0.0779	12.2
201	0.7728	4.64	17.1615	0.717	0.49	0.1230	0.0841	0.0389	8.38
202	0.7071	4.24	17.1100	1.21	1.00	0.2070	0.1694	0.0376	8.87
203	0.6779	4.07	17.1665	1.38	1.24	0.2369	0.2129	0.0240	5.90

Contact Time: 24 Hours in 40 Kh Hanson Ultrasonic Bath

Temperature: 25°C

Samples Filtered through Pellicon Ultrafiltration Membrane PSED.

TABLE B-18

ADSORPTION DATA

URANIUM DIOXIDE ENL-1 (6.0 m²/gr) - FREON E-3 - KRYTOX 157 SYSTEM

Test No.	Powder Weight (Grams)	Surface Area m ²	Weight of Solution (Grams)	Initial Surf Conc In Liquid Wt %	Final Surf Conc In Liquid Wt %	Initial Amt Surf In Liquid (Grams)	Final Amt Surf In Liquid (Grams)	Amt Surf Adsorbed (Grams)	Surf Adsorbed mg/m ²
199	1.2192	7.32	17.1681	0.346	0.12	0.0594	0.0206	0.0388	5.30
200	1.0602	6.36	17.1491	0.534	0.30	0.0916	0.0514	0.0402	6.31
201	0.7728	4.64	17.1615	0.717	0.62	0.1230	0.1064	0.0166	3.57
202	0.7071	4.24	17.1100	1.21	1.27	0.2070	-	-	-
203	0.6779	4.07	17.1665	1.38	1.32	0.2369	0.2266	0.0103	2.53

Contact Time 24 Hours in 40 Kh Branson Ultrasonic Bath

Temperature: 25°C

Samples Filtered through Pellicon Ultrafiltration Membrane P8JM.

TABLE B-19

ADSORPTION DATA

URANIUM DIOXIDE ENL-1 (6.0 μ^2/g) - FC43 - KRYTOX 157 SYSTEM

Test No.	Powder Weight (Grams)	Surface Area (m^2)	Weight of Solution (Grams)	Final Surfactant Conc. In Liquid Weight %	Initial		Final Amount		Surfactant Adsorbed mg/ m^2
					Amt. Surfactant In Liquid (Grams)		Surfactant In Liquid (Grams)	Amount Surfactant Adsorbed (Grams)	
70	4.3511	26.20	31.8899	0.30	0.379		0.113	0.266	10.2
69	3.0409	18.20	36.3579	0.42	0.364		0.153	0.211	11.6
64	2.0752	12.40	37.3049	0.51	0.373		0.190	0.183	14.8
63	1.8138	10.82	36.9296	0.56	0.369		0.207	0.162	14.9
62	1.3836	8.30	37.0825	0.65	0.371		0.241	0.130	15.7

Initial Krytox 157 Concentration: 1.007% by Weight

Temperature: 25 °C

Contact Time: 24 Hours in Sonoblaster 200 Ultrasonic Bath.

Samples Filtered through Millipore VS Ultrafilter.

TABLE B-20
ADSORPTION DATA
URANIUM DIOXIDE ENL-1 (6.0 m²/gm) - FC43-KRYTOX 157 SYSTEM

Test No.	Powder Weight (Grams)	Surface Area m ²	Weight of Solution (Grams)	Initial Surf Conc In Liquid Wt %	Final Surf Conc In Liquid Wt %	Initial Amt Surf In Liquid (Grams)	Final Amt Surf In Liquid (Grams)	Amt Surf Adsorbed (Grams)	Surf Adsorbed/ mg/m ²
107	1.994	7.20	18.6181	0.44	0.19	0.0819	0.0354	0.0465	6.46
108	0.5349	3.21	18.3856	0.44	0.38	0.0809	0.0698	0.0111	3.45
108A	0.5349	3.21	18.3856	0.44	0.37	0.0809	0.0680	0.0128	4.01
115A	1.1711	7.03	18.3600	0.99	0.66	0.1817	0.1212	0.0606	8.61
116A	0.7700	4.42	18.1571	0.99	0.94	0.1796	0.1705	0.0091	2.05
92A	0.7826	4.69	18.6711	0.44	0.32	0.0822	0.0597	0.0225	4.79

Temperature: 50°C

Contact Time: 24 Hours Before Filtration in Branson 40 KHz Ultrasonic Bath.

Samples Filtered Through Pellicon PSJM Ultrafiltration Membrane.

TABLE B-21

ADSORPTION DATA

URANIUM DIOXIDE ENL-1 (5.0 m²/gr) - FREON C-51-12 - KRYTOX 157 SYSTEM

Test No.	Temp °C	Powder Weight (Grams)	Surface Area m ²	Weight of Solution (Grams)	Initial Surf Conc In Liquid Wt %	Final Surf Conc In Liquid Wt %	Initial Amt Surf In Liquid (Grams)	Final Amt Surf In Liquid (Grams)	Amt Surf Adsorbed (Grams)	Surf Adsorbed/mg/m ²
142	16	1.2724	7.63	16.6474	1.08	0.87	0.1798	0.1449	0.0349	4.57
143	16	0.6782	4.07	16.4765	1.08	1.61	0.1779	0.1829	(-0.0050)	-
147	16	1.5430	9.26	16.5307	0.40	0.24	0.0669	0.0405	0.0264	2.85
148	16	0.7006	4.20	16.6103	0.40	0.23	0.0663	0.0382	0.0282	6.71
153	16	1.0723	6.43	16.6581	1.02	0.81	0.1704	0.1366	0.0338	5.25
154	16	1.6024	9.61	16.5482	1.02	0.66	0.1688	0.1092	0.0596	6.20
156	16	1.2200	7.32	16.6400	0.51	0.28	0.0849	0.0466	0.0383	5.23
181*	22	1.2765	7.66	16.6327	1.11	0.72	0.1846	0.1247	0.0599	7.82
182*	22	1.5900	9.54	16.6514	1.11	0.57	0.1848	0.0948	0.0900	9.43
183*	22	0.6918	4.15	16.6660	1.11	0.82	0.1849	0.1366	0.0483	11.60

Contact Time: 24 Hours in Sonoblaster 200 Ultrasonic Bath or Branson 40 KHz Ultrasonic Bath (*).
 Samples Filtered through Pellicon Ultrafiltration Membrane PSM.

APPENDIX C

SURFACE RE-AGGLOMERATION OF DEPOSITED PARTICLES

The agglomeration volume is defined by the surface area of the filter and a height \bar{x} . The latter quantity may be estimated by the following simplified analysis. The flux of particles towards the membrane will be a function of the diffusion coefficient, D , and the flow rate of the wash liquid, v , according to the following equation:

$$J = D \frac{dc}{dx} + vC \quad (1)$$

where

J = flux of particles to the surface.

C = particle concentration, particles/unit volume.

A lower bound on \bar{x} may be obtained by assuming that a pseudo steady state prevails during washing and that the rate at which particles within the agglomeration volume adhere to the membrane is small compared to the magnitude of either term on the righthand side of equation (1), in which case $J \approx 0$.

The concentration decreases from C_W near the filter to zero at a height equal to \bar{x} . As a first approximation, therefore, equation (1) becomes:

$$D \frac{C_W}{\bar{x}} + v C_W = 0 \quad (2)$$

Thus

$$\frac{D}{\bar{x}} = v \quad (3)$$

or

$$\bar{x} = \frac{D}{v} \quad (4)$$

Within the agglomeration volume, particle collisions take place which lead to re-agglomeration. The rate of agglomeration can be expressed in terms of Von Smoluchowski's theory of rapid coagulation of colloidal suspension (3-1). According to this theory the rate of disappearance of primary particles, dc/dt is given by the following equation:

$$\frac{-dc}{dt} = 8\pi D R c^2 \quad (5)$$

where

R = distance of approach for coagulation.

In the simplest case, R is equal to twice the particle radius, or particle diameter, d .

The total number of particles in suspension decreases with time according to the second order kinetic equation which can be integrated to yield the following:

$$\frac{C_t}{C_0} = \frac{1}{1 + t/\tau} \quad (6)$$

where

C_t = Total number of particles in suspension/unit volume at time, t .
This includes the sum of primary particles, as well as binary, ternary, etc., agglomerates.

C_0 = Initial number of particles in suspension/unit volume.

The parameter τ is called the time of coagulation. It is the time in which the number of particles is halved. This coagulation half-life is expressed as follows:

$$\tau = \frac{1}{4 \pi d C_0} \quad (7)$$

Von Smoluchowski's model was developed for flocculation in bulk solutions. It can be applied to the problem of re-agglomeration near a surface of unit area by considering that the ratio n/\bar{x} is an effective bulk concentration, where n is the number of particles per unit area of filter surface and \bar{x} is defined by equation 4 above.

Substituting

$$C = \frac{nv}{d} \quad (8)$$

into equations 5, 6, and 7 yield the following equations:

$$-\frac{dn}{dt} = 8 \pi v d n^2 \quad (9)$$

and

$$\frac{n_t}{n_0} = \frac{1}{1 + t/\tau} \quad (10)$$

$$\tau = \frac{1}{4 \pi d v n_0} \quad (11)$$

It is possible to express equations 10 and 11 in terms of the parameters presented in Figure 5-67, (\bar{D}/\bar{d}) and K_t .

The average number of particles, \bar{n}_1 , in an agglomerate is by definition:

$$\bar{n}_1 = \frac{n_o}{n_t} \quad (12)$$

The volume, \bar{V} , of a mean average spherical agglomerate can be expressed as follows:

$$\bar{V} = \frac{\pi}{6} \bar{D}^3 = \frac{\pi}{6} \left(\frac{\bar{n} \bar{d}^3}{1 - \epsilon} \right) \quad (13)$$

where

\bar{D} = average agglomerate diameter

\bar{d} = average particle diameter

ϵ = volume fraction voids in the agglomerate

or

$$n_1 = \frac{\bar{D}^3}{\bar{d}^3} (1 - \epsilon) \quad (14)$$

Thus

$$\frac{n_t}{n_o} = \frac{1}{(1 - \epsilon)} \left(\frac{\bar{d}}{\bar{D}} \right)^3 \quad (15)$$

The values of surface coverage are related to n_o as follows. For spherical ultimate particles,

$$K_o = n_o \frac{\pi \bar{d}^2}{4} \quad (16)$$

where

K_o = surface coverage due to ultimate particles

or

$$n_o = \frac{4 K_o}{\pi \bar{d}} \quad (17)$$

Equation 11 can thus be rewritten as follows:

$$\tau = \frac{1}{4 \pi v \bar{d} \left(\frac{K_0}{\pi \bar{d}} \right)}$$

or

$$\tau = \frac{1}{16 v K_0 \sqrt{\bar{d}}} = \frac{\bar{d}}{16 v K_0} \quad (18)$$

Substituting equation 15 and equation 18 into equation 10, yields the following relation between \bar{D}/\bar{d} and K_0 :

$$\frac{1}{1-\epsilon} \left[\frac{\bar{d}}{\bar{D}} \right]^3 = \frac{1}{1 + 16 v t \frac{K_0}{\bar{d}}} \quad (19)$$

or

$$\frac{\bar{D}}{\bar{d}} = \left[\frac{1}{(1-\epsilon)} + \frac{16 (vt)}{(1-\epsilon)} \left(\frac{K_0}{\bar{d}} \right) \right]^{1/3}$$

An expression equivalent to Equation 19 can be written in terms of K_t , the surface coverage of agglomerated particles on the filter, which is the measured value reported in Figure 5-67. Using the same principles as above, it can be shown that:

$$K_0 = (1-\epsilon) \frac{\bar{D}}{\bar{d}} K_t \quad (20)$$

so that equation 19 can be written as follows:

$$\frac{\bar{D}}{\bar{d}} = \left[\frac{1}{1-\epsilon} + 16 v t \frac{(\bar{D})}{\bar{d}^2} K_t \right]^{1/3} \quad (21)$$

Equation 19 can also be written in terms of W_0 , the powder loading per unit area of filter surface (gm/cm^2). W_0 is proportional to n_0 , the number of particles per unit area:

$$W_0 = n_0 e v \quad (22)$$

where

ρ = particle density

\bar{v} = average particle volume

By generalizing equation 16, the following relation between K_0 and n_0 is obtained:

$$K_0 = n_0 \bar{a}_c \quad (23)$$

where \bar{a}_c is the average particle cross-sectional area. By eliminating n_0 , the following relation between W_0 and K_0 is obtained:

$$W_0 = K_0 \frac{\rho \bar{v}}{\bar{a}_c} \quad (24)$$

For a given shape, there is a correlation between the cross-sectional area and external surface area of a particle. For a given shape

$$\bar{a}_s = a \bar{a}_c \quad (25)$$

where \bar{a}_s = average surface area of a particle and a is a shape factor as defined in Table C-1. By substitution the following expression is obtained:

$$W_0 = K_0 a \left(\frac{\rho \bar{v}}{\bar{a}_s} \right) \quad (26)$$

The term $\rho \bar{v} / \bar{a}_s$ is equal to the reciprocal of the specific surface area, A_s , for the powder. Thus

$$W_0 = \frac{K_0 a}{A_s} \quad (27)$$

or

$$K_0 = W_0 \frac{A_s}{a} \quad (28)$$

Substituting equation 28 into equation 19 results in the following equation:




$$\frac{\bar{D}}{\bar{a}} = \left[\frac{1}{(1-\epsilon)} + \frac{16 \nu t}{(1-\epsilon)} \left(\frac{W_0 A_s}{a \bar{d}} \right)^{1/3} \right] \quad (29)$$

Reference

- C-1. Kruyt, H.R., Editor, "Colloid Science", Volume I, Chapter VII, "Kinetics of Flocculation", by J.Th.G. Overbeek, p. 278-283, Elsevier Publishing Company, Amsterdam, 1952.

TABLE C-1

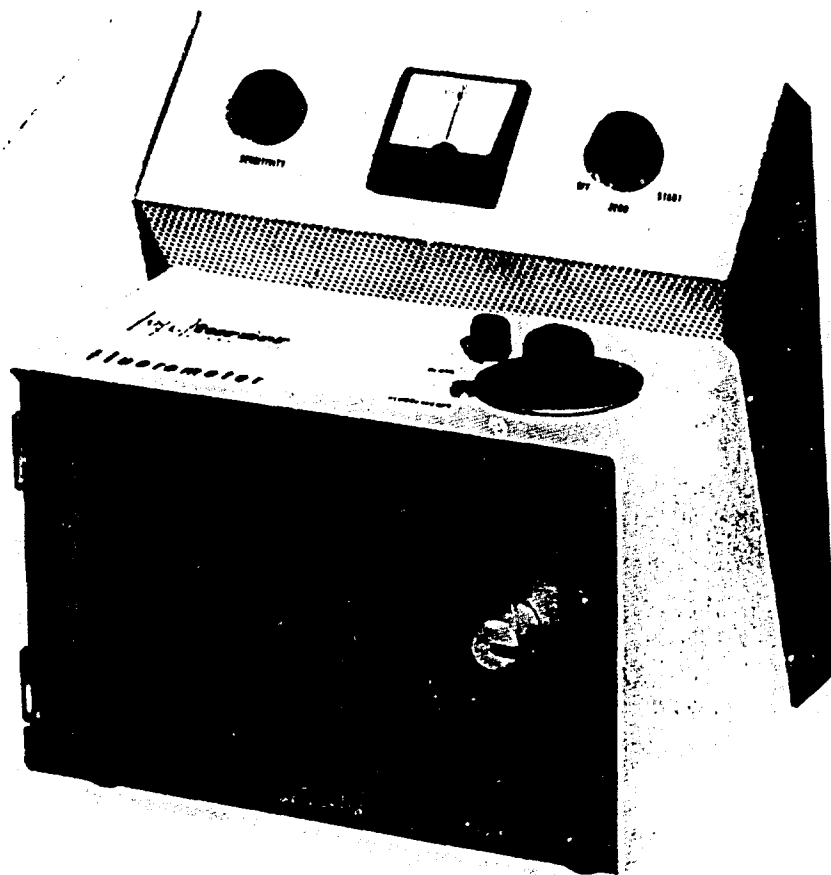
PARTICLE SHAPE FACTOR, k , FOR PARTICLES OF DIFFERENT SHAPE

<u>Particle Shape</u>	<u>Characteristic Dimension</u>	<u>Surface Area</u>	<u>Cross-Sectional Area</u>	<u>k</u>
Sphere 	D	πD^2	$\pi D^2/4$	4
Cube 	a	$6a^2$	a^2	6
Flat Plate (a, b > c) 	a, b sides	$2ab$	ab	2

APPENDIX D

Reproduced from
best available copy.

Model 110



This new fluorometer combines the accuracy, sensitivity, and stability of a research instrument with the rugged simplicity of a routine analytical tool.

It eliminates many of the problems long associated with fluorometric measurements. Easy to operate, the unit is small, occupies a single package, and is moderately priced.

A new concept in fluorometer design...

The ever-widening field of fluorometry has excited the imagination of researchers, laboratory analysts, and technicians in many areas of application. This is especially true where trace analyses in the range of parts per million or parts per billion are encountered. Yet, many of these same people have been waiting for moderately priced equipment which would provide the accuracy, repeatability, and stability which are so essential for an important laboratory tool.

We feel that the Turner Fluorometer will do much to assist today's scientists as they advance the state of the art of fluorometry. It will allow maximum time to be devoted to other phases of research or testing -- with minimum time required for actual measurements. Why? Because the device does not require recalibration and readjustment for each sample, and because the temperature and ultraviolet light levels in the sample compartment are uniquely low, ensuring minimum sample deterioration. Our users report that they no longer resort to timing the length of sample exposure to ultraviolet light.

Clinical laboratories are presently using fluorometers for determining adrenalin and noradrenalin (catecholamines) in urine and blood in a screening test for tumor of the adrenal glands. They also utilize fluorometry in measuring transaminase and lactic dehydrogenase. Many tests now in the research phase are certain to become standard clinical procedures.

Medical and biochemical research laboratories use fluorometers for a host of routine analyses, including determination of DPN, DPNH, steroids, porphyrins, serotonin, DNA, histamine, etc.

Industrial health laboratories use fluorometers for routine determination of beryllium and uranium.

Agricultural and food chemists use fluorometers for vitamin and insecticide residue studies.

Water, air pollution and sanitation engineers find the fluorometer the most effective tool available for studying flow and diffusion of air and water.

An excellent review article appears in ANALYTICAL CHEMISTRY Magazine's Analytical Reviews Issue for April, 1960. In this six-page discussion, Dr. C. E. White summarizes recent developments in fluorometric techniques, covering the period from November 1957 to November 1959. His bibliography contains 238 references of especial significance in fields ranging from metallurgy to agricultural chemistry.

SIMPLE OPERATION DESCRIBED

How to turn the fluorometer ON

1. Turn ZERO knob full c. w. to START for a few seconds, then release. The lucite button next to the FLUORESCENCE dial should illuminate to indicate that power is on. Allow two minutes warmup.
2. Open the sample holder door. Check that the u. v. source is operating by observing through the door-latch opening. Zero the meter to its balanced or "0" center position with the ZERO knob. Occasionally check this setting between samples (with door open).

How to operate the fluorometer

1. Using a standard test tube for a cuvette, place a reagent blank into the sample holder. Close the door.
2. Set the FLUORESCENCE dial at zero, then balance the meter with the BLANK knob.
3. Turn the FLUORESCENCE dial two divisions above zero. Adjust the meter SENSITIVITY knob so that the meter deflects 1/2 to one division to the right of null. Return the FLUORESCENCE dial to zero. Not a critical adjustment, this step need be repeated hereafter only when there are major line-voltage changes. This adjustment does not affect the measurement of fluorescence.
- **4. Insert a known sample and close the door. Balance the meter by turning the FLUORESCENCE dial. Note the reading which you obtain.
5. Open the door, take out the known sample, and replace it with the unknown. Close the door. Balance the meter with the FLUORESCENCE dial. Note the reading.
6. Concentration of the unknown can be determined by a simple ratio of the readings obtained in 4 and 5. Fluorescent light intensity is proportional to concentration over a very wide range.
7. To turn the instrument off, turn ZERO knob to OFF.

****NOTE:** Step 4 need only be accomplished when changes in your chemical processes make this desirable. Tests indicate that step 4 need be done only once a week, or even less frequently. Where chemical processes do cause variability of the sample and standard, the stability of the fluorometer provides an invaluable check on standard preparation.

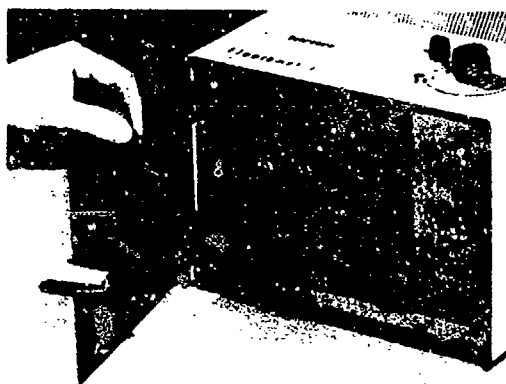
ULTRAVIOLET SOURCES:

Because some samples deteriorate rapidly when exposed to large dosages of u. v. and/or heat, we use a four-watt u. v. source to eliminate such problems. Standard Turner Fluorometers are supplied for 3600A⁰ operation, complete with primary and secondary filters, ultraviolet lamp and spare, and five matched 12 x 75 mm. round Pyrex cuvettes.

Filters are available for operation at 405, 436, and 546 mμ with the lamp normally supplied. A number of secondary filters are available, designed to isolate specific portions of the emission spectrum of the sample.

A unique feature of the Turner fluorometer is the availability of a quartz ultraviolet (254 mμ) light source, filters, and inexpensive non-fluorescent grade

quartz cuvettes. Interchange with the general-purpose light source takes about two minutes. This accessory is particularly useful for the measurement of low concentrations of serotonin, and for many insecticides.



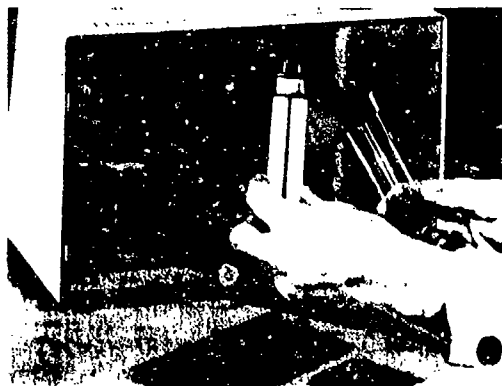
SAMPLE HANDLING

The standard sample holder door pictured here will accept ordinary test tubes as cuvettes. These can be from 10 to 15 mm. diameter, and from 75 to 100 mm. in height. It will also accept square cuvettes, 10 mm. inside and 75 mm. high.

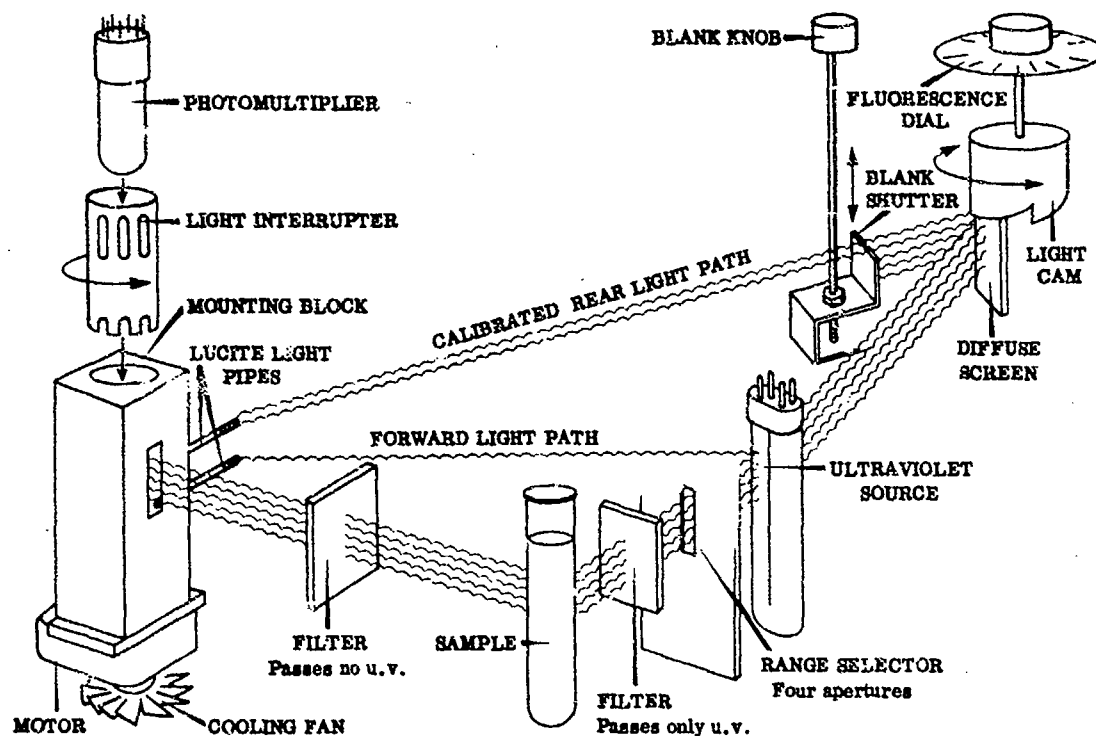
Your Turner fluorometer will always allow you to use the latest techniques. The cuvette holder door is instantaneously interchangeable with doors mounted with continuous flow cuvettes, or solid sample holders such as for uranium fusion pellets, plastic samples or paper chromatograph strips. Your inquiry, detailing your requirements, will be appreciated.

SINGLE PACKAGE CONVENIENCE

This fluorometer is a single unit, supplied ready to plug in and operate. You are freed from the necessity of attaching several units in series, or of supplying any external regulating transformers, galvanometers, light sources, or batteries.



DETAILS OF THE OPTICAL DESIGN



PRINCIPLE OF OPERATION

This fluorometer is basically an optical bridge which is analogous to the accurate Wheatstone Bridge used in measuring electrical resistance. The optical bridge measures the difference between light emitted by the sample and that from a calibrated rear light path. A single photomultiplier surrounded by a mechanical light interrupter sees light alternately from the sample and the rear light path. Photomultiplier output is alternating current, permitting a drift-free A-C amplifier to be used for the first electronic stages. The second stage is a phase-sensitive detector whose output is either positive or negative, depending on whether there is an excess of light in the forward (sample) or rear light path, respectively. Output of the phase detector drives a meter amplifier which is in turn connected to a null meter. A balanced condition, i.e., equal light from the sample and from the rear path, is indicated by the null position of the meter. The quantity of light required in the rear path to balance that from the sample is indicated by the FLUORESCENCE dial. Each of this dial's 100 divisions adds equal increments of light to the rear path by means of a light cam. Note that polarizing filters are not used for light adjustment.

Light in the rear path may also be operator-adjusted with the BLANK control which sets rear-path light to be equal to the residual fluorescence of a solvent blank with the FLUORESCENCE dial set at zero.

Light-source variations do not affect the light balance. Such variations are caused by aging of the ultraviolet source and by line-voltage and frequency changes. Because these affect both the light on the sample and light in the rear path proportionately, light balance is not changed. Variations in photomultiplier sensitivity cancel for the same reason.

Dark current is not a problem because the photomultiplier sees interrupted light and the electronic circuitry detects only the difference in light from the rear path and from the sample.

Persistence of fluorescence does not affect the unit because the light falling on the sample is steady. Only the light emitted from the fluorescent sample is interrupted.

Null-meter sensitivity is always the same, even when high-concentration work is being done with neutral-density filters in the secondary-filter holder.

There is no zero-point error, even with a non-fluorescent blank. This desirable feature is provided by an extra forward light path. Light in the rear path can always be adjusted to be either more or less than that in the forward path. The null meter moves in both directions as the FLUORESCENCE dial is rotated about zero, insuring positive establishment of a true zero.

CONTROLS

Operational controls of the Turner Fluorometer have been human engineered to provide maximum operator convenience. Those controls used during a single series of analyses are on the top and meter panels of the instrument. The range-selector knob and filters, normally changed only when a new analysis is started, are conveniently accessible when the sample holder door is open. The ZERO knob has a START position to insure positive starting of the ultraviolet source. In addition, the pointer for the FLUORESCENCE dial contains a small neon lamp to provide an indication that power is on. Operation of the ultraviolet source may be checked through the door-latch opening.

Although not immediately apparent to the casual observer, the knob used to latch the sample holder door also de-energizes the photomultiplier as the door is opened. Thus the cell cannot be fatigued because it is protected automatically from excess light.

CONSTRUCTION

Long, trouble-free life has been designed into this instrument. Component and material selections have been made with reliability and sturdiness as prime considerations.

Highest quality commercial electronic components have been used wherever suitable. Where these would not handle the requirements, industrial-quality components have been custom made to our rigid specifications.

All circuits have been carefully analyzed and tested to insure reliability, and to eliminate any necessity for special selection of electronic tubes.

Cabinet and structural construction is of carefully reinforced extra-heavy (16 gauge) steel. All critical components, such as the light-interrupter housing, light arm, and the optical-mounting blocks are precision machined from aluminum. They are then black-anodized. No detail has been overlooked; for example, the latch mechanism is made of stainless steel -- and the painted surfaces are solvent-resistant baked enamel.

SERVICE

This instrument is very straightforward in its electromechanical design, . . . and in its operation as well. An easy-to-understand operation and maintenance manual containing schematics and diagrams of both the electronic and mechanical assemblies is supplied with each unit.

With minor exceptions, standard parts are used throughout. Those parts not standard are considered as essentially not subject to wear for the life of the instrument. These and all other parts are always available for same-day Air-Express shipment.

Spare parts kits can be supplied in those cases where the instrument is to be used in an area where parts availability may be questionable. Such kits are tailored to the specific needs of the user.

APPLICATION INFORMATION

We are carrying out a vigorous program of application research. Our records of pertinent articles, procedures, and uses of fluorescent analysis are expanding continually. A letter detailing your analysis problem will bring a summary of the references available in our files. In some cases, we will make measurements of relative fluorescence on an experimental basis. Write.

NEPHELOMETRY

May be used to resolve as little as 0.01 APHA standard turbidity units (about 0.01 ppm silica). Only accessory required is 10 mm I.D. x 75 mm. high square cuvette.

SPECIFICATIONS

Range: About 2 parts per billion quinine sulfate is full scale (100 divisions) on most sensitive range. Range multiplier has approximately 3:1 steps (1:3:10:30). Additional range expansion is easily accomplished through use of neutral density filters.

Resolution: Linear to 1%, readable to 0.5% or better.

Stability: Line voltage variation of 105 to 130 volts or line frequency variation from 50 to 60 c.p.s. cause less than $\pm 2\%$ of full scale variation. These figures assume constant sample temperatures.

Cuvette: Normally supplied for use with standard test tubes 10 to 15 mm. in diameter, and 75 to 100 mm. in height. For all but the most sensitive ranges with 360 mu filters, ordinary test tubes having no visible striations or air bubbles are satisfactory cuvettes. For low concentrations, five cuvettes 12 x 75 mm., selected and matched for similar residual fluorescence are supplied.

Sample Size: 2.5 cc. in a 10 mm. or 4 cc. in a 12 mm. O.D. test tube.

Filter Holders: Accepts any combination of standard 2 x 2 inch filters up to 3/8 inch thick, in both primary and secondary positions.

Finish: Two tones of green baked enamel combine with black knobs and meter to provide a pleasing appearance. FLUORESCENCE dial of precision photo-etched aluminum.

Power Requirements: 50-60 cycle, 117-volt AC, 100 watts.

Size and Weight: 10-1/2 inches deep, 12 inches wide, and 12-1/2 inches high. Net weight, 29 pounds, shipping weight, 34 pounds.

Price: \$985.00, complete with general purpose filters, matched cuvettes, dummy cuvette, dust cover, spare lamp and Operating and Service Manual.

D-5



makers of medical and technical instruments
2524 Pulgas Avenue, Palo Alto, California